Neotectonics of the New York Recess

MEETING PROCEEDINGS AND FIELD GUIDE FOR THE 2015 CONFERENCE OF THE GEOLOGICAL ASSOCIATION OF NEW JERSEY

EDITED BY

Gregory Charles Herman and Suzanne Macaoay Ferguson

NEW JERSEY GEOLOGICAL & WATER SURVEY PENNJERSEY ENVIRONMENTAL CONSULTING

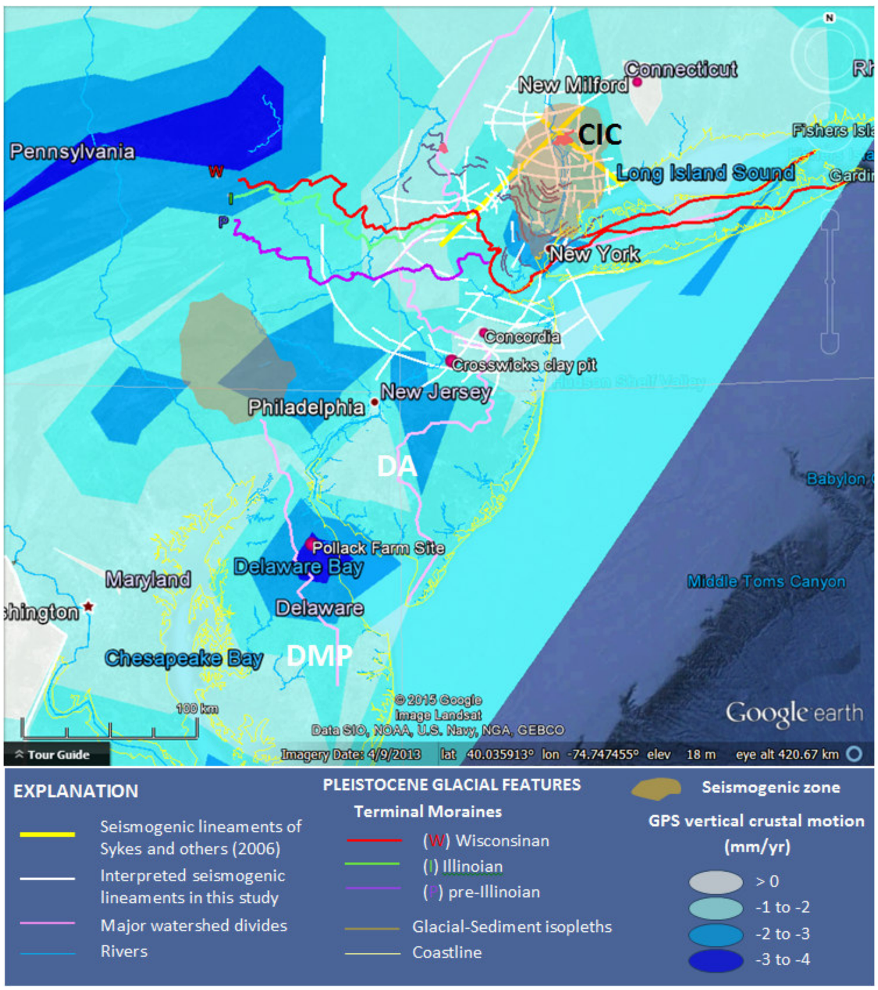

GEOLOGICAL ASSOCIATION OF NEW JERSEY
XXXII ANNUAL CONFERENCE AND FIELD TRIP
OCTOBER 16-17, 2015, LAFAYETTE COLLEGE, EASTON, PENNSYLVANIA

Neotectonics of the New York Recess

2015 CONFERENCE PROCEEDINGS FOR THE 32ND ANNUAL MEETING OF THE GEOLOGICAL ASSOCIATION OF NEW JERSEY

Edited by

GREGORY C. HERMAN

DEPARTMENT OF ENVIRONMENTAL PROTECTION

New Jersey Geological & Water Survey

and

SUZANNE MACAOAY FERGUSON

Pennjersey Environmental Consulting

Friday October 16th annual meeting hosted by Lafayette College

LAFAYETTE

Geology and Environmental Geosciences

Geological Association Of New Jersey
2014-2015 Executive Board

President....................................... Dr. Gregory Herman, New Jersey Geological and Water Survey
Past President .... Dr. Nurdan Duzgoren-Aydin, New Jersey City University
President Elect ....Mr. Michael Gagliano, New Jersey Geological and Water Survey
Recording Secretary .... Mr. Stephen J. Urbanik, New Jersey Dept. of Environmental Protection
Membership Secretary... Ms. Suzanne Macaoay Ferguson, Pennjersey Environmental Consulting
Treasurer .... Dr. Emma C. Rainforth, Ramapo College of New Jersey
Councilor at Large .... Mr. Pierre Lacombe, US Geological Survey
Councilor at Large ....Dr. William Montgomery, New Jersey City University
Councilor at Large ....Mr. Alan Uminski, Environmental Restoration, LLC
Publications Committee ....Dr. Jane Alexander, The College of Staten Island/CUNY
Publications Committee .... Dr. Alan Benimoff, The College of Staten Island/CUNY
Publications Committee ....Dr. Michael Hozik, Richard Stockton College of New Jersey

Field Guides And Proceedings Of Prior Annual Meetings

2015 XXXII - NEOTECTONICS OF THE NEW YORK RECESS,
G. C. Herman and S. Macaoay Ferguson, eds.

2014 XXXI - GLOBAL ENVIRONMENTAL ISSUES AND LOCAL CONSEQUENCES: EARTH SURFACE PROCESSES AND URBAN ENVIRONMENTAL QUALITY, N. Duzgoren-Aydin, ed.

2013 XXX - IGNEOUS PROCESSES DURING THE ASSEMBLY AND BREAK-UP OF PANGAEA: NORTHERN NEW JERSEY AND NEW YORK CITY, A. I. Benimoff, ed.

2012 XXIX - GEOLOGY AND PUBLIC LANDS. J. Alexander, ed.

2011 XXVIII - ENVIRONMENTAL GEOLOGY OF CENTRAL NEW JERSEY,
E. C. Rainforth and A. Uminski, eds.

2010 XXVII - GEOLOGY OF THE GREATER TRENTON AREA AND ITS IMPACT ON THE CAPITAL CITY,
P. Lacombe, ed.

2009 XXVI - NEW JERSEY COASTAL PLAIN STRATIGRAPHY AND COASTAL PROCESSES,
D. Freile, ed.

2008 XXV - ENVIRONMENTAL AND ENGINEERING GEOLOGY OF NORTHEASTERN NEW JERSEY,
M.L. Gorring, ed.

2007 XXIV - CONTRIBUTIONS TO THE PALEONTOLOGY OF NEW JERSEY (II),
E. C. Rainforth, ed.

2006 XXIII - ENVIRONMENTAL GEOLOGY OF THE HIGHLANDS,
S. Macaoay and W. Montgomery, eds.

2005 XXII - NEWARK BASIN - VIEW FROM THE 21ST CENTURY, A.E. Gates, ed.

2004 XXI - PROTEROZOIC, PALEOZOIC, AND MESOZOIC MAFIC INTRUSIONS OF NORTHERN NEW JERSEY AND SOUTHEASTERN NEW YORK, J. H. Puffer and R. A. Volkert, eds.

2003 XX - PERIGLACIAL FEATURES OF SOUTHERN NEW JERSEY AND ADJACENT AREAS,
M. J. Hozik and M. J. Mihalsky, eds.

2002 XIX - GEOLOGY OF THE DELAWARE WATER GAP AREA, D. D'Amato, ed.

2001 XVIII - GEOLOGY IN SERVICE OF PUBLIC HEALTH, P. Lacombe and G. C. Herman, eds.

2000 XVII - GLACIAL GEOLOGY OF NEW JERSEY, D. P. Harper and F. R. Goldstein, eds.

1999 XVI - NEW JERSEY BEACHES AND COASTAL PROCESSES FROM GEOLOGIC AND ENVIRONMENTAL PERSPECTIVES, J. H. Puffer, ed.

1998 XV - THE ECONOMIC GEOLOGY OF CENTRAL NEW JERSEY, J. H. Puffer, ed.

1997 XIV - THE ECONOMIC GEOLOGY OF NORTHERN NEW JERSEY, A. I. Benimoff and J. H. Puffer, eds.

1996 XIII - KARST GEOLOGY OF NEW JERSEY AND VICINITY, R. F. Dalton, and J. O. Brown, eds.

1995 XII - CONTRIBUTIONS TO THE PALEONTOLOGY OF NEW JERSEY, J. Baker, ed.

1994 XI - GEOLOGY OF STATEN ISLAND, A. I. Benimoff, ed.

1993 X - GEOLOGIC TRAVERSE ACROSS THE PRECAMBRIAN ROCKS OF THE NEW JERSEY HIGHLANDS, J. H. Puffer, ed.

1992 IX - ENVIRONMENTAL GEOLOGY OF THE RARITAN RIVER BASIN, G. M. Ashley and S. D. Halsey, eds.

1991 VIII - EVOLUTION AND ASSEMBLY OF THE PENNSYLVANIA-DELAWARE PIEDMONT, M. L. Crawford and W. A. Crawford, eds.

1990 VII - ASPECTS OF GROUNDWATER IN NEW JERSEY, J. O. Brown and R. L. Kroll, eds.

1989 VI - PALEOZOIC GEOLOGY OF THE KITTATINNY VALLEY AND SOUTHWEST HIGHLANDS AREA, NEW JERSEY, I. G. Grossman, ed.

1988 V - GEOLOGY OF THE CENTRAL NEWARK BASIN, J. M. Husch and M. J. Hozik, eds.

1987 IV - PALEONTOLOGY AND STRATIGRAPHY OF LOWER PALEOZOIC DEPOSITS OF THE DELAWARE WATER GAP AREA, W. B. Gallagher, ed.

1986 III - GEOLOGY OF THE NEW JERSEY HIGHLANDS AND RADON IN NEW JERSEY, J. M. Husch and F. R. Goldstein, eds.

1985 II - GEOLOGICAL INVESTIGATION OF THE COASTAL PLAIN OF SOUTHERN NEW JERSEY, R.W. Talkington and C. M. Epstein, eds.

1984 I - IGNEOUS ROCKS OF THE NEWARK BASIN: PETROLOGY, MINERALOGY, AND ORE DEPOSITS, J. H. Puffer, ed.

GANJ 32 CONFERENCE SPONSORS

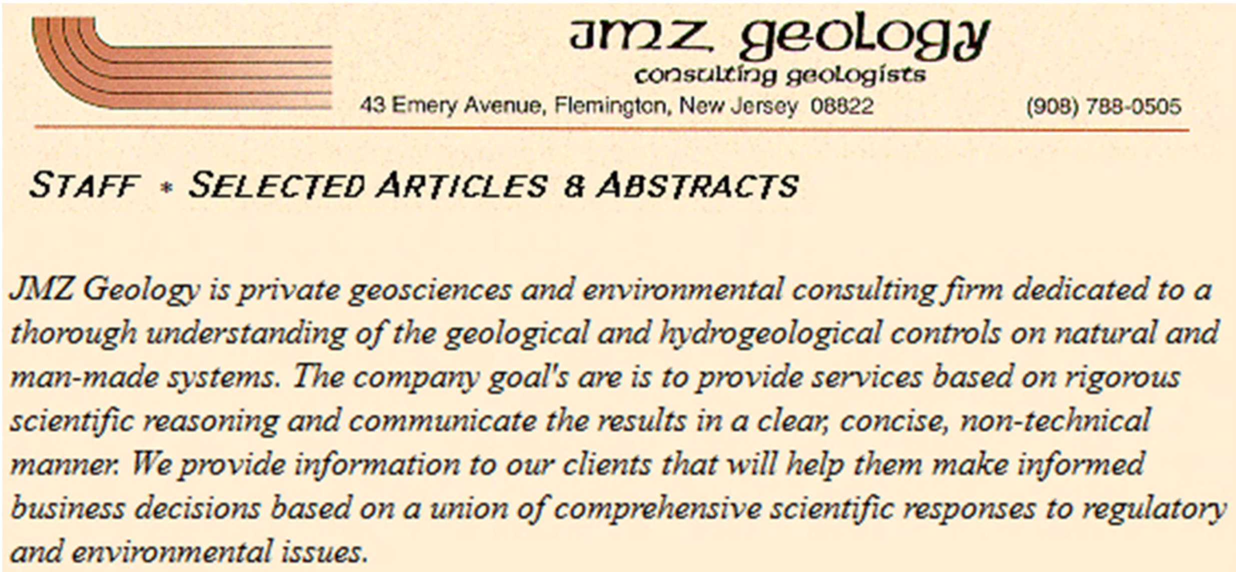

GANJ 32 CONFERENCE SPONSORS

SCHEDULE

Friday, October 16th
Lafayette College Campus

11:30 to 1:30	Conference Registration
12:30 to 1:30	Teacher's Workshop: Teaching Earth Science with Google Earth
1:30 to 1:50	Dr. Gregory Herman - Welcoming comments, State of the GANJ organization, and business meeting.
1:55 to 2:25	Dr. Charles Merguerian, Duke Geological Laboratories - Review of New York City bedrock with a focus on brittle structures.
2:30 to 3:00	Dr. Ryan Mathur, Juniata College – Re-Os isotope evidence an Early Tertiary episode of crustal faulting and sulfide-mineralization in Pennsylvania with probable ties to the Chesapeake Bay bolide impact in Maryland, USA.
3:05 to 3:30	Dr. Frank Pazzaglia, Lehigh University - Geomorphic paleogeodesy and intraplate deformation associated with the Central Virginia Seismic Zone (CVSZ).
3:35 to 4:15	Dr. Dru Germanoski, Lafayette College - Geology museum and department tour, snacks and refreshments.
4:25 to 4:55	Dr. Gregory Herman - Neotectonics of the New York Recess.
5:00 to 5:40	KEYNOTE SPEAKER, Dr. Kenneth Miller, Rutgers University - The role of sea level and mantle dynamic topography on U.S. Atlantic passive-aggressive continental margin architecture.
6:30 to 8:30	Post-meeting dinner

Saturday, October 17th
Assemble at NJ Liberty Village Commuter Lot at 81 RJ-12W

8:00	Leave Flemington NJ Liberty Village Commuter Lot at 81 RJ-12W
8:30 to 10:30	STOP 1: *Eastern Concrete Materials plant,* 1 Railroad Ave, Glen Gardner NJ
11:15 to 1:15	STOP 2: *Mercer County Park,* 48 Valley Road, Lambertville, NJ,
1:20 to 2:00	STOP 3: *Trap Rock Industries Moore's Station Plant,* 1601 Daniel Bray Highway (Rt-29 S), Lambertville, NJ
1:20 to 2:00	STOP 4: *Delaware & Raritan Canal State Park Trail,* 43 Route 29 N, Stockton, NJ
4:50	Return to Flemington NJ Liberty Village Commuter Lot at 81 RJ-12W

Contents

Preface

The theme for the 32nd annual meeting of the Geological Association of New Jersey is the Neotectonics of the New York Recess. As defined in *Wikipedia*, neotectonics, is a sub discipline of tectonics, involving the “study of the motions and deformations of the Earth's crust (geological and geomorphological processes) which are current or recent in geologic time…the term may also refer to the motions/deformations in question themselves.” As such, the purpose of this conference aim is to summarize and communicate the neotectonic setting of our region by integrating the best available geological and geophysical data for the New York Recess, centered on New Jersey. Each of the four technical papers detail post-Jurassic tectonic structural, stratigraphic, and geophysical data that help us gain a better understanding our current geological framework and tectonic setting.

The term ‘neotectonics’ is further defined here, at the outset, by drawing from Steward and Hancock’s (1994) definitive work on the matter as part of a book addressing continental deformation. They primarily differentiate between *neotectonic* (recent) structures, and *palaeotectonic* (ancient) structures. To paraphrase their work, neotectonics is the branch of tectonics concerned with understanding earth movements that both occurred in the past and are continuing at the present day. Thus, *neotectonic structures develop in the current tectonic regime*. There is no need for neotectonism to be regarded as synonymous with a specific period of time, for example Quaternary or Neogene tectonics. When the word is used as an adjective to qualify the age of a structure, it commonly implies that the structure is interpreted to having been propagated or reactivated in *a stress/strain field that has persisted without significant change of orientation to the present day*. Moreover, they separate neotectonics from active tectonics, or those crustal movements that are expected to occur within a future span of time span of concern to human society. Neotectonic structures that are exposed formed within the upper two kilometers of the crust. Deeper structures will only be exposed and distant times in the feature from long periods of uplift and denudation. Neotectonic structures sometimes tie with current and recent geomorphic processes that provide clues as to the duration of neotectonic movements that can also be gleaned from earthquake focal mechanism solutions and in-situ stress measurements. Pattern of historical earthquake distributions and magnitudes can help define neotectonic structural trends in areas undergoing historical crustal fracturing and faulting.

This book of proceedings and field stops begins with the teacher’s workshop, and is followed in order by the technical manuscripts and extended abstracts before ending with the field-trip guide. The teacher’s workshop theme is Using Google Earth to explore the interaction between topography and geological points, polyline, and planes. Parts of different lessons from my introduction geology class at The College of New Jersey are made available to the participants of the teacher’s workshop to explore some aspects of our local geology while learning how to use Google Earth (GE) to access information, and visualize geological features using an interactive 4-dimension (4D) visualization system. For the workshop, there are parts of two GE exercises that help GE users acclimate to the work environment before exploring raster imagery and different settings in GE that provide options for exaggerating the topography, and tracing geological features from scanned and geo-registered imagery.

Our speakers have also contributed manuscripts and extended abstracts that present details contributing to the understanding of our neotectonic setting. Dr. Charles Merguerian, formerly of Hofstra University, and currently a research scientist at Yale University where he is curating his data, provides a retrospective of his extensive work in New York City. His summarizes the different brittle structural discontinuities that he and others have seen in metamorphosed Proterozoic basement and Paleozoic cover rocks seen at the surface and in the subsurface. This work shows that NNE-striking, late-stage, strike-slip faults in NYC may be, or have recently been seismogenically active. Dr. Ryan Mathur of Juniata College, Pennsylvania contributes geochemical work for the eastern parts of the Pennsylvania region into northern New Jersey using Rhenium/Osmium (Re/Os) radioactive parent-daughter isotopes providing Late Eocene to Mid Oligocene ages (~ 39 ± 4 - 27 ± 4 Mya) from brittle faults and rock breccia containing hydrothermal sulfide minerals that demonstrate a, tectonic event in this region. As hypothesized, these crustal features reflect far-field crustal strains lying out in front of a large, hypervelocity asteroid that impacted the head of Chesapeake Bay at ~35.5 Mya. Dr. Gregory Herman provides a summary of modern geological and geophysical data for this region that are compiled and integrated in to GE KMZ file for inspection and download at http://www.ganj.org/2015/Data.hml. Actual-plate motions are examined using ground-fixed Global Positioning Data receiving stations provide 3D plate motion data that are placed in perspective with historical seismicity and physiography to show neotectonic trends that reflect geological heterogeneity in the crust. Some old Appalachian viewpoints are reappraised in light of probable, far-field strain effects stemming from the Chesapeake Impact that helps set the stage for better defining the emerging concept of impact tectonics.

Two technical abstracts include one by Dr.Frank Pazzaglia of Lehigh University on the recently active Central Virginia Seismic Zone. The second one is by this year's keynote speaker, Dr. Kenneth Miller of Rutgers University, where he addresses the role of seal level change and mantle dynamic topography on the US Atlantic continental margin. For our field trip we have four thought-provoking field stops planned, two of which may show brittle, neotectonic overprinting on earlier Mesozoic rocks of the Newark basin. Two other stops are in active commercial quarries and aggregate-processing plants.

Dedication to Butch Grossman by G. C. Herman

It is my honor to dedicate this volume to Mr. Irvin G. 'Butch' Grossman, who passed away earlier this year at age 98. It is only fitting that GANJ 32 provides a forum to dedicate work to a man that both taught and inspired me and countless others in ways that only Butch could. He came to work at the NJGWS in 1984 after retiring from a career with the USGS as a practicing hydrogeologist. He began his second career as the principle content editor for NJGWS reports and maps. He also began teaching us a thing or two. For Butch was not only a hydrogeologist and English editor, but a husband, a father, an artist, an athlete, comedian, and philosopher - to name just some of the many facets of Butch that so endeared him to us. He had a wonderful way of listening to what you were saying, and then pausing before responding. He was a role model that taught me that life's vitality stems from loving, learning, reading, writing, laughing, and moving. In 1989, Don Monteverde and I had just finished mapping the Kittatinny Valley and were excited to share the results with GANJ. That year, as I helped President Michael Hozik organize and run GANJ 6, I was projecting 35 mm photographic slides onto walls, to trace structures in order to make guidebook figures. Now we use 4D computer visualization to do the same. But over this entire stretch of time, Butch never veered away from No. 2, wooden editing pencils with brown lead. I was absolutely shocked when he edited our first work, and second, and third….. I had paid far too little attention to elementary grammar, and Butch helped steer me from the gravel roads of acceptable prose to smoother roads paved by STA (the voluminous USGS publication titled 'Suggestions to Authors'). Back then, I was too inexperienced at writing to edit the GANJ 6 volume, so I asked Butch to, and he graciously accepted. GANJ 6 was a great conference and field experience as we rode across the brand new, yet-to-open, western leg of Route 78 through Alpha, NJ to Morgan Hill, PA and elsewhere. That was also chairman Dru Germanoski's first year with the Lafayette geology department, and so it only fitting that we are reassembled here again for GANJ 32, just 26 years later, in honor of my friend, and many of yours. His influence will always be with me. Thank you Butch.

One of Butch's annual, personalized, and hand-illustrated greeting cards.

Chapter 1. Teachers Workshop: Teaching Earth Science with Google Earth

Gregory C. Herman, New Jersey Geological & Water Survey

The following exercises and methods are part of the laboratory component for an introductory geology class that I teach at the College of New Jersey. We use GE in 4 labs session during the semester to become familiar with the physical expression of land surface and how it works with raster (cell-based), point, polyline, and polygons themes . Please note that this workshop guide is designed for use with Windows PCs. User instructions for a Mac will be different as these exercises use both left- and right mouse buttons and the mouse wheel for program and viewing options. It isn't normal practice to have three button-access on a MAC mouse.

Google Earth KML Terminology:

• KML stands for Keyhole Markup Language (KML), an XML notation for expressing geographic annotation and visualization within Internet-based, two dimensional maps and three-dimensional (3D) Earth browsers (Wikipedia, 2012).

• KML is an international standard of the Open Geospatial Consortium. XML (Extensible Markup Language) is a markup language that defines a set of rules for encoding documents in a format that is both human-readable and machine-readable (Wikipedia, 2012).

• KMZ is a compiled KML file, meaning that it has been encrypted in machine language and is not readily open or read in ordinary language or ASCII text editors.

• You can <File><Save> or <File Save As> from going to KMZ to a KML or vice versa.

• But if you want to manually edit the GE file, <Save As> a KML, then <Open> it using Microsoft (MS) Notepad or Wordpad, common ASCII text editing files for PCs.

Google Earth (GE) and mouse-wheel button interoperability

• A key GE viewing tool is to use the mouse for interactive viewing by <Pressing down>and <Holding> the middle button of your mouse after the cursor is positioned over the feature or area of interest, then moving the mouse with the zoom wheel depressed.

• Depressing and holding the mouse wheel down allows you tilt and rotate the view interactively.

EXERCISE 1: Explore geospatial themes for New Jersey using Google Earth

Copy and paste the following URL into your browser and <Enter>

http://www.impacttectonics.org/gcherman/downloads/PHY120C/LAB4_Google_Earth_1.kmz

This will download a KMZ containing some New Jersey geologic and topographic data that we will open for use in this exercise. This lab is the introductory Google Earth (GE) computer-laboratory session that I run as the first in a series of four GE sessions as part of my introduction to geology curriculum at the College of New Jersey.

You can start the session either by <double-clicking> on the download button upon completion of the download, or start Google Earth, click on the <File><Open > sequence in the Menu Bar (fig. 1), and open the KMZ in the downloads folder.

•The file will load into the GE Temporary folder:

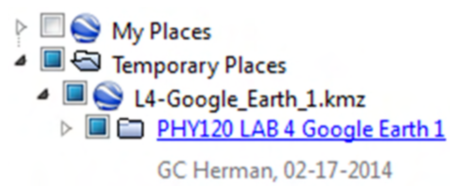

• Upon loading the theme DO NOT TURN ON ALL LAYERS.

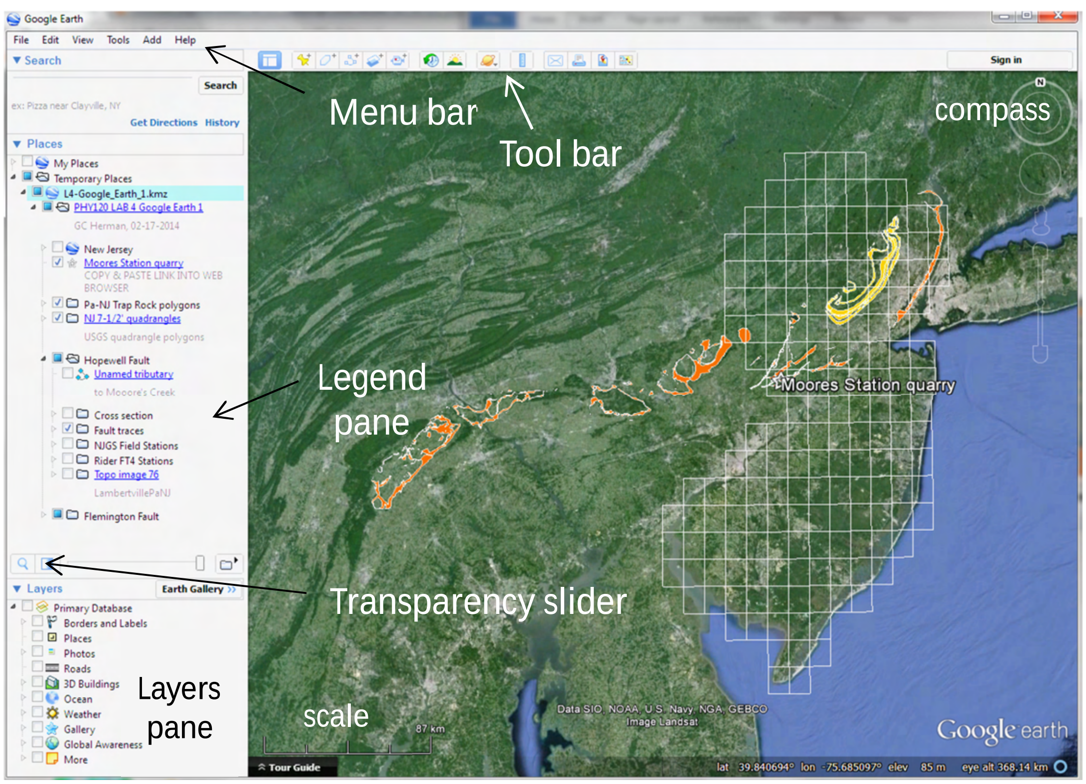

Figure 1. Default view upon opening TCNJ PHY120 Lab4 Google Earth.KMZ

• Be sure to minimize the Tour Guide at the bottom of the GE view and slide the Legend pane downward in order to maximize the space available in which to expand theme folders.

•With the newly loaded theme highlighted and active, grab it by clicking on it once with the mouse, and physically drag it into <My Places> in the Legend pane.

• Then <Right click> on the theme in the Legend pane and specify <Save><Save My Places> or <Save Place As> if you want to save it externally.

•A pop-up menu will prompt you for a location to <Save> the file for future use.

• Expand the theme folder by clicking on the *triangles* to view the theme content before deciding on an approach for *turning layers on and off* (making them visible – see right) →.

• This is a safe approach when downloading and using a file exceeding a couple megabytes size.

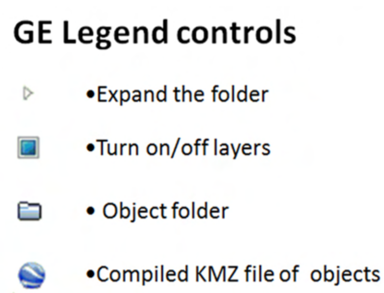

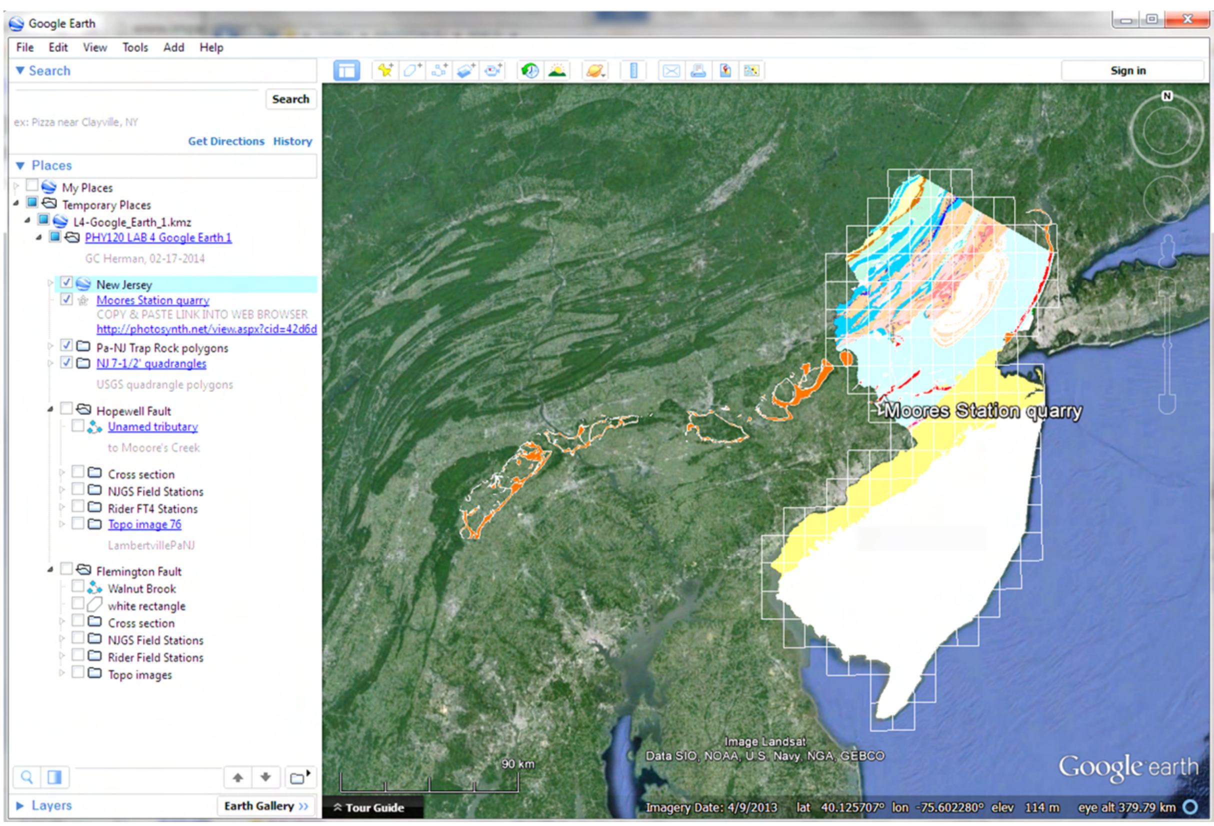

Figure 2. Expanded view showing the 1:100K USGS New Jersey bedrock geology by lithic groups. Note that the *Layers* pane is minimized at the bottom.

•Next, <double-click> on the Hopewell Fault folder

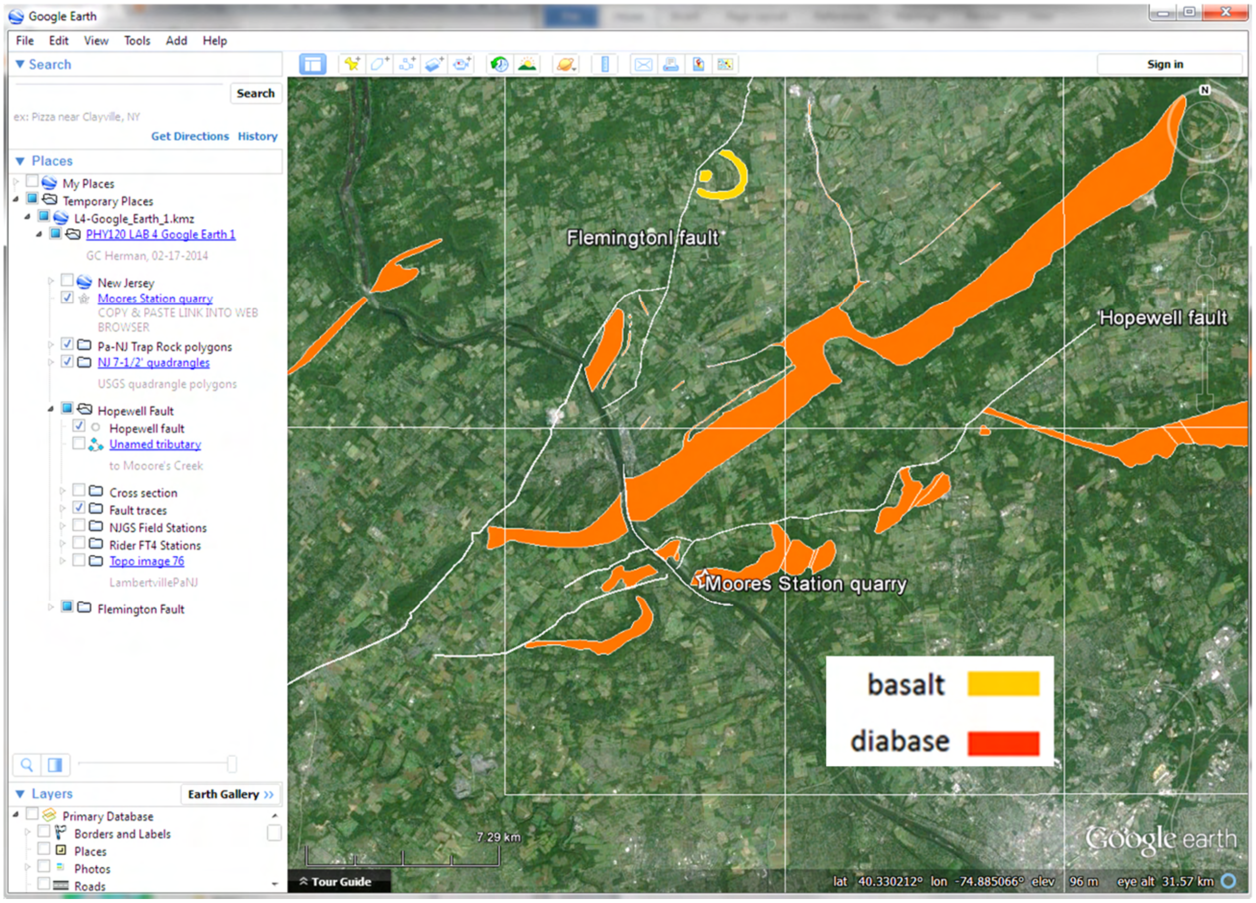

Figure 3. Default view after <double-clicking on the Hopewell Folder.

• The following view will zoom into focus.

• Note that in figure 3 above, the Layers pane has now been restored, but slid down and minimized so that only the Borders through Roads is visible. This maximizes the Places pane availability for displaying a theme's component folders while providing quick access to the built-in GE reference themes such as *Borders and Labels,* and *Roads.*

• Also, note that the Layers Pane has been slid down and minimized so that only the Borders through Roads are visible. This maximizes the Places pane availability for displaying a theme's component folders.

• <Single-left click> on the view to move it into the center of the view, and use the mouse wheel to zoom in to the quarry.

• Depress the mouse wheel and hold it down as you drag the mouse backward toward you to begin dynamically viewing the topography and geology polygon. Release the mouse wheel, <Left click> on the display again and drag it into a desired perspective.

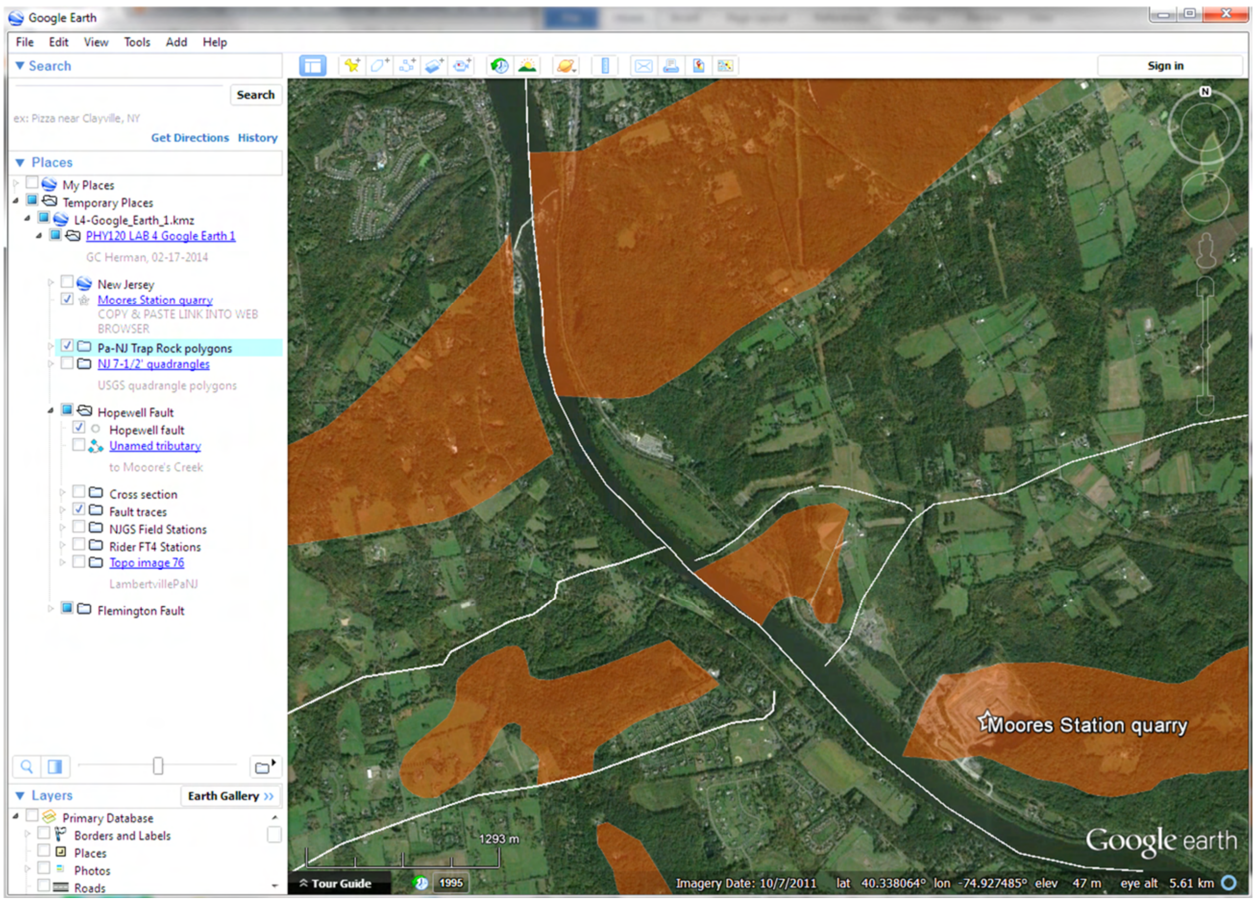

Figure 4. Scaled view after <double-clicking> on the Moores Station quarry placemark. Note that the Pa-NJ Trap Rock polygons folder is active, and that the transparency slider is set at about 50%, making it so that you can see the quarry under the Moores Station quarry placemark toward the bottom right.

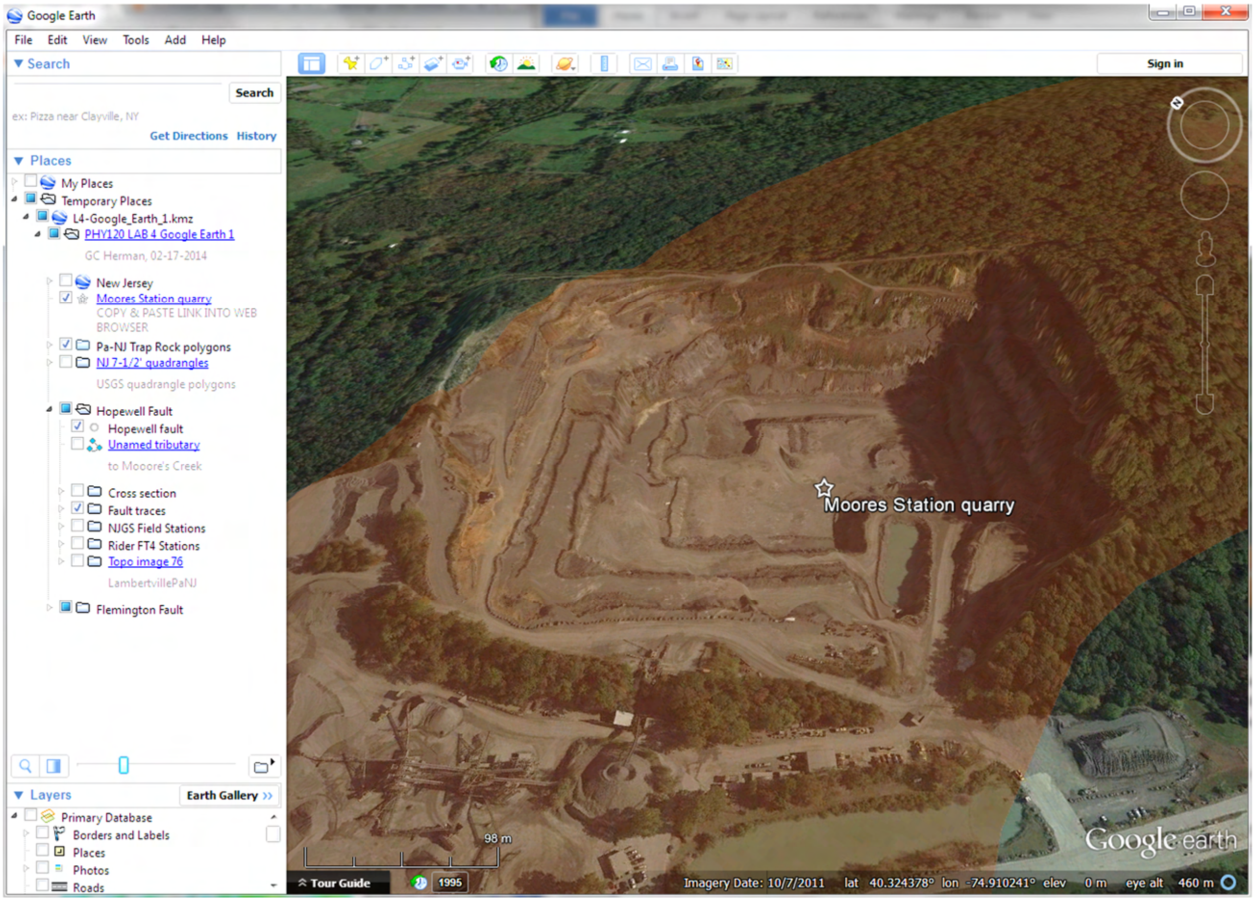

Figure 5. Oblique North-Northeast view of the Moores Station quarry after manually positioning. The Pa-NJ Trap Rock polygons theme is now about 70% transparent.

• <Single-left click>

• In the Legend pane, the balloon pops up in the view with a link to a Photosynth photo collage of the quarry.

• <Right-click<Copy Link> and paste this URL into an Internet browser like MS Explorer or Google Chrome. This will bring you to a Microsoft site that photo mosaics 2D photographic into 3D mosaics called Photosynth (fig. 8)..

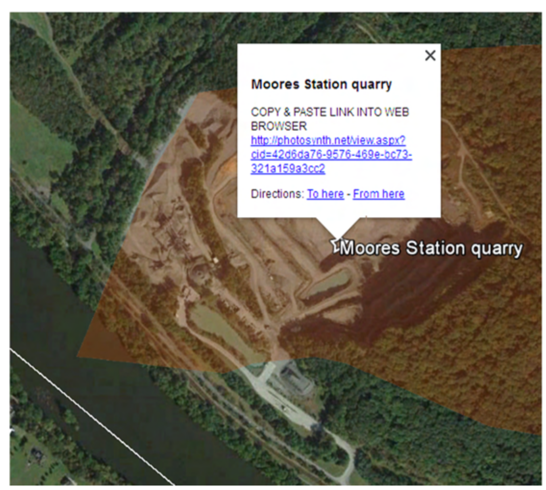

Figure 6. Balloon showing the URL for the MS Photosynth.

• You may get a prompt like this asking your permission for the rendering software to run in your browser.

• If you <Right-click><Run this program> and grant it permission and it works, you will have a view that you can pan and zoom through to see the quarry being worked.

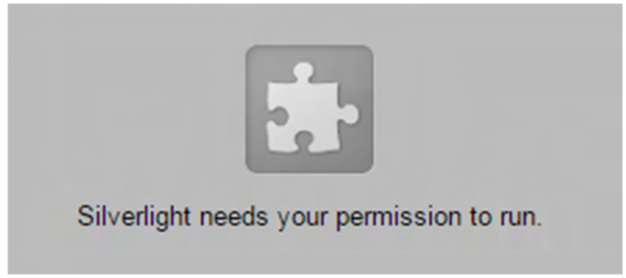

Figure 7. Microsoft Silverlight prompt to run.

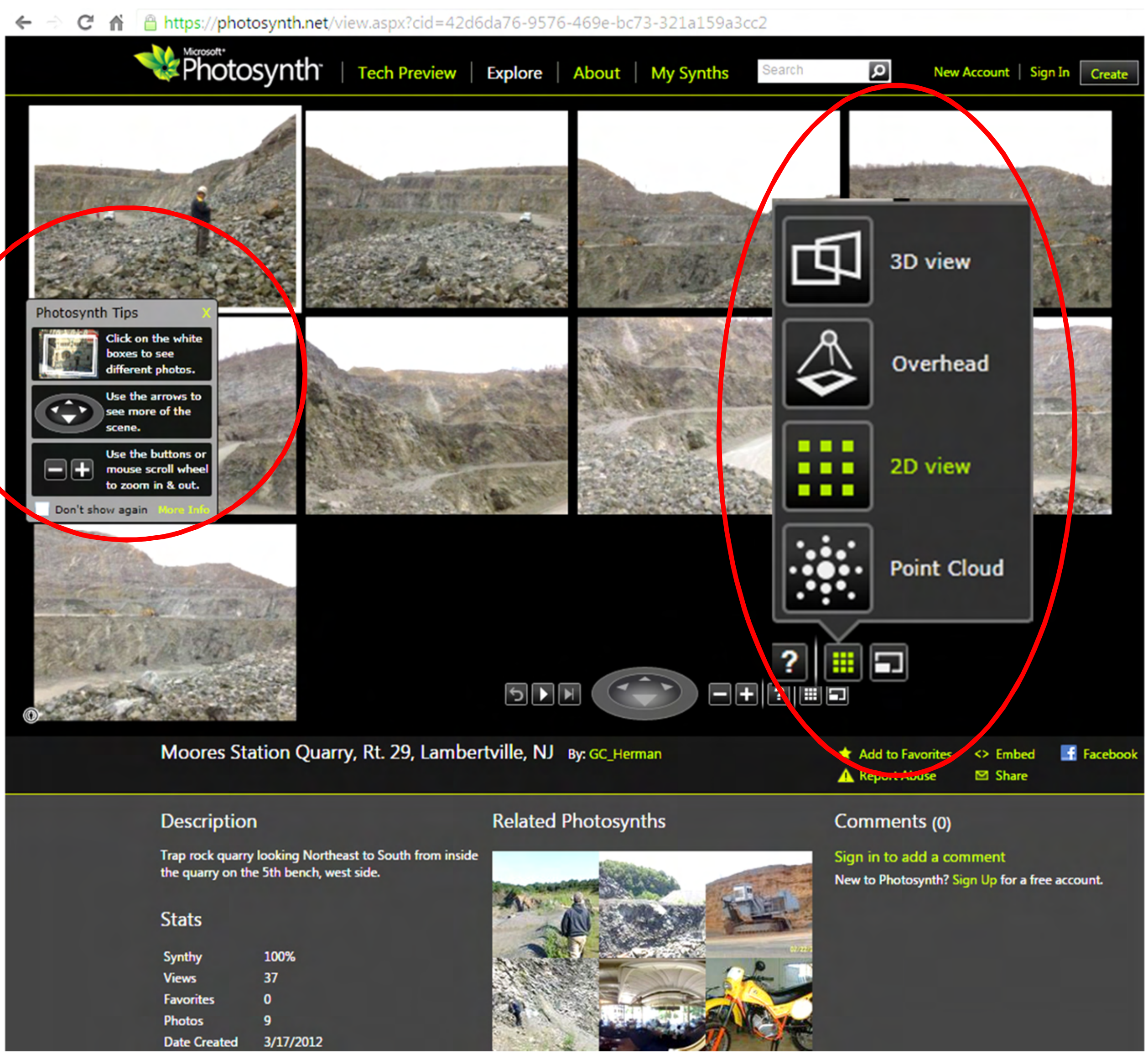

Figure 8. 2D view of the 9-photo mosaic. Note the Photosynth Tips dialog window middle left.

•Now turn on the Topo Image 76 theme and adjust its transparency to about 70%, as demonstrated below.

Figure 9. Bird's-eye view of the Moores Station quarry with part of the U.S. Geological Survey, Pa-NJ Lambertville 7-1/2' topograaphic quadrangle map as an image overlay set at about 70% tranparent. The arrow points to the perspective shown in figure 10 below.

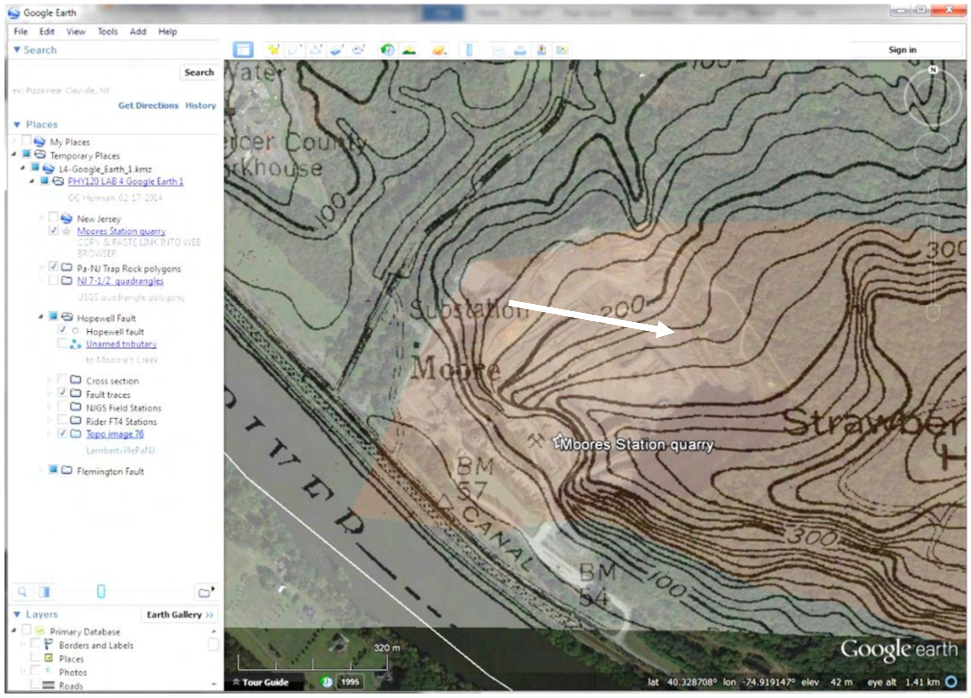

Figure 10. Photograph of quarry benches looking ESE along the viewpoint in fugure 9.

• Now access the <Tools><Options> menu to change the vertical exaggeration to 3.0.

GE and Vertical topographic exaggeration

The command **<Tools><Options…>** take you to the following menu:

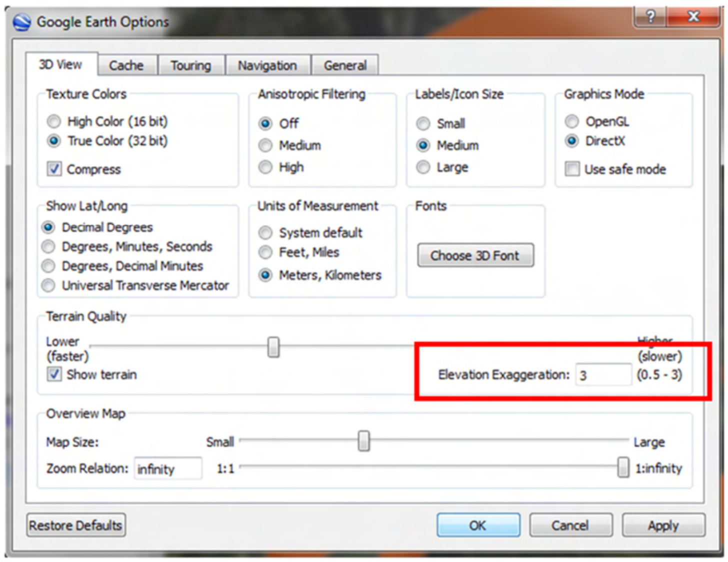

The elevation exaggeration will multiply the height of the topography by the factor entered (up to a maximum 3X)

This function should be used in areas of muted topographic relief, and not for mountain ranges or areas of drastic relief.

Figure 11. This GE options window allows you to set the vertical exaggeration to anyone range of values from a minimum 0.5 and a miximum 3.0.

• The resulting display will look something like this:

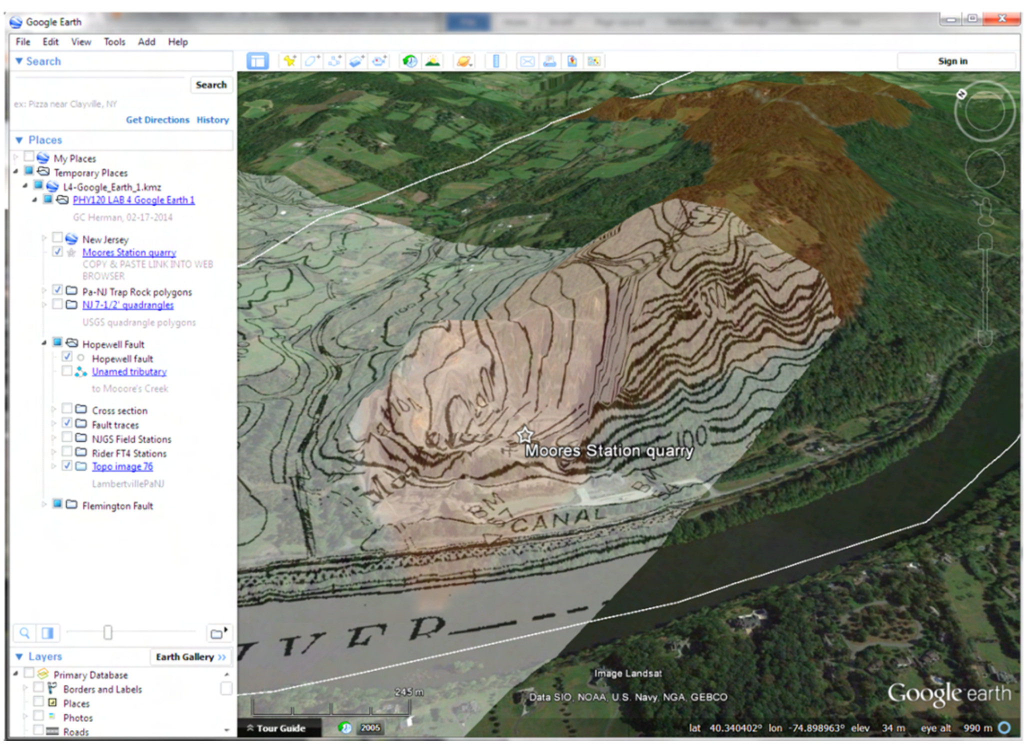

Figure 12. Similar view of the Moore's Station quarry as for figure 8, but with the vertical exaggeration set at 3X.

• Interact with the display, zooming in and out and turning the view to see the exaggerated topographic perspective.

• The last part of this first exercise is to access the KMZ at this URL:

http://www.ngdc.noaa.gov/mgg/global/relief/ETOPO1/tiled/ice_surface/etopo1_ice_surface.kmz

• This opens the colored physiographic theme of the Earth pictured below:

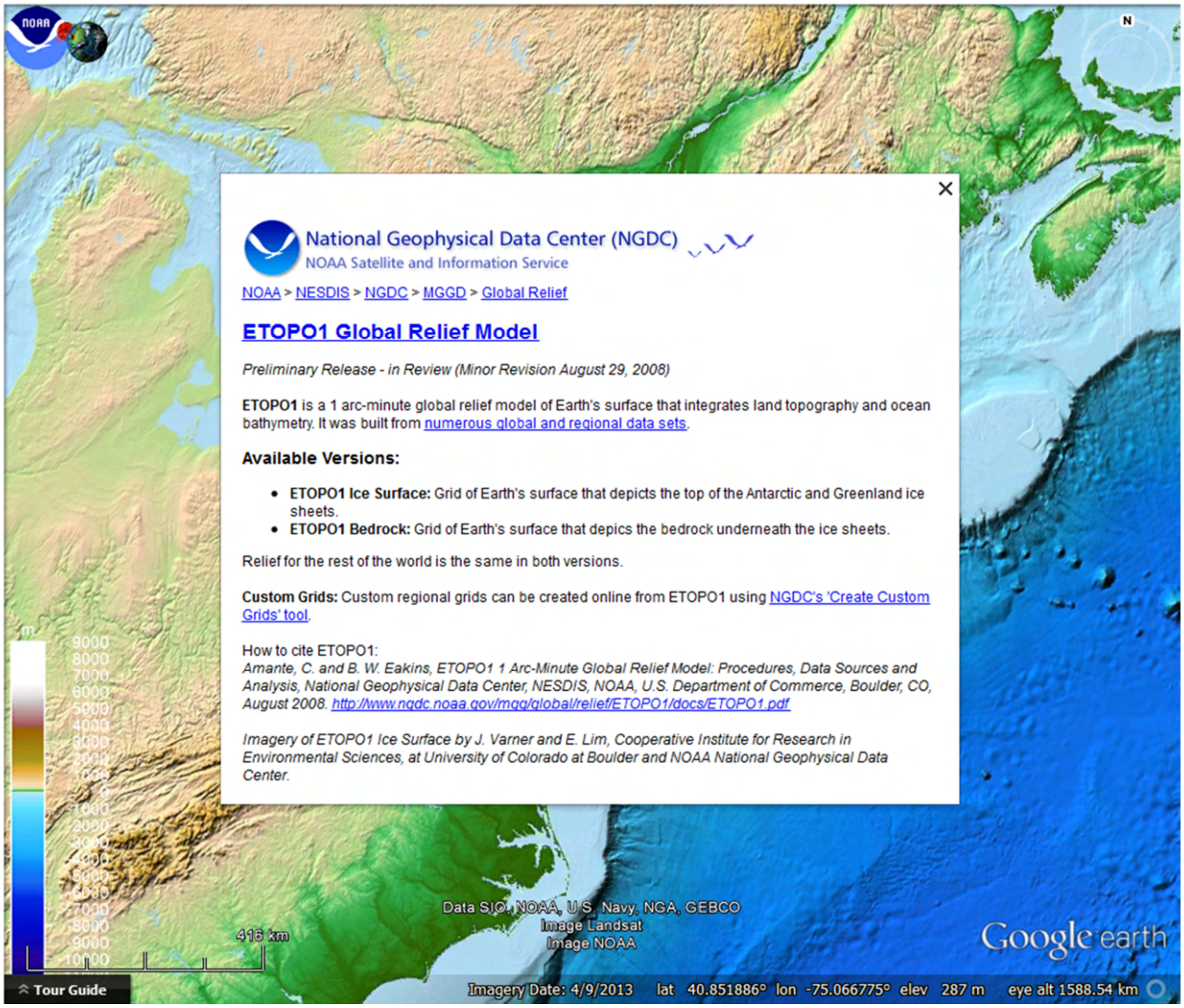

Figure 13. ETOPO1 Globa Relief balloon that is displayed

<Left click> on the newly added 

.

• Use this theme to explore the Andes and the Himalayas, Japan, and wherever on Earth.

EXERCISE 2: TCNJ LAB7_PA-NJ-NY_Glacial_Morraines.kmz (526 KB)

This exercise is the third of four GE labs run in the Physics 120C Introduction to Geology Laboratory. By this time, the students have developed a familiarity with raster imagery and coordinate-referenced points, lines, and polygons, and this lab functions to develop their skills in registering raster imagery for the purpose of extracting polyline-based geoscience themes. For this exercise, three images provide continuous base representation of the Pleistocene terminal moraines and glacial-sediment-thickness contours covering eastern Pennsylvania and western New Jersey (fig. 14). The opening view includes the three maps showing line traces of glacial morainic deposits or thickness isolines of glacial sediments in the New Jersey region. The maps include work by Witte and Germanoski, 2012; Stanford, 2010; and the USGS Geological Survey for Long Island (http://pubs.usgs.gov/of/2000/of00-243/pdf/fig1.pdf).

According to Stone and others (2002), Earth's glacial record shows that the Laurentide ice sheet reached New Jersey at least three times over the last two million years. The limits of these respective events are characterized by Witte and Germanoski (2012) from youngest to oldest in table 1.

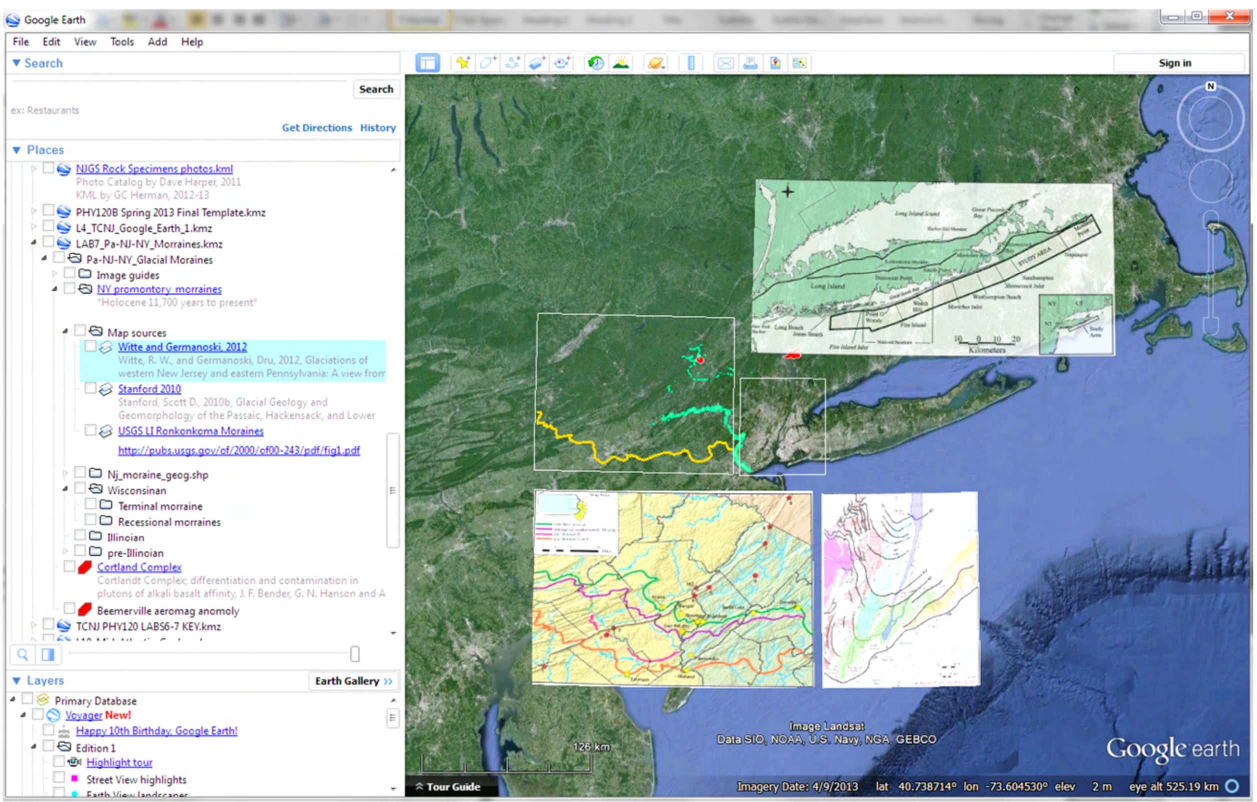

Figure 14. Opening view of TCNJ Lab 7.

Table 1. Pleistocene glacial stages and approximate ages in the NY Recess

Moraines (Marine isotope age)	*estimated glacial-culmination age of terminal deposits*
Holocene 11,700 years to present	
Late Wisconsinan (MIS 2)	~26 – 17.8 Kya
Oldest Late Illinoian or pre-Illinoian B (MIS 6 or 12)	~ 160 - 180 Kya
Two older pre=Illinoian (MIS 16 – 22)	~850 Kya – 2.01 Mya

According to Witte and Germanoski (2012), "Similar to New Jersey's oldest glacial deposits, those in Pennsylvania may represent more than one glaciation. There is some disagreement concerning the age of the older glaciations and number of pre-Illinoian glaciations, but there is a remarkable congruency between the glacial limits mapped on either side of the Delaware River. The youngest glacial deposits laid down during the Late Wisconsinan substage provide the clearest record of glaciation. The glacial record, indicated by the Illinoian and especially the pre-Illinoian deposits, is much less clear due to an extensive and complex periglacial and weathering history".

The opening view in this exercise (fig. 13) includes three raster images that are preloaded in the KMZ along with two white boxes that the two lower images fit in. A third, upper image of Long Island requires matching of the coastline for georegistration. Orange polygons included in the KMZ are polygonal representations of morainic deposits in New Jersey from Stanford and others (2007), subsequently converted from an ESRI shapefile theme in to a KMZ file.

This exercise consists of two parts:

A) Register each image, and then

B) Manually digitize the positions of each moraine using the GE polyline tool 

Part A) Georegister imagery in GE:

1) <Left click> on one of the images to activate it (it becomes highlighted in blue when active) as seen in figure 15 for the Witte and Germanoski (2012) image.

2) Once an image is active, then <Right-click> on the <Properties> menu option (bottom choice). This will place the image in editing mode and activate green handles to manipulate an

image (fig. 15). The different types of handles can be used to resize, stretch, rotate, or drag the image into position.

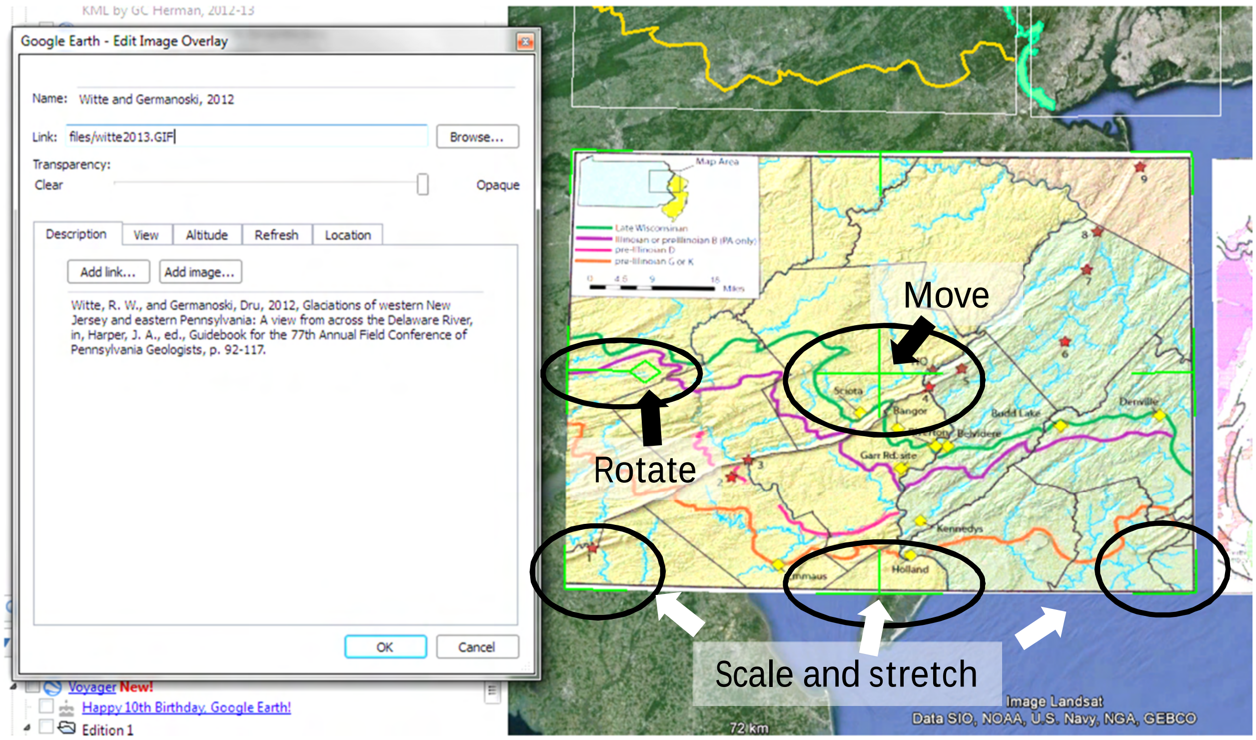

Figure 15. GE view of an image property-dialog box with the image in editing mode. Note the green handles that are used to manipulate the image, and the Trasparency slider on the <Properties>< Edit Image Overlay> menu.

3) Once the correct position is attained, <Left click> <OK> in the Edit Image Overlay window

4) When registering the Long Island image, use the transparency slider to make the image semi-transparent in order to match the coastline on the image with that in GE.

Once each image is positioned, then the next step is to digitize the traces of the glacial moraines.

Part B) Digitize polyline traces of the moraines using the GE polyline tool 

As seen in figure 14, the pre-Illinoian moraine has already been traced as a colored polyline and is useful for checking the alignment of the western geo-registered image. Also, the Wisconsinan terminal moraine in New Jersey (the southernmost green polygon) serves as a reference for continuing the trace of the Wisconsinan from eastern Pennsylvania through New Jersey.

To digitize a feature trace,

1) Activate the folder that is to receive a digital polyline, for example, before tracing the terminal moraine of Wisconsinan age, use the mouse to <Left click> the folder and highlight it before proceeding (like that in figure 14).
2) Next, <Left click> the polyline tool icon in the toolbar. 
The mouse cursor becomes a symbol like this: 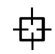
3) Next, position the mouse cursor over the starting point, then repeatedly <Left click> the mouse button as you move along the trace, clicking to place a vertex on the polyline trace.

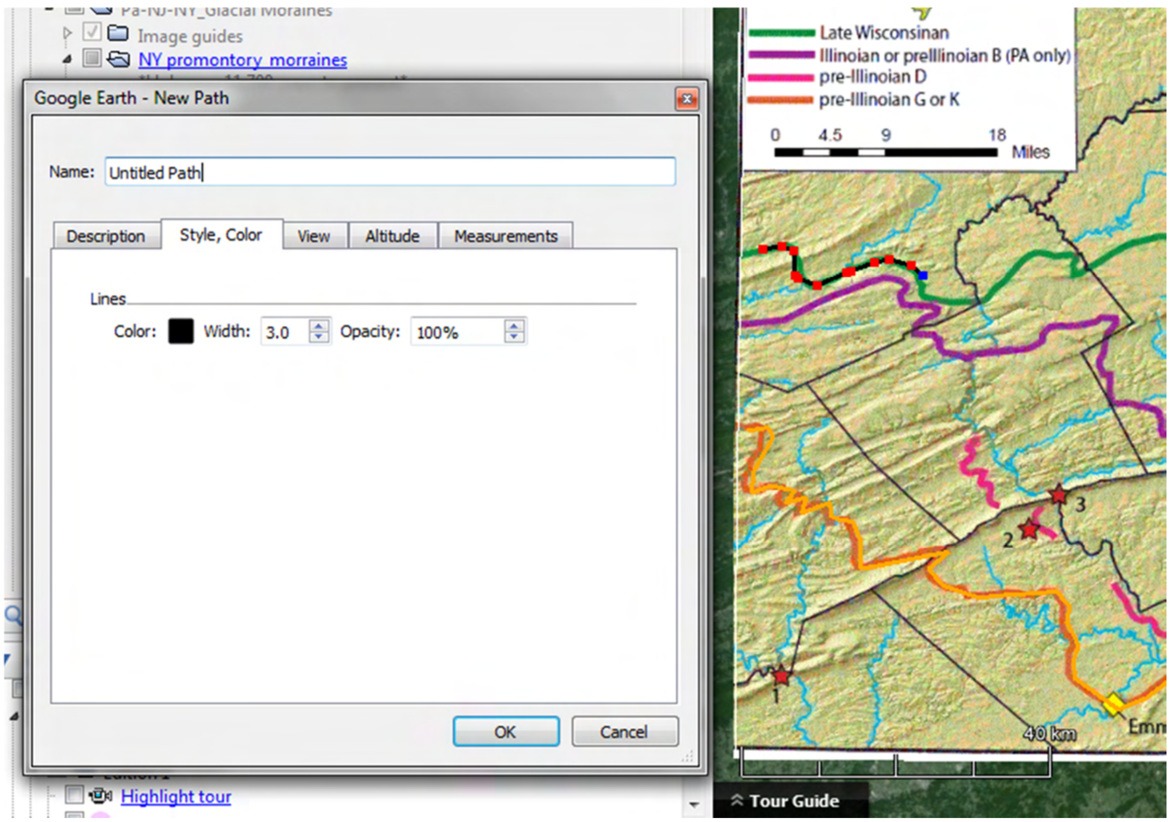

Figure 16. GE view of an image property-dialog box with the polyline in editing mode. Note the black line of Width 3.0 that is being digitzied along the Wisconsinan moraine (beginning on the left and procegressing to the right). Each small, red square is a polyline vertex that can be moved (using the left-mouse button) or deleted (using the right-mouse button)

Note: Once the digitizing environment is active, a feature-dialogue box opens with an <Untitled Path> reference name in the title box (fig. 16). Please type in the name of the feature that you will be digitizing. As long as this dialogue box remains open, you will be in the editing mode and can use the mouse as a digitizing tool to trace the feature line.

4) A <Right click> on a vertex will delete it as you want to refine the line.

Note. There are two modes of digitizing, by holding the left mouse-button down as you drag the mouse along, you can generate a smoot, continuous line that is densely populated with vertices. If you single click between mouse movements, then you can generate a polyline trace adding a single vertex at a time in controlled manner. The choice is yours, experiment using both approaches.

At any time, the dialog box for editing a polyline can be closed by clicking <OK>. To continue digitizing it, or to further edit it, simply <Right click> on the theme in the Legend pane, and continue editing it. Once the vertices are visible, you can select one with a <Right click> to move it (drag it when holding he mouse's left button, or delete it using the right button.)

The goal is to digitize a feature trace representing each of the terminal moraines, and a few of the sediment-thickness lines as part of a new KMZ file.

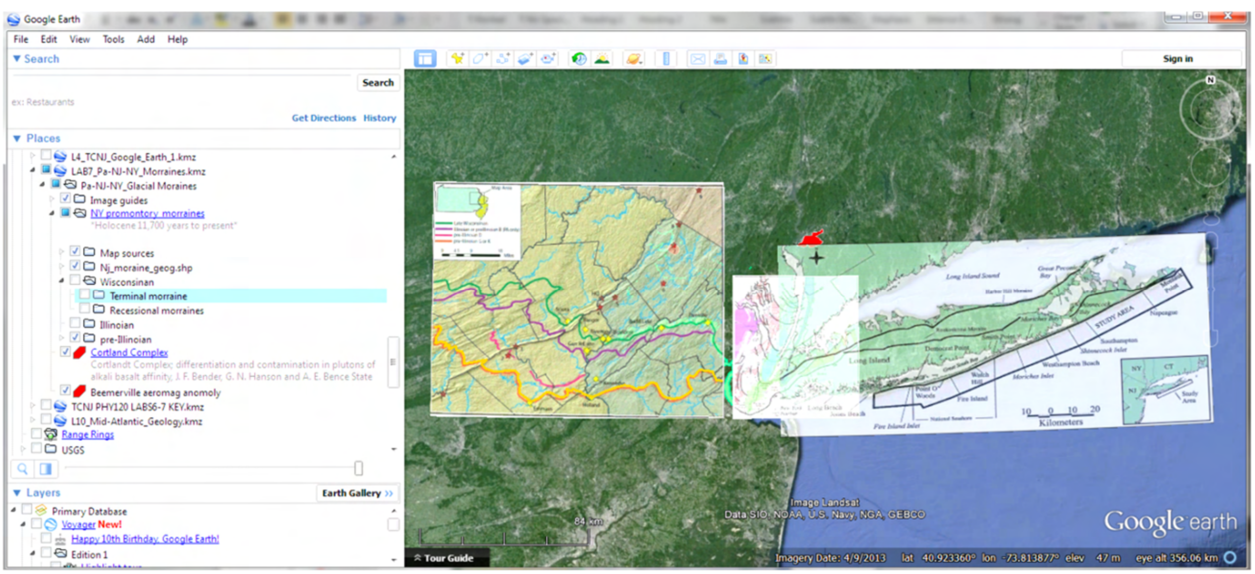

Figure 17. GE view of the correctly georegistered imagery before digitizing the glacial moraines .

Some very important tips:

1) Please <Save> your work periodically. GE crashes, and when it does, you will be sorry if you didn't save your work.

2) To save your work, <Left click> on the folder at its root (highest) level, then in the Menu Bar, <Left click> <File><Save><Save Place As> to save your work to a local hard drive, zip drive, or the cloud.

   Alternatively, after highlighting the top-level folder, use the mouse button to use this shortcut: <Right click> <Save Place As>

3) *How it appears when you saved it last is how it will look when you open it next.*

4) It is also important to repeatedly save your work environment if you prefer by using this sequence of commands:

   Menu Bar, <Left click> <File><Save><Save My Place>

   to save your current work environment.

References

Stone, B.D., Stanford, S. D., and Witte, R.W., 2002, Surficial geologic map of northern New Jersey. U.S. Geological Survey Miscellaneous Investigation Series Map, scale 1:100,000.

Stanford, S. D., Pristas, R. S., Witte, R. W., 2007, Surficial geology of New Jersey: N. J. Geological Survey Digital Geodata Series DGS 07-2, scale 1:100,000.

Witte, R. W., and Germanoski, D., 2012, Glaciations of western New Jersey and eastern Pennsylvania: A view from across the Delaware River, *in*, Harper, J. A., ed., Guidebook for the 77th Annual Field Conference of Pennsylvania Geologists, p. 92-117.

Chapter 2. Review of New York City bedrock with a focus on brittle structures

Charles Merguerian, Principal, Duke Geological Laboratory, Stone Ridge, NY, 12484
Professor Emeritus, Hofstra University, Hempstead, NY 11549
Visiting Research Fellow, Yale University, New Haven, CT 06520

Abstract

Over four decades of mapping of natural exposures and subsurface engineering projects has allowed for a thorough investigation of NYC bedrock features. This paper focuses on young brittle geological features that are superimposed on granulite to amphibolite grade polydeformed bedrock consisting of Proterozoic basement and Paleozoic cover rocks. Two groups of brittle faults prevail in NYC. The older of these are post Permian (295 Ma) and trend NNE with steep dips. These are reactivated by NW-trending discontinuities with steep to moderate dip that locally show post-glacial offset.

Introduction

Geological mapping and geotechnical data from many engineering construction projects in NYC have provided an opportunity for evaluation of brittle discontinuities in NYC bedrock. This paper presents mapping and geotechnical data selected from the Queens Tunnel section of NYC Water Tunnel #3, the East Side Access project across Manhattan into Grand Central Station, the Croton Water Treatment Plant and various NYC parks together with framework data from over 1,000 other locations in and around NYC.

Two pervasive and geomorphologically evident post-Paleozoic fracture sets cut the region. The older of these (Group D - NNE trend) with steep dips exhibits dip-slip offset and local reactivation since these are cut by a younger set (Group E - NNW to NW trend) with moderate to steep dips and strike-slip and oblique-slip mechanisms. Brittle discontinuities affect both the Paleozoic cover and Proterozoic basement sequences but not all groups are found in the cover rocks. The age of Group D fractures is unclear but are possibly associated with Mesozoic rifting as they truncate Permian (295 Ma) rhyodacite dikes in the subsurface of Woodside, Queens (Merguerian 2001, 2002a). Evidence from the Bronx River in the NY Botanical Garden suggests post-glacial offset by the NW-trending Group E Mosholu fault (Merguerian and Sanders 1996a, 1997). The Group E fractures may be the result of contemporary stress or transcurrent fracture propagation away from the Atlantic Ocean ridge into the continental crust. This notion may explain the neotectonic reactivation of brittle crustal features although other mechanisms or combinations of mechanisms are clearly possible.

Physiography of New York City and vicinity

NYC is situated at the extreme southern end of the Manhattan Prong (fig. 1), a northeast-trending, deeply eroded sequence of metamorphosed Proterozoic Y basement to Lower Paleozoic cover rocks that widen northeastward into the crystalline terrains of New England. Southward from NYC, the rocks of the Manhattan Prong plunge nonconformably

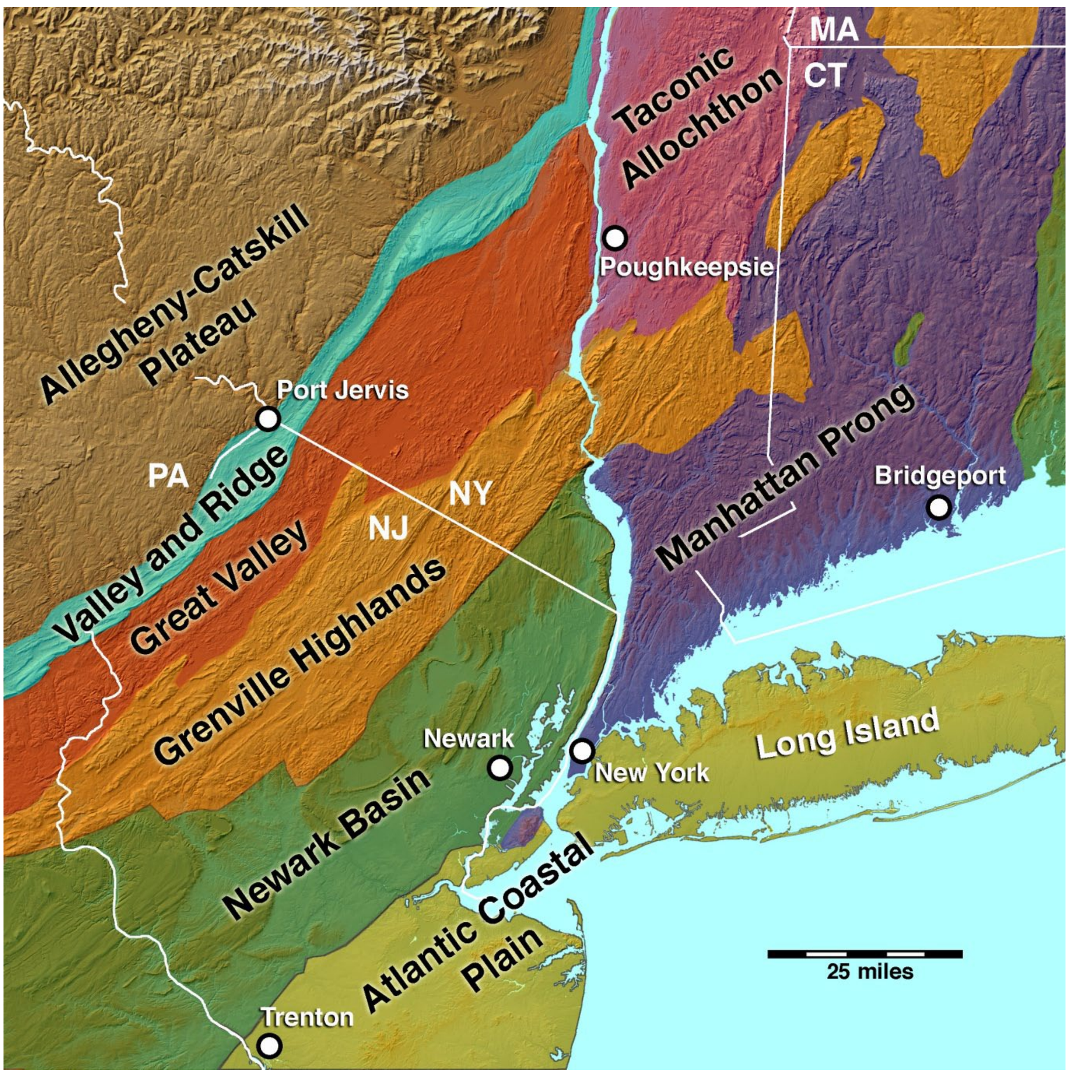

Figure 1. Physiographic diagram showing the major geological provinces in southern New York, northern New Jersey, and adjoining states (From Bennington and Merguerian, 2007).

beneath predominately buried Mesozoic rocks, younger Cretaceous strata, and the overlying Pleistocene (glacial) sediment found capping much of the region, including all of Long Island and much of Staten Island.

The history of NYC bedrock investigations appears elsewhere (Merguerian and Sanders 1991b). My involvement in NYC bedrock studies began in the late 1960s as a City College student in NYC and I have continued my investigations both academically and as a geotechnical consultant, logging over four decades of geological study. The major findings of this period have been presented elsewhere (Merguerian 1983a, 1984, 1994, 1996c, 2002b; Merguerian and Baskerville 1987; Merguerian and Merguerian 2004, 2012, 2014a; and Merguerian and Moss 2005, 2006a, 2007, 2015). Much of the data presented in this paper and posted in the associated online GANJ 2015 web repository is from proprietary reports associated with now long-settled industry claims.

New York City bedrock

Two basic subdivisions of NYC crystalline bedrock (fig. 2) include a substrate of:

1) *Paleozoic cover rocks* including schist, marble, and associated lithotypes that overly

2) *Proterozoic Y basement rocks* including granulite facies gneiss and crosscutting igneous rocks.

Both rock sequences were internally folded and sheared during Paleozoic orogenesis and cut by younger brittle fracturing (faults and joint discontinuities). The following are descriptions of the respective units.

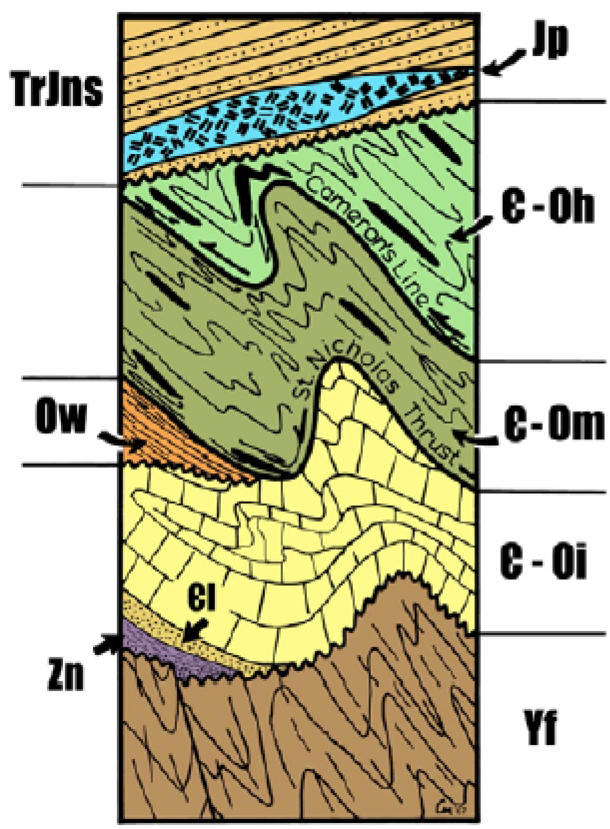

Figure 2. Bedrock stratigraphy of New York City as described in text. The polydeformed bedrock units are nonconformably overlain by west-dipping Triassic and younger strata (TrJns) and the Palisades intrusive (Jp).

Paleozoic cover rocks

***Hartland Formation* (Є-Oh)** - Gray-weathering, fine- to coarse-textured, well-layered muscovite-quartz-biotite-plagioclase±kyanite±garnet schist, gneiss, and migmatite with cm- and m-scale layers of gray quartzose granofels and greenish amphibolite±biotite±garnet. Known for relatively easy excavation because of pervasive jointing parallel to layering, the unit has been encountered in

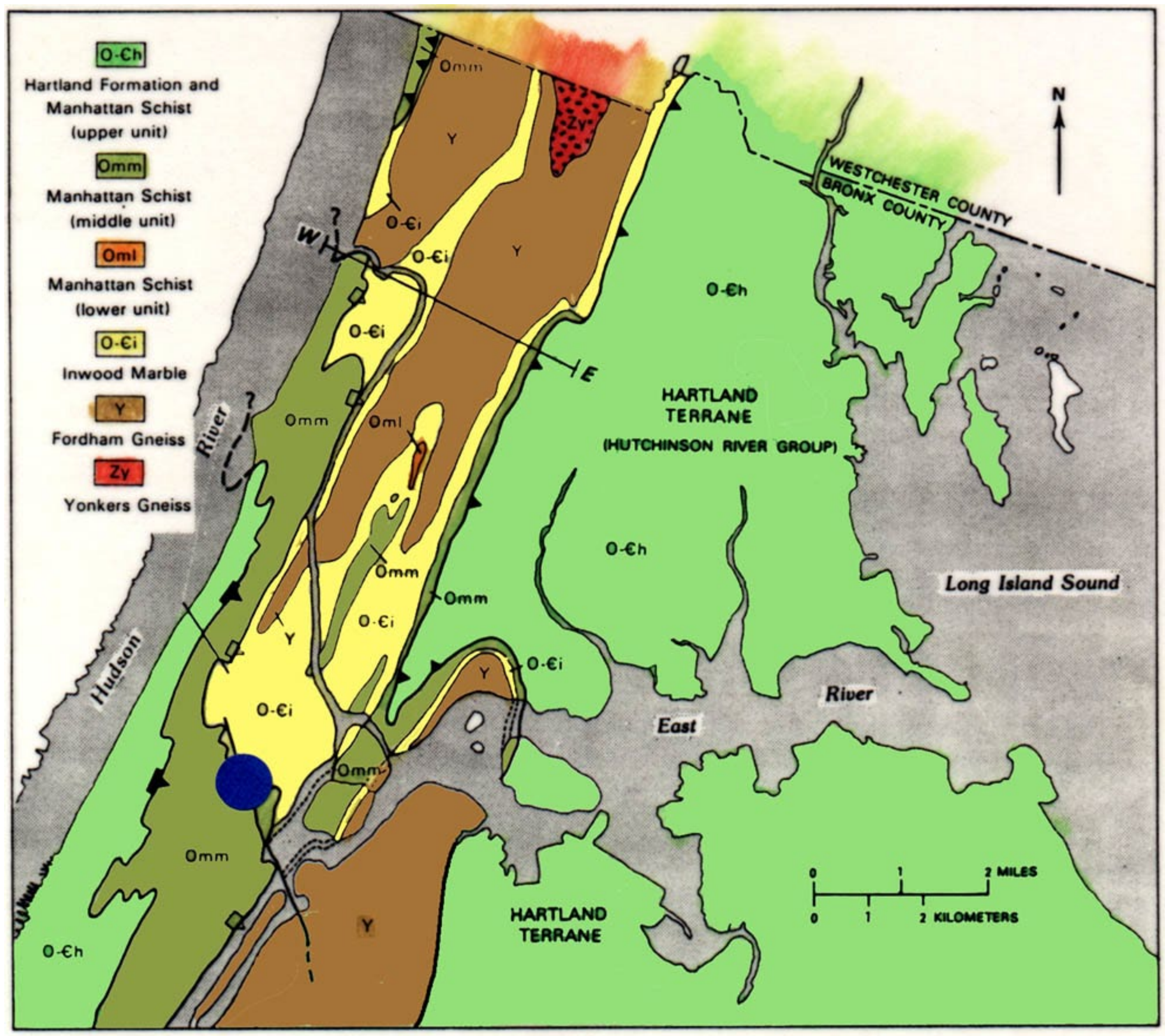

Figure 3. New York City generalized geological map and cross sections adapted from Merguerian and Baskerville (1987). Triangles show the dip of Cameron's Line (solid) and the St. Nicholas thrust (open) and the flagged triangles indicate overturned thrusts. Most brittle faults and intrusive rocks have been omitted. Blue dot shows earthquake epicenter of magnitude 2.4 (21 January 2001) that projects above the trace of the Manhattanville fault (Group E). Cross sections in the Bronx (left and top of map) and Manhattan (right) depict the general, ductile style of folding and faulting involving Cameron's Line and the St. Nicholas thrust. The S-N section is about located were the epicenter symbol near Central Park. Note that the unit Omm is equivalent to Ow in this report.

the East Side Access, Second Avenue Subway, Manhattan Water Tunnel, #7 Line IRT Extension and Con Edison Steam Tunnel projects. It is has been extended into NYC from western Connecticut and Massachusetts based on stratigraphic correlation (Merguerian 1983a) and it is considered a part of the Taconic allochthon (Merguerian and Sanders 1996b).

Manhattan Formation **(Ꞓ-Om) –** Massive, rusty- to sometimes maroon-weathering, medium- to coarse-textured, biotite-muscovite-plagioclase-quartz±garnet±kyanite±sillimanite-magnetite gneiss, migmatite, and schist. Characterized by the lack of internal layering except for kyanite± sillimanite+quartz+magnetite interlayers and lenses up to 10 cm thick, cm- to m-scale layers of blackish amphibolite, and scarce quartzose granofels. It forms the bulk of exposed Paleozoic metamorphic rocks of northern Manhattan including the northern Central Park exposures. These allochthonous rocks are grouped with the Hartland formation as part of a Taconic Sequence.

Walloomsac Formation **(Ow)** – A discontinuous unit composed of fissile brown- to rusty-weathering, fine- to medium-textured, biotite-muscovite-quartz-plagioclase±kyanite± sillimanite±garnet-pyrite-graphite schist and migmatite containing interlayers centimeters to meters thick of plagioclase-quartz-muscovite granofels, layers of diopside±tremolite± phlogopite calcite- and dolomitic marble, and greenish calc-silicate rock. *Amphibolite is absent.* Strongly pleochroic reddish biotite, pinkish garnet (porphyroblasts up to 1 cm), graphite and pyrite are diagnostic mineralogical features of the former pelitic portions of the formation. The lack of amphibolite and the presence of graphitic schist and quartz-feldspar granofels invite the interpretation that this unit is metamorphosed middle Ordovician carbonaceous shale and greywacke of the autochthonous Annsville and Normanskill formations of SE New York and the Appalachian Martinsburg Formation.

Inwood Marble **(Ꞓ-Oi) -** White to bluish-gray fine- to coarse-textured dolomitic and lesser calcitic marble locally with siliceous interlayers containing diopside, tremolite, phlogopite, muscovite (white mica), and quartz together with accessory graphite, pyrite, tourmaline (dravite-uvite), chlorite and zoisite. Layers of fine-textured gray quartzite with a cherty appearance are also locally present. The Inwood is correlative with the Cambro-Ordovician carbonate platform sequence of Appalachians.

Proterozoic basement rocks

Fordham - Queens Tunnel Gneiss **(Yf)** - The oldest rocks in NYC are a complex assemblage of Proterozoic Y ortho- and paragneiss, metasedimentary, metavolcanic and granitoid rocks. Based on detailed studies in the Queens and Brooklyn portions of NYC Water Tunnel #3 (Merguerian, 1999, 2000; Brock, Brock, and Merguerian 2001), the Fordham correlative is known as the Queens Tunnel Complex (QTC) which consists of predominately massive mesocratic, melanocratic and leucocratic orthogneiss with subordinate schist, granofels, and calc-silicate rocks. Grenvillian high pressure granulite facies metamorphism produced a tough, anhydrous interlocking texture consisting of clino- and orthopyroxene, plagioclase, and garnet that has resisted amphibolite grade Paleozoic retrograde regional metamorphism. Geological details of the QTC are presented in a later section.

Paleozoic orogenesis

The venerable Manhattan Schist of NYC, exposed in Manhattan and the Bronx, consists of three separable map units: the Hartland, Manhattan, and Walloomsac formations (figs. 2 and 3). These subdivisions agree, in part, with designations proposed by Hall (1968, 1976, and 1980) but recognize a structurally higher unit that is a direct correlative of the Hartland Formation of western Connecticut (Merguerian 1981, 1983b, 1985c, and 1987). The three schistose tectonostratigraphic units are imbricated along regional ductile faults known as the St. Nicholas thrust and Cameron's Line, as indicated in a simplified cross section across the northern tip of Manhattan into the Bronx (Merguerian 1994, 1996a). The NW-SE section shows the general folded structure of NYC and how the St. Nicholas thrust and Cameron's Line overthrusts place the Manhattan and Hartland formations above the autochthonous Walloomsac and Inwood and the Fordham basement sequence. Major F_3 folds produce digitations of the regional S_2 foliation, which dips gently southward (downward) and out of the page toward the viewer. The NE-SW section illustrates the southward topping of tectonostratigraphic units exposed in central Manhattan and the effects of the yet younger NW-trending asymmetric F_4 folds.

Now metamorphosed to amphibolite facies grade, the exposed Paleozoic metamorphic cover rocks of NYC were originally deposited as sediment and intercalated volcanic and volcaniclastic materials, though in vastly different environments (fig. 4). The Hartland was originally deposited in a deep ocean basin fringed by offshore volcanic islands. The Manhattan originated along the edge of the Laurentian continental margin as thick clay-rich sediment with occasional sand interlayers and mafic dikes or flows. The Walloomsac is mineralogically unique since it originated under restricted oceanic conditions (reducing environment) which consisted of thick accumulations of carbonaceous and sulphidic clay-rich sediment with occasional sandy and calcareous interlayers.

Underthrusting of the accretionary prism associated with the Taconian arc-continent collision produced the deformation, internal shearing, imbrication and amphibolite facies regional metamorphism of the Paleozoic cover rocks with basement involvement. The underlying Fordham-Queens Tunnel Complex basement rocks experienced localized retrograde metamorphism of Grenville granulite facies fabrics during Taconian and younger events.

In NYC and in most crystalline terranes inherent ductile geological structure holds a first-order control on development and geometry of subsequent brittle discontinuities. As such, a brief synopsis of NYC structural geology is here appropriate.

Paleozoic deformational episodes

All Paleozoic cover sequences in NYC have shared a complex structural history which involved three superposed phases of deep-seated Taconian deformation (D_1, D_2, D_3) followed by three or more episodes of open- to crenulate folds (D_4-D_6) in mid- to late Paleozoic or younger time. Synmetamorphic juxtaposition of the bedrock units occurred very early in their structural history (D_2) based upon field relationships. The Fordham-Queens Tunnel basement sequences harbor a more complex history having endured deformation and metamorphism during the Grenville orogeny (~1.1 Ga) in addition to the three Paleozoic orogenies (Taconian, Acadian, and Alleghenian - see chapter 4) whose effects are concentrated in the overlying Inwood, Walloomsac, Manhattan, and Hartland rocks.

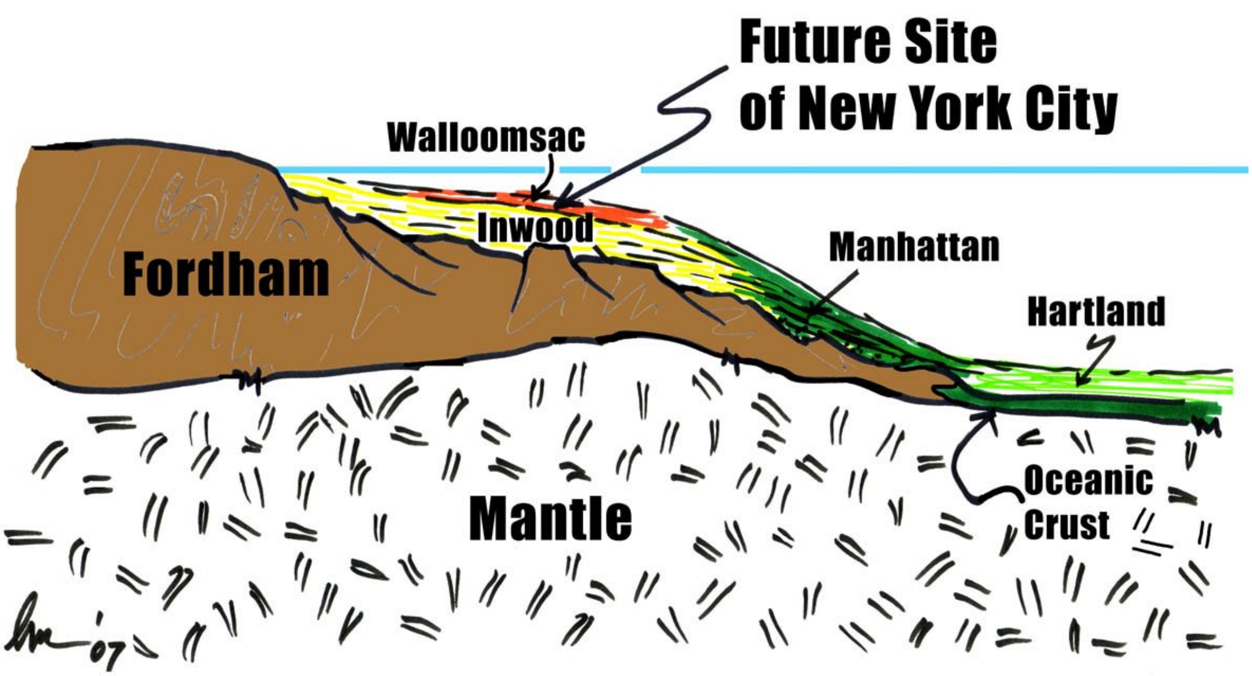

Figure 4. Stylized profile of eastern North America after Late Proterozoic rifting from Rodinia and during deposition of the Paleozoic shelf sequence of the Hartland, Manhattan, and Walloomsac formations. Note the correlation of units and their relationships to the underlying units of the partly coeval Inwood and older Fordham.

The obvious map scale F_3 folds in NYC are those with steep N- to NE-trending axial surfaces (S_3) and variable but typically shallow plunges toward the S and SW (figs. 2 and 3.) The folds are typically overturned to the NW with a steep SE-dipping foliation (fig. 5).

Shearing in fold limbs and along S_3 axial surfaces typically creates a transposition foliation of S_1, S_2, and S_3 that is commonly invaded by granitoids to produce migmatite during both the D_2 and subsequent D_3 events. These third-generation structures deform two earlier penetrative structural fabrics (S_1 and S_2). The older penetrative fabrics trend roughly N50°W and dip gently toward the SW except along the limbs of F_3 folds. I suspect that all of these structures (D_1, D_2, and D_3) are all products of protracted Taconian orogenesis (Merguerian 1995).

During D_2, the rocks acquired a penetrative S_2 foliation consisting of oriented mica and intergrown sillimanite and kyanite with flattened quartz together with staurolite and garnet

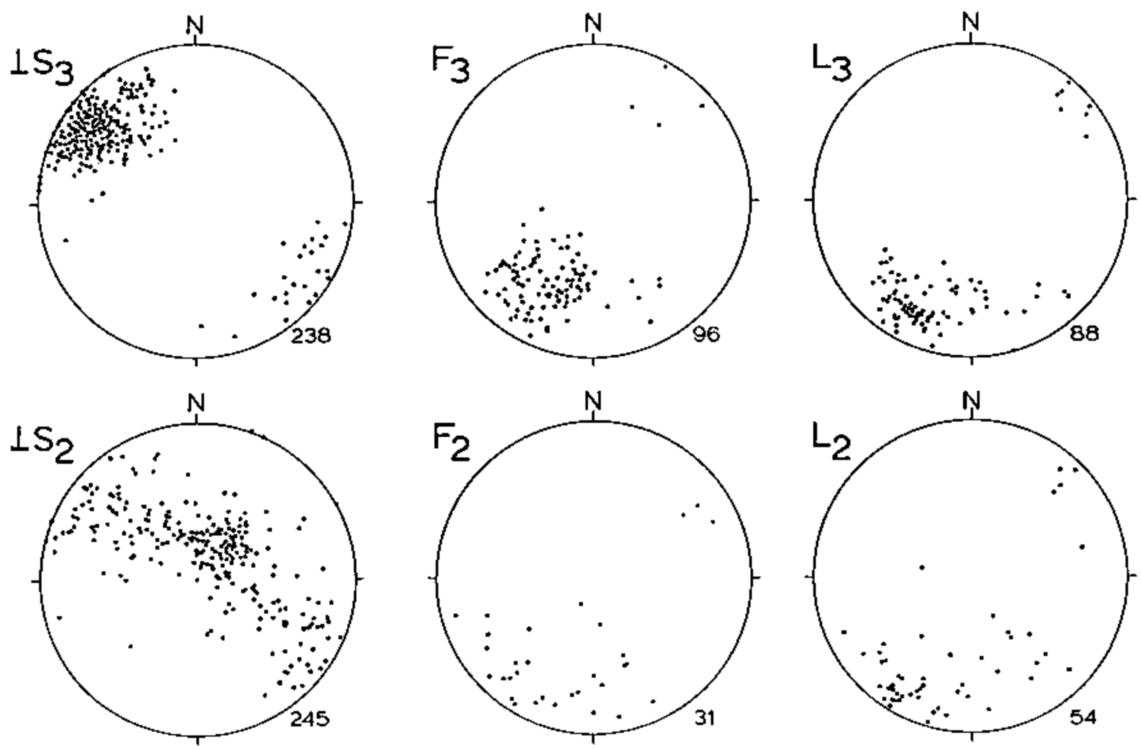

Figure 5. Equal area stereograms showing the distribution of poles to S_2 and S_3, the orientation of F_2 and F_3 fold hinge lines, and the orientation of L_2 and L_3 lineation. The number of plotted points indicated to the bottom right of each stereogram. (Adapted from Merguerian and Sanders 1991, figure 26, p. 113.)

porphyroblasts. Distinctive layers and lenses of kyanite + quartz + magnetite developed in the Manhattan formation and very locally in the Hartland during D_2. Near ductile fault contacts the S_2 fabric is highly laminated with frayed and rotated mica and feldspar porphyroclasts, ribboned and locally polygonized quartz, lit-par-lit granitization, and quartz veins all developed parallel to the axial surfaces of F_2 folds. The D_3 folding event, a period of L-tectonism, smeared the previously flattened kyanite + quartz layers and lenses into elongate shapes parallel to F_3 axes in schistose rocks. Porphyroblasts of tremolite pseudomorphic after diopside also show alignment parallel to F_3 hinge lines in the Inwood Marble of northern Manhattan.

Although the regional S_2 metamorphic grain of the NYC bedrock trends N50°W and dips gently SW the appearances of map contacts are regulated by F_3 isoclinal- to tight folds overturned toward the west and plunging SSE to SW at 25° (fig. 5). S_3 is oriented ~N30°E and dips 75°SE and varies from a spaced schistosity to a transposition foliation often with shearing near F_3 limbs. The F_3 folds and related L_3 lineation mark a period of L-tectonite ductile flow that smeared the previously flattened quartz and kyanite lenses and layers into elongate shapes. Metamorphism was of identical grade with D_2 which resulted in kyanite overgrowths and annealing of former mylonitic textures (Merguerian, 1988).

Originating within the convergent walls of a major subduction zone formerly situated off shore from proto-North America, the D_1 to D_3 folds and fabrics formed during the Taconic orogeny are overprinted by two- and possibly three fold phases that, based on their style and general lack of attendant foliation, undoubtedly took place at much-higher crustal levels than did the three Taconian fabrics. Presumably, the younger fold phases record the effects of the Acadian- and terminal-stage Appalachian orogenies. Stay tuned for news on brittle structures!

Queens Tunnel Complex, city water tunnel #3, stage 2

Between 1996 and 1999, a high-performance tunnel-boring machine (TBM) excavated a 7 m wide, 7.7 km long, and 214 m deep tunnel through the subsurface of southwestern Queens (fig. 6). Taking almost twice as long as expected, low TBM penetration rates resulted from an unusual high-grade metamorphic rock mass and disturbed ground conditions resulting from superposed brittle faults (Merguerian, 2000). Field mapping at 1"=10', petrographic, geochemical, and geochronologic studies conclusively proved that the TBM excavated predominately mesocratic granulite-facies orthogneiss containing broad zones of garnet enrichment. The coarse granoblastic textures of interlocking plagioclase, clino- and orthpyroxenes, and garnet produced an impediment to mining. Proterozoic Fordham Gneiss is now known to underlie western Queens and Brooklyn, a covered region where layered Paleozoic metamorphic rocks of the Hartland formation were formerly anticipated.

In this report, use of the place name *Queens Tunnel Complex* (QTC) for the gneissic rocks exposed in the Queens Tunnel indicate a lithostratigraphic correlation with the billion year old Fordham Gneiss. Results from geochronologic tests have indeed confirmed that the QTC contains ~1 billion year old rocks (Brock, Brock, and Merguerian 2001). A complex ductile and brittle history has emerged from study of the QTC. This paper focuses on the brittle fault history, a protracted episode of fracturing that is superimposed on older ductile structures, summarized in table 1.

Please note that the table reflects current understanding of the geological sequence of events in the QTC (Fordham Gneiss) during analyzed construction. The different deformation metamorphic, intrusive, and folding (F) sequences noted are based on relative timing of crosscutting structures. The events are numbered from oldest (1) to youngest (9) in time. Ongoing petrographic and allied microprobe work may refine this interpretation.

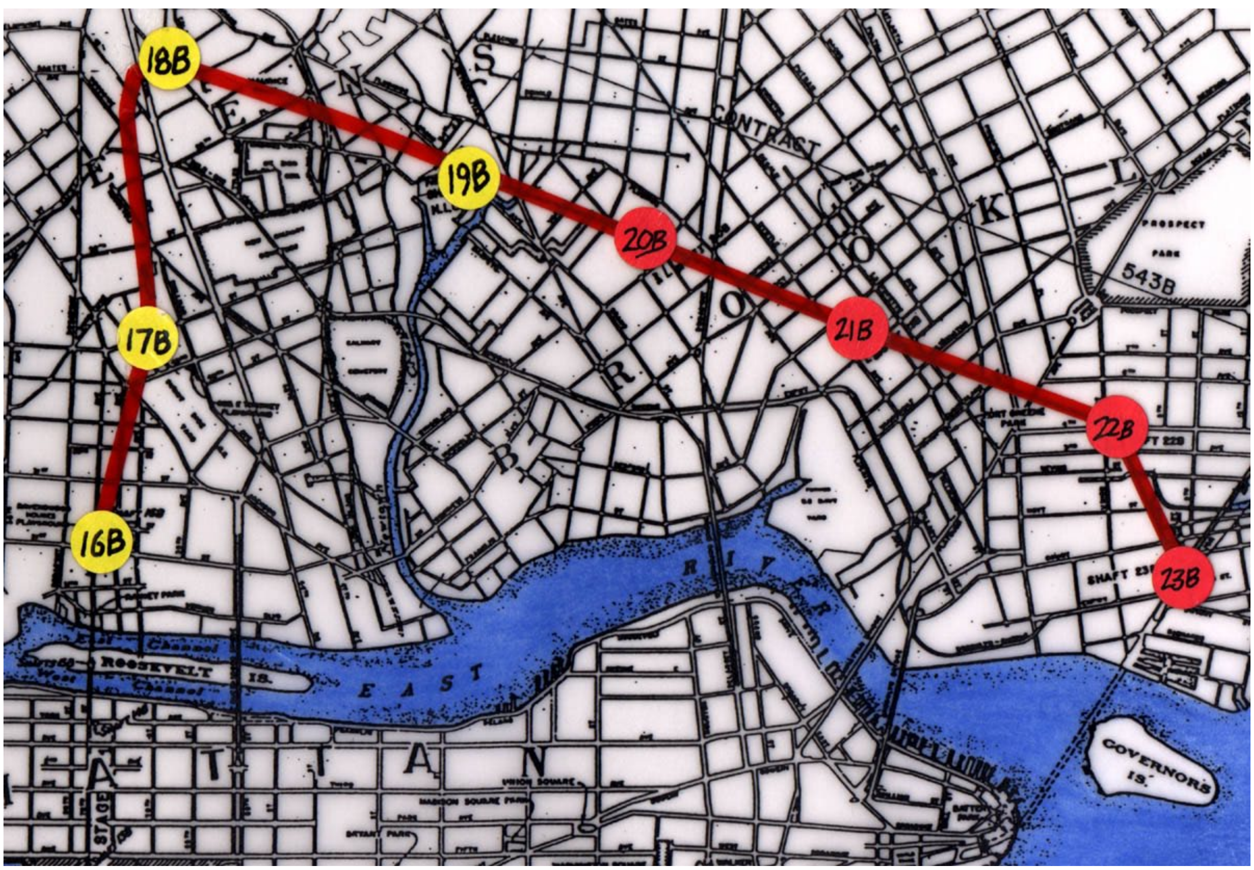

Figure 6. Index map showing the plan view of a part of New York City Water Tunnel #3, Stage 2. The positions of Brooklyn Tunnel (Red colored shafts 23B to 19B) and the Queens Tunnel (Yellow colored shafts 19B through 16B) are shown. North is toward the lower left corner.

Table 1. Geological events recorded in the Queens tunnel

$\mathbf{D_9}$ – Steep NNW-trending strike-slip faults of Group E and sub-parallel joints which continue to affect the region to the present day.

$\mathbf{D_8}$ – NNE-trending, steep oblique slip faults of Group D with thick clay-rich gouge- and crush zones.

$\mathbf{I_6}$ and $\mathbf{M_5}$ – Permian (295 Ma) hypabyssal injections of Woodside rhyodacite dike swarm and retrograde contact metamorphism at former depths of ~ 0.5 to 1 mile.

$\mathbf{D_7}$ – Lengthy sub-horizontal ramp-like faults and fractures of Group C, commonly exhibiting little offset.

$\mathbf{D_6}$ - Steep brittle faults of Group B oriented ~N60°E cut region.

$\mathbf{D_5}$ – Steep NW-trending normal- and reverse faults and joints of Group A. Event is considered to merge with I_5 and D_4.

$\mathbf{I_5}$ - Intrusion of megacrystic K-feldspar pegmatite dikes.

$\mathbf{D_4}$**,** $\mathbf{I_4}$**,** and $\mathbf{M_4}$ – F_4 recumbent to asymmetric folding and ramp-like low-angle ductile faulting with foliated granitoids and pegmatite intruded into brecciated faults (Group A) oriented ~N50°W and low SW dips (<30°). Zones of granitization, biotitization, and retrograde metamorphism found adjacent to fault zones and intrusives. Based on metamorphic grade, these events followed a period of regional uplift and erosion.

$\mathbf{I_3}$ – Intrusion of non-garnetiferous mafic dikes.

$\mathbf{D_3}$ and $\mathbf{M_3}$ – Gentle SW-plunging tight to isoclinal ~N35□Etrending F_3 folds of S_1+S_2 metamorphic layering with localized development of a penetrative foliation and localized D_3 shear zones under conditions of M_3 amphibolite facies metamorphism. Responsible for initial deformation of I_2 Ravenswood-type rocks and slight- to moderate retrograde metamorphism of older granulites.

$\mathbf{I_2}$ – Intrusion of Ravenswood-type (Taconian?) granitoid, dioritic, and gabbroic magmas which later (D_3) form weakly foliated orthogneiss.

$\mathbf{D_2}$ and $\mathbf{M_2}$ – Isoclinal F_2 folding and shearing of both Fordham S_1 and I_1 intrusive suite producing foliated orthogneiss bodies from I_1 intrusives. Development of medium- to coarse-grained S_2 gneissic layering under granulite facies metamorphic conditions. Garnetiferous mafic dikes produced near interlayered amphibolites. Probably progressive with D_1. Unknown age, probably Proterozoic Y.

$\mathbf{D_1}$, $\mathbf{I_1}$,and $\mathbf{M_1}$ – Isoclinal F_1 folding and deep-seated (~20-25 miles) metamorphism under granulite facies metamorphic conditions producing a penetrative S_1 foliation in metasedimentary and probable metavolcanic units of the Fordham. These deformed units were invaded by a vast suite of syntectonic calc-alkaline intrusives as plutons, sills, and dikes. The intrusives of Proterozoic Y age, cross cut S_1 and enclose screens, xenoliths, and cognate xenoliths of older gneiss.

Note: *The list of relative events summarizes my current understanding of the evolution of the Queens Tunnel Complex (= Fordham Gneiss), based on detailed mapping of the as-built tunnel. The relative time of Deformational (D_n), Igneous (I_n), and Metamorphic (M_n) events is based solely on crosscutting field relationships. The events are numbered from oldest (n = 1) to youngest by subscript from the base upward. Ongoing petrographic and geochemical investigations will refine this table.*

Brittle faults of the Queens tunnel and the Woodside rhyodacite dike swarm

Found exclusively beneath the area of Woodside, Queens, a swarm of five thin sub-parallel rhyodacite dikes, all displaying igneous textures, were penetrated during construction of the Queens Tunnel. The dikes are Permian in age (~295 Ma) based on unpublished Ar_{39}/Ar_{40} data of Dr. Sid Hemming and crosscut folded Proterozoic Y granulite facies rocks of the QTC with which they are genetically and temporally unrelated. The rhyodacites are reddish, glassy to aphanitic igneous rocks with no metamorphic fabric and low average density (2.58 g/cm^3). They occur as tabular, discordant injections roughly oriented N53°W and average roughly 3 m in thickness.

The larger dikes vary from 5.3 m down to 1.0 m and taper off to thinner dikelets. The injection of a suite of Permian rhyodacite dikes that are chemically, texturally, and temporally unrelated to their bedrock hosts, mark an anomalous geological event that adds a new chapter to the Paleozoic evolution of the NYC area and provides an important time-stratigraphic marker for geological interpretations.

Over 300 faults have been mapped and studied in the Queens Tunnel over the five-mile extent and the data from these features (Invert Station, Tunnel Bearing, Discontinuity Type, Orientation, Width, Filling, Roughness, Seepage, and Miscellaneous Observations) are presented in spreadsheet form on the GANJ 2015 website[1]. Five generations of brittle faults are superimposed on polydeformed bedrock units of the Queens Tunnel Complex often causing brittle reactivation of ductile faults and pre-existing brittle faults. Brittle faults are typically zones of fault breccia and clay-rich gouge with zeolites ± calcite ± pyrite ± epidote mineralization, and quartz veining. They have created extended areas of high strain prone to stress relief in the form invert heave, rock-wall popping, and jointing. In areas of fault convergence, the brittle faults and sub-parallel regional joints are a persistent cause of blocky ground conditions and related detrimental effects on TBM tunneling (Merguerian and Ozdemir, 2003).

A contoured stereonet plot of brittle faults shows that they cluster into three focused groups (A, D, and E), with A and D more abundant and overlapping with less abundant group B and C structures (fig. 7). Group A include moderately SW-dipping faults (A) and Group D include steeply dipping brittle structures and rhyodacite dikes striking parallel to the regional Appalachian grain. Sub horizontal, reactivated low-angle faults and fractures of Group C are relatively less abundant, relatively young, steeply-dipping, NNE-trending faults that cut Group D dikes. Group E are the youngest structures, are about half as abundant as those in Groups A and D, and strike NW, with oblique and strike slips. Group E structures were seen interacting with both older and younger structures as we will see below.

[1] www.ganj.org/2015/Data/2015_NJGWS_GCH_GANJ32_Merguerian-QWT-stations.xlsx

A preliminary Google Earth (GE) visualization of these various structures was done in conjunction with Gregory Herman of the NJ Geological & Water Survey (NJGWS) for this meeting. He supplemented an existing MS Excel worksheet having structural-feature locations, classifications and orientations and used to produce the GE KMZ[2] theme for this meeting. The various groups of ductile and brittle structures were organized for input into a NJGWS custom-software tool used for automatically positioning and annotating planar objects as components in a KMZ file (see chapters 1 and 5.) For this effort, each representative class of structure was evaluated and represented using scaled 3D planar objects. For example, pegmatite dikes (I_5) are shown in figure 8A, and brittle faults of Group D and E are combined together as brittle faults shown as red ellipsoidal planes in figure 8B.

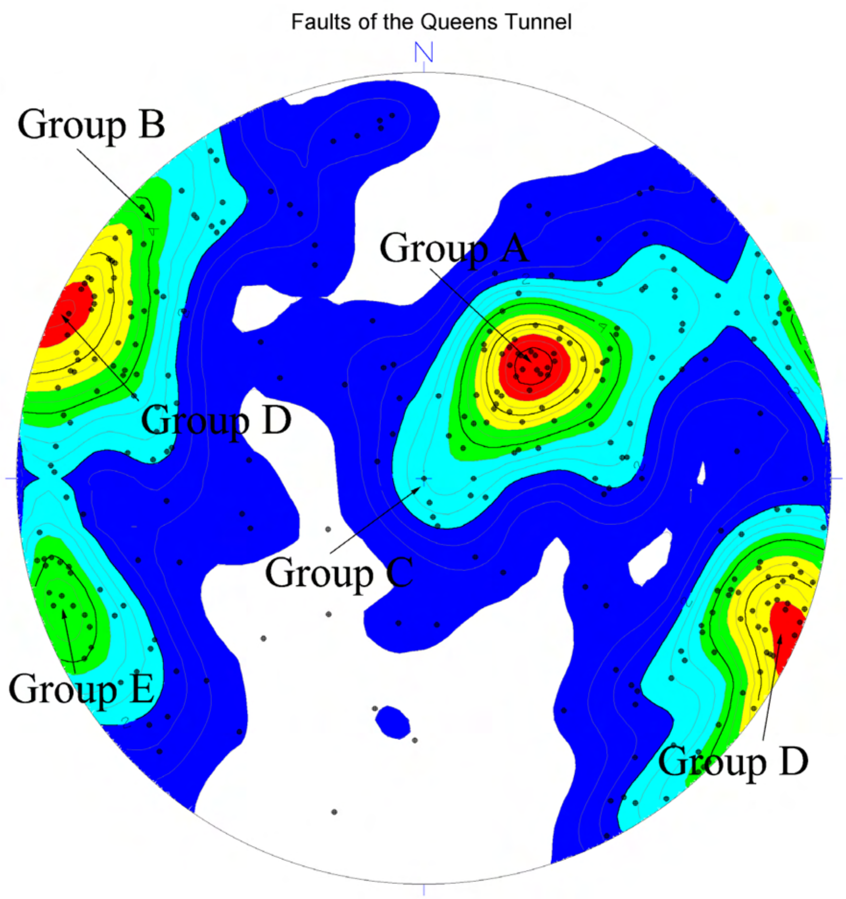

Figure 7. Lower-hemisphere, equal-area stereogram showing the poles to 306 faults mapped in the as-built Queens Tunnel. **Group A** faults strike NW and dip gently SW, **Group B** faults are moderate to steep and strike ENE, **Group C** are sub-horizontal fractures and faults, **Group D** constitutes the NNE-trending fault system of the Queens Tunnel, and **Group E** are the youngest NNW-trending strike-slip faults.

Note in figure 8 how the NNE (Group D) and NW-trending (Group E) faults predominate along both legs of the tunnel. This nicely illustrates in 3D the complimentary orientations of these nearly orthogonal, regional brittle structures. The visualization methods used in GE to generate such features will be covered in this year's teacher's workshop (Chapter 1).

[2] www.ganj.org/2015/Data/2015%20GANJ%2032%20CM%20GCH%20NYC%20Queens%20Water%20Tunnel.kmz

The Group A faults trend ~N46°W with predominately gentle dips and exhibit both normal and reverse offset senses (fig. 9). They are commonly outlined by pegmatite dikes and reactivate NW-trending (D_4) ductile faults (table 1). The brittle Group A faults also occur throughout the entire tunnel in the absence of the ductile faults. The faults are laterally continuous undulating features that persist over 100 m in some tunnel reaches (fig. 10). They vary from tight splays to open features outlined by gouge and crush breccia up to 0.5 m thick. In reactivated zones anastomosing seams of breccia fracture associated granitic intrusives producing local contact dislocations. Group A faults abruptly terminate by ramping steeply into the crown or invert of the tunnel bore. As such, over the course of the tunnel they exhibit variable dip but average ~35°. They dip predominately toward the SW, but a few faults form a conjugate set dipping NE. They are cut by all other faults in the Queens Tunnel (Group B through E). As a result of the persistence of these faults and the development of non-cohesive broken rock as a fault filling, this amalgamated family of ductile and brittle faults exhibit moderate to heavy water inflow and tunnel perimeter instability.

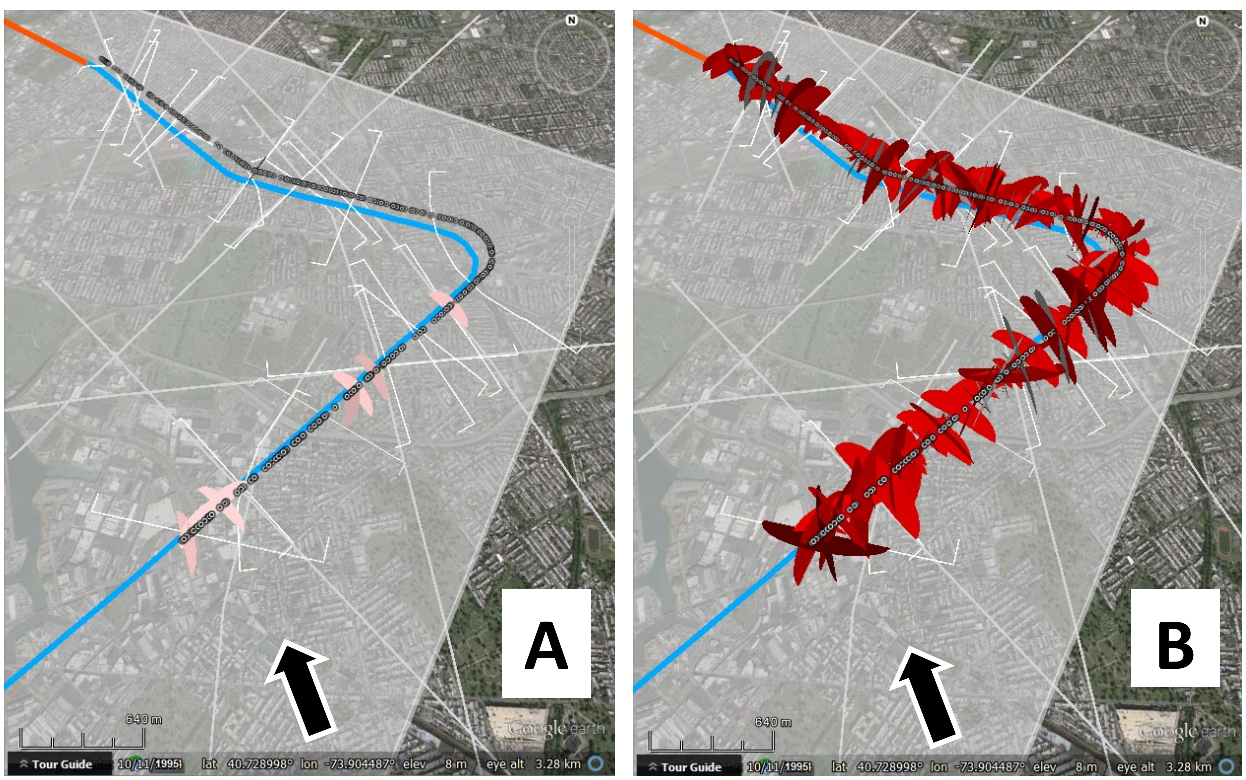

Figure 8. GE views of structures mapped in part of the Queens Tunnel. Data from Merguerian (2000). **A**. Pink ellipses show locations of pegmatite veins. **B.** Red ellipses show brittle fault planes. GE KMZ file available through the GANJ web site, and visualized by G. C. Herman.

Group B, NE-striking faults are minor in total number but can show significant offset. They trend ~N60°E and exhibit moderate to steep dips toward the SE, commonly reactivating NE-trending D_3 ductile fabrics (table 1) and cutting Group A faults. They vary from tight features to open features up to 15 cm in thickness and typically consist of broken rock with a fissile to soft consistency. They cut Group A faults and cut through D_4 zones of biotitization, K-feldspar metasomatism, and granitization. Providing an important relative time control for the fault sequence, one of the Group B faults is truncated by a late Paleozoic rhyodacite dike (fig. 12). Group C, minor brittle faults and fractures can extend for great distances in the Queens Tunnel. They typically show little or no offset and tend to cut or reactivate sub horizontal to gently dipping portions of Group A faults. A number of coincident poles at the

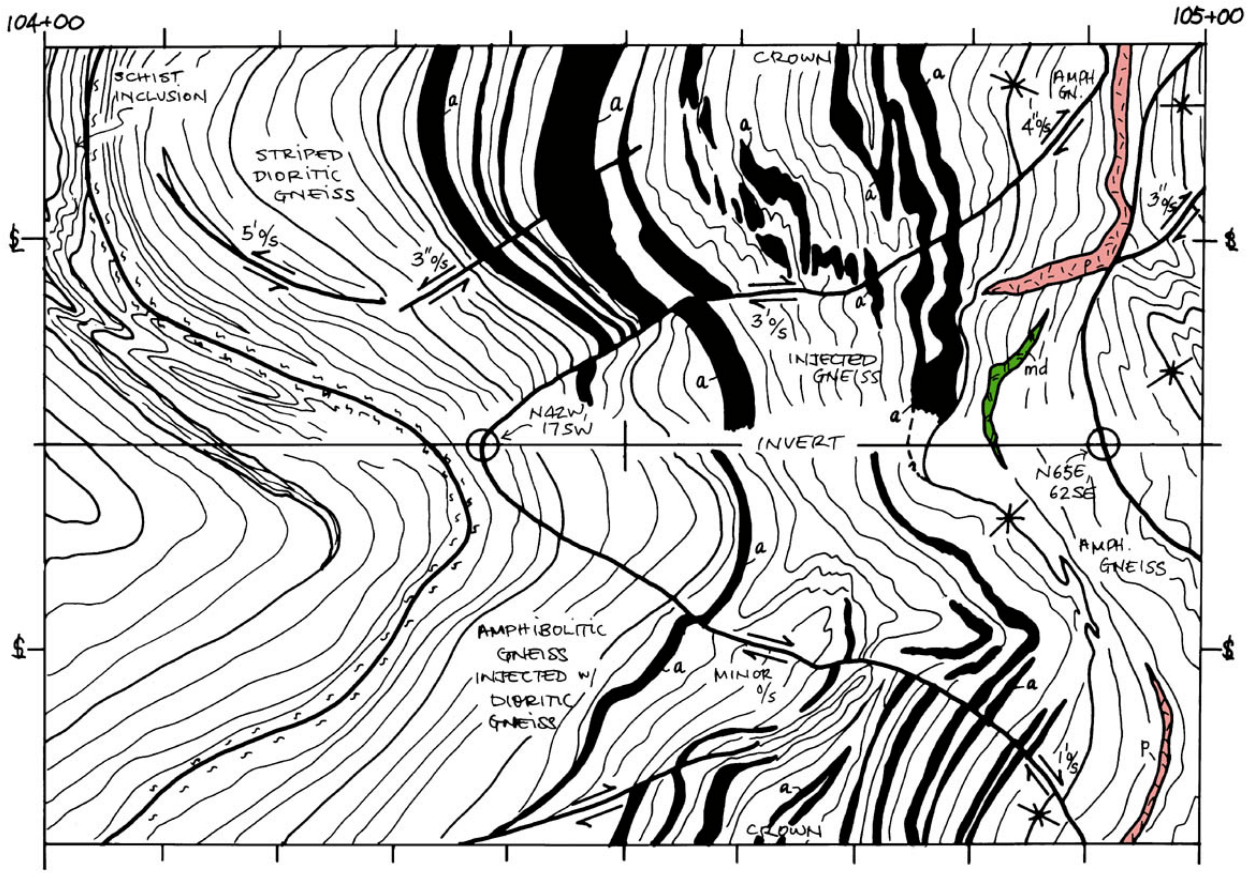

Figure 9. Geologic map of the Queens Tunnel showing Group A fault oriented N42°W, 17° SW that cuts the invert at Station 104+38 (tunnel bearing is N22°E). The fault is only 0.75 cm thick and exhibits 1.0 m maximum offset. **In this and all subsequent map figures the tunnel invert is shown along the center of the map and the tunnel walls curl upward into a cylinder to join at the crown.** Stationing increases from Shaft 19B (to left) to Shaft 16B. The position of the tunnel springline is shown at the map edge. This map covers 100 linear feet of the Queens Tunnel. (Original map scale 1"=10'; tunnel diameter 23' 2".)

center and those clustered near the center of the stereonet (fig. 7) mark the Group C features found throughout the tunnel.

Group D, the 2nd youngest brittle set of NNE-striking, brittle structures, parallel the Appalachian grain and S_3 axial surfaces in NYC and constitutes about a third of all mapped brittle faults (~300 mapped in the 5-mile tunnel segment). They form a system of geologically young dip-slip faults and related joints with an average N21°E strike and have steep dips (figs. 7 and 8).

Figure 10. View of migmatitic amphibolite, dioritic gneiss, and minor biotite schist highly fractured because of composite movement along a SW-dipping Group A fault. The fault is a continuous gently dipping feature for 107 m that originates at Station 195+25 and continues on both tunnel walls to Station 198+50. Here it steepens and disappears into the crown of the tunnel in a zone of ramping imbricate fault splays. Fault gouge and -breccia vary in thickness from 0.4 m thick in areas of fault splay intersection near the central reach of the zone to a hairline fracture at the end. (Digital image by C. Merguerian, 18 November 1999.)

Both normal and reverse slips were recorded. Dip-slip slickensides show reactivation or evolution into oblique-slip mechanisms, presumably reflecting overprinting by Group E structures. Group D faults have thick seams of clay, fault breccia and clayey gouge that vary from 1 cm to 5 m. Minerals found healing the NNE- trending faults show a clear paragenesis of apophyllite and/or heulandite followed by two generations of stilbite (yellow to orange followed by translucent). The stilbite is overgrown with spheres and inter-penetrant cubes of pyrite, calcite, and locally, clear cubic crystals of chabazite (figs. 11A and 11B; table 2).

Figure 11. Photographs of some secondary minerals that infill some fracture interstices in the Queens water tunnel.

Top photo shows orange stilbite with pyrite and calcite overgrowths in Group D faults that form broad zones (up to ~76'- wide) in fractured gneiss. Faults in this zone are oriented N19°-22°E/77°NW to vertical, and N35°E/68°SE, Note hand lens for scale.

Bottom photo shows a fracture with about a 1" interstice that is healed with radiating stilbite (orange) followed by calcite (white) in a Group D fault having ~2 m of offset and a 3 m-wide breccia zone orientation N29°E/72°SE. About the same scale noted above.

Table 2. **Selected Queens tunnel fault/fracture mineral fillings**

Station 077+85 – Upon a substrate of heulandite, cream-colored stilbite in hemispherical masses 2 cm wide and as felted crystalline masses of single sheaf-like crystals. The stilbite is overgrown by calcite and by pyrite. Mineralization occurs in a NS-trending Group D reverse fault cutting interlayered garnet-diorite orthogneiss and garnet amphibolite. Sampled 9/9/99 and 2/8/00.

Station 162+30, RW – Stilbite forming a base with calcite crystals and cubic, clear chabazite overgrowths in a NNE-trending reverse fault zone. Sampled 1/11/99 and 2/8/99.

Station 165+92, RW – Yellowish stilbite as a base to calcite crystals and drusy pyrite. The stilbite crystals, found in Group D N20°E, 71°SE fault, grew as fibers perpendicular to the fracture. Sampled 1/11/99.

Station 166+65, RW – Yellowish stilbite, calcite, and drusy pyrite crystals in N22°E, 77°NW-trending Group D fault zone. Sampled 1/11/99.

Station 167+00, RW & LW – Major 75'-wide NNE Group D faulted pegmatite zone with box-work open cavities and greenish clay gouge. Megascopically, stilbite blades are overgrown by 2-3 mm spherical masses of pyrite. The multifaceted spherical masses are superseded by calcite crystallization, all on a fractured pegmatite or amphibole-gneiss matrix. Sampled 10/6/98, 11/24/98, and 1/12/99.

Station 169+36, RW & LW – Open cavities in 1'-2' wide Group D fault zone (N35°E, 68°NW) through amphibolite in garnet schist containing deep orange stilbite. The stilbite occurs in cavities a few cm in size as rounded sheaf-like clusters. Micro-scale pyrite cubes coat the stilbite. Some late-stage clear acicular stilbite blades occur locally. Sampled 1/12/99.

Station 190+15, RW – Light yellow crystalline stilbite crystals occur in gouge-rich fractured pegmatite. The stilbite crystals are overgrown on massive calcite. Two generations of small, clear crystals (apophyllite and younger analcime) occur next. The analcime crystals are particularly striking because of their facet reflections and clarity. Locally, cm-scale pseudo-cubic calcite crystals are found to overgrow the crystallized matrix. Sampled 1/20/99 and 6/7/99.

Station 190+52, RW – Clear interpenetrating calcite crystals about 1 cm in size in N11°E, 67°NW Group D fault zone overgrow stilbite. Stilbite crystals form a basal substrate found overgrown with massive stilbite then the calcite. Late pyrite cubes here overgrow a second generation of clear stilbite blades. Sampled 6/7/99.

Station 214+25, LW – Radiating masses of orange-colored stilbite surrounded by white calcite in fracture fillings related to a Group D fault oriented N29°E, 72°SE. The fault, which cuts mafic gneiss, has produced a crush breccia zone up to 3 m wide. Mineralization is found in thin veins a few mm thick to irregular nodules up to 10 cm long, all within the brittle fault fabric. Sampled 6/16/99.

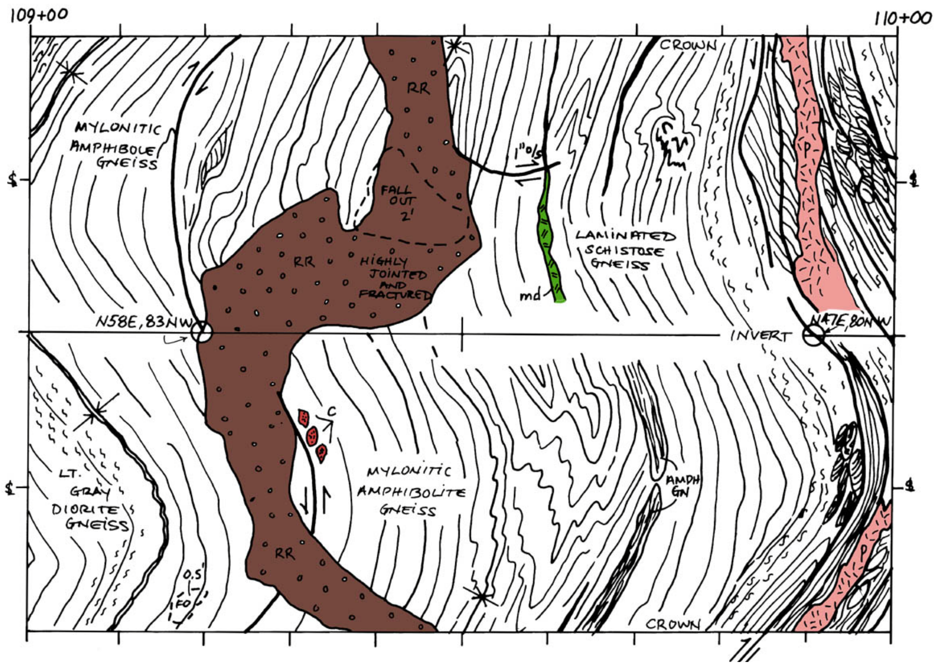

Figure 12. Geologic map showing truncation of N53°E, 83°NW Group B fault by a NW-trending rhyodacite dike of 4 m thickness. (Tunnel bearing is N09°W; Original map scale 1”=10’; tunnel diameter 23' 2".)

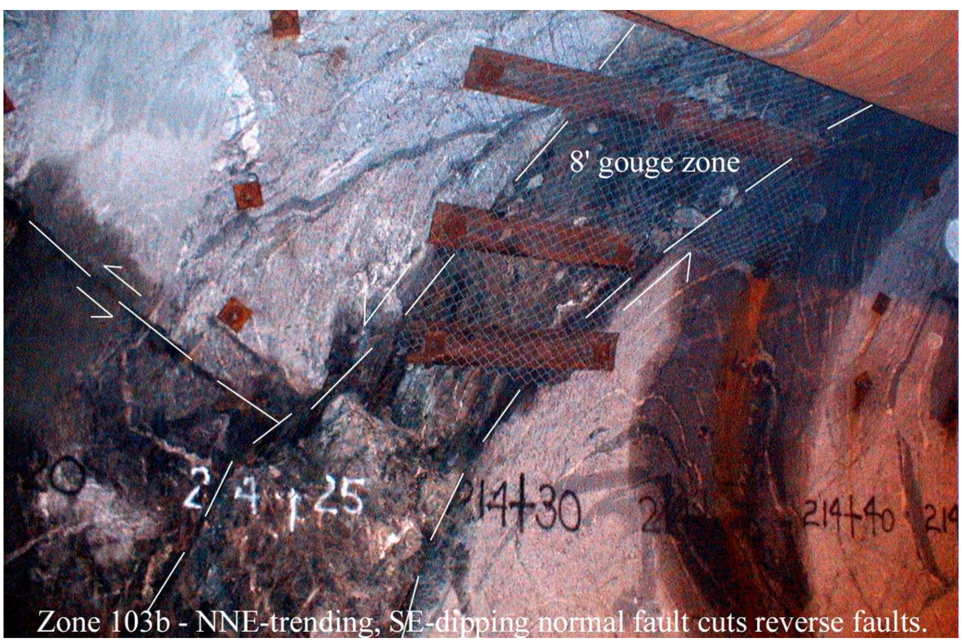

Figure 13. The geology of this disturbed interval (Station 214+30, left wall) is dominated by a major NNE-trending SE-dipping normal fault exposing a 3 m thickness of clay-rich crush breccia. This Group D fault displaces older low-angle reverse faults (Group A) in both the footwall and hanging wall. Fault splays of various orientation and offset sense are found adjacent to the NNE-fault. (Digital image by C. Merguerian, 18 November 1999.)

This group comprises a major fault system that cuts the mapped segment of this tunnel beginning to end, but is most densely concentrated along the NW tunnel leg just beyond the major tunnel bend where orthogonal geometric relationships are easy to spot (see fig. 8B.) Here, the NNE faults crosscut the tunnel at a high angle and contributed to tunnel perimeter instabilities encountered during mining, especially when found in combination with other fractures. They cut the rhyodacite dike swarm and most other geologic features of the tunnel including Group A faults (fig. 13).

The Group E (or Manhattanville) structures are the youngest group of brittle faults and fractures striking NNW from ~N20°W to ~N50°W. They are mostly steeply dipping and show predominately strike-slip offset (figs. 14 and 15). They crosscut every geological feature in the tunnel and mark the youngest structural event to be recorded. These faults dip steeply with sub-horizontal slickensides, flower structure, and little mineralization with the exception of quartz veining. Areas cut by the Group E faults are typically highly fractured and show evidence of high strain in the form of overstress phenomenon including invert heave, spalled rock slabs and rock popping from the crown and tunnel perimeter. These NNW-trending faults are best developed near the western 1.5 km of the tunnel.

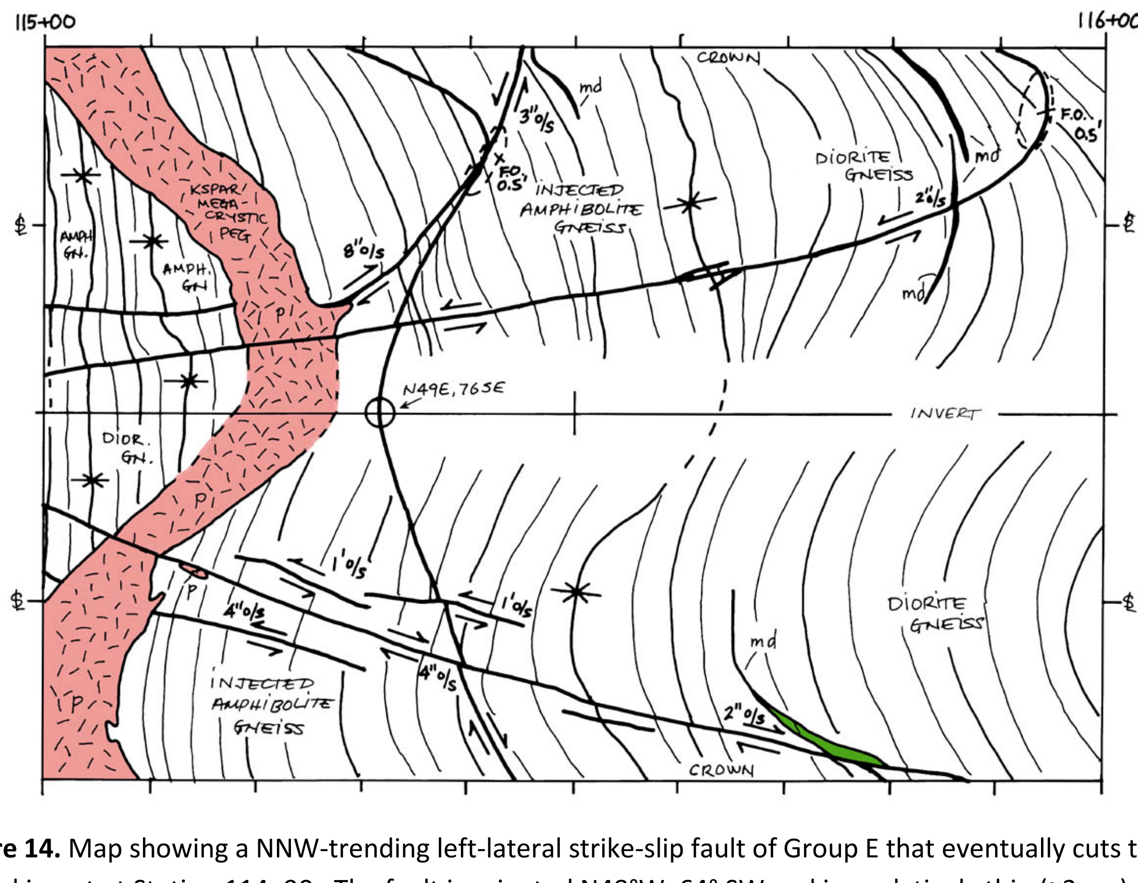

Figure 14. Map showing a NNW-trending left-lateral strike-slip fault of Group E that eventually cuts the tunnel invert at Station 114+90. The fault is oriented N48°W, 64° SW and is a relatively thin (~3 cm) feature.

This western tunnel area marks an extension of the famous "125th Street [Manhattanville] fault" of New York City and parallels many similar faults in the NYC area. Indeed, the Group E faults are part of a regional fracture set along which a recent (17 January 2001) epicenter for a Magnitude 2.6 earthquake occurred[3] (fig. 3).

By contrast to the five-fold fracture history found in the basement rocks of the Queens Tunnel Complex, the Paleozoic cover rocks show a simpler fracture history with an older steep dip-slip NNE-trending fault set (Group D) with thick clay- and zeolite-rich gouge zones. These are cut by NW- to NNW-trending strike-slip faults of the Group E “Manhattanville” fault set.

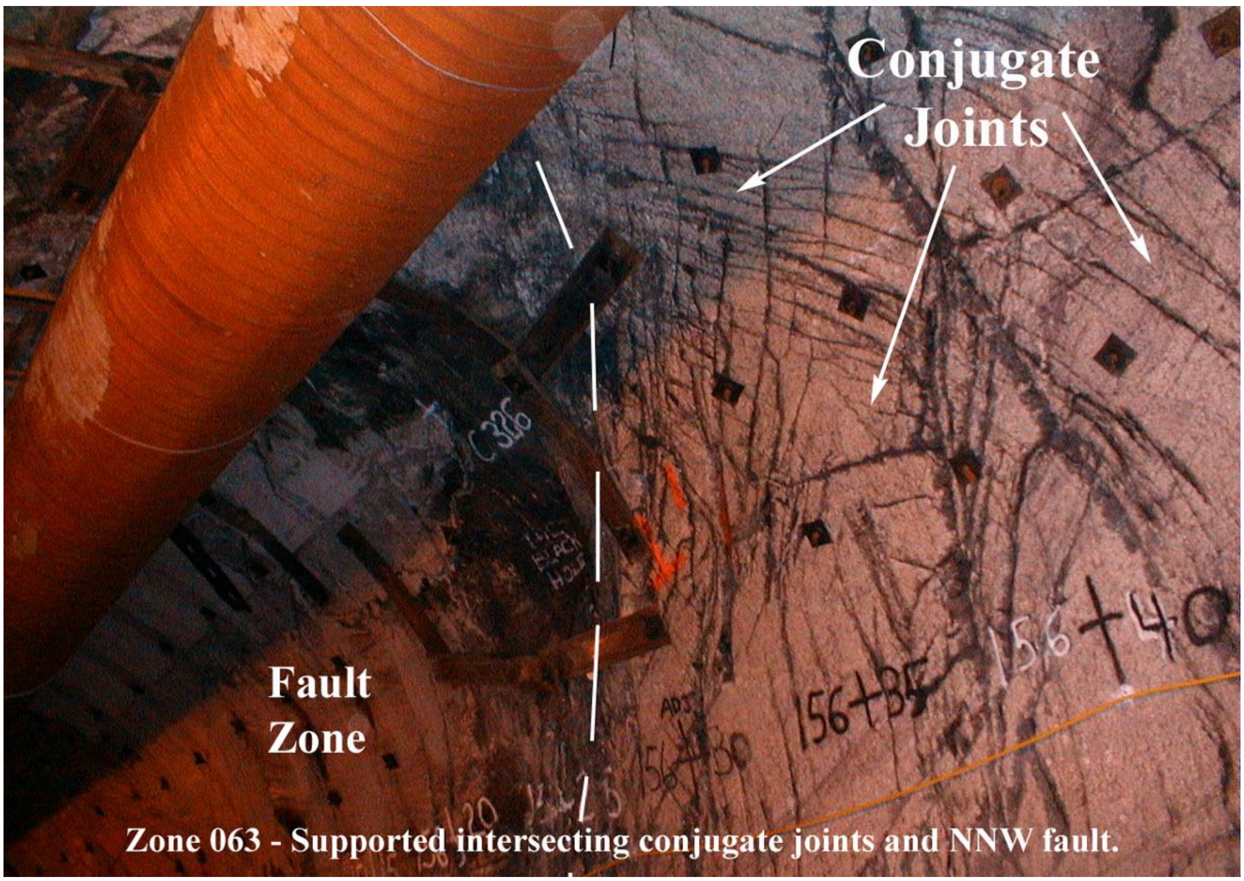

Figure 15. Left wall view of a N20°W fault of Group E that cuts invert at 156+35 with a 0.5 to 1.0 m thick crush breccia and adjacent area of intersecting conjugate joints (flower structure). Tunnel bearing is N41°W; Original map scale 1”=10’; tunnel diameter 23' 2". (Digital image by C. Merguerian, 30 December 1998.)

Intersecting brittle faults are a major contributing factor to the localization, mechanical properties, and alteration of disturbed ground zones in TBM tunnels. Although fracturing generally aids in the TBM excavation of rock, intersecting fractures amplify crown and sidewall instability, cause slippage of TBM grippers, downtime for installation of additional local support and ring steel, and induce damaging water inflows. Such was the case in the East Side Access feature. TBM boring phase both before and after the 90° tunnel bend where significant machine damage and utilization decrease occurred as a result of Group D and Group E fault intersections.

Geology and brittle faults in the East Side Access tunnel

My involvement in the East Side Access project as site geologist for the contractor Dragados-Judlau JV began in 2001 and ended in 2010. This project was to divert a portion of Long Island Railroad trains via curved tunnels to a newly excavated cavern beneath Grand Central Terminal in midtown NYC (fig. 16). Two existing tunnels beneath the East River to 63rd Street constructed in 1980 provided important access from Long Island City for project workers, equipment, TBM launch and maintenance. Two similar open beam TBMs were employed for this project and they were used to punch as many as 8 parallel tunnels into the Paleozoic cover rocks found along the alignment. Except for poor utilization in disturbed ground areas underlain by intersecting faults, excellent penetration rates were experienced because well-layered, gently-inclined micaceous Hartland rocks were found to occupy the much of the tunnel horizon.

Investigations of a number of zones where fault intersection played a role in tunnel perimeter failure allowed for recognition of both NNE- and NW-trending faults in the subsurface Paleozoic cover rocks of the Hartland formation. Two areas in particular were studied. In late 2007, in the EB-2 tunnel between stations 1066+45 and 1067+20, unusual ground behavior took the form of voids which opened up in the crown and sidewalls of the tunnel that caused extensive fallout and downtime for support installation and mucking operations (fig. 17). The voids were over a cubic meter in dimension, laterally continuous and extended upwards to 3-4 m. They contained angular, cobble- to fist-sized blocks of altered slickensided incohesive fault rock and associated clay gouge. The voids were distributed on all sides of the tunnel requiring major downtime during installation of ring steel zone for stability and safety.

In October 2009 a second very similar fractured zone was encountered roughly two years after the zone described above was mitigated and passed. Here, an extensive tunnel reach ~291' in length of the westbound WB-1 tunnel was excavated through nearly identical disturbed ground that was found to unravel fault rock blocks of varying size with little to no stand up time. This produced laterally extensive open voids in the crown and side walls, buried the TBM platforms with loose rock and created interference with support operations. This disturbed ground zone also required pervasive ground support, mucking, and remediation. In both areas, the rock was extremely altered, clay-rich, friable, soft and prone to heaving.

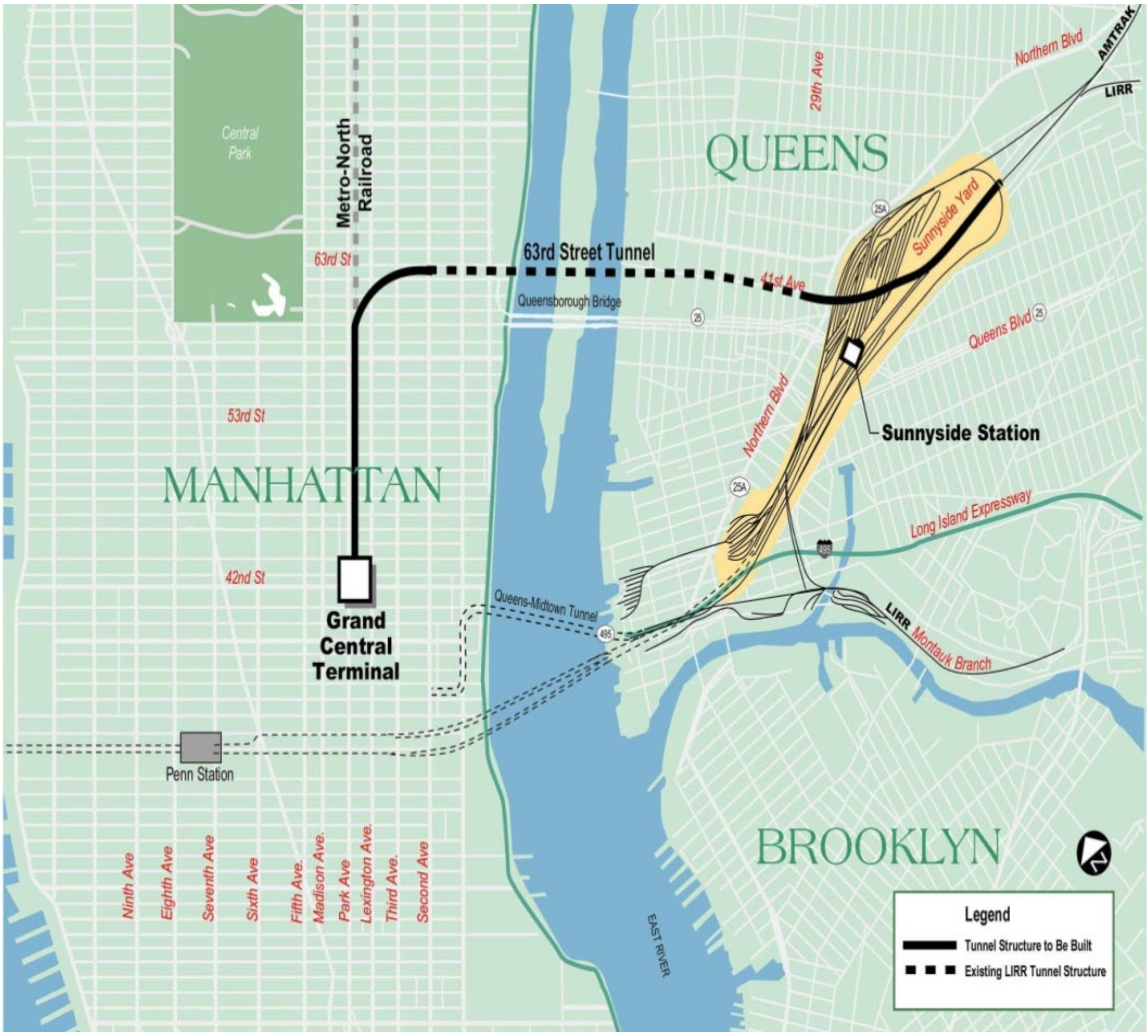

Figure 16. Index map showing the tunnel alignment of the East Side Access Project that will eventually divert MTA Long Island trains from Sunnyside Yard in Queens across the East River via the 63rd Street tunnel into Manhattan. From there the tunnel bends 90 degrees southward to Grand Central Station. (MTA Public Document.)

Even the more quartzofeldspathic granofels interlayers were found to split into thin slabs and were mechanically weak showing clay squeezing and breakage with mild finger pressure. Rock alteration and weakness was the result of pervasive hydration alteration of feldspar and mica to clays which created a weak rock mass not capable of maintaining TBM gripper pressure or load. Similar to the previously described EB-2 zone, this geological condition was the result of a spatial confluence of geological features, including sheared foliation and NNE- and NW-trending brittle faults and joints. A view of a NE-trending fault in this area is shown in figure 18A and the type of ground condition is shown in both figures 17 and 18.

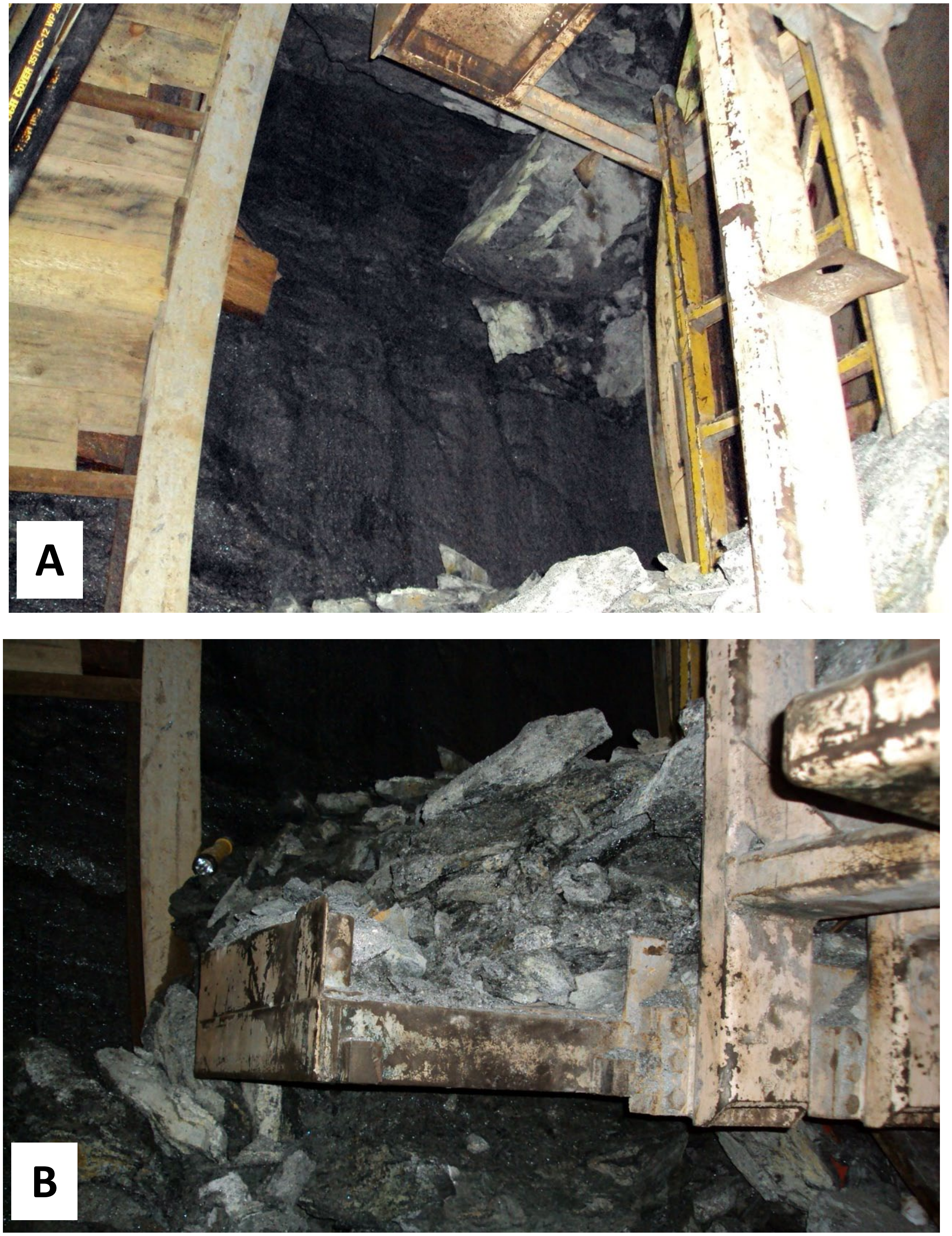

Figure 17. Two views of mucking operations on 09 Dec 2009 showing the extent of poorly-sorted blocky fall out in the left wall rib during mining operations. Upper image (**A**) shows suspended large blocks. Lower image (**B**) shows the magnitude of small rocks and weathered clay-rich matrix of fault breccia and gouge associated with the NE-trending fault that traverses the zone. (Progress Photos 28 and 29 provided by Dragados-Judlau JV.)

Figure 18. Photographs inside the East Side Access tunnel**.**

A. View of N41°E, 85°SE fault (steep through image center) that splays into left wall and crown. This steep Group D fault, together with steep NW-trending cross fractures and gently inclined sheared rock fabrics produced a 291' reach of disturbed ground in the WB-1 tunnel. (Digital image EV010560 taken 01 December 2009.)

B. View of the north wall of EB-2 near Station 1066+70 showing open voids filled with blocky rock and clay behind the support. The voids are scattered throughout the disturbed ground zone and consist of loose angular cobble-sized to fist-sized blocks of highly altered and slickensided rock. (Digital image taken December 20, 2007.)

The redraft of the 1865 Viele map (fig. 19) shows the position of the tunnels in red (EB-2 and WB-1). Note that three NW-trending faults project into the EB-2 tunnel alignment southwest of Station 1066+00. The continuation of mining during 2008 and 2009 looped southward from the area of Station 1066+00 and proved to be an unfortunate geometric situation as the same NE-trending fault zone that affected the EB-1 tunnel in late 2007 traverses southwestward to intersect the WB-1 tunnel starting at Station 1055+71. The width of the disturbed ground zone in EB-2 fault zone along the roughly E-W segment was much less since the fault crossed the tunnel line at a high angle. In the 2009 disturbed ground zone the fault cuts the tunnel at an oblique angle (11°) resulting in an extended zone of tunnel perimeter failure.

To summarize, in the East Side Access excavation unanticipated geological features that converged in these zones produced an extensive reach of open voids, chimneys, and channels that exhibited unraveling with exceedingly short stand up times and deep weathering. This was caused by the presence of a hitherto unknown NE-trending fault zone intersected by NW-trending faults and joints. Because major water courses parallel the NW-trending faults and to a limited extent a NE-trending fault that connects both zones (fig. 19), I suggest that percolating ground water conditions over time affected the fractured, clay-rich ground conditions that plagued the construction effort.

Manhattanville and Mosholu Faults

The venerable 125th Street "Manhattanville" fault has been recognized since Merrill et al. (1902) folio mapping of New York City and in the Berkey (1911) analysis of the New York City Aqueduct (fig. 20). The fault was highlighted in Lobeck (1939) and recognized to be a part of a family of NW-trending faults including faults in Van Cortlandt Park (= Mosholu Fault), Spuytin Duvil, Dyckman Street, Harlem River, and faults to the south in Manhattan (fig. 21). The NW-trending Group E faults of the Manhattan Prong have offset mapped geologic contacts and localized historic seismicity in NYC. Two of these Group E fractures deserve mention in this connection: (1) the famous 125th Street "Manhattanville" fault and (2) the Mosholu fault in the Bronx. Thick zones of fault breccia were diagrammed in Berkey (1948) and redrafted by Fluhr (1969) where a broad U-shaped valley covers 500' of decayed rock above the fault zone (fig. 22).

In 1985, I studied the 125th Street fault during construction of a drill and blast section of NYC Water Tunnel #3 project beneath Amsterdam Avenue where a complex zone of highly crushed fault breccia more than 90 m wide outlined the fault zone (fig. 23). Here, the 125th Street fault strikes N35°W and dips 55° to 75° SW and cuts across and fractured the NE-striking Manhattan Schist (Ꞓ-Om). Where the fault crosses the crown of the tunnel many 2 to 3 m

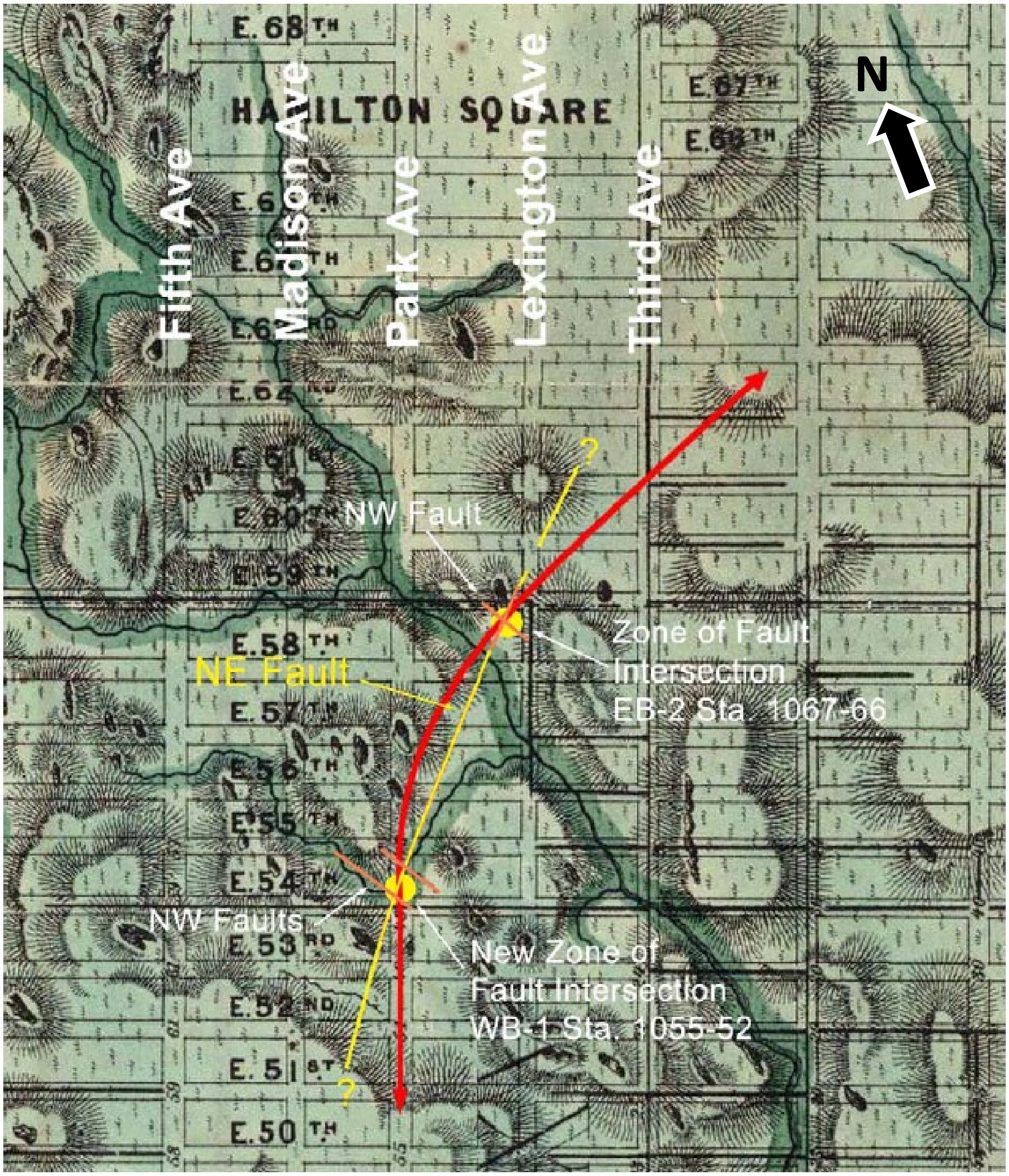

Figure 19. Sanitary and Topographic map of Viele (1865) with the trace of the EB-2/WB-1 tunnels from E. 62nd to E. 51st streets added (red). Note the NW- (orange) and NE- (yellow) trending faults plotted based upon field data (Merguerian and Merguerian, 2004) and by the interpretation of surface drainage patterns. The initial area of disturbed ground from Stations 1067+20 to 1066+45 is plotted in yellow (upper yellow circle). The new zone of intersecting faults and extensive fall out is shown between 54th and 54th streets beneath Park Avenue (Stations 1055+71 to 1052+80; lower yellow circle). Note how drainage patterns are governed by NW- and NE-trending faults and associated fracture zones and how the NE-trending fault extends from the northern disturbed ground zone (upper yellow circle) to the new zone of disturbed ground (lower yellow circle). Main avenues trend ~N30°E so north is tilted to upper left.

Figure 20. Old maps showing the location of the Manhattanville fault, highlighted as a white dashed line.

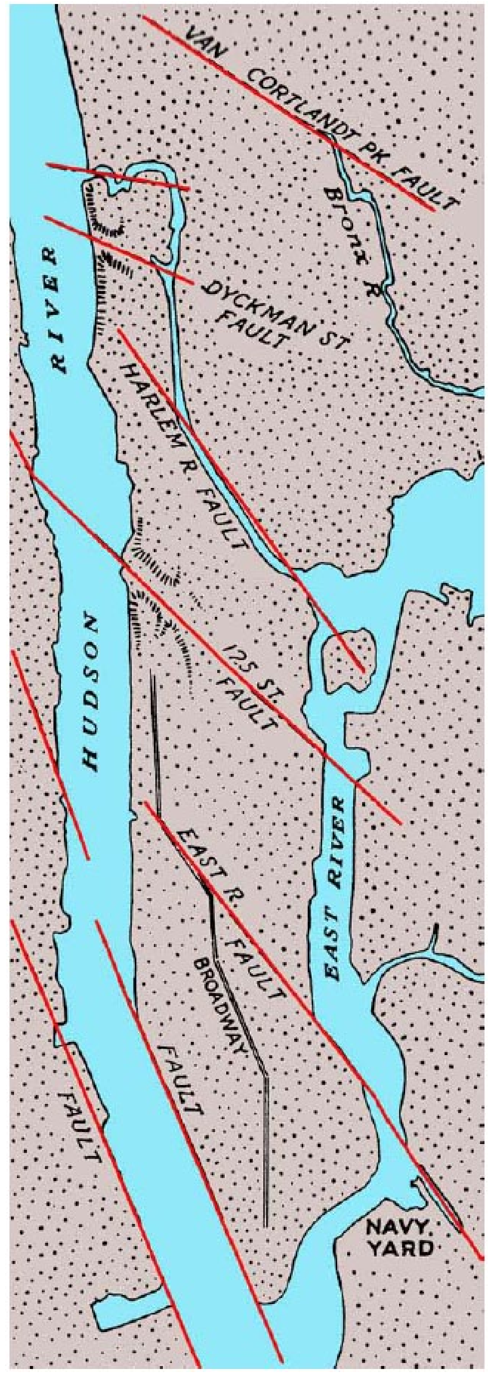

Figure 21. Colorized map of Manhattan showing major faults inferred on the basis of subsurface data in water tunnels and physiographic relationships. (A. K. Lobeck 1939.)

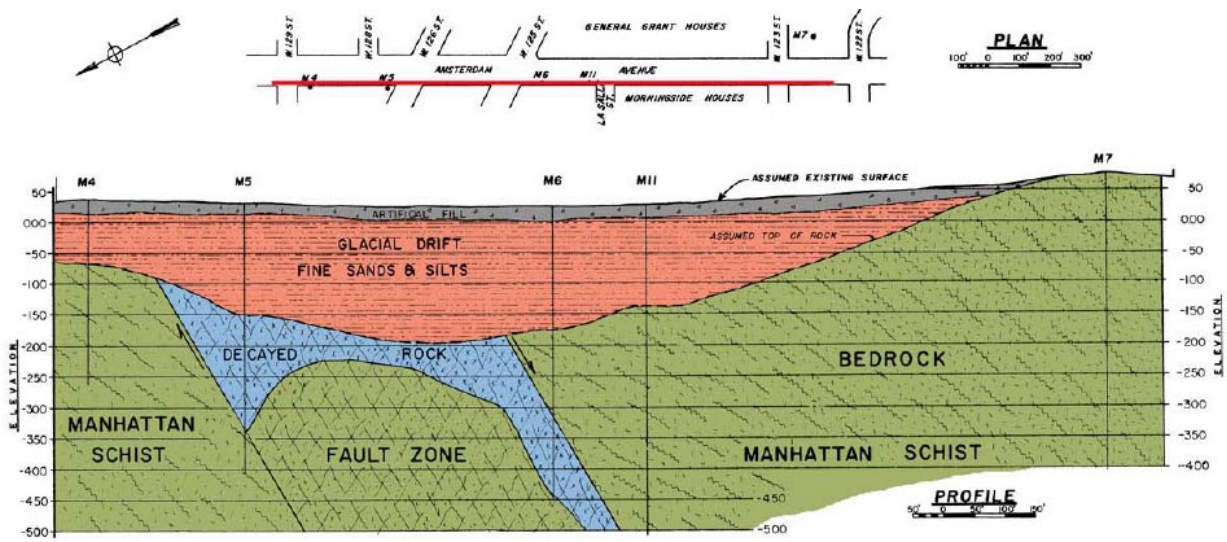

Figure 22. Geological section across the broad U-shaped valley consisting of glacial drift atop the 125th Street "Manhattanville" fault zone. (Colorized from Fluhr 1969, Fig. 4.)

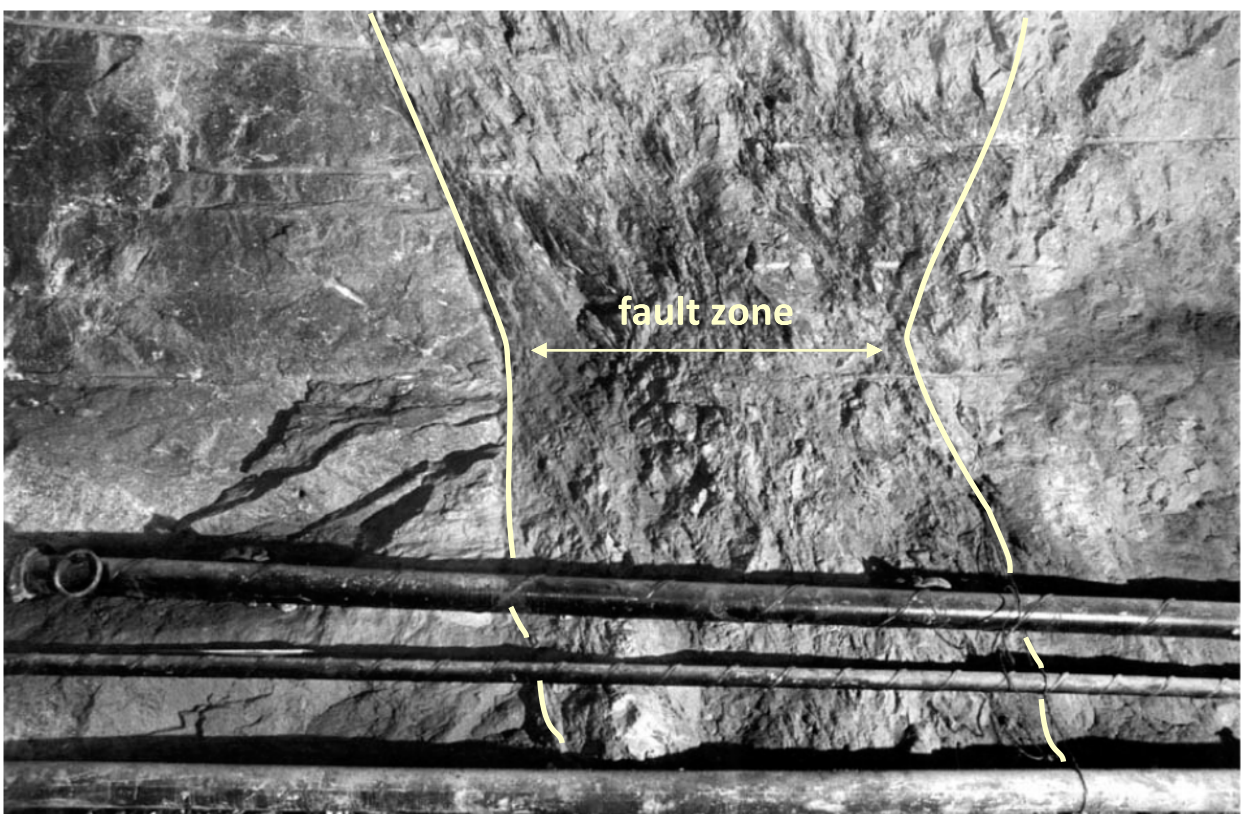

Figure 23. Photograph of the 125th Street fault as exposed in the subsurface of Manhattan in the water tunnel built roughly 250 m beneath Amsterdam Avenue. Note the sharp demarcation of the fault. The photo covers roughly 7 m in vertical dimension and shows the presence of compressed air and water conduits along the bottom. (Carl Ambrose Photo, NYC Bureau of Water Supply.)

blocks of the Manhattan Schist, which remained internally coherent within the broad zone of cataclastic rock, showed a minimum of 90˚ rotation about a vertical axis. The blocks remained internally coherent within an otherwise broad zone of cataclastic rock and fault breccia. Clearly, this observation indicates that along the 125th Street fault, much of the motion has been strike slip. Indeed, slickenlines measured in the tunnel indicate that right-lateral, normal, oblique slip was the most-recent offset sense and that a minimum of 18 cm of slip has been observed along one fault surface (Eileen Schnock, DEP, personal communication). Mapped offset of the prominent Manhattan Ridge in northern Manhattan indicates more than 200 m of composite right-lateral slip along the 125th Street fault valley, a U-shaped valley greatly modified and enlarged by Pleistocene glaciers flowing from the NW and presumably infilled by a younger glacier flowing from the NE (Sanders and Merguerian 1998).

Pelham Bay Park, Bronx, NY

Many excellent examples of brittle faults of contrasting type and offset sense can be found in the bedrock exposures half way up the rock terrace on South Twin Island in Pelham Bay Park in Bronx, NY. Many brittle faults are found in the area including Group D and E faults. Figure 24 shows an eastward view of two brittle faults outlined by quartz veins. Note how the N70°W-trending left-lateral strike slip-fault offsets a quartz vein in the background. This quartz vein was injected into a N30°E fault developed parallel to a sheared foliation in the bounding Hartland gneiss.

A few hundred feet to the south, another NW-trending Group E fault is exposed. This fault trends N66°W and dips 82°SW and shows roughly 0.5 m of composite right-lateral strike-slip offset of an isolated quartz vein. The area around the fault is highly fractured because of a close family of joints oriented N67°W/77°SW. Thus, as found in Central Park (discussed below), both right- and left-lateral offsets occur within close proximity of one another.

Croton Water Treatment Plant, Bronx, NY

Following the excavation of tunnels originating within Van Cortlandt Park for the construction of the Croton Water Treatment Plant in Bronx, NY, project geologists were able to identify and map the contact between the Yonkers Gneiss (Zy) and the Fordham Gneiss (Yf) formations in the side-wall of the TBM tunnel excavations (Isler, Vellone, Merguerian and Merguerian 2009). Based upon analysis of mineralogical differences between the two formations and observations of the textural and megascopic composition of the rock surfaces

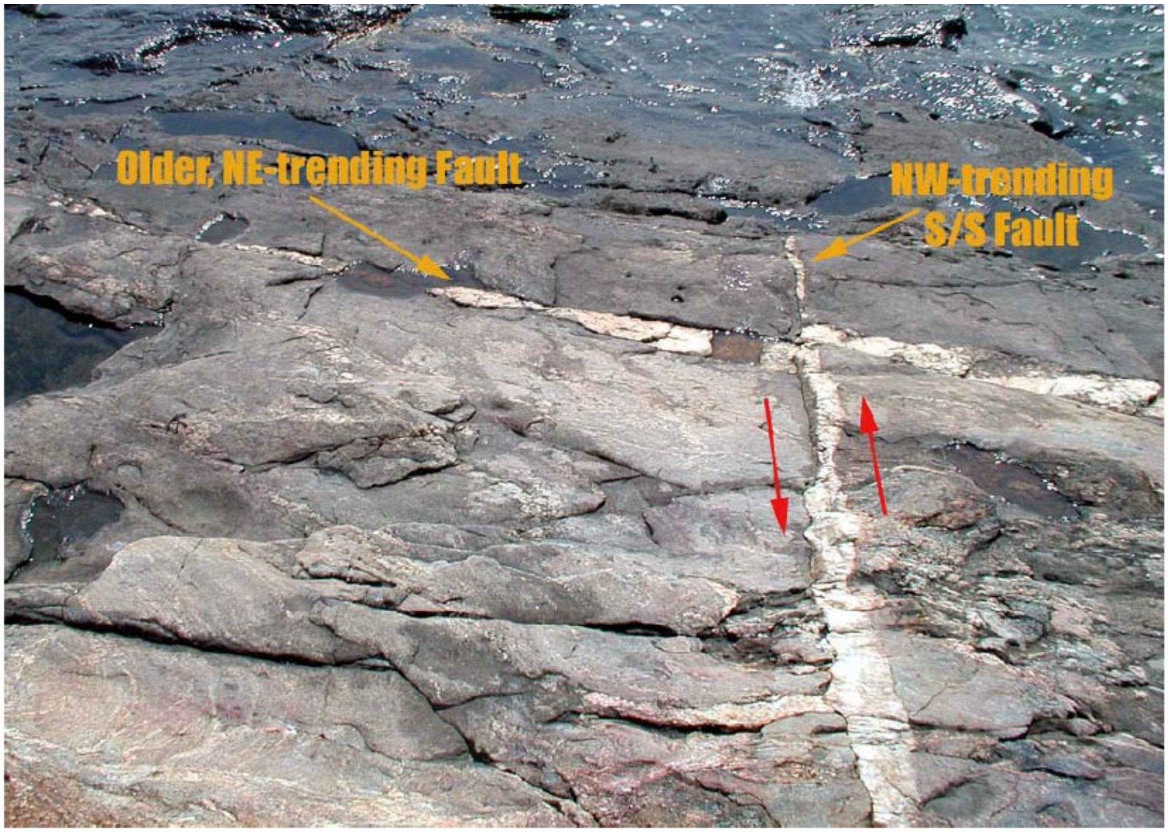

Figure 24. Eastward view of N70°W, 62°NE left-lateral Group E fault (lined by milky quartz vein in foreground). This fault cuts an older Group D NNE-trending fault and parallel foliation (N30°E, 80° SE) in the bounding Hartland gneiss.

exposed during tunneling operations, the contact of the Yonkers gneiss has been re-drawn from its southern limit as shown on Baskerville (1989, 1992) and Fluhr and Terenzio (1984) to extend southward to contact the Mosholu Fault at the southern end of Van Cortlandt Park (fig. 25). The Mosholu fault has ruptured along the Yonkers-Fordham boundary where the Yonkers may have acted as a resistant block and controlled the fault trend and/or location. By contrast to the prediction for a thick fault zone (~350 m wide) by pre-mining geophysical instrument measurements, the actual fault was mapped as a surprisingly narrow (~3 m) zone of dark greenish-black slickensided rock with clay and chlorite coating shear surfaces (figs. 26 and 27). Offset sense is right-lateral strike slip based on mapped contacts (Baskerville 1994) but this is based on very limited exposure. Dan Vellone (personal communication) did much of the mapping at the tunnel. He reports that in the Low Level Service TW tunnel there was 30 cm of offset measured at Station 18+40 and 60 cm of offset at Station 27+98 (fig. 27). The High Level Service TW tunnel exhibited 30 cm of vertical offset at Station 17+06 and ~1 cm of offset at Station 34+55.

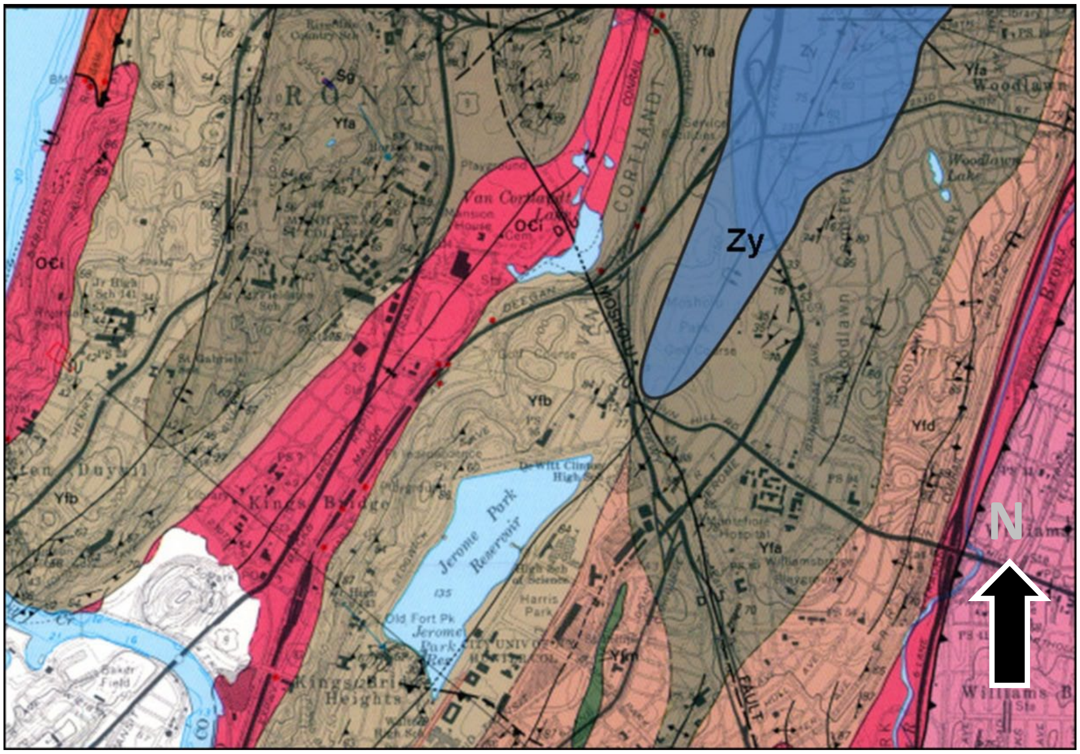

Figure 25. Bedrock map of the tunnel alignment with proposed southward revision of the geologic contact between the Yonkers (Zy - blue) and Fordham (Yf – brown and tan) gneisses based upon observations following the excavation of two tunnels advanced using tunnel boring machine (TBM) methods. (Basemap after Baskerville 1992.)

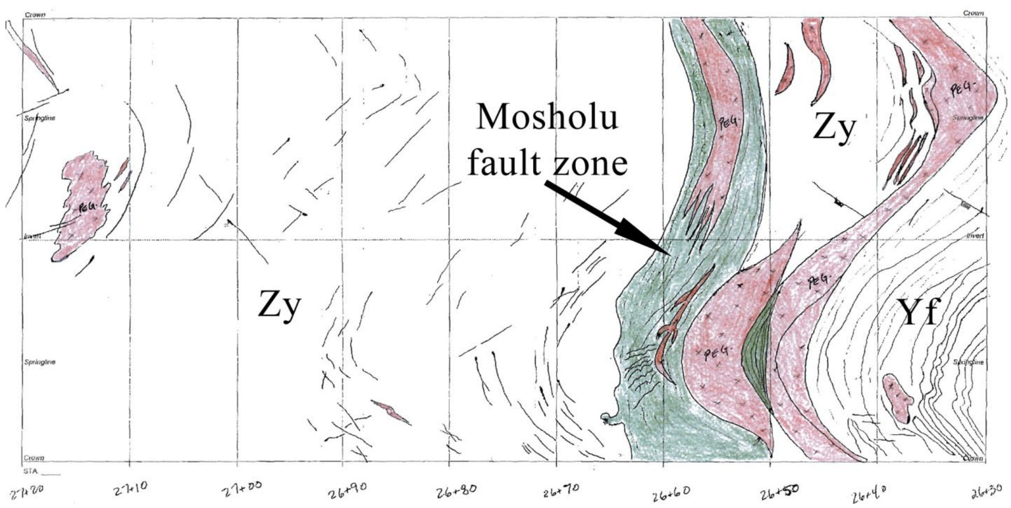

Figure 26. Full-periphery geologic map of the low-level treated water tunnel Station 27+20 to 26+30 that shows jointed Yonkers Gneiss (Zy) in contact with complexly deformed Fordham Gneiss (Yf) along the Mosholu fault zone (green). Younger pegmatite injections are shown in pink (Isler and others 2009; fig. 4).

Figure 27. View of chloritic fault gouge and breccia zone associated with the Mosholu fault in the low-level treated water tunnel (Station 26+60). (Digital image by Dan Vellone.)

Toward the SE, the Mosholu fault extends into the New York Botanical Garden grounds through competent rock (fig. 28).

Central Park, NYC, NY

Hartland, Manhattan and Walloomsac rocks bearing both ductile and brittle structures crop out within Central Park in NYC. A new bedrock map (fig. 29) has modified the position of Cameron's Line and has adjusted the position of bounding lithotypes - the Manhattan and Hartland formations. Cameron's Line shows strong deformation by S-plunging F_3 major and minor folds. The complex sequence of structural events established from other parts of New York City is identical to the structural sequence mapped in Central Park, with three phases of superposed ductile folds crenulated by open folds.

Two generations of brittle faults cut Central Park. They conform to the Group D and Group E faults found in the Queens Tunnel and elsewhere in the city. In some Group D fault surfaces, dip-slip slickensides show overprint by oblique-slip reactivation, the presumable result of younger (Group E) faults. The Group E faults trend N20°W to N50°W, exhibit steep dips and show predominately strike-slip offset. Both right-lateral and left-lateral Group E faults cut the park in three areas.

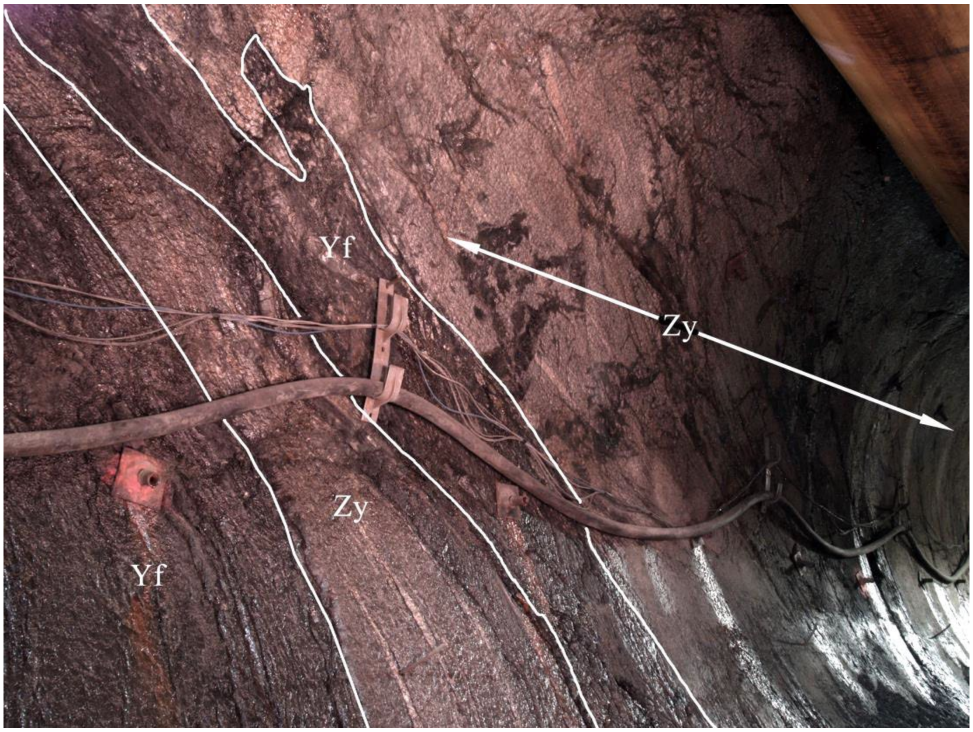

Figure 28. View of southeast wall of high-level treated water tunnel showing permeated and deformed contact of Fordham Gneiss (Yf) with Yonkers Gneiss (Zy). (Digital image of Station 26+95 and annotations by C. Merguerian.)

The 125th Street or Manhattanville fault cuts the NE corner of the park, skirting the Harlem Meer and producing joints oriented N52°W, 75°SW; N19°W 88°NE; and N22°W, 74°NE across the south shore of the meer where gently inclined slickenlines can also be found. Both regional map offsets and the slickenlines indicate right-lateral offset. Two areas south of this locality show evidence for a reversal to left-lateral strike-slip faulting. Near 101st Street and the East Drive, four quartz-healed Group E faults are oriented N12°W, 90° to N39°W, 80°SW-90° with intervening curved splays and healed quartz stringers (colored yellow in fig. 30). From N to S, offsets of 9 cm, 30 cm, 1 cm, and 50 cm (south of outcrop sketch) are the major slip surfaces in the exposure that shows well over a meter of composite offset (fig. 31) and locally up to 0.5 cm of gouge. They cut N44°E sub-vertical isoclinally folded gneiss and amphibolite of the Manhattan formation and offset an isoclinal fold hinge in amphibolite plunging 12° into S45°W.

The most southerly fault in Central Park, adjacent to Eighth Avenue (fig. 29) near the Ladies Pavilion on the west side of The Lake, is oriented N45°W, 90° to N34°W, 81° SW and shows minor left-lateral offset in highly jointed Hartland granofels (fig. 32). Thus, two near orthogonal fault sets cut Central Park, the Group D and Group E faults found elsewhere in NYC. They produce a chocolate block type of brittle fracture pattern in the bedrock units as shown in the magnificent exposure at Umpire's Rock, just south of the ball field. Here, two crosscutting fault generations occur. The older set trends N32°E, 90° with thick gouge and 3 m thick fault breccia at east edge of the sculpted exposure that has been modified by glacial plucking. The field image shows one of the NE-trending faults and shows a NW-trending fracture cutting the exposure at a high angle (fig. 33).

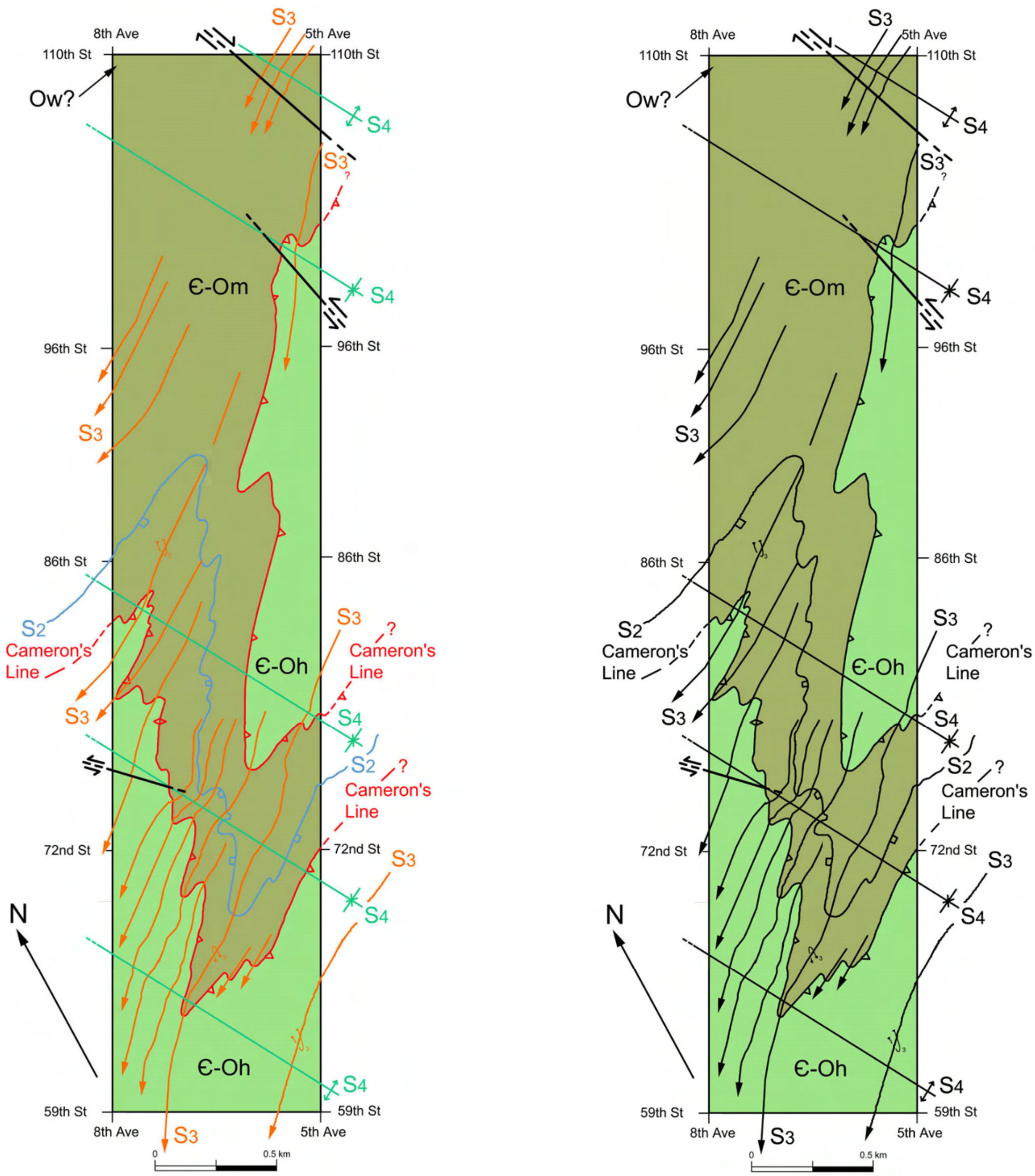

Figure 29. Preliminary bedrock geological maps of Central Park showing ductile and brittle faults and the axial traces of the major structural features, based on re-mapping by Merguerian and Merguerian (2004).

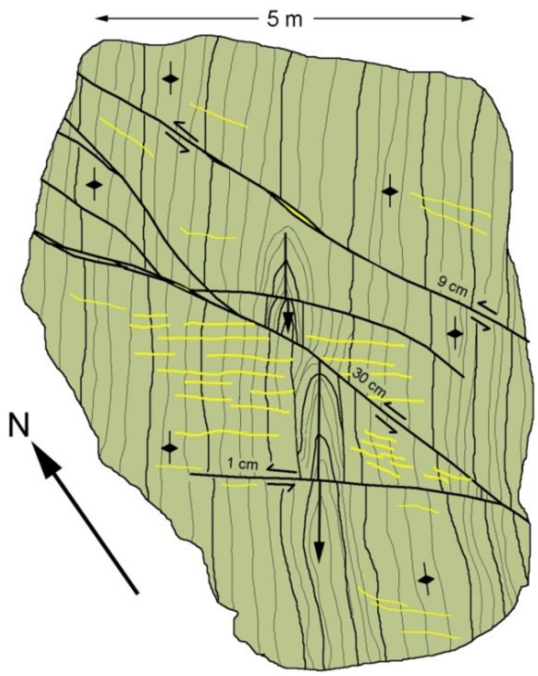

Figure 30. Field-sketch map showing Group E faults in northern Central Park near projected intersection of 101st Street and the East Drive. Yellow lines are healed quartz-filled fractures showing no offset.

Figure 31. Photo looking southward along main fault from center of previous figure. Here a N12°W, 90° left-lateral fault offsets by 30 cm an isoclinal fold hinge in Manhattan amphibolite plunging 12° into S45°W. Foliation and layering in the Manhattan are oriented N44°E/83° NW-90°. Pocket knife at top of image for scale. (CM Stop N537.)

Mt. Morris Park, NYC, NY On the north and south, this small NYC park is a bedrock knoll bounded on the north and south by strike-slip faults. For bedrock enthusiasts low-angle truncation of layering and foliation in the Inwood and Walloomsac by allochthonous garnet sillimanite gneiss of the Manhattan along the St. Nicholas thrust displayed along the knoll's eastern edge (Merguerian and Sanders 1993). At the south end, a slickensided fault surface oriented N75°W, 72°SW exhibits right-lateral oblique-slip offset with slickenlines plunging 28° into W and at the north end of the park another fault is oriented N25°W, 84°NE and shows slickenlines pitching 10°.

Figure 32. Southeastward view of left-lateral N34°W, 81°SW fault zone in Hartland granofels and schist where minor left-lateral offset was detected.

Figure 33. Umpire Rock in Central Park showing two near orthogonal faults. The Group D fault extends from the lower left foreground back into the image and is oriented N32°E, 90° with an eroded 0.5 m gouge zone. This fault is cut by a Group E fault trending ~N50°W, 90° across the image. The outcrop shows another Group D fault defining the east edge which shows a 3 m thick fault breccia modified by glacial action.

New York Botanical Garden, Bronx, NY

Mapping of rocks in the New York Botanical Garden in 2011 showed that Inwood, Walloomsac, Manhattan and Hartland rocks have been imbricated by juxtaposition along the St. Nicholas thrust and Cameron's Line. The overall structure in the park shows an overturned synform of the Inwood-Walloomsac strata with Manhattan and Hartland rocks nestled in the core. The Rocks are cut by the right-lateral Mosholu fault (fig. 34). The trend of the Mosholu fault in the Bronx is similar to that of the 125th Street fault (~N24°W) and its sense of offset is identical. However, the degree of glacial modification is not as great on the Mosholu fault as found along the 125th Street fault, which has been severely modified by glacial action (fig. 22).

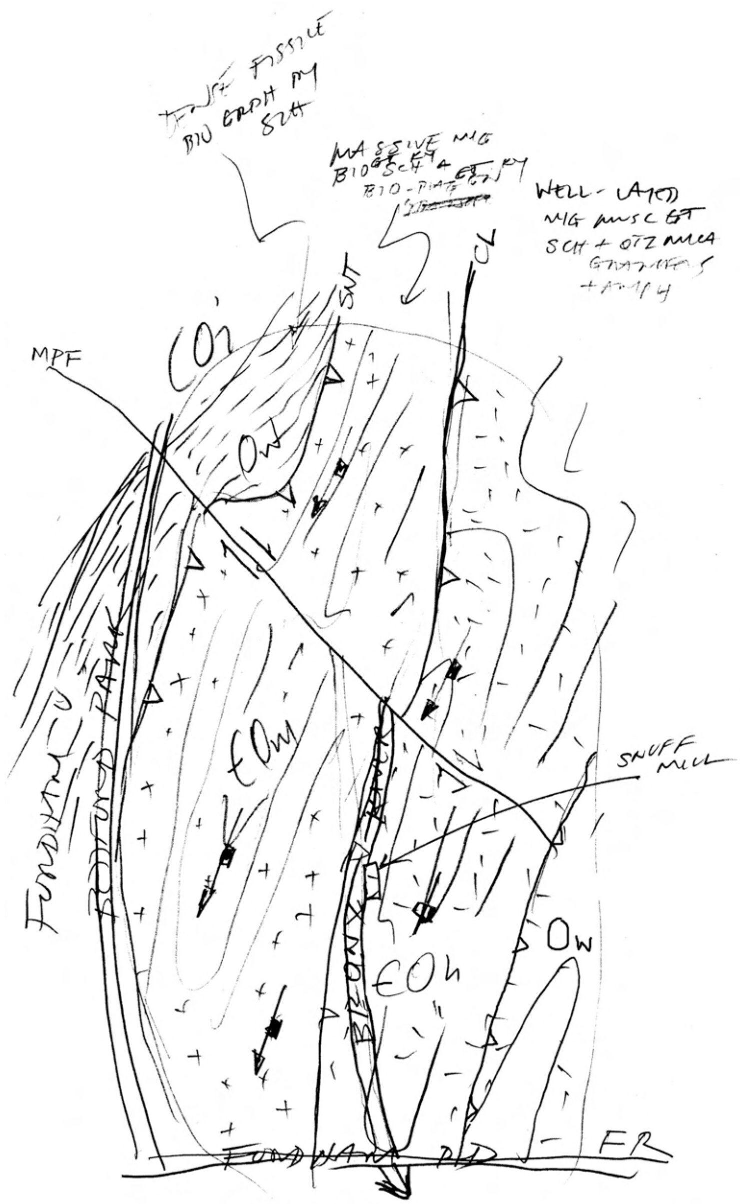

Figure 34. Sketched geological map of the New York Botanical Garden (north to the top) showing a SE-dipping series of thrust slices of Manhattan (Ꞓ-Om), Hartland (Ꞓ-Oh), and Walloomsac (Ow) rocks. The Manhattan is thrust against the Walloomsac and Inwood (Ꞓ-Oi) along the St. Nicholas thrust (SNT) in the NW part of the park. The overall structure is synformal with Manhattan Schist at the center of a SE-plunging F_3 synform whose truncated SE-limb is marked by Cameron's Line (CL) near the course of the Bronx River. Farther SE, a secondary thrust places an imbricate slice of Walloomsac (Ow) against Hartland rocks (Ꞓ-Oh). The thrust zones are marked by imbricated lithologies and broad zones of mylonite ± migmatite. All of the bedrock units and ductile faults are cut by the NW-trending, right-lateral Mosholu fault. (Merguerian, unpublished data.)

Hypotheses on the origin of the Snuff Mill gorge and diversion of the Bronx River

Northeast of the NW-SE-trending Mosholu fault, the Bronx River flows SW in a wide NNE-SSW-trending strike-valley lowland underlain by Inwood Marble (fig. 35). Southwest of the fault is the NNE-SSW-trending Webster Avenue lowland, another equally wide valley underlain by the Inwood Marble, that is offset to the west from the former and lacking a modern-day river but in which the Bronx River undoubtedly flowed in the past.

Just at the point where the NNE-SSW-trending marble lowland has been offset, the Bronx River leaves it and flows southward across resistant gneiss and schist of the Hartland formation in the narrow N-S-trending Snuff Mill gorge. This condition marks a first-order drainage anomaly. If the river did indeed follow the marble lowland SW of the Mosholu fault, then some kind of blockage must have prevented it from continuing to do so. During the time when the river's course to the SW down the Webster Avenue lowland was blocked, the water would have been backed up to form a lake. In such a lake, one would expect that some fine sediment would have been deposited. After a new course to the south through the Snuff Mill gorge had been established, outfall water from the lake would have been locked into this new course across the Hartland, so that even if the locked Webster Avenue lowland became available, the river would not seek to re-occupy it.

Several geologic consequences would be associated with diversion of the Bronx River out of the presumably ready-made course underlain

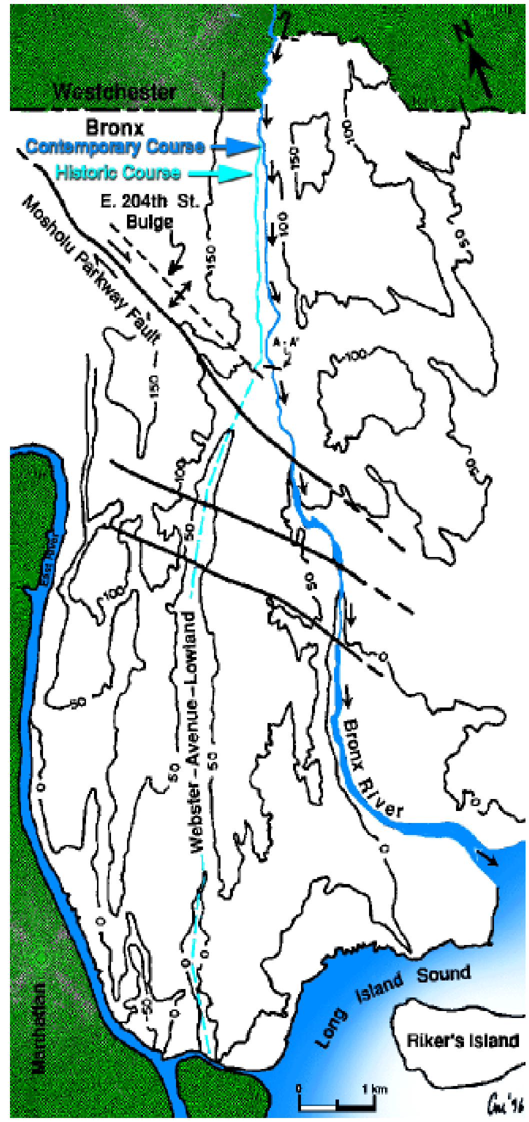

Figure 35. Bedrock contour map showing the present course of Bronx River, its V-shaped gorge, major NW-trending strike-slip faults including the northernmost Mosholu, Bedford Park, and Fordham faults, the E. 204th Street Bulge, the area of the Snuff Mill gorge and section A-A' (fig. 36). The Webster Avenue Lowland marks the previous course of the Bronx River. (Subsurface and fault data from Baskerville (1992), and from engineering records of the NYC Subsurface Exploration Section; bedrock contours in feet).

by the Inwood Marble along the strike-parallel Webster Avenue lowland (fig. 35).

The records archived in the New York City Office of General Services, Subsurface Branch, contain evidence bearing on the diversion of the Bronx River. Figure 36 shows a profile section culled from borings taken across the Bronx River valley from E. 205th Street across to Burke Avenue at a point upstream from the inferred blockage/diversion. Several noteworthy features of these boring records stand out.

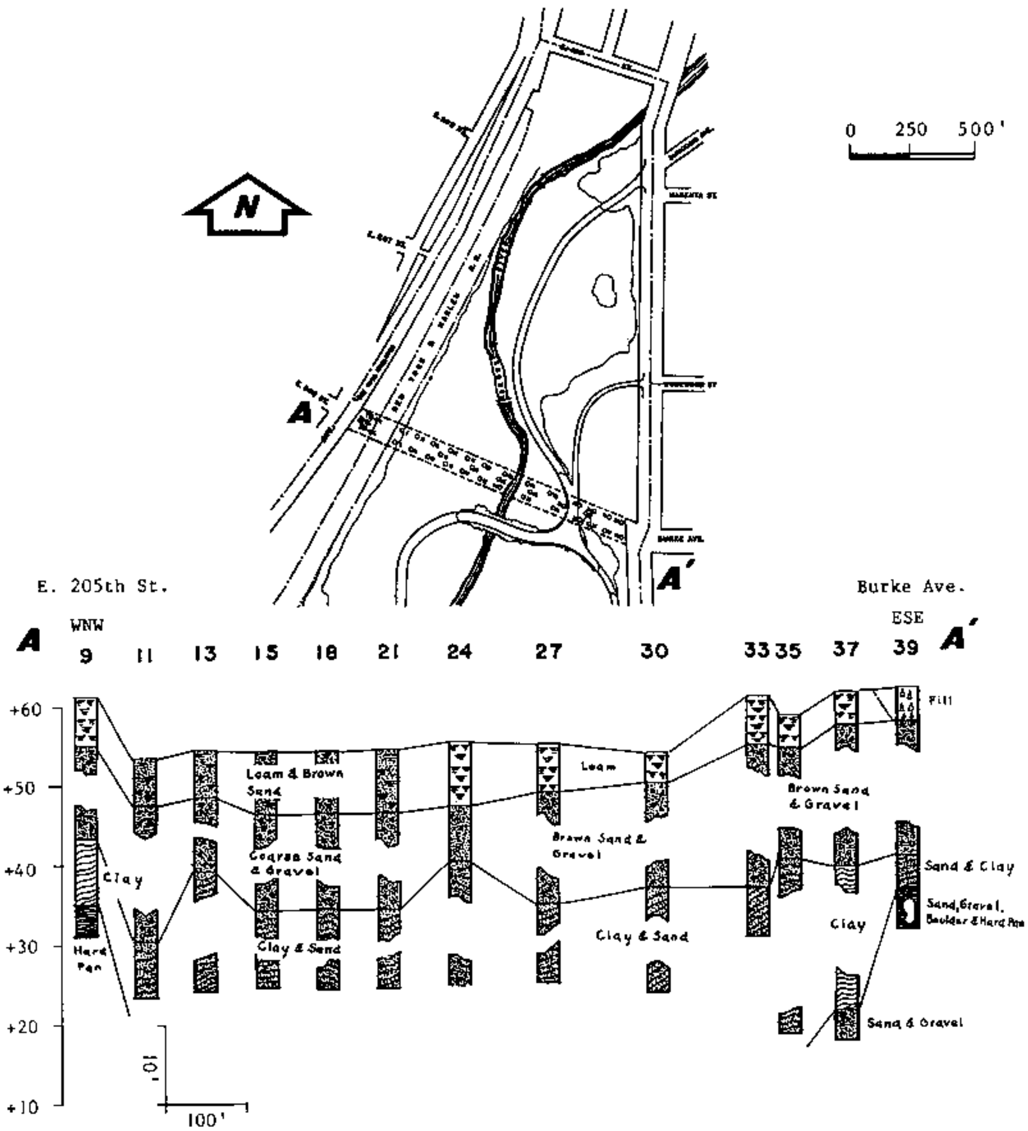

Figure 36. Index map and subsurface stratigraphic section from E. 205th Street east-south-eastward to Burke Avenue in the Bronx, upstream of point of diversion of Bronx River based on records of borings assembled in the 1930s by the WPA rock-line map of the Bronx. Line of section (A-A') also shown on figure 35. Index map shows locations of borings and section A-A'. Stratigraphic correlation diagram using original WPA lithologic symbols for individual boring logs. (Drawn at 10X vertical exaggeration by J. E. Sanders. Elevations are Bronx Highway Datum.)

First, at the bottoms of several borings are what probably should be classified as till ("hardpan," "boulders"). Overlying the putative till is pebbly coarse sand. Next above is thick clay. The clay infers deposition within a lake that formed in connection with the diversion. The clay is both underlain and overlain by coarse +/- pebbly brown sand. Not shown on this section is the deposit of cobbles having an exposed thickness 20 feet in the excavations for the new Bronx River sewer mentioned by Kemp (1897, p. 19).

No clay unit comparable to that found north of the Mosholu fault is present in any of the boring records we have examined along the Webster Avenue lowland, where a capping of artificial fill was emplaced before the railroad and streets were built. The records of sediment in the fill of the Webster Avenue valley contain gray sand below, which is overlain by brown sand. Notably absent is any reddish-brown sediment, key indicators of one- or more pre-Woodfordian glacial episodes. As mentioned above, figure 35 shows contours on the bedrock surface. Note that the Webster Avenue valley is youthful with a narrow, V-shaped profile.

Kemp (1897) inferred that the diversion of the Bronx River was a byproduct of Pleistocene glaciation. Merguerian and Sanders (1997) accepted Kemp's post-glacial age assignment but did so for a reason Kemp did not mention. Namely, had the Snuff Mill gorge been in existence before the latest glacier arrived in the NYC region, then the ice would surely have changed the profile from its present narrow V-shape to a broader U-shaped valley. The narrow V-shaped profile of the Snuff Mill gorge (fig. 37) and absence of smoothed-, polished- and striated rock surfaces on the jagged fresh bedrock exposed in the valley walls by contrast to glacially polished and striated rock on the upland surfaces away from the gorge are powerful arguments in favor of a post-glacial age for the Bronx River diversion, erosion and downcutting of the Snuff Mill gorge. Merguerian and Sanders (1997) considered the NW-trending Group E faults of NYC, along with the Mosholu and Dobbs Ferry faults in Westchester to be seismically capable faults with a history of offset of geological and geomorphic features. They associate the bedrock bulge in figure 36, right-lateral offset of the Bronx River, and diversion of the Bronx River with neotectonic (post-glacial) seismicity along the Mosholu fault.

Faults and Seismicity in NYC

NYC paleozoic cover rocks are cut by two main sets of brittle faults trending ~N30°E [paralleling the long axis of Manhattan] and ranging from N20°W to N50°W [diagonally across Manhattan] with steep to moderate dips toward the SW. Proterozoic basement rocks show a more complex brittle fault history. The NNE-trending faults, which locally reactivate annealed ductile fault zones (Cameron's Line and the St. Nicholas thrust) are steep- to vertical and show dominantly dip-slip motion. The NW-trending faults show complex movement dominated by strike-slip offset followed by dip-slip or oblique-slip reactivation. The NW-trending faults have produced map-scale offset in NYC and geomorphic evidence from the Bronx River implies post-glacial ground rupture.

Figure 37. View of Snuff Mill gorge showing non-glaciated bedrock exposures along V-shaped course of the Bronx River through non-glaciated Hartland rocks. (CM digital image taken 02 June 2011.)

North of NYC, contemporary seismicity along the NW-trending Dobbs Ferry fault in late October 1985 included two small (~4.0) tremors and many aftershocks. As shown in figure 38, more robust earthquakes in and around the vicinity of NYC were recorded in 1884, 1783, and 1737. Unequivocal post-glacial ground rupture is difficult to demonstrate in NYC where most bedrock faults are deemed (especially by seismologists) to have formed at depth and then later elevated to the surface. Yet, the Bronx River, which formerly flowed SSW in an open valley underlain by the Inwood Marble, shows diversion away from its "pirated" marble valley along the NW-trending right-lateral Group E Mosholu fault.

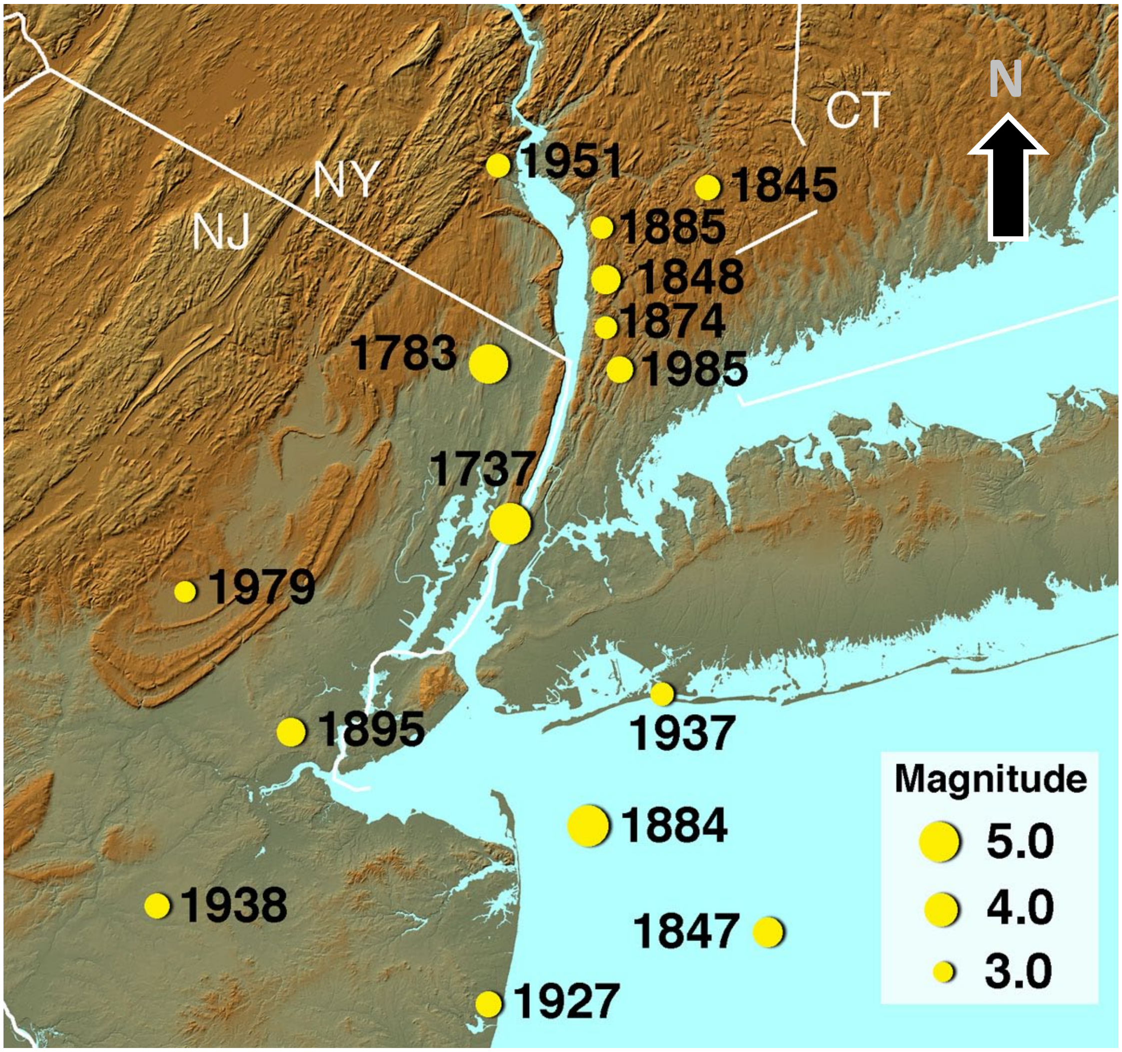

Figure 38. Map showing historic seismic activity in the vicinity of New York City showing a diffuse zone of seismicity and the position of M3 and greater events before 1986. (From Bennington and Merguerian 2007.)

Merguerian and Sanders (1997) did not prove that the surface displacement of the bedrock adjacent to the East 204th Street bulge accompanied an earthquake generated along the Mosholu fault, nor did they prove that surface rupture took place. However, in many seismically active zones, surface displacement, such as the bulging mentioned above adjacent to the Mosholu fault, typically is associated with earthquakes (for example, the Palmdale Bulge along the San Andreas fault in California). No surface offset has been previously reported in connection with any of NYC's strongest earthquakes of 1737 (~M5.2), 1783 (~M4.9), and 1884 (~M5.2). Yet, the August 1884 earthquake produced 4 m long by 3 m deep soil openings, cracked buildings and chimneys in Brooklyn and was felt over a hundred miles from the epicenter, which was located in the New York Bight. Equivalent seismic shaking in NYC today would likely cause failure of older masonry walls, shatter glass windows in skyscrapers and rupture water and gas mains as soils liquefy during ground shaking.

The epicenter of a small earthquake (~2.4 Richter) localized in NYC on 17 January 2001 plots adjacent to the trace of the 125th Street fault near 102nd Street and Park Avenue in Manhattan. Later that same year, on 27 October 2001, another similar earthquake (~2.6 Richter) struck NYC with an epicenter near 55th Street and Eighth Avenue. The two epicenters are plotted on figure 39 to show that they are parallel to Group E Central Park faults (shown in red with offset arrows) as described above.

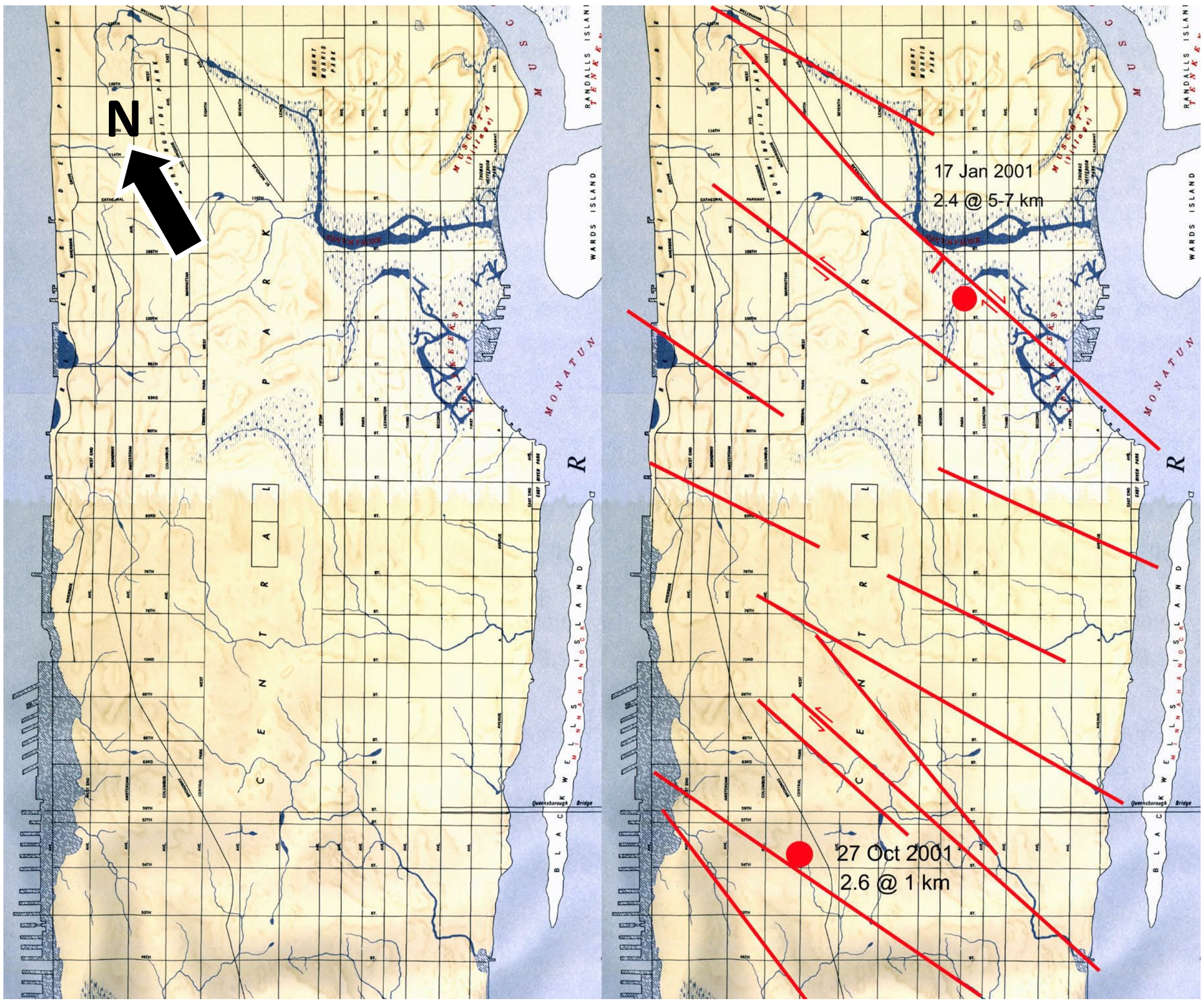

Figure 39. Old topographic map of Manhattan (McCoun 1609) showing pre-industrial era drainage on left following structural weaknesses (typically faults) in crystalline rocks. Note the pronounced NNW- to NW- trend of creeks and streams. The map on the right includes mapped fault with arrows showing slip directions in Central Park Other faults are inferred from stream patterns and topography. Epicenters of two small earthquakes in 2001 beneath Manhattan Island are also shown.

Because the contemporary stress regime in the lithosphere is oriented N64°E and also about NW-SE (Sykes and others, 2008), NYC faults are well-oriented to exhibit neotectonic activity. Arm waving aside, perhaps the Group E fractures may result from Atlantic Ocean ridge push with transform- fracture propagation into the edge of the continental crust (fig. 40). This model, proposed over twenty years ago at a GSA meeting while the audience snoozed loudly, is deemed a possible mechanism for neotectonic reactivation of these young brittle features though other mechanisms or combinations of mechanisms are clearly possible given the numerous potential inputs of neotectonic overprint.

Thus, given the modern stress regime, the presence of Group D and Group E faults in the NYC area portend seismic risk. Given the known history of time-separated moderate intensity seismic activity in New York City, the potential that a damaging earthquake may affect this densely populated area should not be ruled out. Because earthquakes *have* happened here, *can* happen here, and *will* happen here, effective pre-emptive planning to mitigate seismic hazards is an urban necessity.

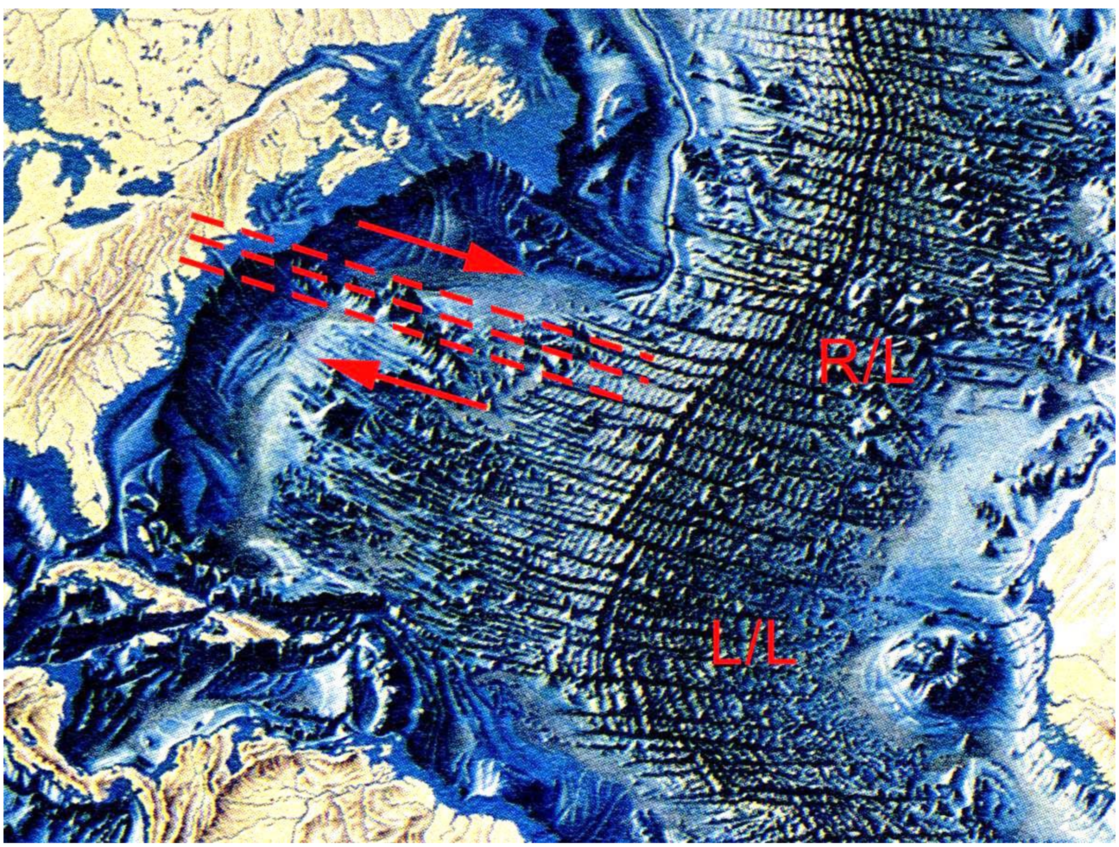

Figure 40. Contemporary NYC seismicity seems to be localized along NW-trending brittle faults. As diagrammed above, the right-lateral and left-lateral offset sense of active NYC faults may be caused by varied offset along the transcurrent faults that segment the mid-ocean ridge of the Atlantic Ocean basin. (Base map from Heezen and Tharp 1968.)

Acknowledgements

I am deeply indebted to Grow-Perini-Skanska JV, Dragados-Judlau JV, Mueser-Rutledge Consultants and the New York Botanical Garden for allowing permission to publish the scientific results of my consulting work over the years. My heartfelt gratitude is extended to these contractors, owners, and engineering firms who have provided me decades of continual access to this information and to their job sites for geological investigations. I also thank conference organizer Greg Herman for his support and interest in this work on brittle structures and his careful computer-based input and Google Earth analysis of the field data.

The support of my research by the Geology Department of Hofstra University and help from legions of students are gratefully acknowledged. Drs. Sidney Hemming of Lamont Doherty Earth Observatory and Gil Hanson of SUNY Stony Brook have provided preliminary age data on the rhyodacite dikes. The dedication of the staff at Duke Geological Laboratory (G. Glasson, H. Manne) has been instrumental in providing the assistance to perform this work.

References

Baskerville, C. A., 1989, New York City: juxtaposition of Cambrian and Ordovician miogeoclinal and eugeoclinal rocks: p. 39-48 in C. A. Baskerville, ed., Geology and engineering geology of the New York Metropolitan area, International Geological Congress, 28th, Washington, D. C., Guidebook to Field Trip T361, 59 p.

Baskerville, C. A., 1992, Bedrock and engineering geologic maps of Bronx County and parts of New York and Queens Counties, New York: U. S. Geological Survey Miscellaneous Investigations Series Map I-2003 (scale 1:24,000).

Berkey, C. P., 1911, Geology of the New York City (Catskill) aqueduct: New York State Museum Bulletin 146, 283 p.

Berkey, C. P., 1948, Engineering geology in and around New York: in Creagh, Agnes, ed., Guidebook of Excursions: Geological Society of America, 61st Annual Meeting, New York City, p. 51-66.

Brock, Pamela Chase; Brock, Patrick W. G.; and Merguerian, Charles, 2001, The Queens Tunnel Complex: a newly discovered granulite facies Fordham orthogneiss complex that dominates the subsurface of western Queens: p. 1-8 *in* Hanson, G. N., *chm*., Eighth Annual Conference on Geology of Long Island and metropolitan New York, 21 April 2001, State University of New York at Stony Brook, NY, Long Island Geologists Program with Abstracts, 128 p.

Fluhr, T. W., 1969, Recent engineering data on the New York City Group of formations, p. 1-11 *in* Alexandrov, E. A., *ed*., 1969, Symposium on the New York City Group of Formations: New York State Geological Association Annual Meeting, 40th, Flushing, New York: Flushing, NY, Queens College Department of Geology Geological Bulletin 3, Queens College Press, 83 p.

Fluhr, T. W., and Terenzio, C. G., 1984, Engineering geology of the New York City water supply system: Albany, New York, New York State Museum and Science Service, Geological Survey Open-File Report 05.08.001, 183 p.

Hall, L. M., 1968, Geology in the Glenville area, southwesternmost Connecticut and southeastern New York, Section D-6, p. 1-12 *in* Orville, P. M., ed., Guidebook for field trips in Connecticut: New England Intercollegiate Geological Conference, Annual Meeting, 60th, New Haven, Connecticut, October 1968: Connecticut Geological and Natural History Survey Guidebook 2

Hall, L. M., 1976, Preliminary correlation of rocks in southwestern Connecticut, *in* Page, L. R., ed., Contributions to the stratigraphy of New England: Geological Society of America Memoir 148, p. 337-349.

Hall, L. M., 1980, Basement-cover relations (sic) in western Connecticut and southeastern New York, p. 299-306 *in* Wones, D. R., ed., International Geological Correlation Project, Proceedings, Project 27: The Caledonides in the U. S. A.: Blacksburg, Virginia, Virginia Polytechnic Institute and State University, Department of Geological Sciences, Memoir 2, 329 p.

Heezen, B. C. and Tharp, M., 1968, Physiographic diagram of the North Atlantic Ocean (rev. ed.): Boulder, CO, Geological Society of America.

Isler, D. E., Vellone, D. A., Merguerian, Charles; and Merguerian, J. M., 2009, Redefining the southern terminus of the intrusive contact between the Yonkers and Fordham gneiss in Van Cortlandt Park, New York City, NY: *in* Hanson, G. N., *chm*., Sixteenth Annual Conference on Geology of Long Island and Metropolitan New York, 28 March 2009, State University of New York at Stony Brook, NY, Long Island Geologists Program with Abstracts, 15 p. http://www.geo.sunysb.edu/lig/Conferences/abstracts-09/isler.pdf

Kemp, J. F., 1897, The glacial or postglacial diversion of the Bronx River from its old channel: New York Academy of Sciences Transactions, v. 16, p. 18-24 (map).

Lobeck, A. K., 1939, Geomorphology. An introduction to the study of landscapes: New York and London, McGraw-Hill Book Company, Inc., 731 p.

Merguerian, C., 1981, Tectonic history of the New York City area (abstract): Empire State Geogram, v. 17, p. 28 (only).

Merguerian, C., 1983a, The structural geology of Manhattan Island, New York City (NYC), New York (abstract): Geological Society of America Abstracts with Programs, v. 15, no. 3, p. 169 (only).

Merguerian, C., 1983b, Tectonic significance of Cameron's Line in the vicinity of the Hodges Complex--an imbricate thrust model for Western Connecticut: American Journal of Science, v. 283, p. 341-368.

Merguerian, C., 1984, Revised stratigraphy of the Manhattan Schist, New York City (abstract): Empire State Geogram, v. 20, p. 28-29.

Merguerian, C., 1985c, Geology in the vicinity of the Hodges Complex and the Tyler Lake granite, West Torrington, Connecticut, p. 411-442 *in* R. J. Tracy, *ed*., New England Intercollegiate Geological Conference, 77th, New Haven, Connecticut: Connecticut Geological and Natural History Survey Guidebook No. 6, 590 p.

Merguerian, C., 1987, The geology of Cameron's Line, West Torrington, Connecticut, p. 159-164 *in* Roy, D. C., ed., Northeastern Section of the Geological Society of America, Centennial Fieldguide, Volume 5, 481 p.

Merguerian, C., 1988, Annealed mylonitic textures in polyphase deformed metamorphic terrains (abstract): Geological Society of America Abstracts with Programs, v. 20, no. 7, p. A214 (only).

Merguerian, C., 1994, Stratigraphy , structural geology , and ductile- and brittle faults of the New York City area (extended abstract), p. 49-56 *in* Hanson, G. N., *chm*., Geology of Long Island and metropolitan New York, 23 April 1994: Stony Brook, NY: Stony Brook, NY, Long Island Geologists Program with Abstracts, 165 p.

Merguerian, C., 1995, The Taconic problem--alive and well in New York City (NYC) (abstract): Geological Society of America Abstracts with Programs, v. 27, no. 1, p. 68.

Merguerian, C., 1996a, Cameron's Line mylonite zone in Connecticut and New York City - evidence for Taconian accretionary tectonics (abs.): Geological Society of America Abstracts with Programs, v. 28, no. 3, p. 81.

Merguerian, C., 1996c, Stratigraphy, structural geology, and ductile- and brittle faults of New York City, p. 53-77 *in* Benimoff, A. I. and Ohan A. A., chm., The Geology of New York City and Vicinity, Field guide and Proceedings, New York State Geological Association, 68th Annual Meeting, Staten Island, NY, 178 p.

Merguerian, C., 1999, Techniques of TBM tunnel mapping - the Queens Tunnel, NYC, p. 8-12 *in* Hanson, G. N., *chm*., Sixth Annual Conference on Geology of Long Island and

Metropolitan New York, 24 April 1999, State University of New York at Stony Brook, NY, Long Island Geologists Program with Abstracts, 143 p.

Merguerian, C., 2000, Rock mass properties of the Queens Tunnel Complex: Duke Geological Laboratory Report QT0010, 257 p., including Geological Field Map Album, Scale 1"=10' (Stations 3+65 to 254+00).

Merguerian, C., 2001, Young rhyodacite dikes found in the Queens Tunnel, beneath Woodside, Queens: p. 9-19 *in* Hanson, G. N., *chm*., Eighth Annual Conference on Geology of Long Island and metropolitan New York, 21 April 2001, State University of New York at Stony Brook, NY, Long Island Geologists Program with Abstracts, 128 p.

Merguerian, C., 2002a, Rhyodacite dikes of the Queens Tunnel Complex, NYC Water Tunnel #3 (abs.): Geological Society of America Abstracts with Programs, v. 34, no. 1, p. A75.

Merguerian, C., 2002b, Brittle faults of the Queens Tunnel Complex, NYC Water Tunnel #3: p. 63-73 *in* Hanson, G. N., *chm*., Ninth Annual Conference on Geology of Long Island and metropolitan New York, 20 April 2002, State University of New York at Stony Brook, NY, Long Island Geologists Program with Abstracts, 116 p.

Merguerian, C. and Baskerville, C. A., 1987, The geology of Manhattan Island and the Bronx, New York City, New York, p. 137-140 *in* Roy, D. C., *ed*., Northeastern Section of the Geological Society of America, Centennial Fieldguide, v. 5, 481 p.

Merguerian, C., Brock, P. C., and Brock, P. W. G., 2001, The Queens Tunnel Complex – a granulite facies orthogneiss terrane exposed in NYC Water Tunnel #3 (abs.): Geological Society of America Abstracts with Programs, v. 33, no. 6, p. A46.

Merguerian, Charles; and Merguerian, Mickey, 2004, Geology of Central Park – From rocks to ice: *in* Hanson, G. N., *chm*., Eleventh Annual Conference on Geology of Long Island and Metropolitan New York, 17 April 2004, State University of New York at Stony Brook, NY, Long Island Geologists Program with Abstracts, 24 p. http://www.geo.sunysb.edu/lig/Conferences/abstracts-04/merguerian/merguerian.htm

Merguerian, C. and Merguerian, J. M., 2012, Structural geology and metamorphism of the Inwood Marble, NYC, NY: Geological Society of America Abstract # 199974, Abstracts with Programs, v. 44, no. 2, p. 73.

Merguerian, C. and Merguerian, J. M., 2014a, Stratigraphy, structural geology and rock mass properties of the Hartland Formation, Second Avenue Subway, NYC, NY: Geological Society of America Abstract # 235972, Abstracts with Programs, v. 46, no. 2, p. 90.

Merguerian, C., Merguerian, J. M., and Cherukupalli, N. E., 2011, Stratigraphy, structural geology and metamorphism of the Inwood Marble Formation, northern Manhattan, NYC, NY: *in* Hanson, G. N., *chm*., Eighteenth Annual Conference on Geology of Long Island and Metropolitan New York, 09 April 2011, State University of New York at Stony Brook, NY, Long Island Geologists Program with Abstracts, 19 p. http://www.geo.sunysb.edu/lig/Conferences/abstracts11/merguerian-2011.pdf

Merguerian, C. and Moss, C. J., 2005, Newly discovered ophiolite scrap in the Hartland Formation of midtown Manhattan: *in* Hanson, G. N., *chm*., Twelfth Annual Conference on Geology of Long Island and Metropolitan New York, 16 April 2005, State University of New York at Stony Brook, NY, Long Island Geologists Program with Abstracts, 7p. http://www.geo.sunysb.edu/lig/Conferences/abstracts-05/merguerian-moss.htm

Merguerian, C. and Moss, C. J., 2006a**,** Structural implications of Walloomsac and Hartland rocks displayed by borings in southern Manhattan: *in* Hanson, G. N., *chm*., Thirteenth Annual Conference on Geology of Long Island and Metropolitan New York, 22 April 2006, State University of New York at Stony Brook, NY, Long Island Geologists Program with Abstracts, 12 p. http://www.geo.sunysb.edu/lig/Conferences/abstracts06/merguerian-06.pdf

Merguerian, C. and Moss, C. J., 2007, Newly discovered serpentinite bodies associated with the St. Nicholas thrust zone in northern Manhattan: *in* Hanson, G. N., *chm*., Fourteenth Annual Conference on Geology of Long Island and Metropolitan New York, 14 April 2007, State University of New York at Stony Brook, NY, Long Island Geologists Program with Abstracts, 13 p. http://www.geo.sunysb.edu/lig/Conferences/abstracts07/abstracts/merguerian-07.pdf

Merguerian, C. and Moss, C. J., 2015, Structural geology and metamorphism of the World Trade Center Site: *in* Hanson, G. N., *chm*., Twenty-second Annual Conference on Geology of Long Island and Metropolitan New York, 11 April 2015, State University of New York at Stony Brook, NY, Long Island Geologists Program with Abstracts, 12 p. http://www.geo.sunysb.edu/lig/Conferences/abstracts-15/merguerian-moss.pdf

Merguerian, C.; and Ozdemir, L., 2003, Rock Mass Properties and Hard Rock TBM Penetration Rate Investigations, Queens Tunnel Complex, NYC Water Tunnel #3, Stage 2: p. 1019-1036 in Robinson, R. A. and Marquardt, J. M., eds., Rapid Excavation and Tunneling Conference, 2003 Proceedings, 1334 p.

Merguerian, C. and Sanders, J. E., 1991b, Trip 16: Geology of Manhattan and the Bronx, 21 April 1991: New York Academy of Sciences Section of Geological Sciences Trips on the Rocks Guidebook, 141 p.

Merguerian, Charles; and Sanders, J. E., 1993b, Trip 26, Cameron's Line and The Bronx parks, 08 May 1993 (revision of Trip 21, 24 November 1991): New York Academy of Sciences Section of Geological Sciences Trips on the Rocks Guidebook, 126 p.

Merguerian, Charles; and Sanders, J. E., 1993d, Trip 28, Geology of southern Central Park, New York City, 26 September 1993: New York Academy of Sciences Section of Geological Sciences Trips on the Rocks Guidebook, 143 p.

Merguerian, Charles; and Sanders, J. E., 1996a, Diversion of the Bronx River in New York City - evidence for postglacial surface faulting?, p. 131-145 *in* Hanson, G. N., *chm*., Geology of Long Island and metropolitan New York, 20 April 1996, State University of New York at Stony Brook, NY, Long Island Geologists Program with Abstracts, 177 p.

Merguerian, Charles; and Sanders, J. E., 1996b, Contrasting styles of the Taconic orogeny in New York: deep- vs. shallow thrusts, p. 116-130 *in* Hanson, G. N., *chm*., Geology of Long Island and metropolitan New York, 20 April 1996, State University of New York at Stony Brook, NY, Long Island Geologists Program with Abstracts, 177 p.

Merguerian, Charles; and Sanders, J. E., 1997, Bronx River diversion: neotectonic implications (abs.): Paper No. 198, p. 710 *in* Hudson, J. A. and Kim, Kunsoo, *eds.*, International Journal of Rock Mechanics and Mining Sciences, Special Issue, 36th U.S. Rock Mechanics Symposium, Columbia University, New York, June 29-July 02, 1997, v. 34, no. 3/4, 714 p. Full version on CD-ROM, 10 p.

Merrill, F. J. H.; Darton, N. H.; Hollick, Arthur; Salisbury, R. D.; Dodge, R. E.; Willis, Bailey; and Pressey, H. A., 1902, Description of the New York City district: United States Geological Survey Geologic Atlas of the United States, New York City Folio, No. 83, 19 p. (Includes colored geologic map on a scale of l:62,500).

Sanders, John E., and Merguerian, Charles, 1998, Classification of Pleistocene deposits, New York City and vicinity – Fuller (1914) revived and revised: p. 130-143 *in* Hanson, G. N., *chm*., Geology of Long Island and Metropolitan New York, 18 April 1998, State University of New York at Stony Brook, NY, Long Island Geologists Program with Abstracts, 161 p.

Sykes, L., R., Armbruster, J. G., Kim, Won-Young, and Seeber, Leonardo, 2008, Observations and tectonic setting of historic and instrumentally located earthquakes in greater New York City - Philadelphia area: Seismological Society of America Bulletin, Vol. 98, No. 4, pp. 1696-1719.

Chapter 3. Re-Os isotope evidence of Early Tertiary crustal faulting and sulfide-mineralization in Pennsylvania with probable ties to the Chesapeake Bay bolide impact in Maryland, USA.

Ryan Mathur[1] David P. Gold[2], Chad J. Ellsworth[3], Arnold G. Doden[4], Marc Wilson[5], Joaquin Ruiz[6], Barry E. Scheetz[3], and Gregory C. Herman[7]

[1] Juniata College Department of Geology, Huntington, PA
[2] The Pennsylvania State University Department of Geosciences, University Park, PA
[3] The Pennsylvania State University Department of Civil Engineering, University Park, PA
[4] Geologic Mapping and Resource Evaluation, Inc., State College, PA
[5] Carnegie Museum of Natural History, Pittsburgh, PA
[6] Department of Geosciences, University of Arizona, Tucson, AZ
[7] New Jersey Geological & Water Survey, Trenton, NJ

Abstract

Re-Os isotope measurements of sulfide minerals from 11 occurrences that span a radial distance of over 200 Km serve to geochemically link epithermal mineralization in Pennsylvania and New Jersey to an Eocene event. The most likely geologic event that could have influenced the area during the Eocene is the Chesapeake Bay impact event. The significance of the discovery is twofold: no epithermal mineralization has been linked to the Chesapeake Bay impact to date nor has the process been clearly identified throughout the region.

Introduction

During the construction of a major interstate road (I-99) in Centre County, Pennsylvania (fig. 1) an epithermal pyrite deposit was unearthed. The study by Mathur (2008) examined the origin of the sulfide mineralization at this location. With Re-Os data measured in sulfide minerals and fluid inclusion data from co-genetic quartz, they interpreted a younger 33.8 ± 4MA, high temperature (>200^{o}C) mineralization event (represented by fault breccia pyrite) overprinted the Mississippi Valley type mineralization (termed MVT and represented by vein pyrite). The timing of the younger mineralization event coincides with two Cenozoic events in the Appalachian Basin: the Chesapeake Bay impact and Eocene volcanism in the southern portion of the Nittanny anticlinorium (Dennison, 1971).

The significance of the overprinted Eocene age becomes apparent by examination of previous models that described sulfide deposit genesis related to older mineralization events. Two timeframes for mineralization have been suggested for MVT deposits in the Appalachians:

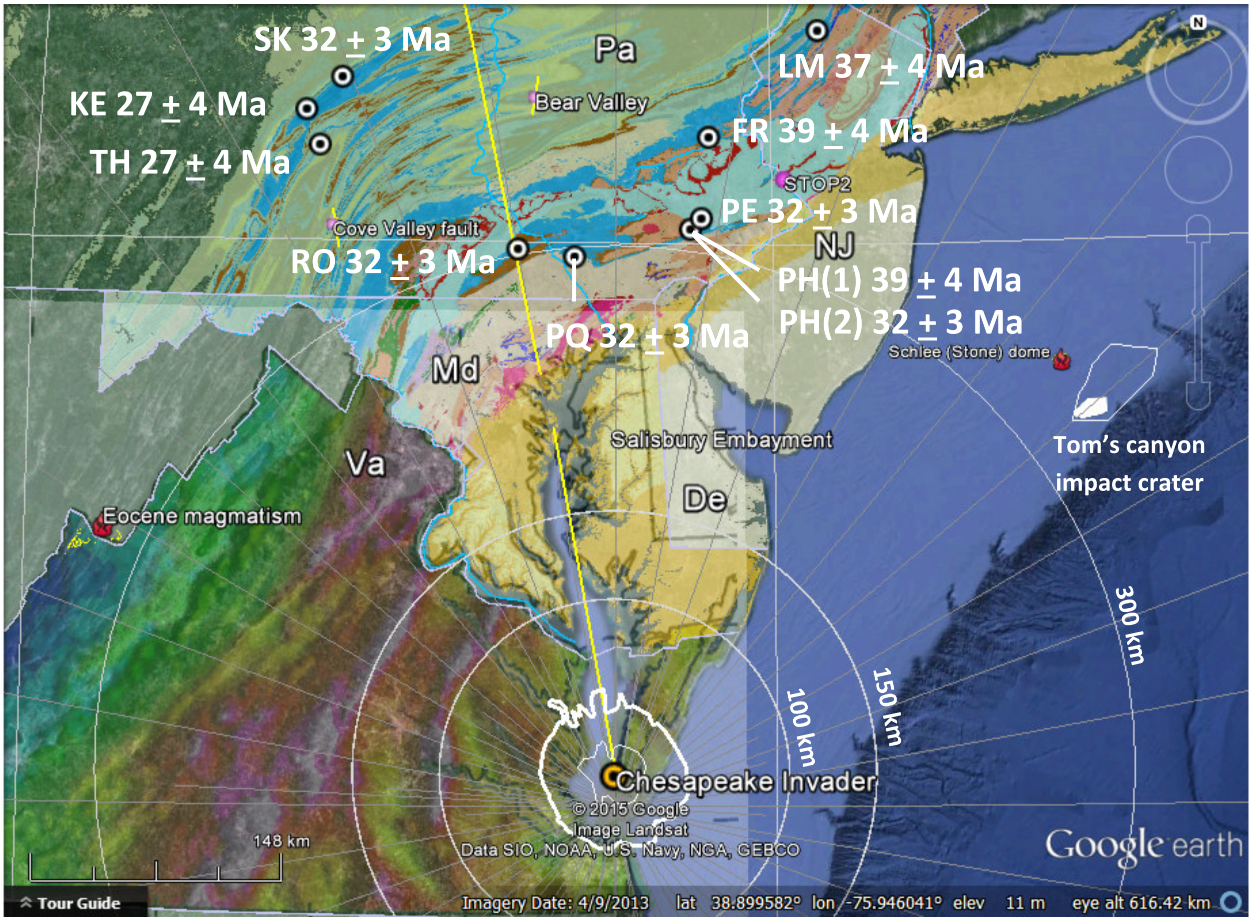

Figure 1. Location map of nine of eleven (11) epithermal sulfide deposits in Pennsylvania and New Jersey analyzed in this report for Re-Os radioisotope ages. Also shown are the locations of late Eocene igneous rocks in West Virginia and Virginia (Southworth and others, 1993; Tso and others, 2004), and the Tom's Canyon impact structure (Poag and Pope, 1988). The two base themes include an integrated, generalized, geological theme covering Maryland through New Jersey adapted from the USGS (see Chapter 4 for explanation and unit key), and a Bouger Gravity anomaly map of Virginia (http://pubs.usgs.gov/of/2005/1052/html/va_grav_large.htm) showing rings of 100- and 150-km radii surrounding the Chesapeake impact crater. The presumed direction of bolide flight is from the SSE to NNW along the bright yellow line extending from the crater up the spine of Chesapeake Bay, following a primary direction of crustal compression resulting from a directed, oblique, hypervelocity strike of the crust. The light gray lines project from the crater outward into the surrounding, like wheel spokes, one which symmetrical bisects the Tom's Canyon impact structure.

1) Radiometric dates from alteration silicates indicate that mineralization occurred in the late Permian age (Hearn, 1987), and

2) Structural geology (Kesler, 1990) indicates a Devonian age.

Traditional models of sulfide deposition in the area have favored two different models (similar to the genesis of base metal occurrences in the mid-continent): as related to an extension of a larger MVT system (Heyl, 1982) or as related to diagenesis (Kutz, 1989). For instance, fluid inclusion studies of quartz in the gossans and sulfur isotope studies of sulfides from Pb-Zn occurrences by Howe (1981) indicated that MVT processes occurred in the area. The second model relates mineralization could have formed during diagenesis. Rose (2005) used trace and major element geochemical signatures from the veined sulfides and host rocks to argue that the sulfides formed during diagenesis as a result of sulfidation of the host rock.

Mineralization throughout central and eastern Pennsylvania has been geochemically linked to MVT-like processes. Kesler and van der Pluijm (1990) (the study identified similarity of Pb isotopic composition of ore from the Keystone mine and Friedensville to other Appalachian MVT deposits), Kesler et al., 1995 (the study identified similarities of fluid inclusion evidence from the Schad and Keystone to other Appalachian MVT deposits), and Appold (1995) (the study correlated sulfur isotope data for the Appalachian MVT and the data collected by Howe (1981) to indicate a common source of sulfur for these deposits) link Pb + Zn mineralization in Pennsylvania to Appalachian MVT deposits. The results were interpreted to indicate that mineralizing fluids formed by a combination of connate and formation water brines most likely mobilized by Alleghanian orogenesis (between 280-310 Mya), with ore deposition analogous to Mississippi Valley-type Pb-Zn deposits (further described in Oliver, 1986).

This contribution explores the extent and overall impact of the previously unknown Eocene event. Previous studies identified and described Pb-Zn sulfide occurrences in Paleozoic strata in this area of the Valley and Ridge Province and several other locations in eastern Pennsylvania (Howe, 1981; Rose, 1999; Smith, 1977). Thus, to further understand the origin of epithermal sulfide deposits in the area and the extent of the younger mineralization, we measured the Re-Os contents of sulfides from 10 different mineral locations (fig. 1) spread throughout eastern to western Pennsylvania and New Jersey. The selection of the suite of deposits provides the following comparative analysis:

1. We chose both minor occurrences (Thompson mine, Keystone mine, and Roosevelt mine) along with the historically largest Pb-Zn mines in Pennsylvania (Pequa mine, Friedensville mine and Phoenixville mine).

2. The selected deposits span a large geographic region. The inclusion of eastern Pennsylvania and New Jersey sulfide occurrences allows for improved interpretation for the causes associated with the Eocene mineralization event.

Methods

Samples for the Pennsylvania sulfides were obtained from the collections at the Carnegie Museum of Natural History, Hillman Hall of Minerals; samples for the New Jersey sulfides were obtained from drill cores and hand specimens. No fresh sulfides from the historic mine sites were collected due to the chemical weathering of sulfides in a humid climate. The samples were hand-picked and powdered for analyses.

To characterize the mineralogy and chemistry of the samples, powdered X-ray diffraction (XRD) were performed on the sulfides. XRD analysis was conducted using a Scintag X-ray powder diffractometer. XRD scans were completed in slow, step-scan mode for precision analysis. For Re-Os analysis, 0.7 to 2.1g sulfide mineral powders were completely dissolved by the carius tube method (Shirey, 1995). Os and Re were separated by distillation and ion exchange chromatography, respectively (Mathur, 2000c). Samples were loaded into a thermal ionization mass spectrometer as salts (Creaser et al., 1991) and concentrations of Re and Os were determined by isotope dilution. Blank measurements for Re and Os ranged from 24-41 picograms and 0.4-1.2 picograms respectively, and the measured 187Os/188Os of the blank was 0.20 ± 0.02 throughout this study. All measurement errors have $2\sigma<0.5\%$; however, the greatest source of error in the measurement is the Os blank. Therefore, errors reported in Table 1 were calculated by varying the concentration of the Os blank between 1 and 2 picograms (further discussion in Mathur, 2000).

Results

The XRD mineral identifications as well as the Re-Os concentration and isotope ratios are reported in table 1. The concentration of Re and Os range from 0.2- 2.3 part per billion (ppb) and 3-50 parts per trillion (ppt), respectively. A comparison of average concentration with 1 sigma errors of Re and Os in sphalerite (0.92 ± 0.80 ppb and 10 ± 9.2 ppt), pyrite (0.95 ± 0.9 ppb and 9 ± 6 ppt) and galena (1.1 ± 0.4 ppb and 33 ± 14 ppt) does not reveal any mineral phases containing higher concentrations of either element. The overall average concentrations of Re and Os are similar to those measured in porphyry copper deposits and other types of epithermal mineralization (Mathur, 2000a, b, 2002, 2005; Mathur et al., 2003).

Isochron plots of the data reveal three linear trends (fig. 2). The calculated ages of the trends were determined using a conventional isochron plot with the ratios of daughter (^{187}Os/^{188}Os) versus parent (^{187}Re/^{188}Os) plots: $^{187}Os_m = {}^{187}Os / {}^{187}Os_i + {}^{187}Re_m(e^{\lambda t}-1)$; where: m= measured, λ= decay constant, t= time, i= initial (Ludwig, 2001). The decay constant we used for Re is $1.66 \times 10^{-11}\ yr^{-1}$ (Selby et al., 2007). Four samples from Phoenixville and Freidensville lie on a trend that yields a Model 1 age of 39 ± 4 Ma, $^{187}Os/^{188}Os_i$= 0.27± 0.03, MSWD= 1.3. Three samples from Keystone and Thompson lie on a trend that yields an age of 27 ± 4 Ma,

$^{187}Os/^{188}Os_i = 0.05 \pm 0.04$; because three points does not possess statistical significance no MSWD is reported. Sixteen samples from Skytop, Pequa, Perkiomen, and Roosevelt lie on a trend that yields a Model 3 age of 32 ± 3 Ma, $^{187}Os/^{188}Os_i = 0.23 \pm 0.03$, MSWD= 5.3. The ages overlap within reported errors, with the exception of the samples from the Keystone and Thompson mines, which lie slightly younger than the other trends on the isochron plot. The initial Os ratio is relatively consistent for all isochrons and possesses a significant non-radiogenic source for Os.

Table 1. Re-Os analytic analyses from Ten Mines in Pennsylvania having late Eocene hydrothermal event with sulfide minerals

Mine-sample #	County	Mineral	Re (ppb)	Os (ppt)	$^{187}Re/^{188}Os$	error	$^{187}Os/^{188}Os$	error
Thompson	Mifflin	pyrite	2.30	19	1142	103	0.53	0.03
Roosevelt	Mifflin	sphalerite	0.33	17	90	8	0.29	0.02
Keystone-Gn-1	Juniata	galena	1.15	19	377	34	0.21	0.01
Keystone-Sph-1	Juniata	sphalerite	3.03	18	833	75	0.43	0.03
Perkiomen	Montgomery	pyrite	0.65	11	365	33	0.41	0.02
Perkiomen	Montgomery	sphalerite	1.10	5	574	52	0.47	0.03
Perkiomen-657	Montgomery	sphalerite	0.41	5	371	33	0.41	0.02
Perkiomen	Montgomery	pyrite	1.08	3	1906	172	0.23	0.01
Perkiomen- 700	Montgomery	pyrite	0.20	5	224	20	0.32	0.02
Perkiomen- 25692	Montgomery	sphalerite	1.24	30	203	18	0.29	0.02
Friedensville- 702	Lehigh	sphalerite	0.54	4	699	63	0.71	0.04
Friedensville- 703	Lehigh	sphalerite	0.31	15	118	11	0.36	0.02
Phoenixville- 1-689	Chester	sphalerite	0.76	5	849	76	0.88	0.05
Phoenixville- 1-690	Chester	sphalerite	0.82	2	894	107	0.90	0.07
Phoenixville- 1-6920	Chester	galena	1.48	30	250	23	0.32	0.02
Phoenixville 2-1	Chester	sphalerite	0.65	3	1049	126	0.66	0.06
Phoenixville 2-2	Chester	galena	0.43	21	106	10	0.29	0.02
Phoenixville 2-3	Chester	pyrite	0.50	7	2312	208	0.91	0.05
Pequa Gal	York	galena	1.29	50	119	11	0.29	0.02
Pequa Gal	York	galena	1.20	46	110	10	0.27	0.02
Little Juniata	Centre	pyrite	0.495	19.000	1309	118	0.850	0.051
Little Juniata	Centre	pyrite	0.543	24.000	1319	119	0.870	0.052
Lafayette	New Jersey	sphalerite	3.32	5	9004	540	6.4	0.38

Discussion

The Re-Os results from the sulfides serves to geochemically link the epithermal deposits to an Eocene age and relatively non-radiogenic sources of Os. Two aspects of the results tie the 10 analyzed occurrences (spanning over 200 Km radial distances to one another) to a similar event. First, multiple deposits that exist in western and eastern Pennsylvania (Pequa, Skytop, Roosevelt, and Perkiomen) fall along similar trends on the isochron diagram indicating a similar source fluid precipitated mineralization. Secondly, the calculated age and initial Os ratios for Layfayette, Pequa, Skytop, Roosevelt, Perkiomen, Phoenixville and Friedensville overlap. This overlap indicates that mineralization age and source could be the same. The Thompson and

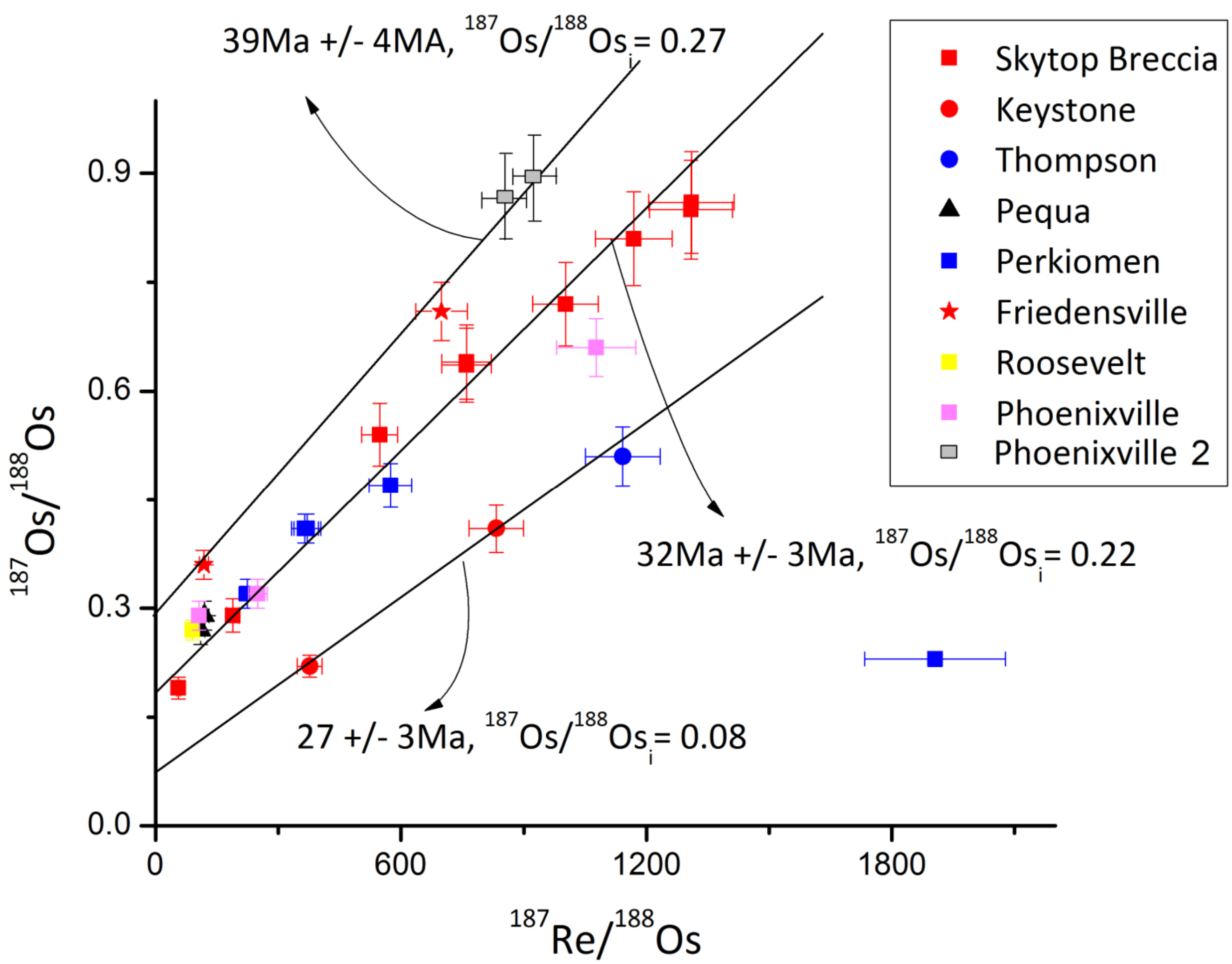

Figure 2. Re-Os isochron plots of sulfide minerals analyzed for eight (8) locations in Pennsylvania (fig. 1). Results from Lafayette Meadows (LM) are not plotted because the Re/Os ratios are significantly larger and the trends become difficult to view.

Keystone results do not overlap with the Eocene age and have an Os initial ratio that barely overlaps with chondritic mantle. Although inconsistent with the other 8 occurrences, the young age and non-radiogenic Os initial ratio clearly point to a process not related to MVT-style mineralization.

Mathur and others (2008) hypothesized the young mineralization event related to two possible causes, the Chesapeake Bay impact or Eocene volcanism present in southerly portions in the same geologic structure (the Eocene volcanics are labeled in fig. 1). However, because the deposits analyzed span a larger geographic region, the Eocene volcanism present in the West Virginian portions of the Appalachians (Southworth and others, 1993; Tso and others, 2004) could not be a cause for the mineralization in eastern Pennsylvania. No geologic relationships tie the Lafayette, Phoenixville, Friedensville, Perkiomen or Pequa with the alkalic volcanism present in West Virginia. Also kimberlites occur in this that could have caused mineralization area (Bikerman and others, 1997), however the ages of known kimberlite activity do not coincide with the Re-Os ages determined here. Therefore, the young event that might have impacted mineralization in eastern Pennsylvania is the Chesapeake Bay impact. Tom's Canyon impact identified in the Atlantic Ocean tens of kilometers east of New Jersey could also be important as it occurred at roughly the same time (Poag, 1998b).

Constraining the cause to the Chesapeake Bay impact is the most significant interpretation of the dataset. The impact crater sits at the mouth of Chesapeake Bay (fig. 1) and is currently the fifth largest recognized meteoric impact crater on Earth. As first identified by Wiley Poag in 1997, it represents a major tectonic event for the eastern continental margin of the North American Plate (Koeberl and others, 1996; Poag, 1996; Poag and others, 2009). Dating of the impact places it at 35±0.5 million years ago. Manifestations of this event include tsunami deposits on the Atlantic shelf to the north, and a tektite ejecta field in the Atlantic Ocean, and as the source for the locally distributed jasper-pebble deposits in northeastern Virginia. One of the authors, as part of an FHWA SHRP program in 1985, identified echelon quartz twinning in petrographic thin sections of the Townson gravel, a quartz aggregate use locally for concrete formulations. But just how the impact lead to the genesis of the epithermal sulfide veining event throughout Pennsylvania remains unclear. Links between ore deposits and impacts is not a new discovery. Many studies have demonstrated impacts such as Sudbury, Canada and the Vredefort dome in South Africa caused mineralization (Grieve, 1994; Grieve, 2005; Reimold and others, 2005). In fact, Grieve defined three general types of mineralization associated with meteor impacts: progenetic (ores existing before impact), syngenetic (formed during) and epigenetic (post impact). The isotopic and field evidence indicate that the mineralization analyzed here is epigenetic.

The exact processes that lead to mineralization could be related to two general mechanisms: hydrothermal convection cells driven by the heat of the impact or release of mantle fluids analogous to antipodal volcanism associated with impacts. With respect for the hydrothermal-convection mecahanism, breccias and ores associated with the Sudbury and Vredefort large impacts are thought to be associated with hydrothermal flow of meteoric fluids associated with convective flow spanning up to 8 km (Pirajno, 2005). But the distribution of breccia and mineralization seen in this region would require meteoric-driven mineral sources driven by heat to occur over hundreds of square kilometers, making it highly unlikely. However, two factors associated with the Chesapeake Bay impact may have allowed for the existence of a larger hydrothermal system. The Chesapeake impact occurred near or within seawater and the surrounding crust contains several overlapping joints and faults that would serve as ideal conduits for fluid flow. The preexisting fracture network is not clearly defined; however the Roosevelt, Thompson and Keystone sites are associated with the well documented and studied Tyrone/Mt. Union lineament (Gold, 1999), where mineralization has been recognized for nearly 200 years. Gold (1999) also reports an alignment of sulfide mineralization along a short lineament in Montgomery County which included the Perkiomen mine. The Skytop deposit represents a juncture of a minor lineament and a recognized fault. Many other lineaments exist throughout the eastern and western Pennsylvania that could have served as conduits due to an orogenic history that has at least four mountain building events (Grenville, Taconic, Acadian, Alleghanian) impacting the area over the past billion years.

The second mechanism that could lead to mineralization is for the ground shock of impact to drive a fluid release from mantle depths, as evidenced by fluid inclusion temperatures of 400^{o}C (Howe, 1981; Mathur and others, 2008). The fluids would have risen to the surface through a plumbing system comprised of either preexisting fractures, impact-generated fractures, or a combination of both. The nearly 0 ‰ per mil sulfur isotope data for Friedensville presented by Kesler and van der Plujm (1990) could be interpreted as a magmatic sulfur isotope signature. Continued analyses of other sulfide occurrences throughout the radial impact area should illuminate which pathways served as channels for the epithermal mineralization.

Aside from understanding processes associated with impacts of meteors, this identification of large-scale mineralization in Pennsylvania associated with the Chesapeake Bay impact has long-range implications for future exploitation of economic resources, as well as a direct impact on the civil transportation infrastructure. The Interstate 99 example resulted in $80 million dollar expenditure by the Commonwealth of Pennsylvania to remediate the effects of acid rock drainage that was a direct consequence of the exposure and weathering of pyrite in this deposit. The extent of the mineralization proposed in this hypothesis has not yet been fully delineated. There is no reason to believe that the observed regional mineralization is limited just to Pennsylvania and New Jersey. Applying a systematic radius about the impact crater for a radial distance to Lafayette Meadows, NJ or Skytop, PA suggests that areas as far south as South Carolina and as far north as Connecticut including West Virginia, Virginia, Maryland, New York, and Delaware may contain similar structures and mineralization. As seen in figure 1, Eocene magmatism occurs at radial distances of over 300 km from the crater.

Acknowledgements

We would like to thank MAUTC, ACS and the Pennsylvania DCNR for their kind support of the project. The project was greatly aided by the assistance of D. Nicholas and G. Huston.

References

Altamura, R.J., Weil, A.B., Van der Voo, R., 1999, Paleomagnetic results provide evidence for Early Triassic extension in the Valley and Ridge terrane, central Appalachians: Geological Society of America Annual Meeting Abstracts with Programs, v. A-476.

Appold M.S., K.S.E., Ah J. , 1995, Geochemical constraints on the genesis of Mississippi Valley-type mineralization in the central Appalachians: Economic Geology, v. 90, p. 902-919.

Bikerman, M., Prellwitz, H.S., Dembosky, J., Simonetti, A., and Bell, K., 1997, New phlogopite K-Ar dates and the age of southwestern Pennsylvania kimberlite dikes: Northeastern Geology and Environmental Sciences, v. 19, p. 302-308.

Creaser, R. A., Papanastassiou, D. A., and Wasserburg, G. J., 1991, Negative thermal ion mass spectrometry of osmium, rhenium and iridium: Geochimica et Cosmochimica Acta, v. 55, p. 397-401.

Dennison J. M, Jr., 1971, Tertiary instrusions and associated phenomena near the 38th parallel fracture zone in Virginian and West Virginia: Geological Society of America Bulletin, v. 111, p. 501-508.

Gold, D. P., 1999, Lineaments and their interregional relationships: Special Publication - Geological Survey of Pennsylvania, p. 306-313.

Grieve, R. A. F., 1994, The economic potential of terrestrial impact craters, *in* Masaitis, V. L., ed., International Geology Review, Volume 36: United States, Winston & Son : Silver Spring, MD, United States, p. 105-151.

—, 2005, Economic natural resource deposits at terrestrial impact structures, Geological Society Special Publications, Volume 248: United Kingdom, Geological Society of London: London, United Kingdom, p. 1-29.

Hearn P. P, Sutter, S. J., Belkin HE, 1987, Evidence for late Paleozoic brine migration in Cambrian carbonate rocks of the central and southern Appalachians: Implications for Mississippi Valley-type sulfide mineralization: Geochimica et Cosmochimica Acta, v. 51, p. 1323-1334.

Heyl A. V., W. W. S., 1982, Outlying mineral occurrences related to the Upper Mississippi Valley mineral district, Wisconsin, Iowa, Illinois, and Minnesota: Economic Geology, v. 77, p. 1803-1817.

Howe, S. S., 1981, Mineralogy, fluid inclusions, and stable isotopes of lead-zinc occurrences in central Pennsylvania State College, Pennsylvania State University.

Kesler S. E, van der Plum, B., 1990, Timing of Mississippi Valley-type mineralization: Relation to Appalachian orogenic events: Geology, v. 18, p. 1115-1118.

Koeberl, C., Poag, C. W., Reimold, W. U., and Brandt, D., 1996, Impact origin of the Chesapeake Bay structure and the source of the North American tektites: Science, v. 271, p. 1263-1266.

Kutz K. B., Spry, P. G., 1989, The genetic relationship between Upper Mississippi Valley lead-zinc mineralization and minor base metal mineralization in Iowa, Wisconsin, and Illinois: Economic Geology, v. 85, p. 2139-2154.

Mathur, R. D., 2000a, Different crustal sources for Au-rich and Au-poor ores of the Grasberg Cu-Au porphyry deposit, *in* Ruiz, J., Titley, S., Gibbins, S., and Margotomo, W., eds., Earth and Planetary Science Letters, Volume 183: Netherlands, Elsevier: Amsterdam, Netherlands, p. 7-14.

—, 2000b, Relationship between copper tonnage of Chilean base-metal porphyry deposits and Os isotope ratios, *in* Ruiz, J., and Munizaga, F., eds., Geology [Boulder], Volume 28: United States, Geological Society of America (GSA): Boulder, CO, United States, p. 555-558.

—, 2002, Age of mineralization of the Candelaria Fe oxide Cu-Au deposit and the origin of the Chilean iron belt, based on Re-Os isotopes, *in* Marschik, R., Ruiz, J., Munizaga, F., Leveille, R.A., and Martin, W., eds., Economic Geology and the Bulletin of the Society of Economic Geologists, Volume 97: United States, Economic Geology Publishing Company : Lancaster, PA, United States, p. 59-71.

—, 2005, A Re-Os isotope study of sedimentary rocks and copper-gold ores from the Ertsberg District, West Papua, Indonesia, *in* Titley, S., Ruiz, J., Gibbins, S., and Friehauf, K., eds., Ore Geology Reviews, Volume 26: International, Elsevier: Amsterdam, International, p. 207-226.

Mathur, R. D., Mutti, L., Barra, F., Gold, D., Smith, R. C., Doden, A., Detrie, T., Mc Williams, A. , 2008, Fluid inclusion and Re-Os isotopic evidence for hot, Cenozoic mineralization in the central Pennsylvanian Valley and Ridge Province: Mineralogy and Petrology, v. 93, p. 309-324.

Mathur, R., Ruiz, J., Herb, P., Hahn, L., and Burgath, K. P., 2003, Re-Os isotopes applied to the epithermal gold deposits near Bucaramanga, northeastern Colombia: Journal of South American Earth Sciences, v. 15, p. 815-821.

Mathur, R. D., 2000c, Re-Os isotopes of base metal porphyry deposits: United States.

Oliver, J., 1986, Fluids expelled tectonically from orogenic belts: Their role in hydrocarbon migration and other geological phenomena.: Geology, v. 14, p. 99-102.

Pirajno, F., 2005, Hydrothermal processes associated with meteorite impact structures; evidence from three Australian examples and implications for economic resources, Australian Journal of Earth Sciences, Volume 52: Australia, Blackwell Scientific Publications for the Geological Society of Australia: Melbourne, Victoria, Australia, p. 587-605.

Poag, C. W., 1996, Structural outer rim of Chesapeake Bay impact crater; seismic and borehole evidence: Meteoritics, v. 31, p. 218-226.

Poag, C. W., 1997, The Chesapeake Bay bolide impact-a convulsive event in Atlantic Coastal Plain evolution, in Seagall, M., Colquhoun, DJ, and Siron, ed., Evolution of the Atlantic Coastal Plain-sedimentology, stratigraphy, and hydrogeology: Sedimentary Geology, v. 108, no. 1-4, p. 45-90.

—, 1998a, The Toms Canyon structure, New Jersey outer continental shelf; a possible late Eocene impact crater, *in* Poppe, L. J., ed., Marine Geology, Volume 145: Netherlands, Elsevier: Amsterdam, Netherlands, p. 23-60.

Poag, C. W., Koeberl, C., Miller, K. G., and Reimold, W. U., 2009, Paleoenvironmental recovery from the Chesapeake Bay bolide impact; the benthic foraminiferal record: Special Paper - Geological Society of America, v. 458, p. 747-773.

Poag, C. W., Koeberl, C., and Reimold, W. U., 2004, The Chesapeake Bay Crater: Geology and geophysics of a Late Eocene Submarine Impact Structure.: Berlin, Springer.

Poag, C. W. and Pope, L. J., 1998, The Toms Canyon structure, New Jersey outer continental shelf; a possible late Eocene impact crater, *in* Poppe, L.J., ed., Marine Geology, Volume 145: Netherlands, Elsevier: Amsterdam, Netherlands, p. 23-60.

Reimold, W.U., Koeberl, C., Gibson, R.L., and Dressler, B.O., 2005, Economic mineral deposits in impact structures; a review Impact studies: Federal Republic of Germany, Springer Verlag: Berlin, Federal Republic of Germany, 479-552 p.

Rose, A.W., 1999, Metallic mineral deposits; zinc-lead-silver: Special Publication - Geological Survey of Pennsylvania (1999), p. 582-587.

Selby, D., Creaser, R.A., Stein, H.J., Markey, R.J., and Hannah, J.L., 2007, Assessment of the 187Re decay constant by cross calibration of Re-Os molybdenite and U-Pb zircon chronometers in magmatic ore systems: Geochimica et Cosmochimica Acta, v. 71, p. 1999-2013.

Shirey S., Walker, R., 1995, Carius tube digestion for low-blank rhenium-osmium analysis: Analytical Chemistry, v. 67, p. 2136-2141.

Smith R. C, II, 1977, Zinc and lead occurrences in Pennsylvania: Harrisburg, Pennsylvania Geological Survey mineral resources, p. 318.

Smith, R. C., II, Foland, Kenneth A., and Nickelsen, Richard P., 2004, The Lower Silurian Clear Springs volcanic suite; Sword Mountain olivine melilitite (433 ±3 Ma) and Hanging Rock Diatreme, Washington County, Maryland Geological Society of America NE and SE Sections, Abstracts with Programs, v. 36, p. 71.

Southworth, C. S., Gray, K. J., Sutter, J. F., and de Witt, W., 1993, Middle Eocene intrusive igneous rocks of the central Appalachian Valley and Ridge Province; setting, chemistry, and implications for crustal structure: U. S. Geological Survey Bulletin, p. J1-J24.

Tso, J. L., McDowell, R. R., Avary, K. L., Matchen, D. L., and Wilkes, G.P., 2004, Middle Eocene igneous rocks in the Valley and Ridge of Virginia and West Virginia: U. S. Geological Survey Circular, p. 137-161.

Chapter 4. Neotectonics of the New York Recess, USA

Gregory C. Herman, NJ Geological & Water Survey, Trenton, NJ 08625

Abstract

The present-day (neo-) tectonic framework of the west central Atlantic continental margin centered on New Jersey is mapped using digital geophysical and geological data with Google Earth (GE). The incorporated data themes are available from our internet web site www.ganj.org/2015/data.html. These data include some samples of high-precision, laser-based (LiDAR) topographic surveys in the form of hill-shaded raster imagery that were used in conjunction with GE's aerial imagery to help portray our neotectonic setting. Other incorporated geological themes include 1) historical earthquake occurrences, some of which provide focal-mechanism solutions for the current state of crustal stress, 2) current crustal motions including long-term determinations of horizontal drift and vertical ground motion gained from ground-fixed and continuously monitored global-positioning-systems (GPS), 3) and regional geological themes portraying geological strata and trends of secondary tectonic structures including fold axes and major facture systems. These themes are used to gain a perspective on the latest brittle structures that may have originated in our current state of crustal stress, that are seen in outcrop or the shallow subsurface using geophysical methods, and that overprint older paleotectonic (ancient) structures. A simple set of chronostratigraphic groups are used that divide our regional strata into sections separated by major unconformities that are then used to summarize, review, and discuss structural features within each section with respect to their spatial distribution and kinematics. This systematic approach towards cataloguing our current geological setting results in the portrayal and definition of some newly recognized regional geological features and points to the need for a reappraisal of some older, classic interpretations of structural and tectonic stages that have impacted our region during the Mesozoic and Cenozoic eras. Although Mesozoic structures and their overprint of earlier Paleozoic and Proterozoic ones aren't neotectonic in nature, recognition of these older features in the various chronostratigraphic groups is important when considering the latest brittle structures occurring here that may have formed in our current state of crustal stress, or were reactivated in the relatively recent geological past because of their favorable orientations with respect to on-going Earth processes that incite brittle failure of the crust. Because of the geological complexity of this region, and the voluminous tectonic and structural data available for inclusion, it is impractical to cover all of the details involved in this process. Instead, an approach is taken where particular, detailed studies that best exemplify the end goals are integrated and illustrated to set the stage for further efforts along these lines.

Introduction

The theme for this year's GANJ conference and field trip is *Neotectonics of the New York Recess*. This is the first time in our organization's three decade long history that we have tackled the topic of our current tectonic setting. Perhaps it's because we sit on the eastern margin of the North American continent, a region of extreme human population and infrastructure that is generally considered to be tectonically passive by virtue of a lack widespread orogenic activity, and where only occasional, subtle glimpses of contemporary or historical tectonic activity occur. Or perhaps recent technological breakthroughs have led us to this point where precise and robust data sets are now available for the type of integration and comparison that enable characterization of the relatively subdued tectonic effects occurring here.

Only recently have Earth scientists gained free and open access to the kinds of universally uniform computer platforms and visualization software necessary to access, integrate, generate, and communicate the myriad data sets needed to characterize the subtle neotectonic aspects of a geologically complex region. With these tools and data, a vast number of spatially referenced geoscience themes are now easily compared and contrasted, allowing us to explore the more elusive links between our current states of crustal stress, current plate motions in 3D, and hence our current, or neotectonic, setting. These tools also provide the means by which to emphasize the distribution and nature of the youngest brittle structures in our region. This focus on brittle structures is simply because most common strain responses to imposed stresses on Earth's crust at land surface are elastically bending and fracturing. Earthquakes for example signal brittle-fracture response within the upper 20 km of our crust (Sykes and others, 2006). Widespread and pervasive tensile fractures associated with Mesozoic rifting distributed across broad swaths of the Appalachian foreland culminations and basins have control over the uneven and scalloped nature of our continental margin. Yet, superimposed on these Mesozoic tensile and transtentional features are younger brittle features that are commonly discordant with respect to all earlier finite-strain axes.

As presented in this chapter, integration of neotectonic aspects of this region noted in earlier chapters with the results of the above types of evaluation lends support to new tectonic interpretations, introduced here, that begin to shed light on some of the unexplained, relatively recent epeirogenic movements noted in our region. This chapter summarizes what is currently known about the neotectonic setting and structural framework of the Appalachian region centered about New Jersey, near geographic coordinate's 40^{o} N latitude and 74^{o} W longitude. This region happens to comprise the ill-defined junction between the central and northern Appalachians, including such prominent physiographic features as the Pennsylvania Salient, New York Recess, Salisbury Embayment, and the Adirondack Mountains (fig. 1). This small section of the continental land mass located on the North American plate (NAP) has been repeatedly tectonized by a series of well-constrained geological events associated with various convergent (mountain-building) and divergent (ocean building) tectonic events (fig. 3). Older, widely recognized events include the Grenville (Proterozoic), Taconic (early Paleozoic), Acadian (mid Paleozoic) and Alleghanian (late Paleozoic) orogenies, each of which contributed major tectonic components to our region. The Early Mesozoic Newark rift basin, the archetype rift basin and significant component in a continental-scale rift system that shredded the entire eastern continental seaboard of the NAP, spans New Jersey as well as parts of neighboring Pennsylvania and New York. With respect to more recent upheavals in our region, Woodworth (1932) and Davis (1963) both chronicled crustal arching and relatively abrupt changes in base level elevation that took place during Jurassic and Tertiary times that can now be placed into a neotectonic perspective.

This work benefits from a computerized, multi-variable analysis of the geology in our region that provides snapshots of our present day physical setting with respect to our current state of crustal stress and absolute crustal-plate movements. Complexities that arise with working with such large sets of geospatial data are addressed by grouping geological units into lithic groups (figures 1 and 2) and implementing a simple feature-accounting system reflecting our tectonic history in order to itemize and systematically compare strain features and effects (fig. 3). This allows a close examination of the different groups of brittle strain features and kinematics. When coupled with constraints stemming from work focused on lithospheric crustal responses to glacial and sedimentary loading of the continental margin, this work may help explain how and when our neotectonic stress regime switched polarity and evolved to where we are today. What certainly becomes clear from this process is a picture of our current neotectonic framework showing coincident and congruent breaks in crustal motion with clusters of recorded earthquakes. With further scrutiny, other tectonic controls can be evaluated with respect to measured plate motions, including lithospheric flexuring and local crustal failure stemming from a host of tectonic processes including erosion, denudation, sedimentation, and periodic advance and retreat of continental glaciers and marginal seas.

What has not been determined is the manner and/or source of the tectonic stresses on our region during the Tertiary period that resulted in late-stage, brittle shear fracturing and oblique wrenching of this region from east-central Pennsylvania through New Jersey and southern New York which increase in intensity towards the Chesapeake Bay impact site. Regional data indicate a post Newark-aged northward push into and through our region of that not only sheared the crust, possibly compacting it by as much as 10%, but also thickened and hence uplifted it, perhaps by as much as a few kilometers. These observations are placed into context with the working hypothesis that I published in an abstract almost ten years ago (Herman, 2006) that related large, hypervelocity bolide (asteroid or comet) impacts on Earth to geodynamic processes and measureable lithospheric strains.

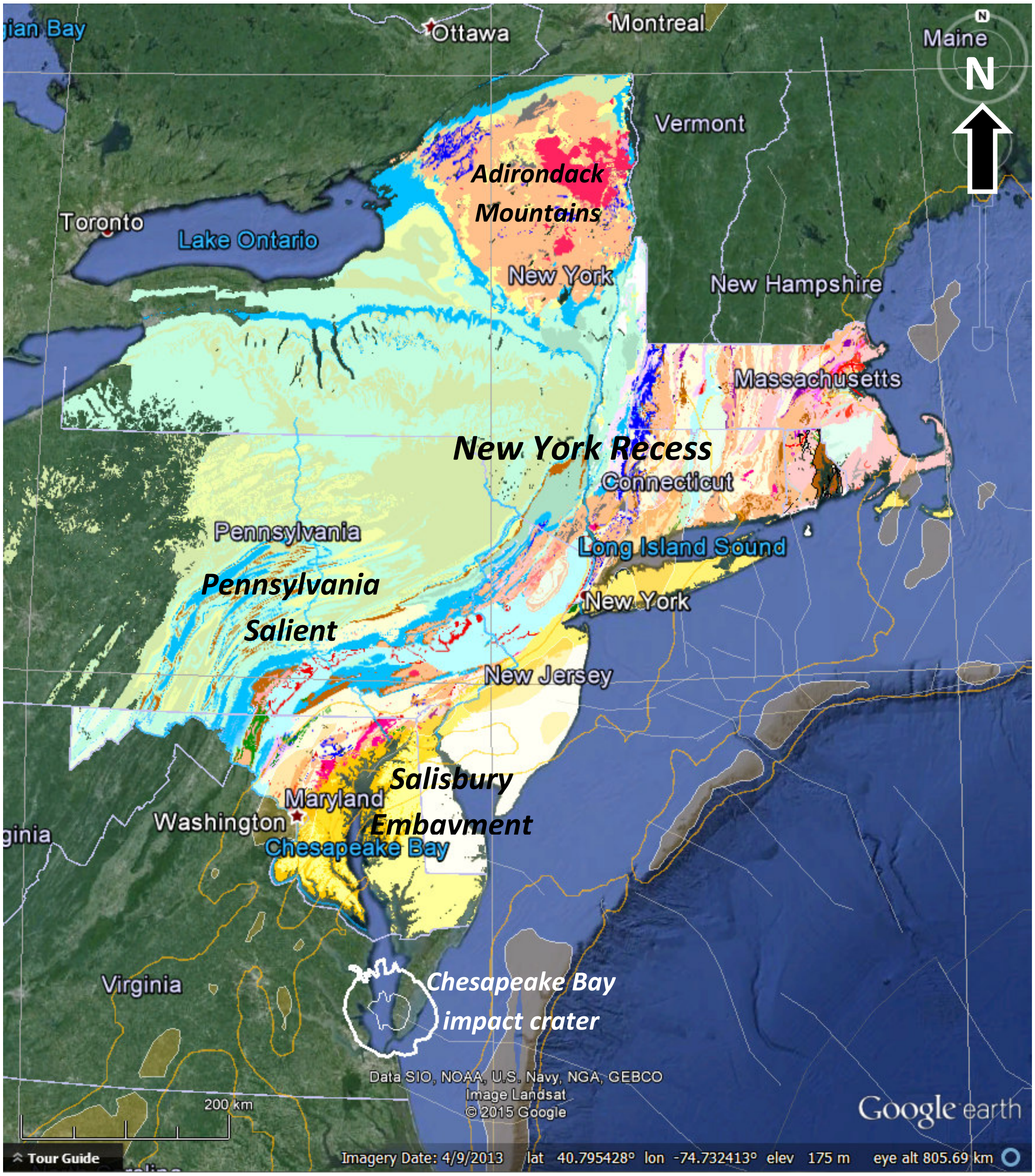

Figure 1. Integrated USGS geological themes covering parts of seven states, centered about New Jersey. Bouguer gravity isolines (Herman and others, 2013) and interpreted oceanic fractures covering the coastal and shelf areas are shown. The Cheseapeake impact crater, depicted by the white lines, are buried beneath ~3 km of sediment at the mouth of Chesapeake Bay. To allow tectonic analyses on a regional scale, and integrated geological base map was compiled using thirty-one (31) lithic groups to color the statewide themes. Each lithic group and its associated color is defined in figure 2.

	RGB	Unit
1	100 100 100	Amphibolite
2	250 30 80	Anorthosite
3	240 220 250	Argillite and hornfel
4	0 170 250	Carbonate
5	200 50 150	Conglomerate
6	250 220 100	Cretaceous sedimentary
7	250 180 180	Felsic intrusive and granofel
8	220 150 150	Felsic extrusive and metavolcanic
9	250 170 120	Gneiss and paragneiss
10	150 200 175	Graywacke
11	240 110 110	Intermediate intrusive
12	250 90 170	Intermediate extrusive
13	210 0 0	Jurassic plutonic
14	210 250 210	Jurassic sedimentary
15	250 170 0	Jurassic volcanic
16	0 0 250	Marble and calcareous metasedimentary
17	0 128 0	Mafic extrusive, metavolcanic, greenstone and serpentinite
18	255 0 130	Mafic intrusive
19	170 230 200	Mudstone and shale
20	220 180 250	Phyllite
21	190 210 150	Sandstone
22	250 230 200	Schist
23	220 250 150	Siltstone
24	230 200 250	Slate
25	235 235 190	Taconic allocthons and Jutland Formation
26	250 230 10	Tectonic breccia, mélange and mylonite
27	250 250 220	Tertiary sedimentary
28	170 250 250	Triassic sedimentary
29	160 80 0	Quartzite
30	255 255 135	Quaternary sediment
31	192 0 0	Ultramafic

Figure 2. Stratigraphic units and associated Red-Green-Blue (RGB) computer palette used for compling an integrated geological base map for regional tectonic compilation and interpretation of the NY Recess region, as presented in figure 1. Grouping units in this manner enables the integration of state-geology themes that are otherwise coded by formation and provide too much detail.

This chapter includes known details and processes that help us understand our neotectonic setting, but much is left to be desired. Written and photographic accounts of disrupted Late Mesozoic and Cenozoic coastal plan deposits are rare. Most clay pits and artificial outcrops are largely reclaimed and developed. Foreland penetrative crustal compaction of classic Appalachian foreland affinity are found sparingly in the Newark Supergroup where late-stage penetrate strains and reverse faulting point to a more recent brittle event that may correspond to some of the regional uplifts that have been chronicled in this region by workers over the past century. But detailed subsurface work in this region by many workers over the past few decades, occurring in both fractured bedrock and post-Jurassic strata of the coastal plain, have helped identify relatively young, igneous intrusives, brittle faults, and nearby bolide-impacts of considerable size that may share a linked tectonic heritage. For example, brittle strain effects of late Jurassic or Cretaceous crustal transtention in the New

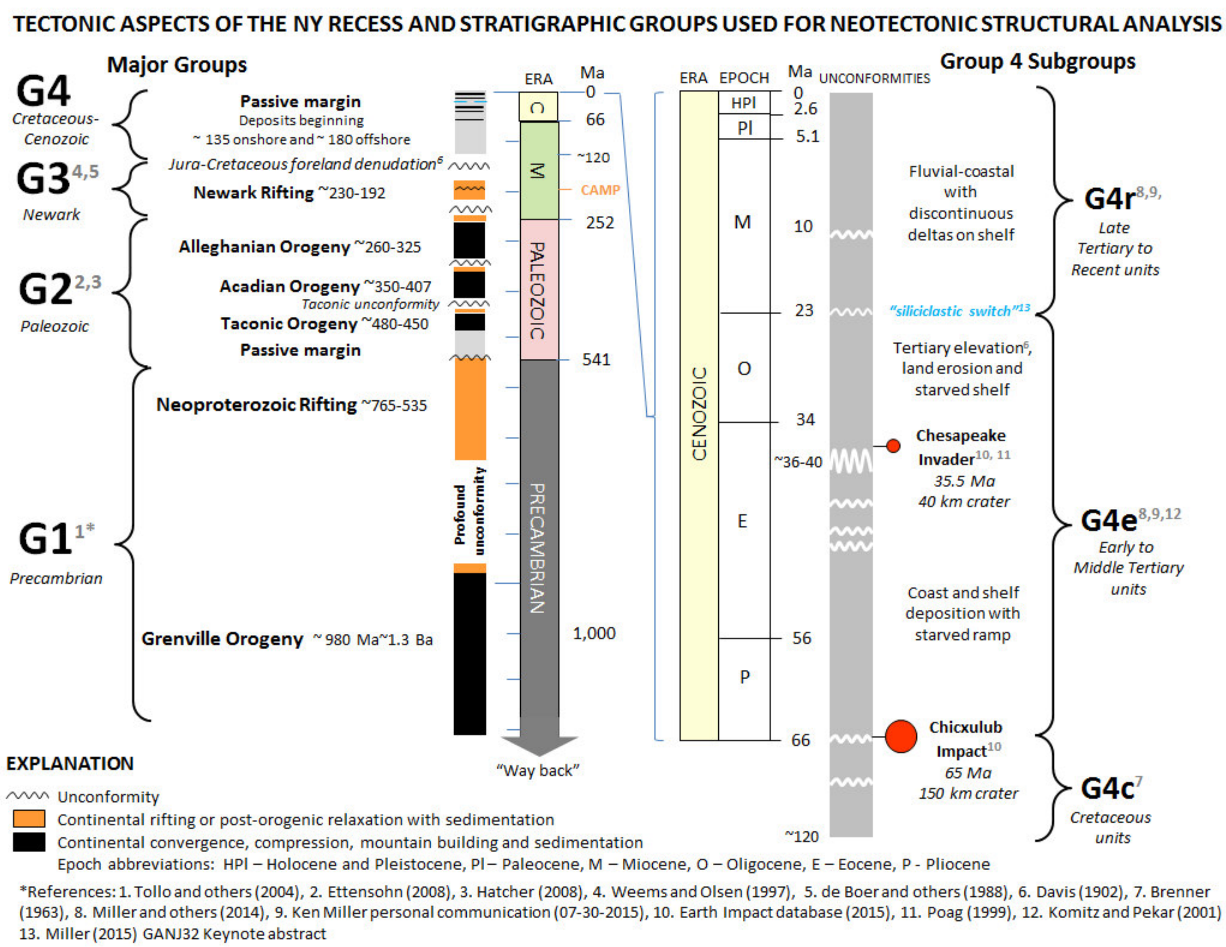

Figure 3. Chronostratigraphic groups used for a neotectonic structural analyses of NAP mid-Atlantic region. Two large-bolide impacts on the NAP during the Cenozoic are shown relative to time and stratigraphic aspects. References for the tectonic and stratigraphic aspects are footnoted after group names and abbreviations. Era and stage boundary ages are from www.stratigraphy.org.

Jersey highlands can now be seen clearly on modern, laser-derived base imagery to cross-cut and segment Musconetcong Mountain with discordant faults showing both normal and oblique slips (see Chapter 5, STOP 1). These trends appear to link with cross-strike fracture cutting Cretaceous coastal plain units, pointing to probable eastward- to northeastward-directed transtentional collapse of the New York Recess including part of the Early Cretaceous coastal plain. This region was subsequently compressed and elevated yet again, more than once, as indicated by the orientation of the current stress regime, and a brittle, non-coaxial overprint that subtlety affects all pre-Cretaceous bedrock in the region. Because late-stage, uplift events in this region are apparently sub-vertical or epeirogenic in nature from a geomorphological viewpoint, recent work of Herman and others (2013) in GANJ 30 becomes relevant for helping to explain Mesozoic crustal inversion, first outlined by Woodworth (1932), that probably stems from distributed thermal welting and emplacement of intrusive bodies of the Central Atlantic Magmatic Province (CAMP) along the eastern continental margin of the NAP. However, this fails to account for Cenozoic-aged tectonic disruptions that produced pronounced continental unconformities, such as the mid-Cenozoic one in the region of the NY Recess that temporally coincides with the arrival of the Chesapeake Invader (fig. 3 and Poag, 1999).

The following work is organized to show the un-interpreted graphic data first for review and consideration, before discussing ensuing interpretations. The methods of data integration, processing, and display are noted for the various themes, including current, crustal-plate motions, recorded earthquakes, and 3D vectors summarizing our current state of crustal stress. Aspects of other regional and global Bouguer gravity and aeromagnetic geophysical themes are included to help decipher and constrain the ensuing, interpreted tectonic trends. The various brittle geological features found in the region are then discussed using chronostratigraphy to systematically assess their occurrence, spatial distribution, and kinematic behaviors, beginning with the most recent ones and progressing backwards to relatively older ones. The results of this process leads us past conventional thinking to cautiously consider whether some of the neotectonic effects we see, particularly those that don’t fit current tectonic paradigms, could have formed as far-field brittle effects imparted by catastrophically large-bolide impacts on the NAP during the Cenozoic Era. In other words, can impact tectonics fill in current gaps in our tectonic history that conventional orogenic processes cannot fully explain? Can catastrophic impacts help explain documented, epeirogenic episodes of crustal compression and ’out-sequence’ orogenic structures like those reported in the Juniata Culmination of Pennsylvania (Herman, 1984)? These thoughts are not commonly held or entertained by the general geological community at this time, but they are bolstered by recent radiometric work conducted in Pennsylvania and northern New Jersey using Rhenium and Osmium (Re/Os) isotopic age dates obtained from sulfide-mineralized faults zones (Chapter 3; Mathur and other, 2015). All signs at this time point to a widespread episode of tectonic disruption in our region at the time of and immediately following the Chesapeake impact. But are there other, more plausible explanations? If one merely entertains the notion of tectonic catastrophism, then why not extend the plank farther and wrestle with the notions of what tectonic and geodynamic effects can (or do) stem from very large, extremely energetic bolide impacts such as Chicxulub, the one that hit the Gulf of Mexico at the dawn of the Cenozoic Era! Could the Chicxulub impact have subsequently altered global plate dynamics? Can the Chicxulub impact be responsible for the current state of crustal stress and NAP plate motions in places as far removed as New Jersey? At the end of this chapter and forum, I hope that we land securely on solid footing, where we can not only consider catastrophism in a neotectonic sense, but begin seeing it in a global sense. For if these hypotheses are tested and ring true, then they must blend seamlessly with uniformitarianism in order to fully account for the geodynamic processes observed around us.

Digital Geospatial Themes in a GE KMZ format

Over the past two decades digital-mapping systems and methods have arisen that provide extremely accurate measurements and visualization of grounded field positions and surface geologic structures. These also provide timed measurements of crustal-plate motions from over a decade of Global Positioning System (GPS) data. Terrain maps in some places are now measured with sub-meter precision using airborne laser mapping (LiDAR). This chapter reflects the use of such data and methods to integrate, interpret, and share geospatial data using this forum so that anyone can access and use them in the same environment in which they were organized. This allows one to place discrete, geology observations into context with the sequences of Appalachian tectonic events that shape our region.

As noted previously, this study is centered between the Adirondack Mountains of New York and the Chesapeake Bay as part of the Salisbury Embayment of Maryland and Delaware. Both raw and interpreted data are compiled, including preliminary tectonic interpretations of geological features over parts of New Jersey, Maryland, Delaware, Connecticut, Massachusetts, and the eastern parts of New York State and Pennsylvania (fig.1). This was done in order to place New Jersey and the New York City area into geospatial context within a broader region that shares geological processes and products. The figures represented herein that use Google Earth (GE) were generated using the data that are available from download from the GANJ web site. These databases are mostly reprocessed and packaged source themes from the US Geological Survey, the Geological Society of American (DNAG magnetic and gravity potential field data), the National Oceanic and Atmospheric Administration (NOAA) and the National Space and Aeronautical Administration (NASA), among others. The methods used to generate new data and interpretations are intertwined herein with descriptions of how each theme was accessed, processed and used for regional visualization.

This work used Microsoft's MS-Excel spreadsheet software to handle parametric data, and both ESRI's Arc-GIS and Google Earth (GE) to integrate and interpret the data. GIS was mostly used to conduct structural analysis of bedrock ridges exposed in high-resolution topographic maps (see Chapter 1). GE on the other hand, is a free, 4D global-visualization tool that is used both for viewing and interpreting the data, and for easily communicating the results. GE is a time-variant, virtual globe that works with geographic spatial coordinates and is a recognized standard for data sharing among the scientific and general community using the internet, including our GANJ web site. Most of the figures in this report were generated by capturing visual displays of various geospatial themes at various viewing scales directly from the computer-display screen. Therefore within this report, the term 'view scale' is used rather than the more common 'map scale', because the figures are simply graphics capture, or a 'screen grab' of a computer display when one is satisfied with the view. Representation of our current geological and geophysical state in this manner can be a risky task as the various geological units and geophysical data nomenclature are constantly in flux, and stem from varying periods of record and source scales, so each figure should be considered a static snapshot of the geodynamic processes that we dwell on. We are still learning the uses and limits of these technologies, which from my perspective, are getting better at an accelerated rate. Nevertheless, the visualized raw data serve to base new interpretations of how our region has evolved tectonically, and care is given to not only to outline the methods that have been employed, but also reference the source material and pertinent metadata for each theme that is needed to build a reliable foundation for the regional tectonic analyses.

Integrated USGS Geology using generalized lithic groups

Current statewide geological maps are compiled and distributed in a computerized format by the USGS for the entire United States by state, and for most of the world for hydrocarbon exploration[1]. These data are provided for download in various data formats, including those for GE as Keyhole Markup Language (KML) files or the compressed variety (KMZ files), as described in Chapter 1. The available USGS state-based KML files for Delaware, Maryland, New Jersey, Pennsylvania, New York, Connecticut, Massachusetts, and Rhode Island were manually reprocessed for generalization and use in conducting this regional, neotectonic structural evaluation. For example, rather than the default display mode based on individual geological formations as standardized by the USGS, this study includes a regional geology theme in a KMZ format that was customized for display using lithic groups. Data integration was done manually using Microsoft's freeware XML (extended mark-up Language) editor, XML Notepad 2007, as computer software that can read and display the KML folder structure, as well as allow addition of new folders with customized names of lithic groups that can receive groups of formations that were manually placed in each new folder using the primary rock type

[1] http://energy.usgs.gov/OilGas/AssessmentsData/WorldPetroleumAssessment.aspx

listed for each formation for each theme. Upon grouping adjoining themes in this manner, continuous patches of similar rocks or sediment visually emerge that aid in identifying tectonic structural discontinuities that correspond to folds and faults (figs. 6-9). Some mismatched stratigraphic units still occur along contiguous state boundaries (fig. 1) but many disappear from using this approach. Figure 2 details the 31 lithic groups that were used e to contrast certain lithologies that may lend clues into the occurrence of secondary structures by their fold and faulted patterns. A RGB color screen was worked out (fig. 2) to recombine each USGS state files including those for (fig. 1).

Current plate movement using ground-fixed Global Positioning Systems (GPS)

I began studying the neotectonics of this region in 2003 while conducting fracture-bedrock aquifer research for the NJGWS (Herman, 2005). Don Monteverde suggested in 2005 that I look into using ground-fixed receiving stations that use global-positioning-systems (GPS) technology to facilitate this work. At that time, NASA maintained an open-access internet portal through their Jet Propulsion Laboratory (JPL) that included almost 800 global stations where crustal movements were continuously being monitored (table 1), with most located on the NAP (Herman, 2006). The GPS includes a constellation of Earth satellites in geosynchronous orbits that are used for global navigation and precise geodetic position measurements. A GPS includes the navigation payloads that emit radio signals, receiving station on or close to the ground, the data links, and the associated command and control facilities operated and maintained by the US Department of Defense in conjunction with civil and commercial service providers. GPS provides determinations of three dimensional positions referenced to N-S, E-W, and UP-DOWN, with velocities along each position in mm/yr, and time records kept for about 95% of the time, for 24 hours a day, in all weather, and around the globe (Assistant Secretary of Defense, 2001). Daily positions are collected and analyzed by various organizations and institutions that then deliver these geodetic data to the California Institute of Technology under contract with NASA's Jet Propulsion (sideshow.jpl.nasa.gov/mbh/series.html, and to NOAA through their CORS (Continuously Operated Reference Stations) web portal with data covering the USA (geodesy.noaa.gov/CORS/). Record keeping began for some stations in 1989, with each station having come on line at various dates with unique types of data records, and sampled at varying frequencies. GPS time-series data for each receiver location are analyzed by various sources to determine short- and long-term positional changes of the station through time relative to a fixed, mathematical reference frame (calculated ellipsoids or spheroids). But reference frames and instrumentation are periodically modified and improved, and different adaptions evolve for use by international and national agencies and programs requiring standardized and robust data sets. Prior to September 6, 2011, CORS GPS data were compiled and released as long-term data using a reporting format standardized with NASA-JPL data that referred to an International

Terrestrial Reference Frame of 2008 using 2005 coordinates for the GRS80 ellipsoid. Since 2011, CORS data update new a new coordinate reference frame and are no longer available as tabular data sets using customized queries to simultaneously access data records for multiple stations. COPS data users must now access single records at a time and statistically process each data set to analyze long-term trends. We're currently investigating ways to automate this process at the NJGWS, but for now, the 2009 data are used for this work, and are only spot checked for validity with respect to variations of long-term trends over time. Table 1 provides a basic statistical summary of four different GPS data sets that used as part of this work. It shows that the number of global, ground-fixed receiving stations has increased by over 300% in a span of only 10 years. This table also includes a comparison of the formal positional and velocity errors for global data sets downloaded one decade apart. For more information on GPS and recent development in the technology see www.gps.gov/systems/gps/space/ and www.ngs.noaa.gov/CORS/coords.shtml.

Table 1. Basic statistical summary of four, ground-fixed GPS data sets used for analyzing and representing long-term crustal-plate motions. Rates of motion stated in mm/yr.

Data set	No.	Avg. X vel.	Avg. Y vel.	Avg Z vel.	Avg horiz. vel. (calc)	Avg. X vel. error (+-)	Avg. Y vel. error (+-)	Avg Z vel. error (+-)	X-vel. range	Y-vel. range	Z-vel. range
NASA 2005 GLOBAL	778	23.4	12.2	3.7	27.0	0.2	0.3	0.6	> -71.5 < 66.8	> -35.2 < 57.4	> -90.9 < 125.4
NASA 2015 GLOBAL	2485					0.2	0.2	0.7			
NOAA 2009 NY REGION	67	0.4	0.6	1.2	-	-	-	-	> -1.6 < 1.2	> -1.4 < 2.4	> -3.9 < 0.2
NOAA 2014 SPOT	7										

I suppose it was just good fortune that I visited the CORS web portal in 2009 and downloaded a data set covering this region before the aforementioned changes in CORS positional recording and data access policies took effect, as the use of these data are rapidly becoming more sophisticated and difficult to use because of growth and specialization of the industry. The 2009 data set includes records for 67 ground-fixed, GPS receiving stations in the region of the NY Recess (fig. 4). I used ESRI's ArcView's 3D Analysts GIS software to produce a simple triangular integrated network (TIN) surface map based on the interpolation of point values and showing areas with the same ground motion. Upward rates are positive and

Figure 4 *(Legend and explanation below figure on opposing page).* GE display of the mid-Atlantic , continental and oceanic margin of the North American Plate (NAP), centered near 40^o latitude and -75^o longitude showing recent crustal motions determined using ground-fixed GPS receiving stations, crustal seismogenic zones, princial axes of crustal compression reported from focal-mechanism solutions from well-constrained earthquakes, and some key structural analyses used for interpretations. Note the parabolic line connecting the seismic zones wrapping arond the rising Adirondack Mountains, which appear to act as a buttress that is resisting the slow, northwestward plate drift with rates that slowly increase NE up the spine of the Appalachian Mountains.

NASA-JPL[2] and NOAA-CORS[3] ground-fixed GPS data to capture 'long-term' horizontal and vertical crustal movement - The large white vectors show the horizontal component of current crustal motion in mm/yr based on NASA-JPL[2] global data downloaded in May 2015. Different stations came on line at different times and use different sampling rates. Some vectors include white labels showing magnitude (mm/yr) and bearing (azimuth 0-359^o). Current regional horizontal motion is to the WNW at rates that gradually increase from ~14 mm/yr at the Chesapeake Bay in the SW to ~16 mm/yr in the northast (NE) near the Adirondacks. The blue and white polygons comprise an equal-velocity surface capturing a snapshot of 'long-term' trends in vertical ground motion captured from NOAA's on-line data portal referred to as 'CORS'[3]. This surface was derived using the 151 ground-fixed CORS records located with the small, white, open circles. These time-series records also have varying record lengths and sampling rates. The polygons were generated as a GIS triangulated integrated network (TIN) with break lines set to the 5 velocity ranges detailed in the figure explanation below right. See text for more information on how long-term GPS-series data were obtained, plotted, statistically analyzed, and spot checked for accuracy.

Crustal seismogenic zones - Orange polygons represent the historical, crustal-seismogenic zones derived using a GIS grid of uniform cell size (50 km) to quantify the density of earthquake epicenters falling within a 1^o search radius from cell centers within a geographic range of latitude 90^o S to 90^o N and longitude 30^o E to 150^o W (Herman, 2006). Epicenter densities were derived for each cell from a GIS point shapefile of 27,852 earthquake epicenters with a magnitude 2.0 or greater, obtained from on-line earthquake records maintained by the USGS-NEIC, the New Jersey, Ohio, and Indiana geological surveys, and Harvard's Weston Observatoy (see text). A 2D polygon shapefile of seismogenic zones was generated from the gridded results where the density of earthquake epicenters exceeded 0.001 events per km^2.

Current, horizontal orientations of primary crustal compression - The thicker, gray, 3-dimensional vectors with yellow labels depict directions current orientation of the crustal stress regime by depicting the bearing and plunges of the principal-axes of crustal compression calculated from well-constrained earthquakes that give 'focal-mechansim solutions' that are reported on-line and in the literature (table 2).

Detailed structural analyses – Small white vectors with orange labels indicate penetrative tectonic compaction (%) of calcite grains that fan out beyond the Pennsyania Culimination and Paleozoic rocks into New Jersey Mesozoic rocks (Engelder, 1979; Lomando and Engelder, 1984). See text for details.

2. NASA's Jet Propulsion Laboratory (http://sideshow.jpl.nasa.gov/post/series.html.
3. NOAA's National Geodetic Survey's Continuously Operating Reference Station (CORS) network (www.ngs.noaa.gov/CORS)

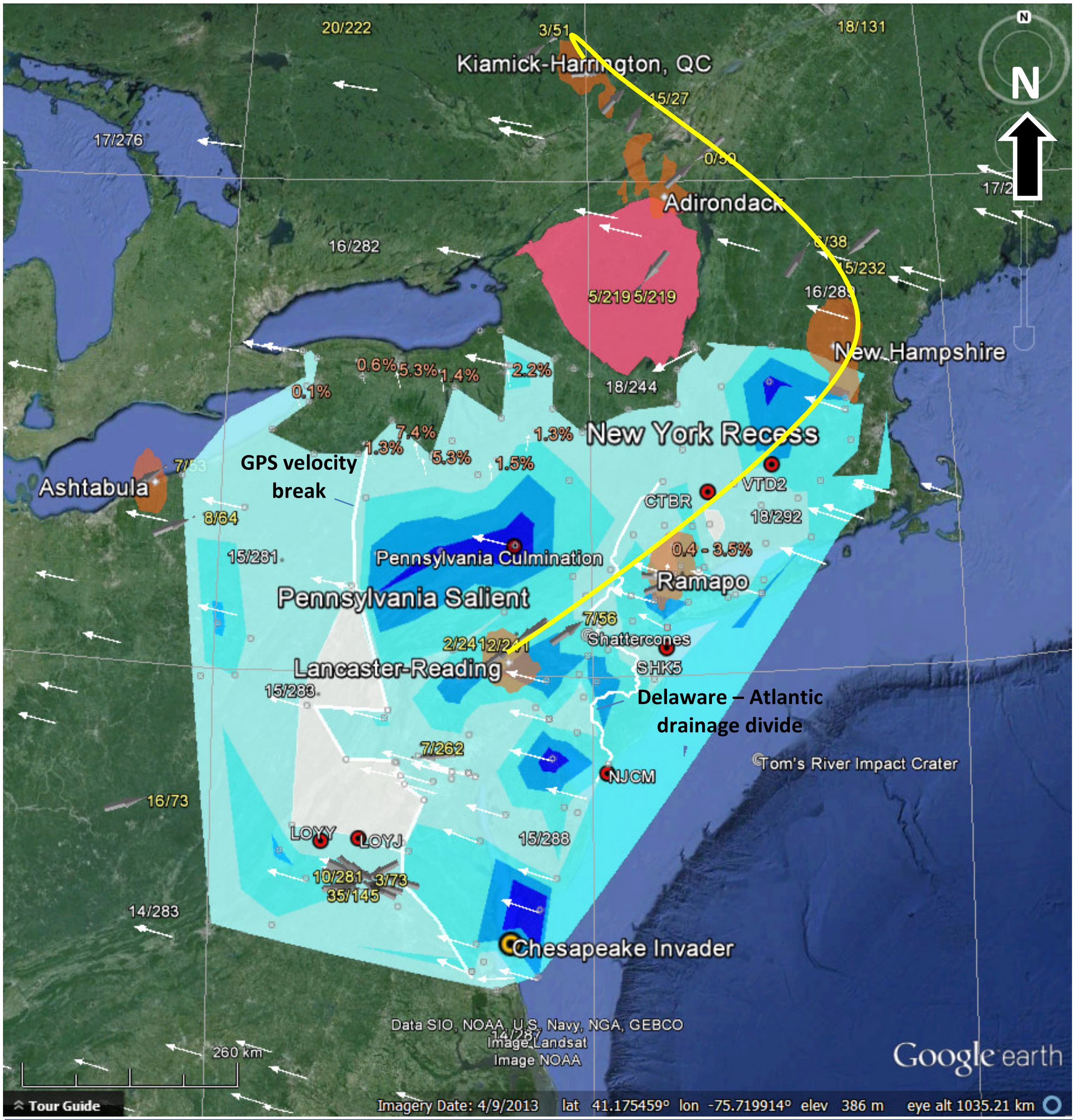

EXPLANATION

Rivers

Polyline trace of bow wave connecting seismogenic zones wrapping around the Adirondack uplift

GPS VERTICAL CRUSTAL MOTION (mm/yr)

- > 0
- -1 to -2
- -2 to -3
- -3 to -4

Adirondack Mountains

Historically active crustal seismic zone (see caption)

Horizontal component of GPS crustal-plate motion

Current crustal, principal-compression-axis orientation determined from earthquake focal-mechanism solutions (details explained on caption on opposing page). Plunge (0-90) and bearing (0-359) of axes shown with yellow annotation.

downward are negative with ranges of about 0 to 4 mm/yr. The TIN uses three break line values to separate four ranges of vertical ground motion as summarized in figure 4. It is important to note that this 2009 representation of vertical ground motion is only a snapshot of how Earth's surface was moving at that time in a 'long-term' sense, which translates into a period of about a decade for some stations, but only shorter periods of as little as two or three years for others (figs. 4 and 5). But as a theme used for neotectonic studies when viewed together with complimentary themes including regional watershed divides, hydrography, and earthquakes, we will see that the geometry of this TIN surface conforms to map trends of historical crustal seismicity as well as the current physiographic expression of our landscape. But because the NOAA data are not as defined and inclusive with respect to formal error reporting, an additional study was done using spot GPS locations around this region for individual records downloaded in 2014 to further assess the variations and limitations seen in these data sets. Figure 5 is a summary of scatter graphs depicting timed variations and oscillations in the vertical component of crustal motion for the seven CORS stations shown in figure 4. For all charts, the vertical rate is plotted on the Y-axis and time is plotted on the X-axis. All spot locations have a negative (downward-trending) motion values determined using linear-regression statistics in MS Excel (red straight lines in figs. 5 and 6). The Wilkes Barre (WIL1) station has one of the longest records in the region and is used to compare results with 5 other stations having overlapping records and to characterize yearly oscillations in vertical ground motion (fig. 6). Note the variable monitoring periods charted in figure 5. Also note that a plot of a seven-day moving average through the raw data accentuates periodic, oscillatory trends with more clarity. Figure 6 is used to show that in our region, yearly fluctuations of our land surface systematically vary on the order of about 10mm/yr owing to solar gravitational induction of annual Earth tides. Seeing such systematic variability in timed GPS signals is important when deriving and assessing longer term, derivative TIN surfaces for used in regional kinematic analysis. A close look at these data show that the TIN surface uses velocity break lines at 2mm intervals, or at about 20% of the value of the overall expected annual range in vertical ground motion that we experience here. Table 1 also shows that positional accuracies in the vertical dimension are the least precise of all GPS positional coordinates because of such surface oscillations. Nevertheless, as we will see below, the geometry of this TIN surface, derived using statistical linear regression of data reflecting periodic, systematic oscillations of our land surface does indeed conform to complimentary geospatial physiography, hydrography, and crustal seismicity.

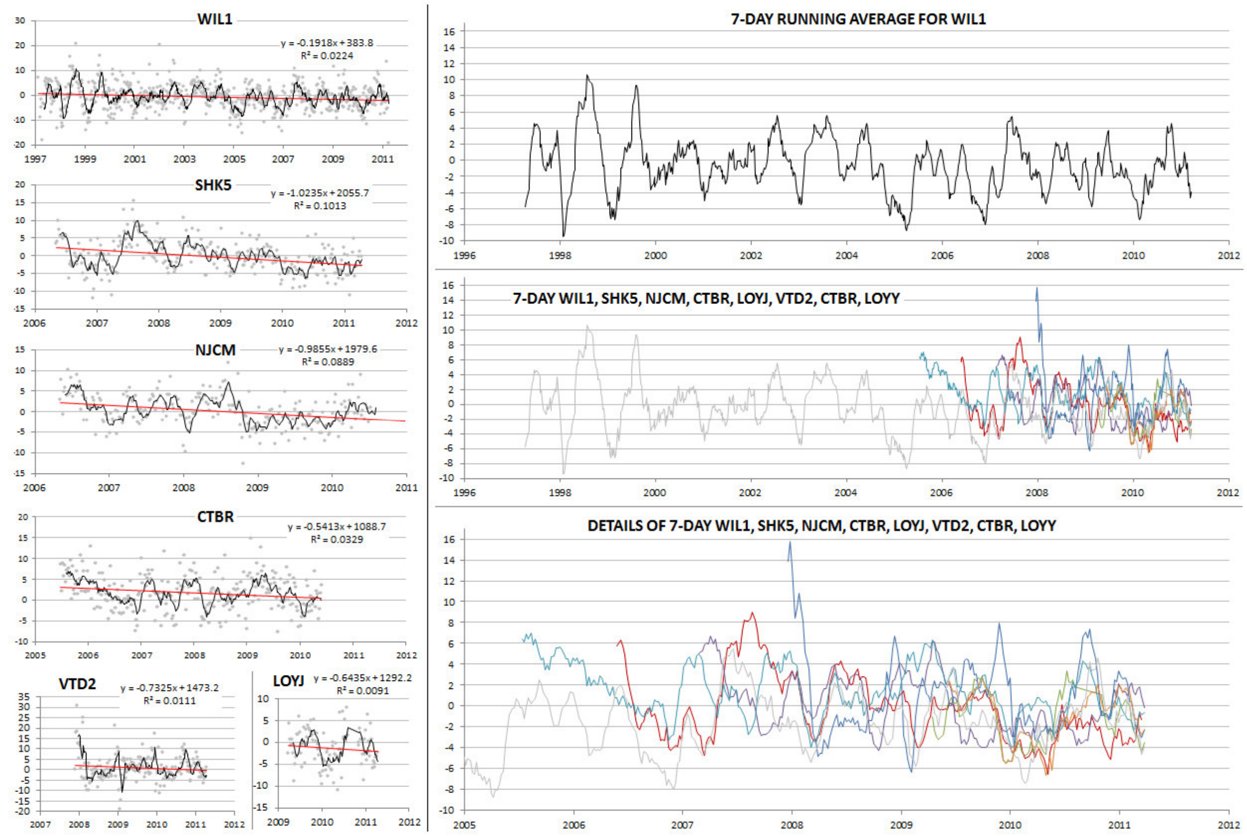

Figure 5. – Spot NOAA CORS data analysis showing unfiltered, filtered, and simple linear-regression lines summarizing data trends used to derive parametric data for the velocity axes.

Regional earthquake catalogs, crustal seismogenic zones, and depicting crustal compression

Five different sets of historical earthquake data are integrated into this work (figs. 4 and 6 to 8). The earthquake seismic zones named in figure 4 stem from the aforementioned, preliminary neotectonic assessment in this region (Herman, 2006). That work produced a GIS point theme using ESRI's (Environmental Systems Research Institute, Inc.) shapefile format with 28,139 earthquake events recorded from 1900 to 2005 between latitudes 39°N to 60°N and longitudes 46°W to 83°W. Of this total 26,625 included depth values and 27,852 are greater than or equal to magnitude 2. Most events were retrieved by a computer-based search from the USGS National Earthquake Information Center (NEIC) for the period of 1973 to 2001, but other instrumental and non-instrumental records were added from other earthquake catalogues maintained by Weston Observatory at Boston University and US States including New Jersey, Ohio, and Indiana. All records were combined and parsed to eliminate duplicate records. At this point is important to point out that earthquake magnitudes have been

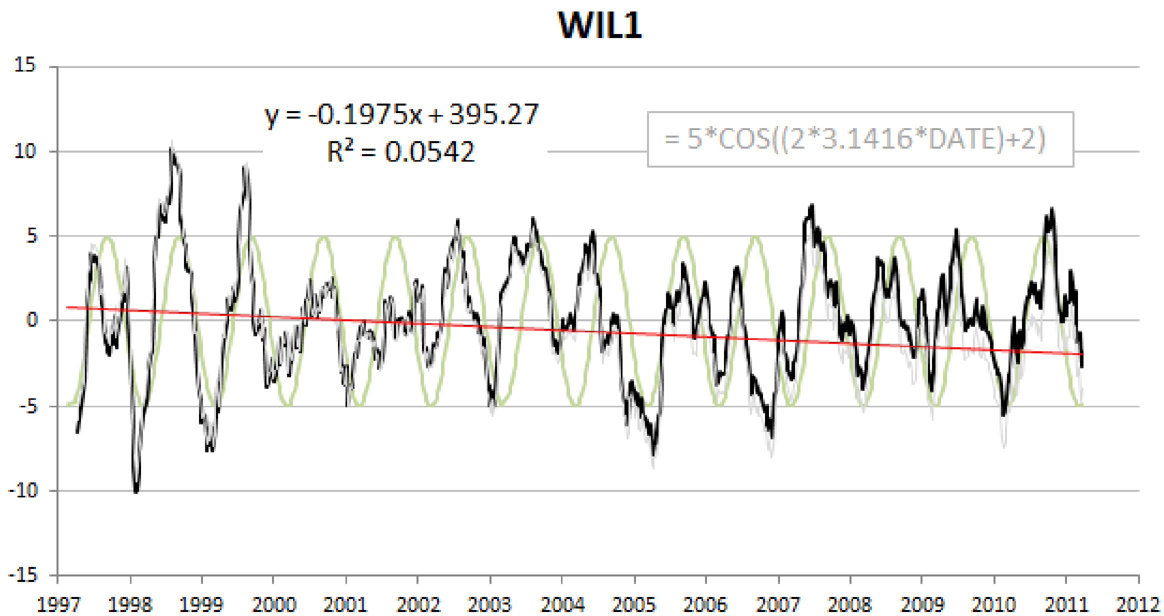

Figure 6. Fourteen years of vertical (Z-component) ground-position monitoring from Wilkes Barre, Pa station WIL1. Superimposed on the curve for the 7-day running average (thin, light-gray line) is the linear regression (red) line of the 7-day curve, an adjusted 7-day curve from removing the regional, sinking effect (regression value at time X) and a simple COSINE function showing a 31.7 nHz cycle manually fit to the data spread by trial and error. The COS function signals the amplitude variations stemming from solar-induced Earth tides with amplitudes in our region averaging about 5 mm/yr, and ranges in oscillatory motion of land surface of about 10 mm/yr. The largest range in 1998 occurred when our solar system was temporarily aligned in the Milky Way galactic plane as it crossed through during a 26,000-year periodic event (Meus, 1997).

historically defined in various manners, with the most recent, most quantitative form (Moment magnitude) having superseded the more familiar Richter magnitude value. Because of the relatively low-magnitude ranges of earthquakes in our region (fig. 7), most of the different magnitude values compiled over the historical record are comparable and only differ slightly when using magnitude classification schemes. For it's the larger and longer-period earthquake events above magnitude ~7 that the more modern methods are better formulated to assess (Aki, 1970). For this work, magnitudes were catalogued using the best methods available at that time, and we simply view then as representing systematic, logarithmic steps representing about a 30-fold increase in the amount of energy released per one-integer increase in magnitude (http://earthquake.usgs.gov/learn/topics/measure.php).

The earthquake GIS point theme assembled in 2005 was used with ESRI's cell-based modeling (GRID) program in the ArcView 3.2 GIS environment to calculate the density of earthquake epicenters lying within 1-degree square cells using a search radius of 50 miles from cell centers. A set of closed polygons were then generated that represent crustal seismogenic zones where grid density values were equal to or greater than 0.001 earthquakes per square

Figure 7. A scatter graph showing number of earthquakes grouped by the magnitude ranges showing in figure 10. This NEIC catalogue query includes over 3500 historical events recorded between LON 55W to 95W and LAT 30N to 50N. Most earthquakes in our region are in the 1-3 magnitude range.

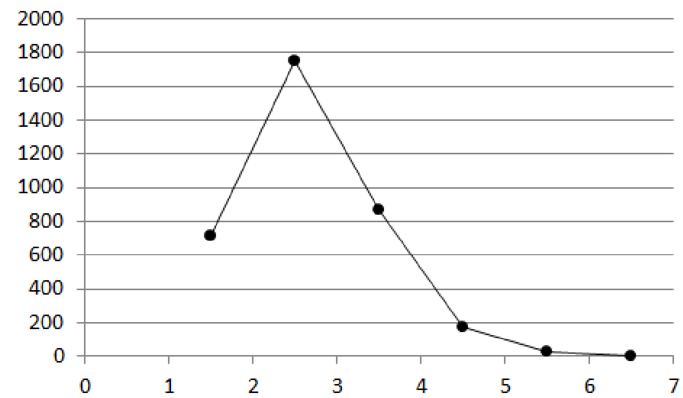

kilometer area. These values were derived at and symbolized using trial and error densities, search radii, and grid-cell sizes. This work was completed shortly before the work of Sykes and others (2006), the second of five data sources, that supersedes the earlier work by providing a more accurate, open-access earthquake catalogue covering the Philadelphia to New York region (figs. 8 and 9). But the aforementioned seismogenic zones are used here because they extend well beyond the geographic range of this newer catalog. A third earthquake catalog was obtained from the NEIC portal earlier this year by issuing a custom query for historical earthquakes lying within a region bounded by longitudes 55^{o} to 95^{o}W and latitudes 30^{o} to 50^{o}N (fig. 10). This query returned 3532 historical events that were subsequently parsed into folders holding point records of specific magnitude ranges as shown in figure 10 and tallied in figure 7.

Current crustal stress in our region using earthquake focal-mechanism solutions of principle stress axes (P-axes).

The remaining two data sources of earthquake parameters are listed in table 2 along with data from Sykes and others (2000) that detail locations, measurements, and reference sources for 45 principal axes of crustal compression (P-axes) found in our region that were derived by seismologists using analytic methods for some of the well-monitored earthquakes depicted in figure 10. The techniques surrounding the derivation of these data surpass the scope of this work, but simply state, the uneven manner in which energy is released during an earthquake indicates two possible planes of rupture, or fault planes that could have resulted in the observed energy release. By analyzing the various forms in resulting ground waves, directions, and travel times as received at various seismographic stations, the state of crustal stress that produced that energy release can be defined. The actual fault plane cannot be strictly determined, but is reduced to only a couple of geometric solutions predicated by rock mechanics. It is left to experienced professionals to determine which of two 'nodal' planes best characterizes a specific earthquake rupture based on many considerations, including field

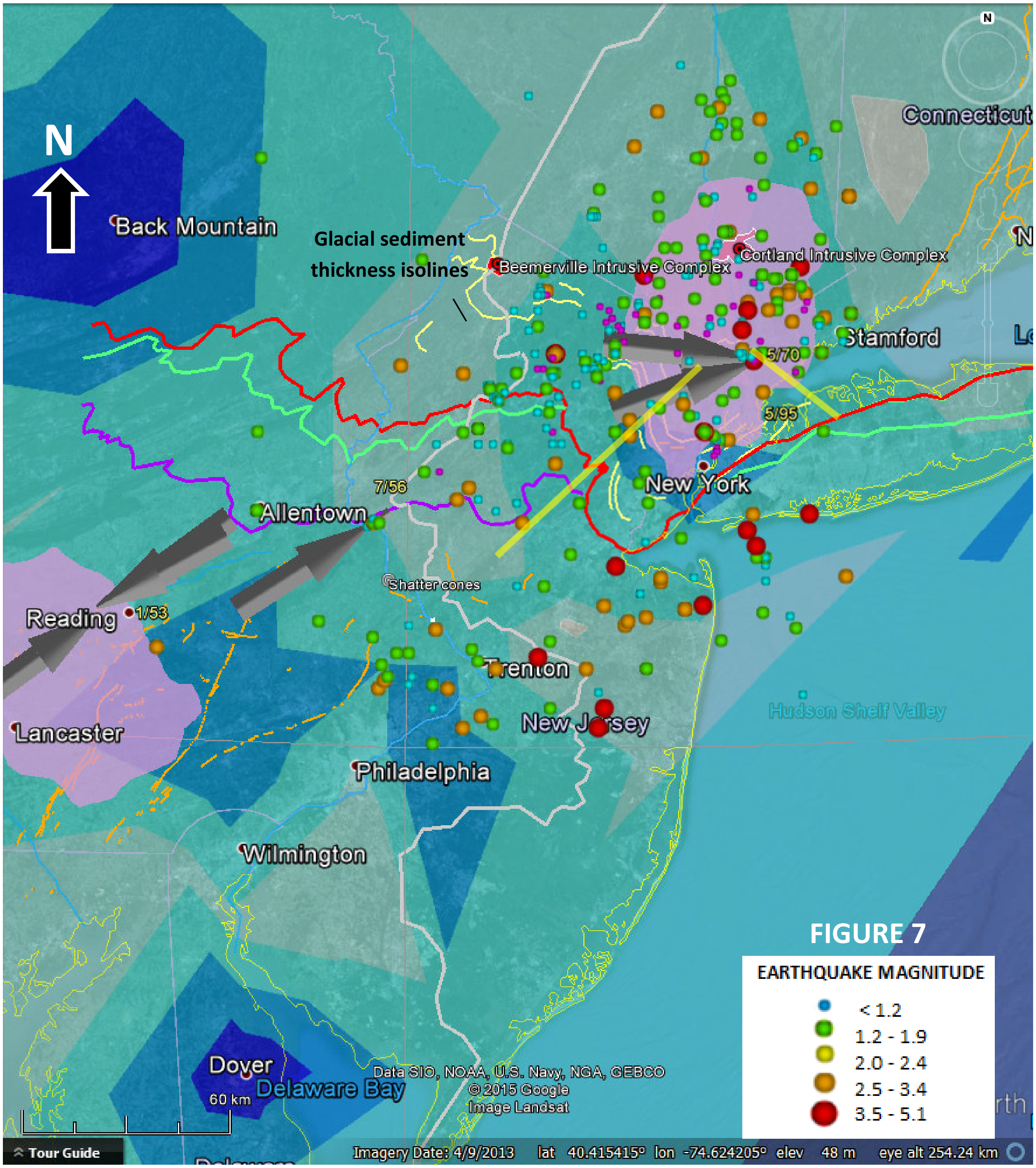

Figures 8 and 9 (on opposite page with map legend). Locations of historical earthquakes (Sykes and others, 2006) shows ranges of magnitudes (fig. 7) and depths (fig. 8). The blue and gray polygons summarize the long-term vertical ground motion from the 2009 CORS data (fig. 4). Also shown are seismic zones (pink polygons), Jurassic dolerite dikes, Pleistocene terminal moraines and sediment-thickness contours (bright-yellow) and shorelines, rivers and streams from unpublished USGS hydrography (1:500,000 scale). Place names are default GE labels that appear when using a 60 km GE scale. The Beemerville and Cortland intrusive complexes are marked for reference. See text for further explanation of data sources. Straight yellow lines are seismogenic lineaments of Sykes and others (2006).

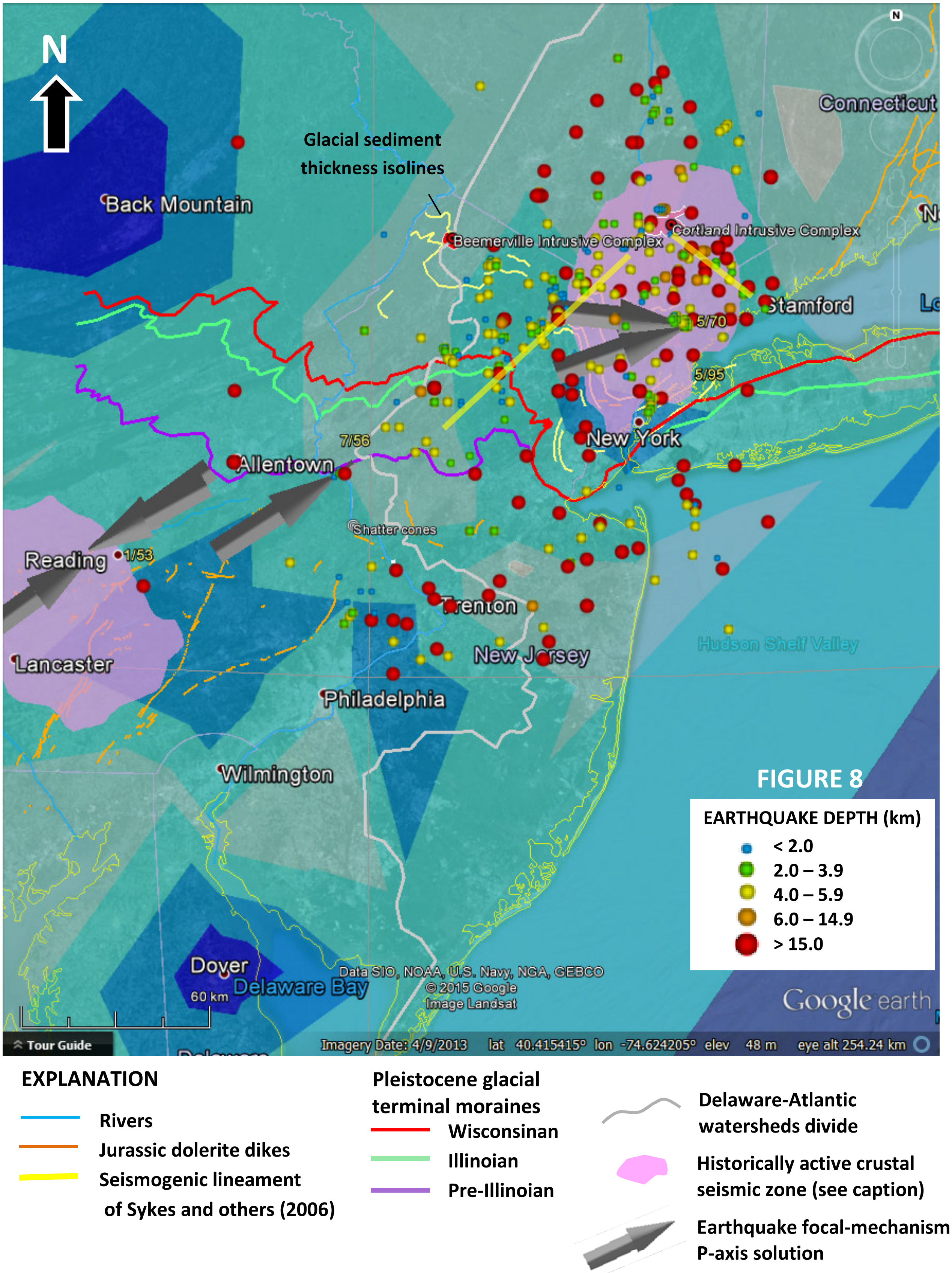
N
Glacial sediment thickness isolines
Back Mountain
Connecticut
Beemerville Intrusive Complex
Cortland Intrusive Complex
Stamford
5/70
5/95
New York
7/56
Allentown
Shatter cones
Reading
1/53
Trenton
New Jersey
Lancaster
Philadelphia
Hudson Shelf Valley
Wilmington
FIGURE 8
EARTHQUAKE DEPTH (km)
< 2.0
2.0 – 3.9
4.0 – 5.9
6.0 – 14.9
> 15.0
Dover
60 km
Delaware Bay
Data SIO, NOAA, U.S. Navy, NGA, GEBCO
© 2015 Google
Image Landsat
Google earth
Tour Guide
Imagery Date: 4/9/2013 lat 40.415415° lon -74.624205° elev 48 m eye alt 254.24 km
EXPLANATION
Rivers
Jurassic dolerite dikes
Seismogenic lineament of Sykes and others (2006)
Pleistocene glacial terminal moraines
Wisconsinan
Illinoian
Pre-Illinoian
Delaware-Atlantic watersheds divide
Historically active crustal seismic zone (see caption)
Earthquake focal-mechanism P-axis solution

Accordingly, the parametric data in table 2 includes the locations and azimuthal bearing and plunge for each calculated P-axis derived for 28 earthquake events in the mid-Atlantic US region (table 3). These data were input into a KML-symbol-generating tool built by the NJGWS to geospatially plot and orient 3D object symbols in GE (Herman, 2013). The results summarized in figures 3, 8 and 9 show shaded, 3D gray vectors aligned along axes of principle crustal compression. Most of the P-axes in our immediate region plunge gently NE at angles less than 10°, but some variability is seen in and near New Jersey were some axes point to the east, or plunge at shallow angles back to the SW (figs. 8 and 9). But one unexpected consequence of

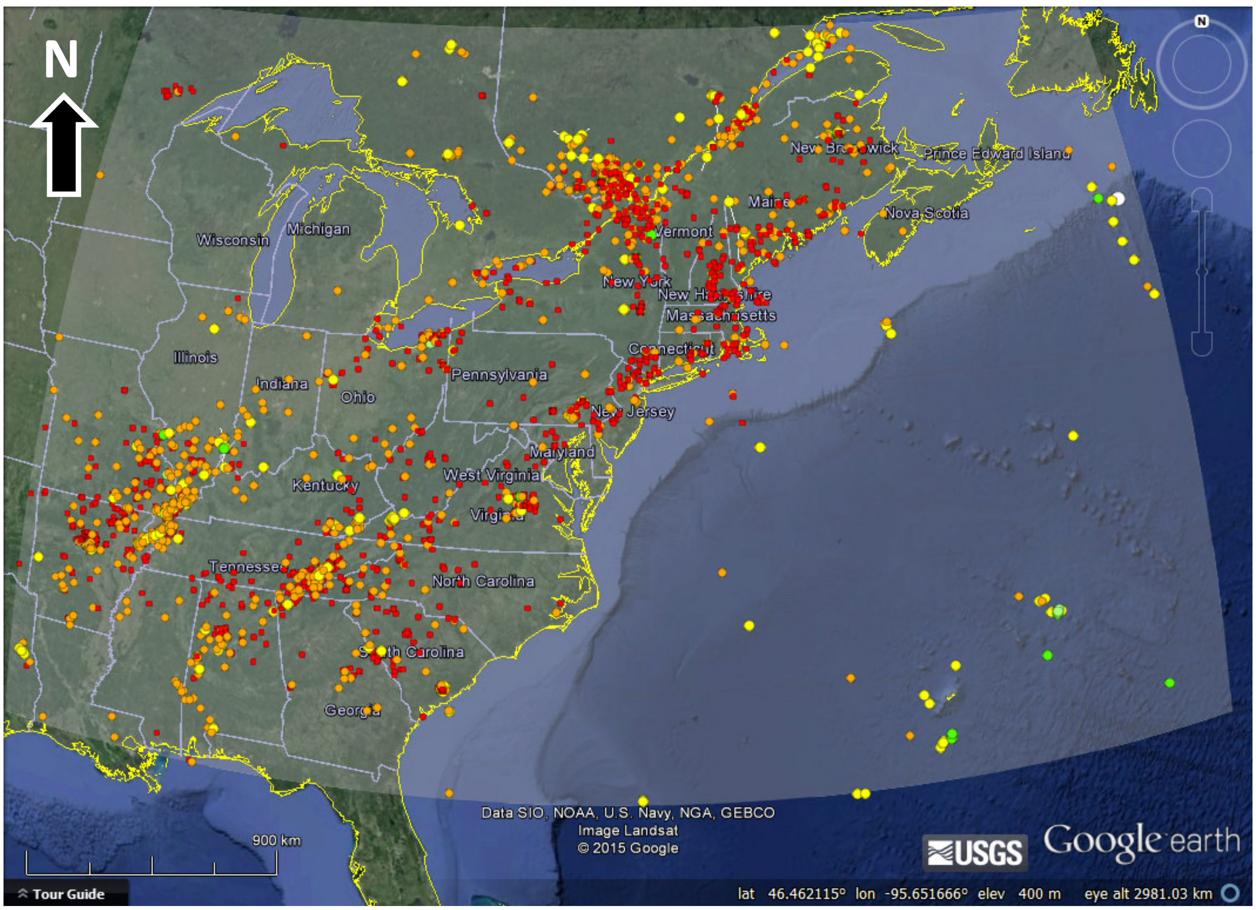

Figures 10 (above). A NEIC search for historical earthquakes between Latitude's 30° to 50° N and Longitudes of 55 to 75° W returned 3532 event records. The light-gray mask highlights the search area with the results displayed using ranges of magnitude detailed in the figure 11 legend.

Figure 11 (opposite page). Neotectonic interpretation of the NEIC earthquake data with respect to seismogenic zones and lineaments, and the horizontal component of NAP motion. The bright-yellow, polylines highlight patterns of crustal seismicity and are systematically distributed about the Adirondack shield. The light-blue polyline with opposing arrows notes a keel line separating structures plunging SW off the Adirondack uplift and NE off of the Pennsylvania culmination.

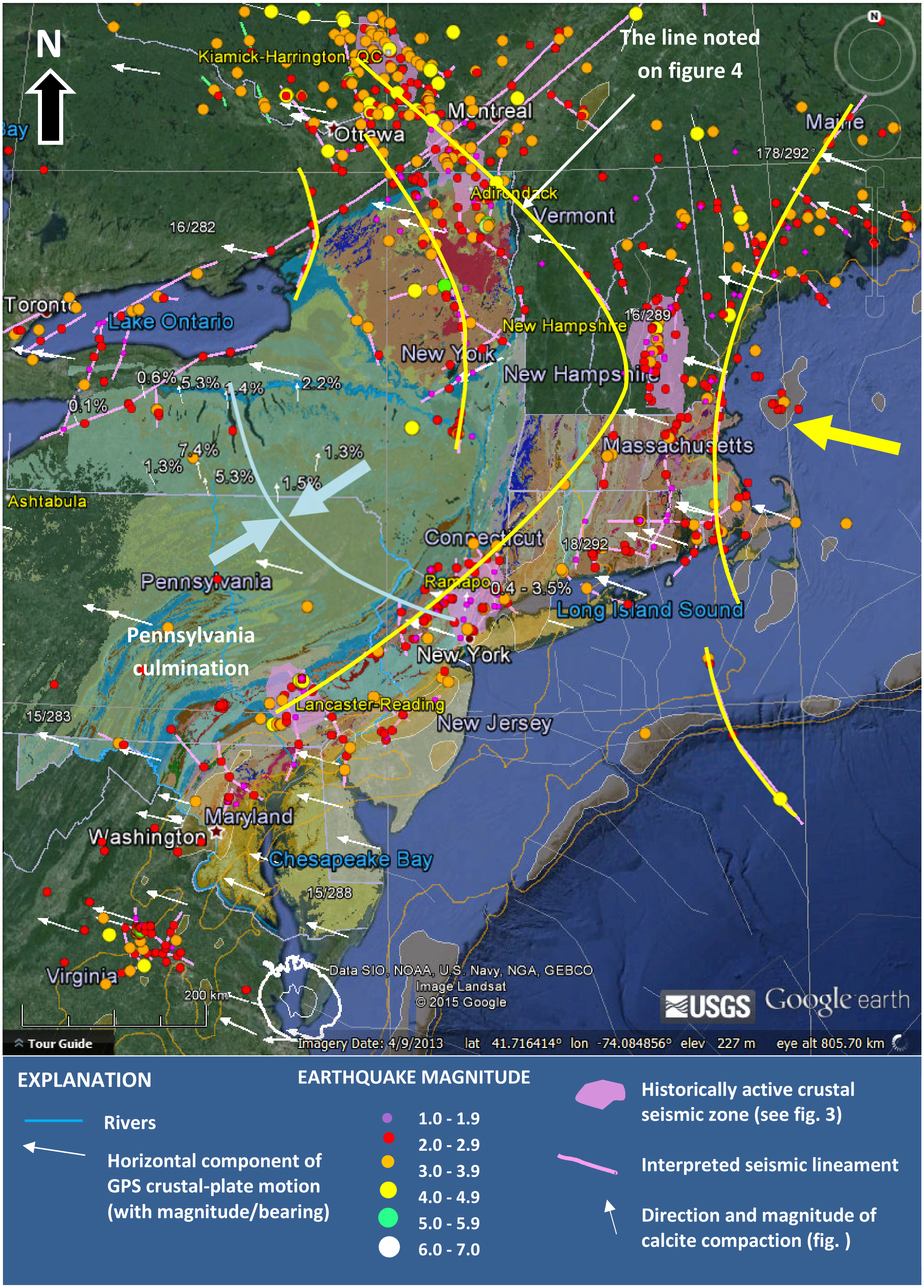
N
Kiamick-Harrington, QC
Montreal
Ottawa
The line noted
on figure 4
Maine
178/292
Adirondack
Vermont
16/282
Toronto
Lake Ontario
New Hampshire
16/289
New York
New Hampshire
0.6%
5.3%
1.4%
2.2%
0.1%
7.4%
1.3%
1.3%
5.3%
1.5%
Massachusetts
Ashtabula
Connecticut
18/292
Pennsylvania
Ramapo
0.4 - 3.5%
Long Island Sound
Pennsylvania
culmination
New York
15/283
Lancaster-Reading
New Jersey
Maryland
Washington
Chesapeake Bay
15/288
Virginia
200 km
Data SIO, NOAA, U.S. Navy, NGA, GEBCO
Image Landsat
© 2015 Google
USGS
Google earth
Tour Guide
Imagery Date: 4/9/2013 lat 41.716414° lon -74.084856° elev 227 m eye alt 805.70 km
EXPLANATION
Rivers
Horizontal component of
GPS crustal-plate motion
(with magnitude/bearing)
EARTHQUAKE MAGNITUDE
1.0 - 1.9
2.0 - 2.9
3.0 - 3.9
4.0 - 4.9
5.0 - 5.9
6.0 - 7.0
Historically active crustal
seismic zone (see fig. 3)
Interpreted seismic lineament
Direction and magnitude of
calcite compaction (fig.)

Table 2. Regional earthquake location and source parameters for focal-mechanism P-axes determinations .

ID	Longitude	Latitude	Depth	Trend	Plunge	Source*
1	-73.82	40.98	6	70	5	1985 Seeber and Dawers (1989)
2	-73.82	40.98	5	95	5	1985 Seeber and Dawers (1989)
3	-75.59	46.47	11	51	3	1990 Du and others (2003)
4	-73.46	45.20	12	50	0	1993 Du and others (2003)
5	-76.01	40.34	2	53	1	1994 Du and others (2003)
6	-76.05	40.34	2	241	2	1994 Du and others (2003)
7	-71.91	44.29	-6	38	6	1995 Du and others (2003)
8	-74.43	45.99	18	40	9	1996 Du and others (2003)
9	-71.35	44.18	7	232	15	1996 Du and others (2003)
10	-74.19	45.81	22	27	15	1997 Du and others (2003)
11	-69.91	47.67	5	102	20	1997 Du and others (2003)
12	-71.35	46.75	22	131	18	1997 Du and others (2003)
13	-80.39	41.50	2	64	8	1998 Du and others (2003)
14	-74.72	46.17	12	71	19	1998 Du and others (2003)
15	-66.39	49.65	18	118	18	1999 Du and others (2003)
16	-78.9	46.87	13	222	20	2000 Du and others (2003)
17	-74.25	43.95	8	219	5	2000 Du and others (2003)
18	-80.83	41.99	2	53	7	2001 Du and others (2003)
19	-73.510	44.650	15	252	30	2002 ISC-HRVD
20	-85.629	34.494	19.6	230	7	2003 ISC-NEIC
21	-86.968	33.203	5	146	74	2004 ISC-NEIC
22	-78.253	43.693	5	250	4	2004 ISC-NEIC
23	-85.796	39.594	6.1	273	0	2004 ISC-NEIC
24	-82.8	35.88	8	43	81	2005 ISC-NEIC
25	-77.287	39.184	5	262	7	2010 ISC-NEIC
26	-77.710	37.970	11	281	10	2011 ISC-NEIC
27	-77.933	37.936	6	104	9	2011 ISC-NEIC
28	-77.951	37.912	7.9	120	16	2011 ISC-NEIC
29	-77.948	37.825	0.1	92	5	2011 ISC-NEIC
30	-77.896	37.940	5	237	14	2011 ISC-NEIC
31	-77.814	37.903	4.9	145	35	2011 ISC-NEIC
32	-77.976	37.907	7.2	109	14	2011 ISC-NEIC
33	-77.932	37.950	3.4	114	5	2011 ISC-NEIC
34	-77.988	37.925	4.8	73	3	2011 ISC-NEIC
35	-77.993	37.935	3.8	107	18	2011 ISC-NEIC
36	-77.983	37.940	4.1	129	26	2011 ISC-NEIC
37	-77.951	37.946	3.1	144	30	2011 ISC-NEIC
38	-77.930	37.910	12	283	4	2011 ISC-NEIC
39	-73.699	44.513	11	92	7	2011 ISC-NEIC
40	-77.983	37.945	3.2	128	27	2012 ISC-NEIC
41	-77.984	37.913	2.9	74	48	2012 ISC-NEIC
42	-77.988	37.906	8.6	289	9	2012 ISC-NEIC
43	-87.1	32.83	12.7	230	10	2012 ISC-NEIC
44	-83.054	37.139	17.1	63	33	2012 ISC-NEIC
45	-80.836	38.642	9.2	73	16	2013 ISC-NEIC

using GE to plot these data arose from using the default placement setting in GE that clamps symbols to the ground. Each of the p-axis symbols uses a model built by positioning two 3D vectors pointing toward one another with the origin of the symbol in the center of the symbol (→•←). But when generated, each symbol was plot using the plunge value so that when it is clamped to the ground at the symbol center point, only the downward plunging half of the full symbol is revealed as the other half is masked beneath ground. This plotting effect reveals some very interesting pattern of historical seismicity, particular at the southern reaches of this region (fig. 3). These patterns merit further inspection and will be discussed in more detailed below.

When viewed collectively, these earthquake data define local and regional earthquake clusters, or swarms that commonly have a linear character that reflects systematic linkage of aligned fault segments comprising a fault system with individually segments active at different times. Historical seismic activity has been proposed to occur on old, ancient, deeply rooted faults such as the Ramapo fault in New Jersey (as detailed later) and appears to occur along linear trends that locally cut older Appalachian trends across-strike with fault systems such as the fault system that are detailed in STOP 1 of Chapter 5. But the geometric arrangement of seismogenic zones and linear trends seen in epicenter plots certainly display systematic distribution relative to the Adirondack Mountains (figs. 4, 8, 9 and 11). Patterns of historical crustal seismicity splay outward around this actively rising Proterozoic basement block as illustrated in figures 3, 8, 9 and 11. As the NAP slowly rotates about a hub that's more or less fixed on the Gulf of Mexico (Herman, 2006), the crust appears to be driving against a resistant Adirondack 'buttress' that is cored by deep-seated ultramafic igneous plutons (fig. 1). Other subsidiary seismic zones and lineaments in this part of the NAP point to other 'sticking areas' that are resisting plate rotation where similar, deeply seated igneous stock appear to pin the crust to the mantle. For example, the Cortland ultramafic intrusive complex of Late Ordovician age heads up, and may cause the Ramapo seismic zone (figs. 8 and 9). The lower arm of the parabolic fracture envelope extend from the Adirondack region SW through the Hudson Valley and the Ramapo seismic zone before dissipating somewhere past the Lancaster-Reading seismic zone (fig. 9). This arm parallels the Ramapo seismic line mapped by Sykes and others (2006) and plotted in figure 11. We can also use the various vectors of plate motion and the pattern of seismogenic responses to predict, oblique-slip motions on the varying old and new faults, and perhaps even examine seismic gaps more closely now. But with respect to the vertical-velocity field, we need to further account for both local and regional elastic strain effects in the crust stemming from erosion and sedimentary loading, glacial unloading, and probably anthropogenic loading, especially near the mouths of bays where humans tend to flock to and build up. Some of these aspects will be addressed in more detail below after some new tectonic representation are first presented that are based on highly detailed, laser-based surveys of land surface.

LiDAR- and aerial-photographic geological interpretations of tectonic structures

A series of regional structural interpretations of parts of northern New Jersey and eastern Bucks County, Pennsylvania were conducted at the NJWS during 2013 to 2015 because of the uncertainty of prior mapping and the new availability of high-precision, laser-based, topographic imaging referred to as LiDAR (see http://oceanservice.noaa.gov/facts/lidar.html), that includes derivative map products like grayshade, topographic relief maps showing bedrock ridges of relatively small relief that are absent from older maps and ortho-photo imagery (see Chapter 5 STOP 1). Currently, detailed, LiDAR surveys of New Jersey are available, but with varying coverage areas and spatial resolutions. The NJ Dept. of Environmental Protection (NJDEP) GIS group recently produced a statewide, standardized, LiDAR-based digital-elevation-model (DEM) and shaded-relief base theme having 15 m^2 cells for use in GIS. At this time, LiDAR data for New Jersey are not available on-line and are only released to the public after personal inquiry to the NJ State Dept. of Treasury[4]. In contrast, Pennsylvania maintains a user-friendly internet portal for distributing their LiDAR data and imagery through the Pennsylvania State Geospatial Data Clearinghouse (http://www.pasda.psu.edu/). For this study, LiDAR hill-shaded LiDAR imagery for areas of Buck's County Pennsylvania that are adjacent to 7-1/2' topographic quadrangles that were, and are currently being mapped by the NJGWS were captured on screen from display in a web browser and saved as separate raster images using a *.PNG file format. Each image was then manually registered in GE to result in a set of overlapping tiles that provide seamless coverage for mapping LiDAR-based bedrock features (fig. 12). These data were used as a basis for tracing bedrock ridges (tan lines on maps) and structural discontinuities from intrusive nonconformities (green contact lines) and other secondary structural features including faults (white lines) and the traces of fold hinges for both synclines (blue) and anticlines (red). Historical GE imagery was very helpful with these interpretations because syncline keels commonly contain a series of ponds or small water bodies' connected by streams running along the keel of the fold hinge. A scanned image of the geologic map of Buck's County, Pa. (Willard and others, 1950) was added to aid in the interpretation of structures that cross the Delaware River (figs. 12 and 15)

The New Jersey part of this work was done using ESRI's ArcGIS platform that provided proprietary access to the NJ LiDAR themes within the NJDEP. For this work, the various sets of LiDAR-based hill-shaded imagery were loaded into an ESRI ArcGIS project in order to trace noticeable bedrock ridges in areas having little sedimentary cover, and generate GIS shapefile themes of the various structural components (figs. 13-15). The same approach was used here, tracing and color-coding noticeable bedrock ridges, nonconformable lithic contacts, folds, and faults in conjunction with previous mapping, and thereby using detailed base imagery to augment the structural interpretation of our tectonic setting. Once a LiDAR theme was interpreted and finished for western (fig. 13) and eastern (fig. 14) parts of the state, they were

[4]https://njgin.state.nj.us/NJ_NJGINExplorer/jviewer.jsp?pg=lidar

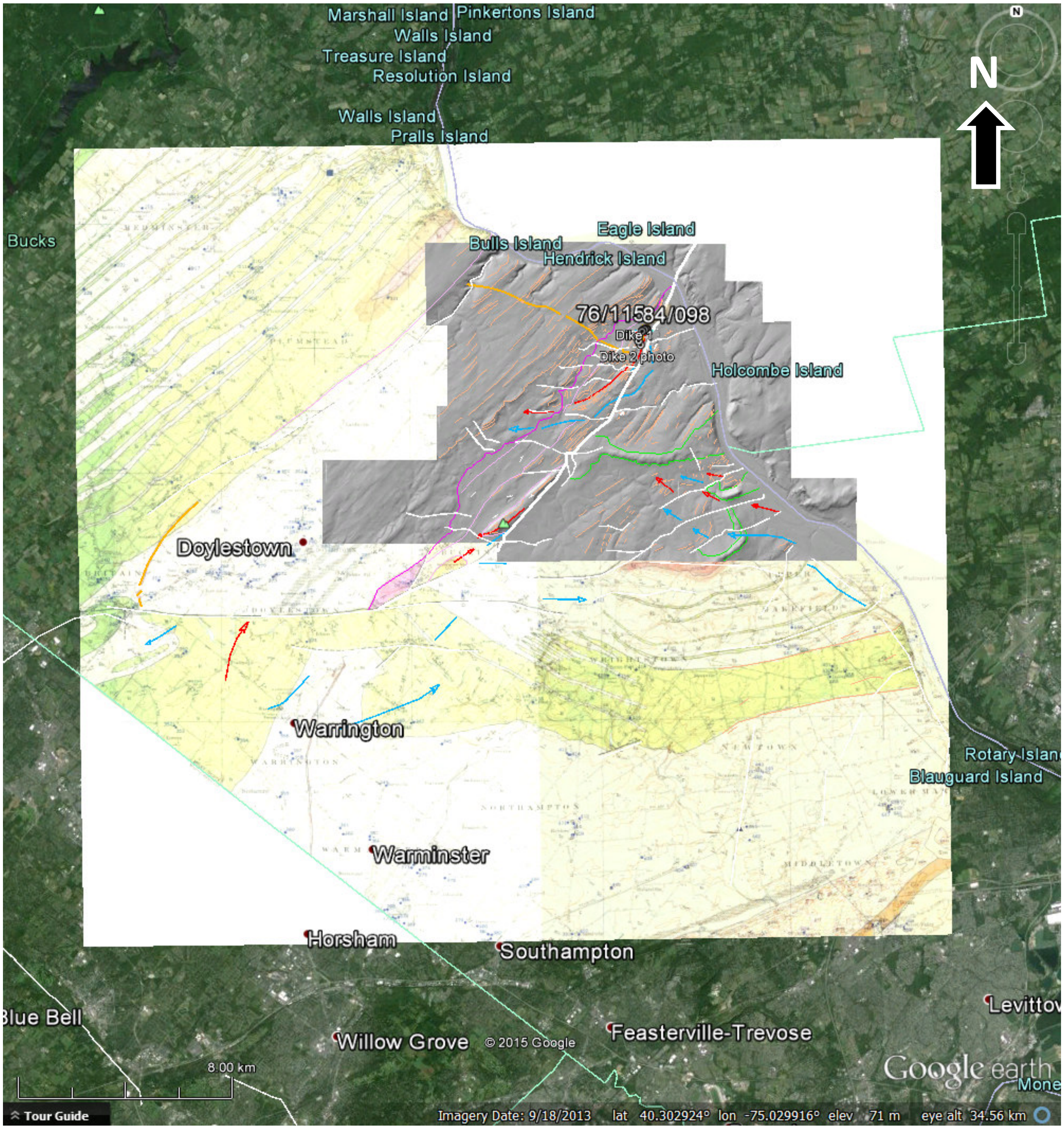

Figure 12. GE display of the Buck's County Geology compilation that is available for download from the GANJ web site. This KMZ file includes part of the Willard and others (1950) geological map of Bucks County, Pa. Large, (centered light-greenish image) and 9 gray LiDAR, hill-shaded images were screen captured from the PASDFA web site and manually tiled together to serve as a detailed base for resolving State-boundary issues stemming from earlier mapping in this area. Colored lines denote faults (white), Jurassic Dikes (orange), anticline axes (red), syncline axes (blue), and nonconformable contacts (green). This work is still in progress and the data files and interpretations are preliminary.

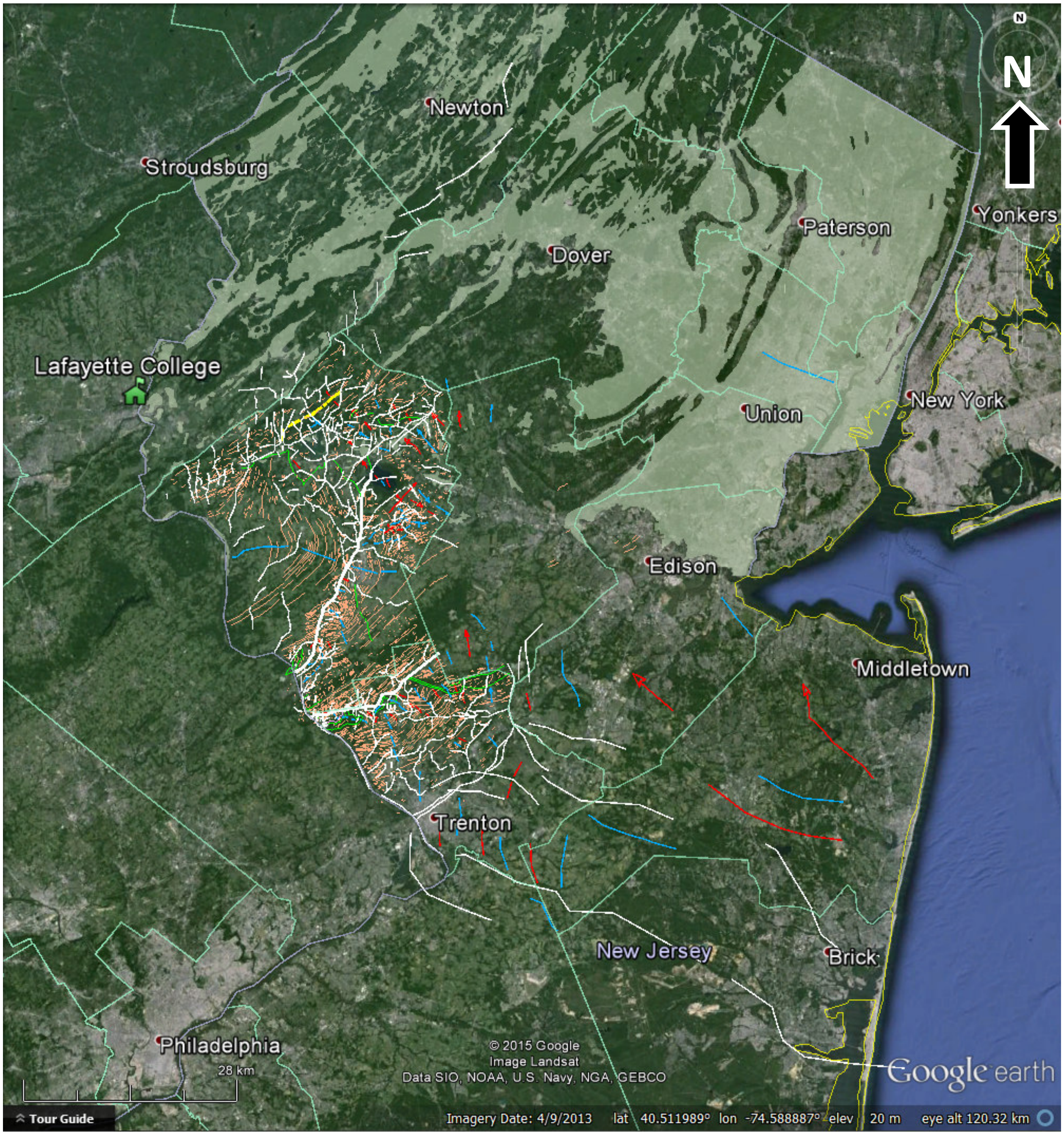

Figure 13. GE display of preliminary, LiDAR-based structural interpretation of western parts of New Jersey. The light green shaded area is a GE KMZ file based on NJ Geological Survey DGS96-1 showing areas of thick sedimentary cover that mask bedrock. Colored lines denote mapped and interpreted faults (white), anticline axes (red), syncline axes (blue) and nonconformable contacts (green). This work is still in progress and the data files and interpretations are preliminary.

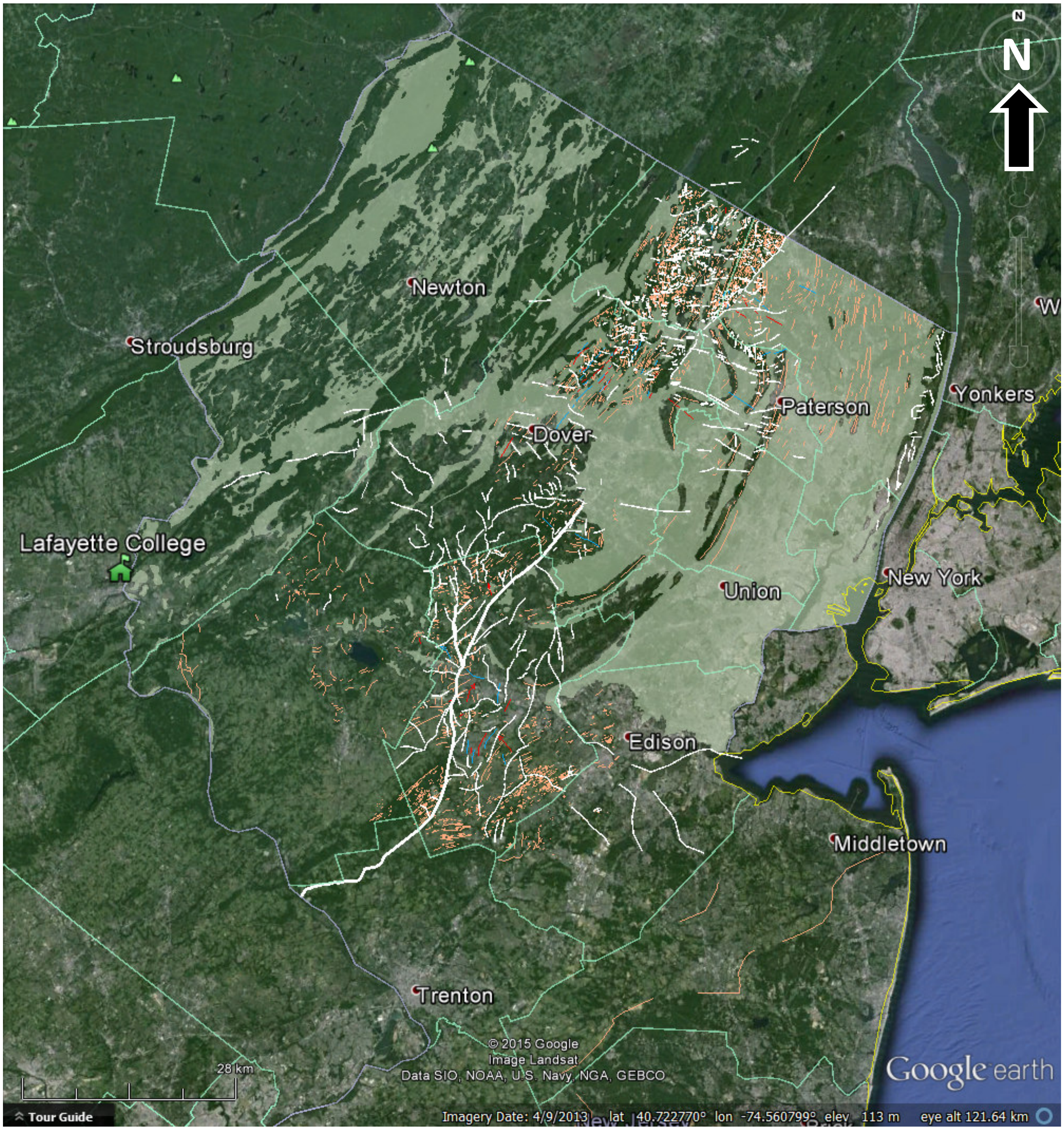

Figure 14. – GE display of preliminary, LiDAR-based structural interpretation of eastern parts of northern New Jersey. The light green shaded area is a GE KMZ file based on NJ Geological Survey DGS96-1 showing areas of thick sedimentary cover that mask bedrock. Colored lines denote mapped and interpreted faults (white), anticline axes (red), syncline axes (blue), and nonconformable contacts (green). This work is still in progress and the data files and interpretations are preliminary.

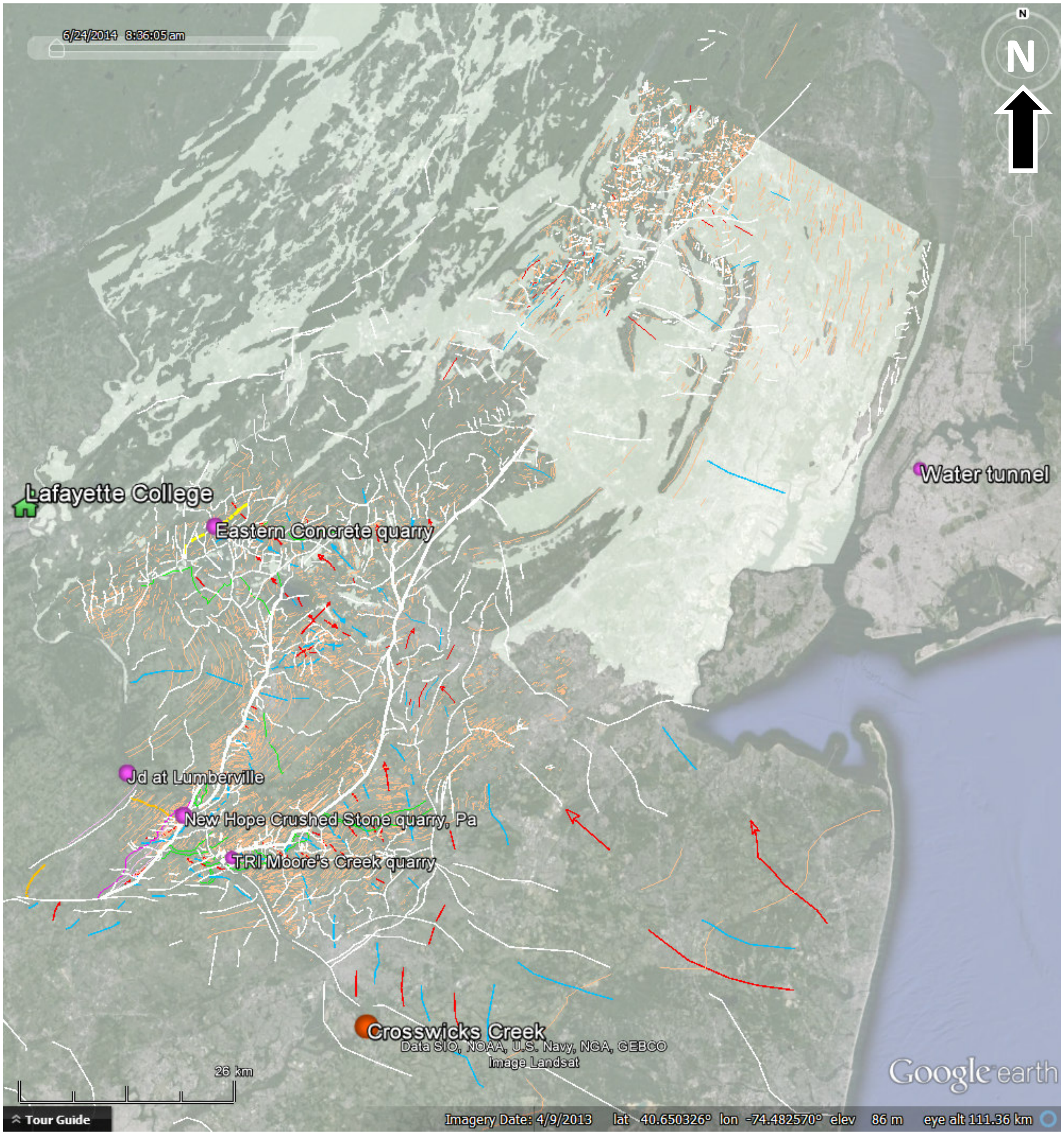

Figure 15. GE display of preliminary, LiDAR-based structural north-central New Jersey resulting from combining work for areas shown in figures 13 and 14. The light green shaded area is a GE KMZ file based on NJ Geological Survey DGS96-1 showing areas of thick sedimentary cover that mask bedrock. Colored lines denote mapped and interpreted faults (white), anticline axes (red), syncline axes (blue), and nonconformable contacts (green). This work is still in progress and the data files and interpretations are preliminary. Locations of the GANJ 32 field STOPS and some other points of interest are noted.

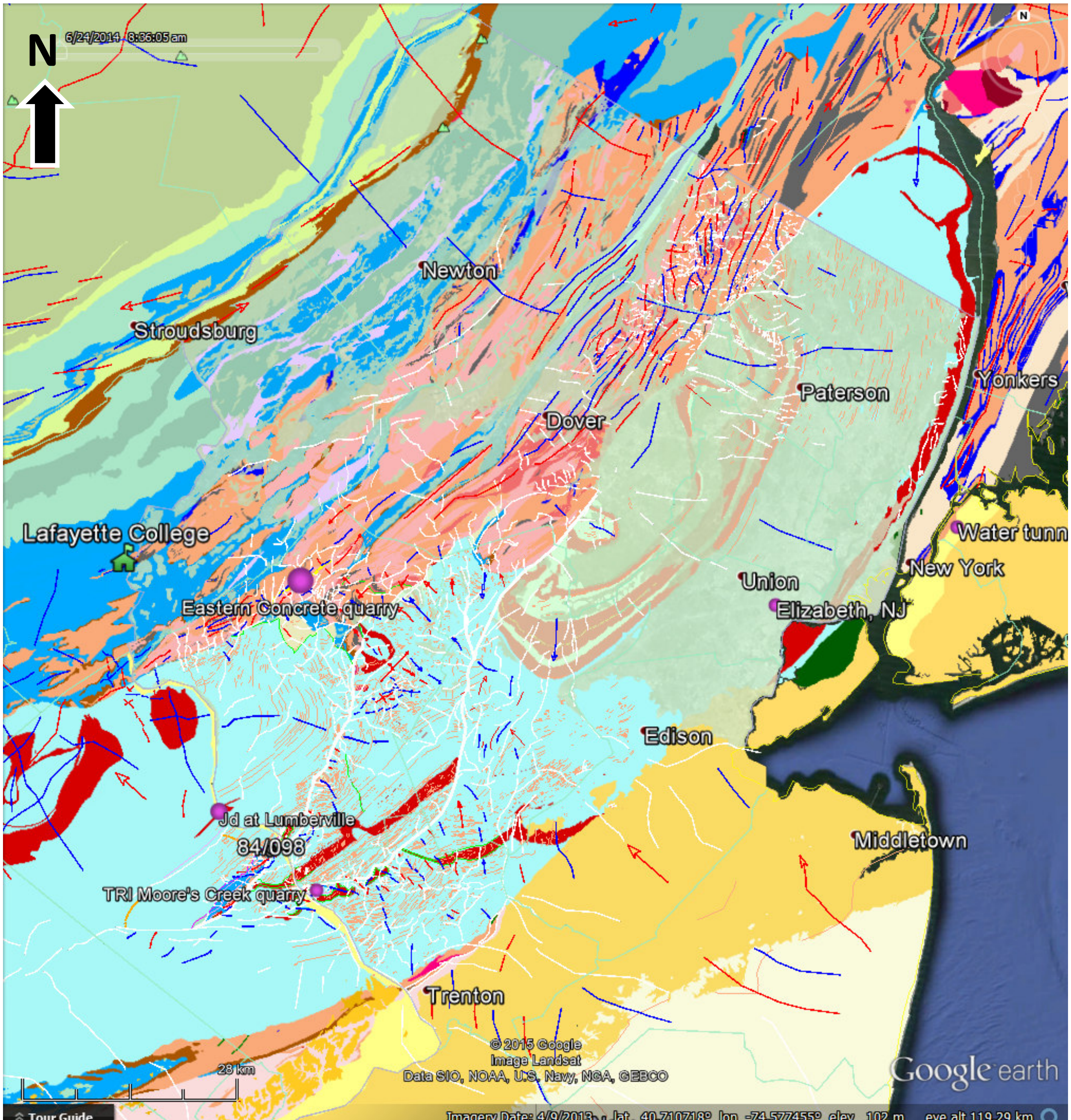

Figure 16. GE display of northern New Jersey and surrounding areas combining themes shown in figures 1 and 12 - 15. The legend for the lithic groups is shown on figure 2. Note the labels denoting the physiographic provinces and border faults along the NW edge of the Newark Basin, including the Ramapo fault. The Newark basin comprises most of the Piedmont province.

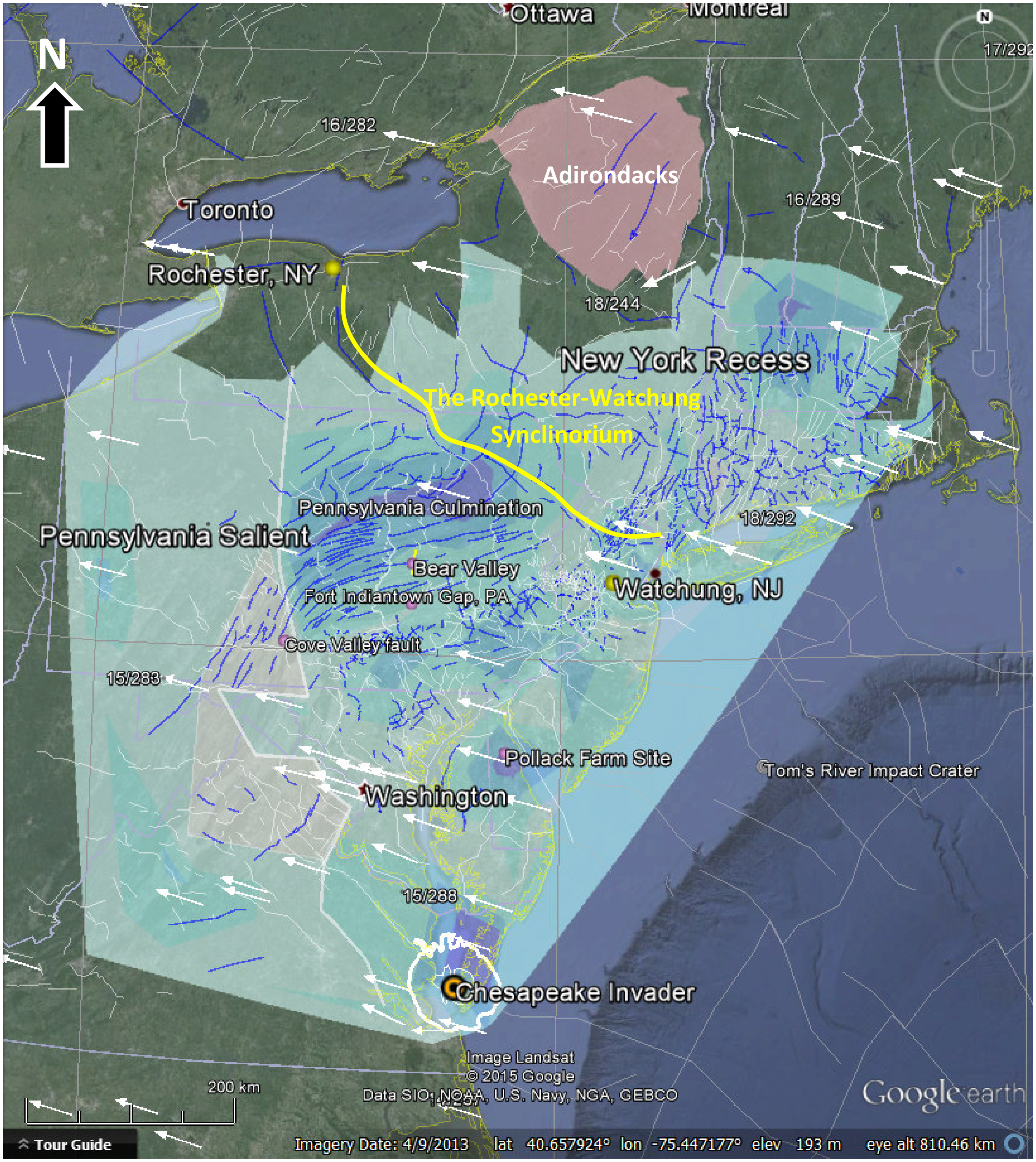

Figure 17. GE display showing aspects of the preliminary , regional neotectonic compilation in the region of the New York Recess showing traces of major fractures systems on and near land (white lines), interpreted oceanic transform faults (gray), current direction of horizontal plate drift, and syncline axes (blue lines) . Also noted is the Chesapeake Bay impact structure with the thicker white line noting the carter's outer rim, and other places referenced in the text.

converted to GE KML files, and then combined into a single theme for continued editing and refinement in GE (fig. 15). These themes are only preliminary bedrock interpretations that have yet to be reviewed and as such are provided through the GANJ web portal as open-file products that come with the caveat that they are still subject to revision and modification as they are in draft form and may be useful as a base for further work in adjacent areas lacking details or for whatever the user may have in mind.

The next step in the interpretation process was to take the LiDAR-based interpretations and compare them to the generalized, regional geological theme for further refinement. For this regional part of the structural analysis, the more prominent fracture traces (including faults) and fold axes were added to a new KMZ file with individual subfolders so that the interpretation could be augmented using GE imagery in combination with the USGS geology theme (fig. 17). The focus of the interpretation was one fracture systems that imparted structural discontinuity to older Appalachian grain, as well as cross-strike folds or flexures that were either added from published state geological maps, or were apparent with respect to the geological map pattern and landforms as seen in the historical photographic imagery within GE.

Data added from State geological maps within the region of study ranged in scale from 1:100,000 to 1:250,000. Many of the USGS GIS statewide geology themes include subthemes of digitized fault traces as part of the retrieved KML files, and these were incorporated as available. Other computer-based interpretation tools were used to constrain the directions and dips of some bedrock panels that define fold limbs. These software tools include the 3D GE and NOAA 3-point problem solving applications recently developed by the NJGWS as described and exemplified in Chapter 1. During interpretation, traces of major fracture systems, anticlines, and synclines were systematically organized into different subfolders in the KMZ file 2015_NJGWS_GANJ_32 GCH_NY_Recess Bedrock _Structure_Compilation.kmz that is available for download through the GANJ web site. Figures 16 through 19 show aspects of this regional structural synthesis with respect to part of the USGS geology theme, the ground-motion TIN (of fig. 3), and global geophysical, potential-field themes of Bouguer gravity and total magnetic field intensity that were compiled by different sources using a GE KMZ file format. These geophysical themes are very useful when used with GE theme-transparency settings to help constrain the form of interpreted regional structures. Note that major fracture systems are commonly mapped along surface-water drainage, and folds include an arrow head in many places indicating a probable direction of axial plunge. As a result, some unexpected regional-scale fold patterns emerged, such as a regional synclinorium that separates the Pocono Plateau from the Pennsylvania Culmination, referred to as the Rochester-Watchung Synclinorium. This major structural depression consists of a series of en echelon synclines stretching from Rochester NY through the Watchung syncline of NJ over a distance approaching 400 kilometers. This line appears to mark the current boundary between structures plunging SW off of the rising Adirondack shield, and NE off the eastern limb of the slowly subsiding Pennsylvania Culmination (fig. 17). This cross-strike trend appears common throughout the New Jersey, southern New York, and New England region, and lays sub-parallel to current, horizontal plate motions (fig. 17). Such features are candidate neotectonic structures as they appear to also conform to current plate motions and one of two statistical populations of current p-axes orientations in the region (fig. 18). Perhaps these broad, open folds and warps are a neotectonic strain response in the NAP as it continuously and slowly grinds over deep-seated, igneous intrusions that once pinned the crust to the mantle within the old Appalachians roots, and thereby resist current separation. These structures and such processes will be considered further in the concluding discussion.

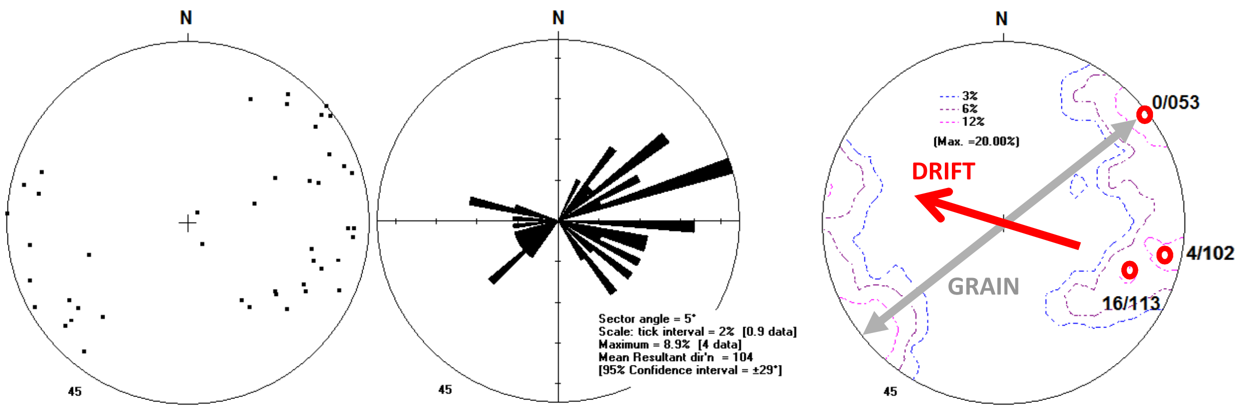

Figure 17. Lower-hemisphere, equal-angle plots of the 45 p-axes orientations compiled in table 2. Most current compression axes plunge eastward, and show three statistical 'maximums', one trending along the Appalachian tectonic grain (~053^{o} azimuth), and two others that nearly oppose the current horizontal direction of plate drift (~287^{o}).

Chronostratigraphic summary of tectonic stages and brittle structures in rock and sediment in the region of the New York Recess.

It is impractical for this chapter to thoroughly review and summarize all of the nuances stemming from the collective body of work detailing the different Appalachian structures in this region, not to mention the probability of their involvement in neotectonic activity. Rather, select studies are summarized that emphasize key concepts, or that include details pertinent to this report on the characteristic occurrences and distributions of known, probable, and possible neotectonic structures in our region. A systematic grouping of possible neotectonic features is done beginning with the least numerous and relatively youngest features before proceeding systematically backward through time and structural complexity using the chronostratigraphic units detailed in figure 3. Further discussion of the respective brittle, crustal strains is placed

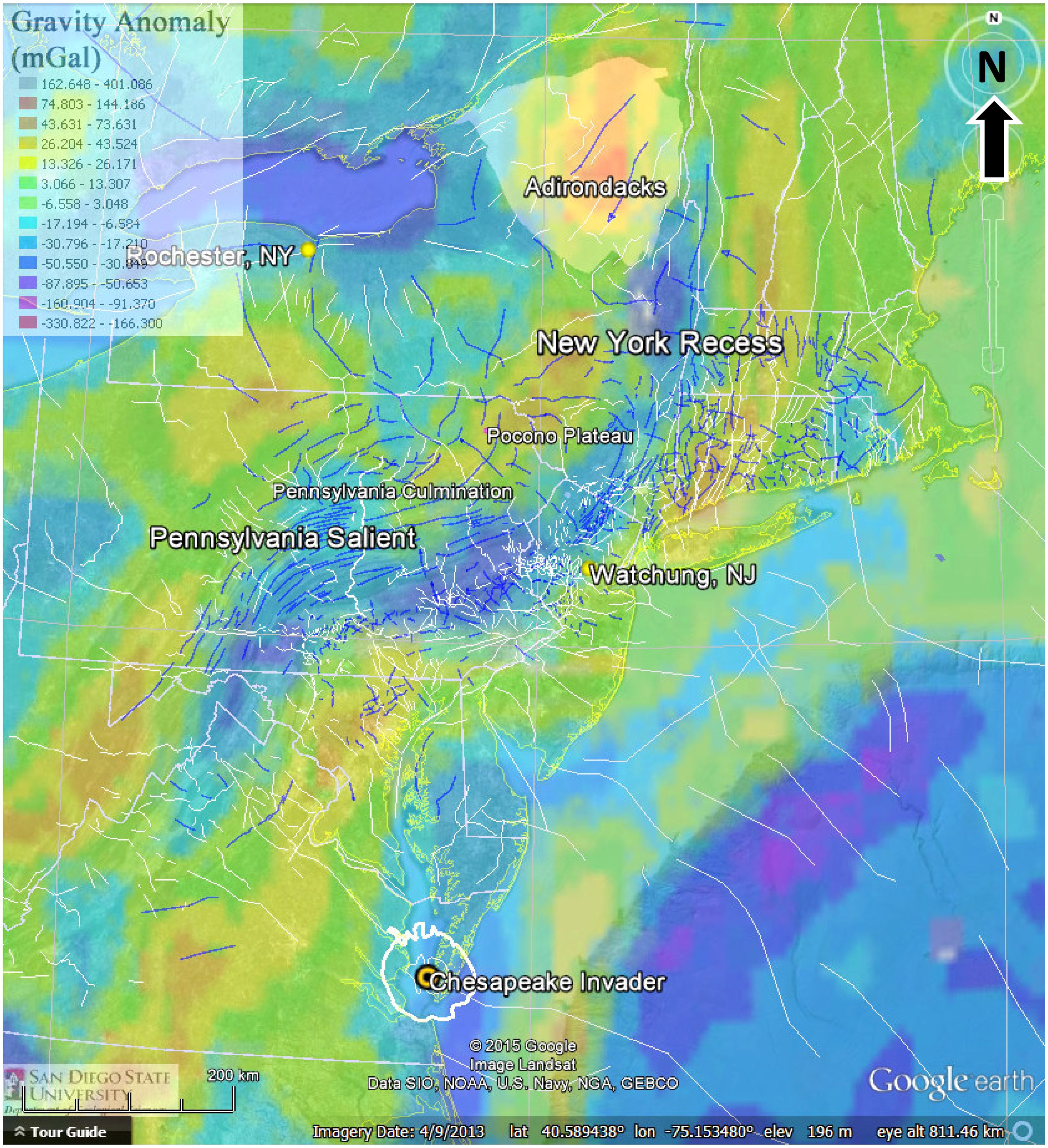

Figure 18. GE display showing the same interpreted geological structures noted in figure 17 with the GRACE Global Gravity Model 2 activated and set to about 60% transparency. For more information on this geospatial theme, please refer to:

Tapley, B., J. Ries, S. Bettadpur, D. Chambers, M. Cheng, F. Condi, B. Gunter, Z. Kang, P.Nagel, R. Pastor, T. Pekker, S.Poole, F. Wang, 2005, GGM02 - An improved Earth gravity field model from GRACE: Journal of Geodesy, http://www.csr.utexas.edu/grace/.

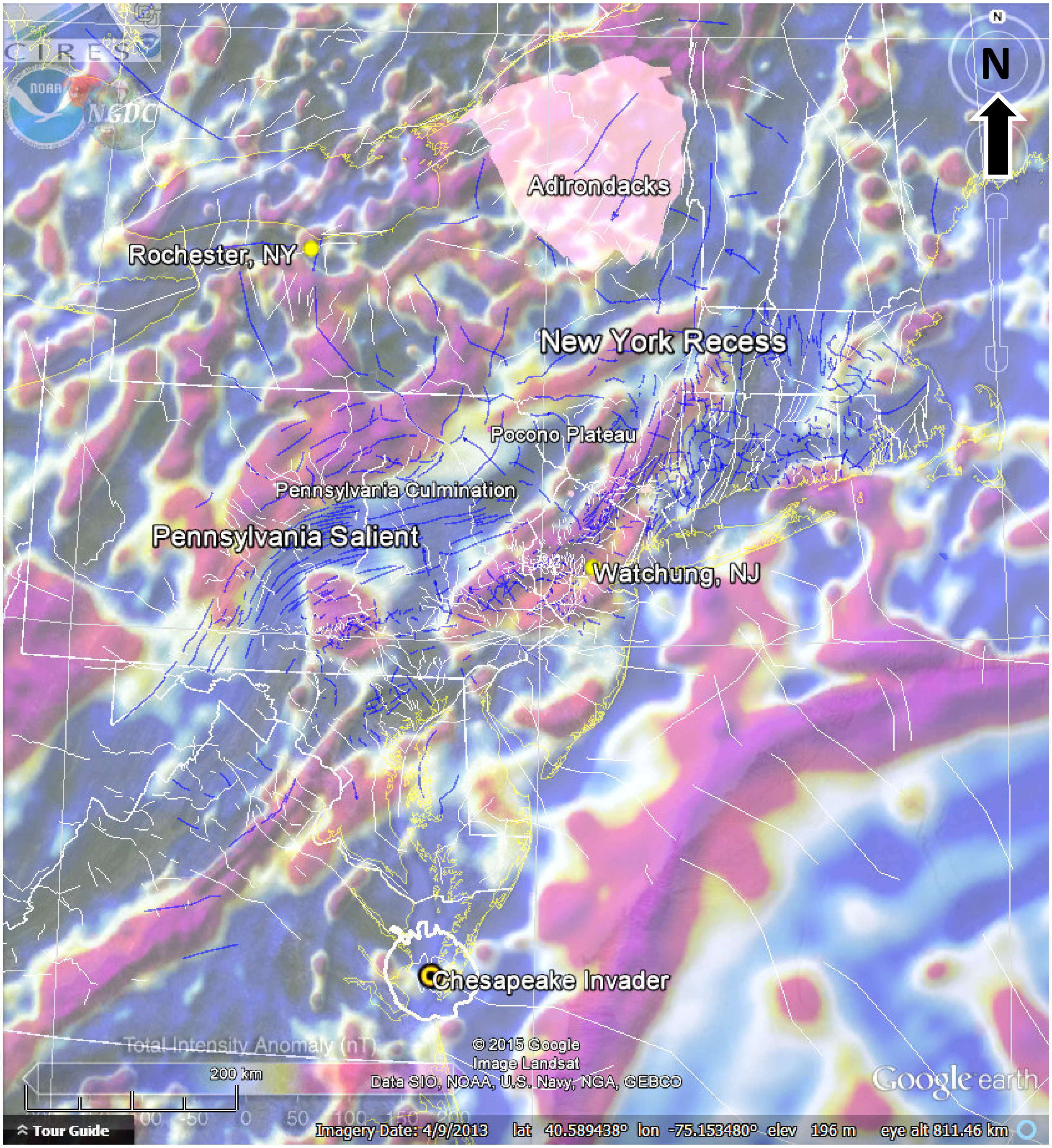

Figure 19. GE display showing the same interpreted geological structures noted in figure 17 with the Earth Magnetic Anomaly Grid EMAG2 activated and set to about 60% transparency. For more information on this geospatial theme, please refer to:

Maus, S., U. and 22 others, in review, EMAG2: A 2-arc-minute resolution Earth Magnetic Anomaly Grid compiled from satellite, airborne and marine magnetic measurements: http://geomag.org/info/Smaus/Doc/emag2.pdf. http://geomag.org/models/emag2.html into context with hypothetical stressors and other critical, neotectonic considerations including glacio-isostasy, sedimentary loading and lithospheric flexure at the end of this report. For now, we progress backward through time and deeper into the lithic section to summarize what we currently know about known or suspected neotectonic structures occurring in this region.

Tectonic Group 4 Cretaceous and Cenozoic age (<120 Ma years)

As depicted in figures 3 and 20, a treatment of neotectonic structures in strata of Cenozoic age requires further use of subgroups that reflect the stratigraphy of the NJ coastal plain and nearby Atlantic shelf region, where the most complete sedimentary record is preserved. This primary grouping includes the glacial and pro-glacial detritus on land of Pleistocene age and the more recent Holocene alluvium (fig. 20). The Cenozoic Era into six epochs covers the past 66 Ma and is nearly halved at the Eocene-Oligocene boundary ~34 Ma, just above a pronounced unconformity found throughout the eastern margin of the NAP (fig. 20). There are a number of disturbances and sedimentary pulses both on land and in the costal and submarine stratigraphic record during this time, some of which must stem from the 'Tertiary elevation' of our region as previously noted. This uplift episode, or series of episodes, probably resulted in the rapid erosion of Appalachian cover, the amount of which is reserved later for late discussion and speculation. After the Oligocene, the seas returned and retreated onto the coastal plain of our continental margin many times (Pazzaglia and Gardner, 1994; Browning and others, 2008). Consequently, this stratigraphic record is complex but has been studied in detailed using drill core and multi-channel seismic reflection data throughout the mid-Atlantic region (for example, see Miller's keynote abstract and Metzger and others, 2000). As illustrated in figure 20, chronostratigraphic units are separated into groups that are bounded my major unconformities with both continental and submarine expression within strata deposited on the continental shelf. Focused consideration is given to a few records that show clear representations of stratigraphic and structural relationships pertinent to this neotectonic theme.

The description of this group is comparatively easy insofar as there has been no direct, confirmed, visual geological evidence of Quaternary to Late Tertiary geological faulting seen in the New Jersey, or the New York City area historically. There are isolated incidences where indirect evidence of Pleistocene sediment thickening across possible faults scarps (Stanford and others, 1997), or perhaps deposited and preferentially preserved along a reactivated Mesozoic fault (Herman and others, 2014), but the entire area has been mapped in detailed beginning around 1900 and there are no photographic reports or noted visual records of structural disruption of strata of this age. Owens and Minard (1979) report that a reorientation of Pliocene gravel of Late Pliocene age in the New Jersey Coastal Plain from south to southeast and speculated on a tectonic control, but they state that "no faults or folds have been detected in Cretaceous formations in the area to support his hypothesis". Late Pliocene to Pleistocene deposits offshore in this region have been extensively studies using high-resolution, seismic-reflection profiling like that of Metzger and others (2000), and there are also no know reports of visual, structural disruptions in subsurface records of this age strata, explicitly including the Cohansey Sand and Kirkwood Formation. The only indirect, subsurface interpretation invoking structural disruption of strata in the Coastal Plain of New Jersey is that of Sheridan and others (1991) from the southern part of the province where a deep seismic-reflection profile was run in an attempt to decipher upper crustal structures in the 2 to 6 km depth range. From this study they interpreted Mesozoic rift basins beneath Coastal Plain units based on horizontal velocity contrasts, and they depict in profile, half- and full-grabens from the line that have border faults cutting up section through most of the coastal plain units almost to the sediment-water

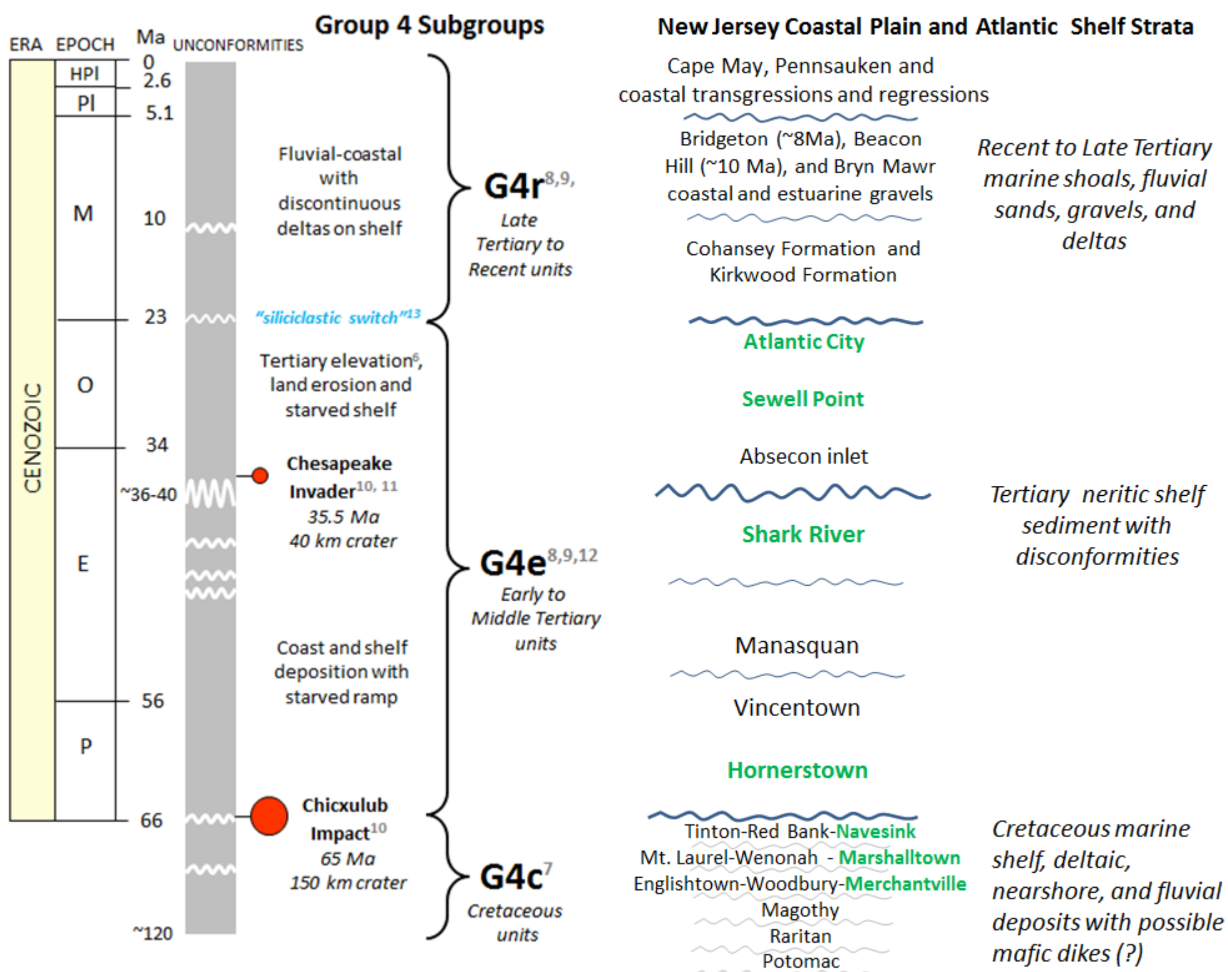

Figure 20. Chronostratigraphic tectonic subgroups for the Cenozoic Era with respect to strata of the New Jersey coastal plain and Atlantic continental shelf (fig. 3). Glauconitic formaitons are colored green.

interface. Offset on these faults is minimal; however the raw stacked records do not clearly show stratigraphic disruption, leaving these faults and their penetration of the coastal plain units as uncertain.

The lower –middle Miocene sequence in the coastal plain reflect a strong influence of riverine sources of sediment in contrast to subjacent marine strata (Browning and others, 2008). There is one well-documented site in this region where lower Miocene strata contain chaotic and folded beds with visible, brittle fractures and faults. It's noted in figures 17 and 23 as Pollack's Farm, and is situated across the Delaware River from New Jersey. Andres and Howard (1998) photographed fractures, joints, and faults in Lower Miocene strata here, but provided no orientation data. They attribute sedimentary disruption and some brittle fracturing to probable cryoturbation processes stemming from seasonal freezing in near periglacial climates, but state that some of these features appear to have formed in an extensional stress field, possibly related to reactivation of the nearby border fault zone associated with an inferred, buried Mesozoic rift basin, such as those reported by Sheridan and others (1998). However, they also note that some of the brittle features may have formed in response to erosion and unloading or weathering and mineralization processes. Ramsey (1998) also depicts sub-vertical fault here in cross section that repeatedly offset Lower Miocene strata along steeply dipping faults that terminate upward into blanketing Quaternary alluvium. So it is probable that brittle fracture and faults occur elsewhere in the region in strata of this age, but they remain elusive, and apparently spotty in their spatial distribution.

Crone and Wheeler (2000) summarized known occurrences of Quaternary faults, liquefaction features, and possible tectonic features in the Central and Eastern United States, east of the Rocky Mountain front. They report "in each case, paleoseismological fieldwork and other studies found no clear geological evidence of prehistoric earthquakes larger than the small or moderate shocks known historically". They included a review of reports pointing to the possibility of Quaternary tectonic activity based on pollen data, sea-level curves from tidal marshes, soft-sediment deformation observed in cored sediments from a glacial lake, and geomorphic observations. None of these provided evidence of sudden seismic slip as opposed to slow aseismic creep. Most are inconsistent with the orientation of the existing compressional stress field and the absence of significant post-Mesozoic slip. Nevertheless, modern geological and geophysical work have failed to directly demonstrate secondary tectonic structures in New Jersey or bordering parts of NYC and Pennsylvania for this group of strata.

Subgroup G4e – Early to Middle Tertiary (~23 - 66 Ma)

During the early Tertiary, the northern African plate boundary shifted from transtention to compression (Klitgord and Schouten, 1986), and our regional stress shift may have occurred during this time as well. There is a pronounced unconformity at the Cretaceous-Tertiary (K/T) boundary (fig. 20), and afterwards, the deepest water depths of the Cenozoic were attained in this region during the lower to lower middle Eocene (Browning and others, 1997). Land and coastal areas were elevated and eroded during this time (fig. 20), and the only coastal plain strata of Oligocene age in New Jersey are found in the subsurface in the southernmost area of the state (Miller, 2015). The New Jersey coastal plain strata contain other, pronounced unconformities within upper Eocene through Oligocene strata that were deposited in starved ramp and shelf environments (Miller, 2015). The pre-Miocene disconformity separating the Kirkwood Formation from subjacent Eocene strata in the NJ coastal plain is widely recognized in both outcrop and the subsurface as the longest hiatus in the northeast Atlantic continental margin, and resulted from a drop in sea level near the of Eocene time (Olsson and others, 1980). Moreover, seismic-reflection data in some areas of the shelf show pronounced channeling of a seaward-prograding wedge of sediment that was subsequently scoured by a down-slope erosional event that produced submarine canyons just above Eocene/Oligocene boundary (Miller and others, 1985). A subsequent, rapid rise in sea level began sometime during mid-Oligocene time but sedimentation rates remained slow then and the entire continental margin in the region was sediment-starved, not only of siliciclastic but also of pelagic carbonate (Browning and others, 1997). According to Malisnky and Barlett (1975), the stratigraphic sequences during this time to our north in Nova Scotia and Newfoundland are eroded on shore, and those offshore are the result of differential preservation with less than one half of Middle Eocene to Miocene time is represented, including 12 Ma hiatus separating Middle Eocene and Lower Oligocene units. Other, smaller-duration hiatuses separate Oligocene and Middle Miocene strata, as well as the Middle and Upper Miocene units to our north as well as here (fig. 20).

The only reported occurrence of brittle structures found in the Early- to Middle-Tertiary strata in New Jersey are localized, strangely-disrupted sandstone beds in the Vincentown Formation of Late Paleocene age, where thin beds of lithified, coarse sand are impregnated with limonite and appear to be rolled up and folded (fig. 21). However, these distortions may not be tectonic as they may stem from diagenetic alterations (Peter Sugarman, personal communication, November, 13, 2014). More exposures of these and-or other similar beds of this age are needed in order to better assess the nature of these secondary structures. Nevertheless, measured fracture orientations and possible fold axes in the unit are included on figure 21 to demonstrate that the trend of the apparent folding in this unit is nearly orthogonal to the current horizontal component of plate drift.

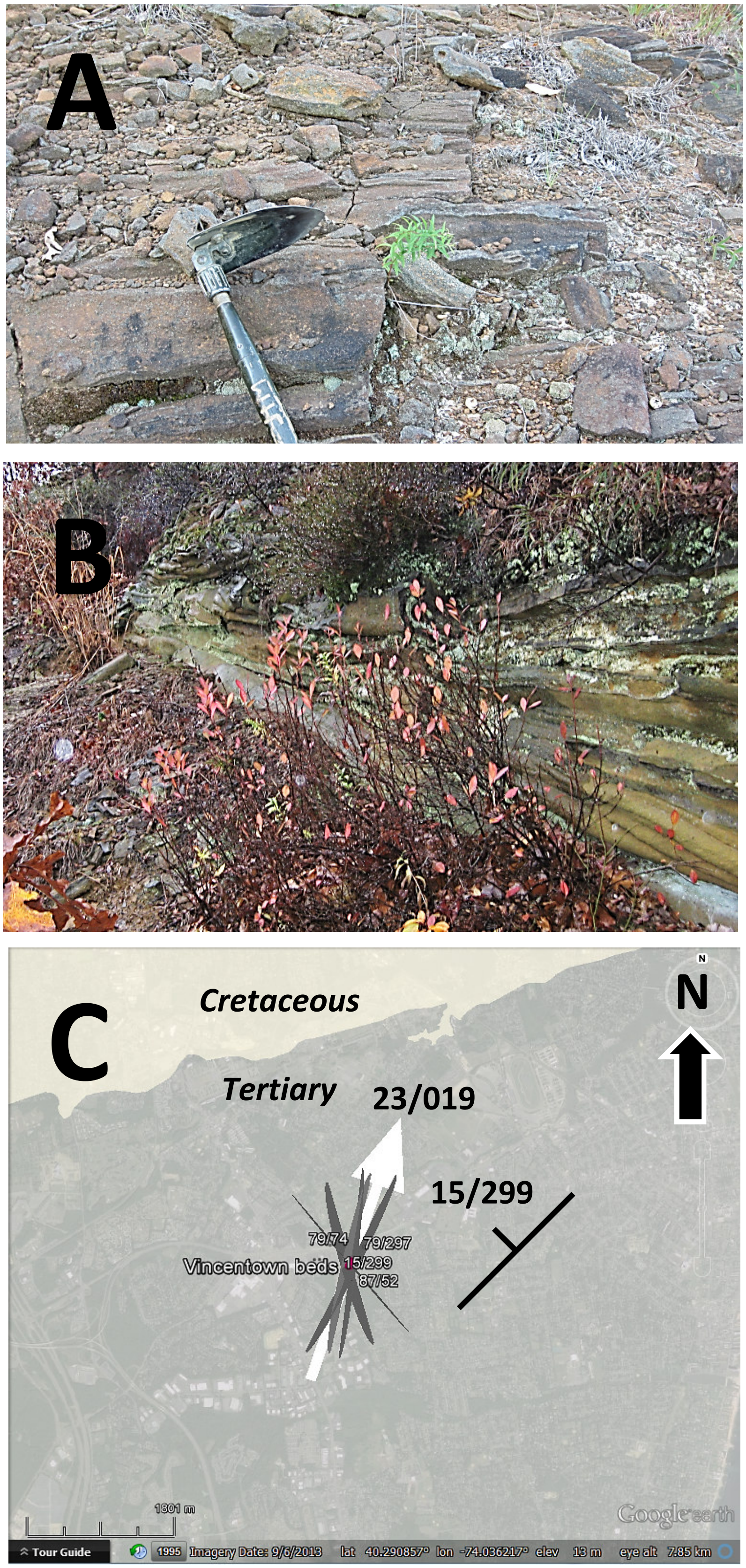

Figure 21. Photographs (A and B) and GE plot (C) of potential, secondary tecotnic structres in the Vincentown Formation of Early Tertiary age (fig. 20). (A – SE view and B NE view) GPS site coordinates are ~LAT 40.157 LON -74.657. The contorted, Fe-cemented sandstone beds are apparently rolled up and folded with a possible plunge/trend of ~23/019). Fracture planes (3D gray ellipses) strike parallel and across beds oriented ~15/299 (dip /dip azimuth). See text for further discussion.

Subgroup G4c - Cretaceous (~ 66 to 120 Ma)

Secondary structures cutting steeply dipping Cretaceous strata in the New Jersey Coastal Plain (fig. 22) have been mapped as cross-strike discontinuities (fig. 23). Old reports such as Ries and others (1904) also note structural disruption in Cretaceous clay, including small faults, iron-oxide veining, folding, and warping of these units in our region. They point out that tilting and folding of these units exert an "important influence of the form and extent of the outcropping beds", but "faulting is rarely seen". Dombroski (1987) noted fracturing, slickensided shearing and disturbed zones in the Cretaceous Woodbury Clay as part of a hydrogeological assessment of the Woodbury-Merchantville confining layer. I have also seen steeply dipping, slickensided, and pyrite-mineralized small faults cutting Cretaceous clay many years ago, but at the time was unappreciative of the tectonic implications, and unprepared to measure and record specific structural and locational information. The Cretaceous units of the Coastal Plain have been structurally disrupted, and today's drainage patterns reflect rather subtle tectonic structural controls that are generally poorly understood, but are generally attributed to large-scale warping of the crystalline basement underlying the coastal plain (Owens and others,1986). Much more evidence of Cretaceous and Cenozoic tectonic structures occurs further south along the Appalachian margin beginning near Virginia and Maryland (York and Oliver, 1976).

Figure 22. Photos of steeply dipping beds (A) and faulted Cretaceous strata (B) described in NJGWS permanent notes from the Crosswick Creek clay pit circa 1956. This was noted as possibly stemming from soft-sediment slumping and sliding of beds into an old stream channel. But structural disruption of innner Coastal Plain strata has been reported in the Woodbury Clay, the Navesink Formaiton, Englishtown, and Raritan Formations that is probably tectonic is origin.

The New England Seamount Chain formed just to the east of this region about 70 to 124 Mya during active continental rifting as basin growth accelerated in the North Atlantic to the east of Canada and west of Greenland (Duncan, 1984). At this time, our region was probably being stretched in a northeastwardly direction (fig. 24) , as indicated by the latest-stage extension fractures cutting early Jurassic strata in our region along cross-strike trends of ~160^o to 180^o that we will cover in more detail below.

The set of oceanic transform faults referred to as Kelvin-Cornwall displacement (Drake and Woodward, 1963) coincides with the New England seamount chain (fig. 24) that is an integral structural component in stretching this part of the evolving NAP northeastward as spreading propagated northward along the Appalachian margin. The cross-strike secondary structures that cut Cretaceous units of the NJ Coastal Plain (fig. 23) display right-lateral and normal-slip components (Klewsaat and Gates, 1994) that are the same displacement noted along the Kelvin-Cornwall displacement. The zero (0) mGal Bouguer gravity anomaly exemplifies this stretch (fig. 24) if we assume that its current expression along the NAP's Atlantic margin reflects segmented CAMP bodies that were emplaced during the Jurassic and subsequently stretched during the Cretaceous (Herman and others, 2013).

Tectonic Group 3 - Newark (~120-260 Ma)

The rift-basin setting of the Newark basin is well known, and different sets of tensile brittle structures are systematically distributed, oriented, and arranged with respect to one another in Early Mesozoic strata (fig. 25, and Herman, 1997; 2005; 2013). Fractures generally strike parallel to nearby, mapped faults with steep dip angles (~60^o to vertical). They are densest near border faults that parallel the Appalachian grain (S1 of fig. 25) and large intrabasinal faults such as the Flemington and Hopewell (S2 of figs. 24 and 25, also see chapter 5, STOP 2). These three groups of extension fractures and faults developed with an upward, helical twist in strike through strata and time (fig. 26). The oldest (S1) fractures occur in the oldest strata and locally show signs of stratigraphic compaction, indicating that they formed early in the depositional history of the basin (Herman, 2001). Fractures of intermediate strike cluster about N10^o -N20^{o}E and are among the most widespread and pervasive joints in the region. These fractures probably formed during an accelerated phase of crustal extension and concurrent igneous intrusion of CAMP bodies as the crust was being rapidly pulled apart (Herman and others, 2013). Jurassic dolerite dike swarms in Pennsylvania bearing this strike penetrate far into the Appalachian foreland where they bound the eastern side of the Pennsylvania Culmination and coincide in trend with an intermediate reach of the Susquehanna River (fig. 27). The youngest set of extension fractures (S3) strike across the Appalachian grain and overprints and locally offset earlier structures (fig. 25). These fractures are also recognized in the NJ Highlands (Chapter 5 STOP 1) as well as the NYC area in Proterozoic and Paleozoic

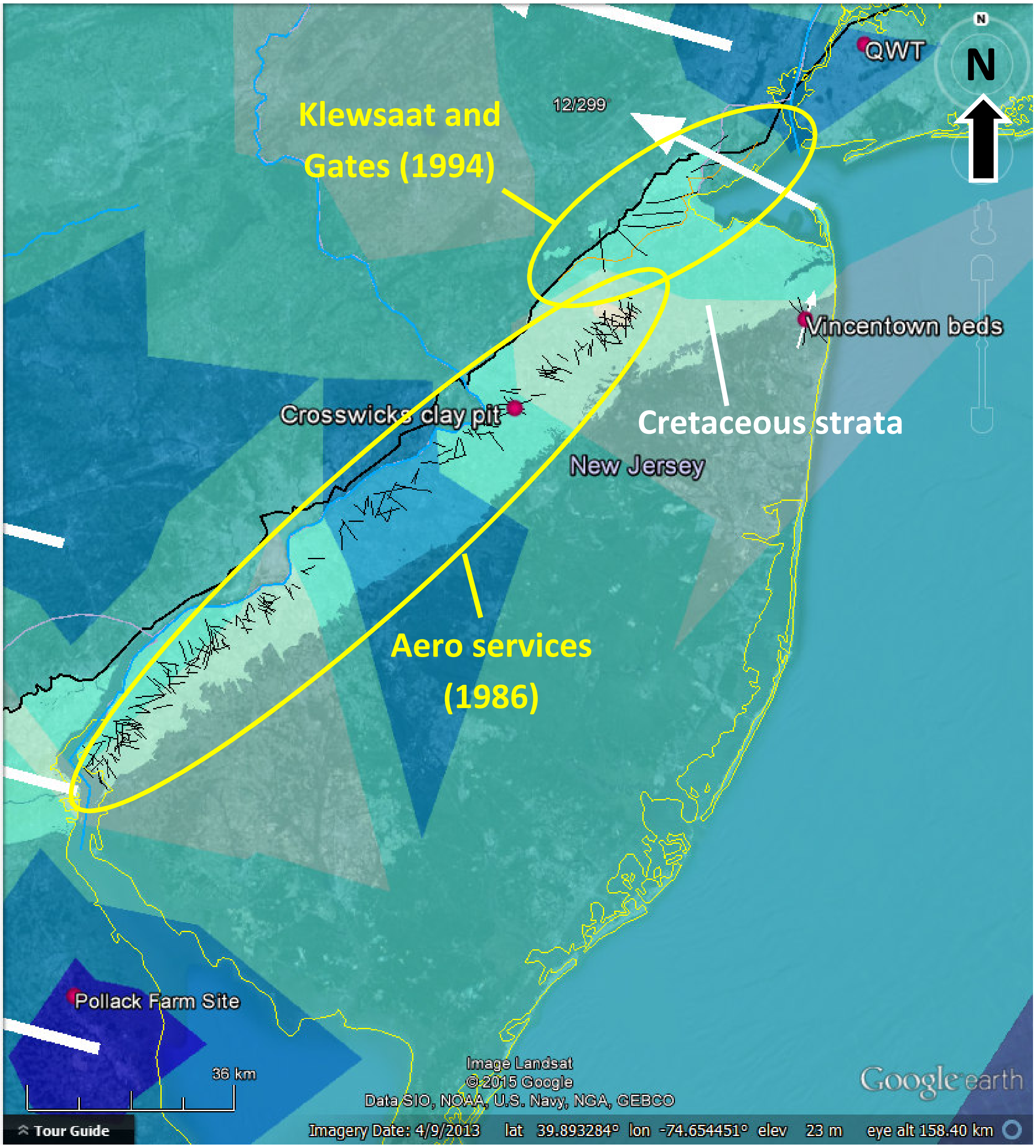

Figure 23. GE map centered on outcropping Cretaceous strata in New Jersey showing the TIN velocity surface (fig. 3), mapped topographic linements in the Woodbury Formation (Aero Services, 1986), concealed faults offsetting the buried extension of the Palisades Sill (Klewsaat and Gates, 1994), and other locations where apparently disrupted strata are reported in the NJ Coastal Plain (see text for further discussion) . QWT – Queen's Water Tunnel.

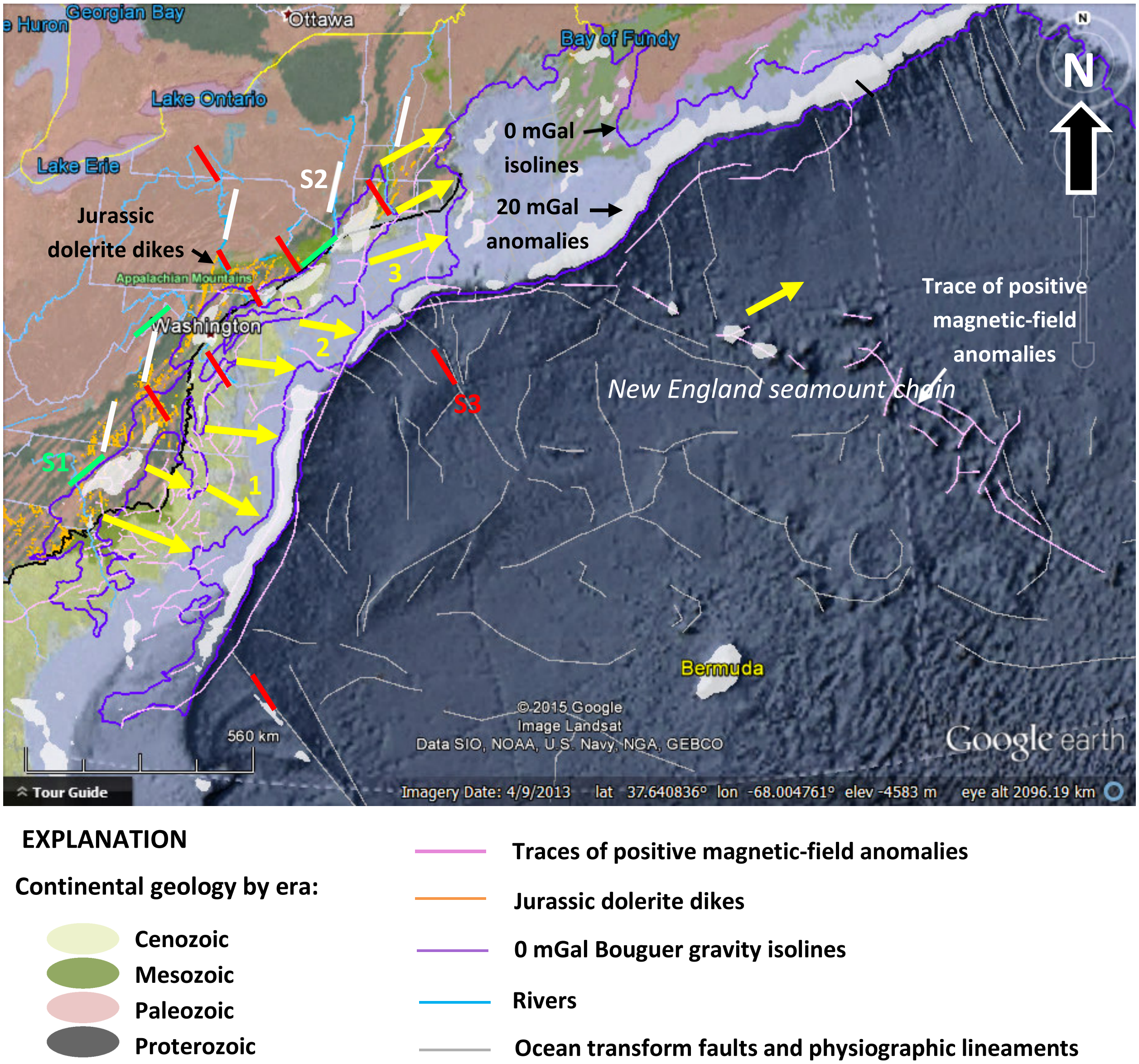

Figure 24. GE map centered between the Appalachian Mountains and Bermuda with yellow arrows highlighting three, incremental stretching directions (1 – 3) of the NAP continental margin based on overlapping tectonic extension fractures identified in Mesozoic rocks of New Jersey (Herman, 2009) and assuming that the 0 mGal Bouguer gravity isolines (purple polylines) along the continental margin were once joined prior to continental rifting (Herman and others, 2013). A semi-transparent base image shows continental geology by Era and grayshade sea-floor physiography[5]. These three proposed stetches during the Mesozoic correpsond to steeply dipping fracture sets highlighted using thick, colored lines aligned parallel (S1), oblique (S2), and almost normal (S3) to the NAP continental margin, and account for the trends of Jurassic dikes and major river segemnts.

[5]http://www.impacttectonics.org/KMLZs/GCH%20Impact%20Tectonics%2001-2015.kmz

rocks (Merguerian 2015; Chapter 2 of this volume). Together they reflect a systematic counter-clockwise rotation of the finite-stretching direction of our continental margin during Mesozoic rifting. This fracture record therefore also records the systematic rotation of the NAP Atlantic margin as it was being incrementally stretched apart, opened, and filled by growing oceanic crust (Herman, 2009). The latest-stage fracture geometry found in the Newark Basins is also seen in the Cretaceous strata detailed above and in crystalline basement as we see in Chapter 5, STOP 1. These structural systems form rhombohedral-shaped fault slices and blocks that dip moderately to steeply SE-E that are bounded by both SE-E (synthetic) and NW-N (antithetic) dipping extension structures that worked together to accommodate bulk stretching and sagging of crustal rocks (for example see Chapter 5, STOPS 1 and 3). Now that the systematic nature of these brittle rift structures is recognized, not only on the basis of structural geometry but also

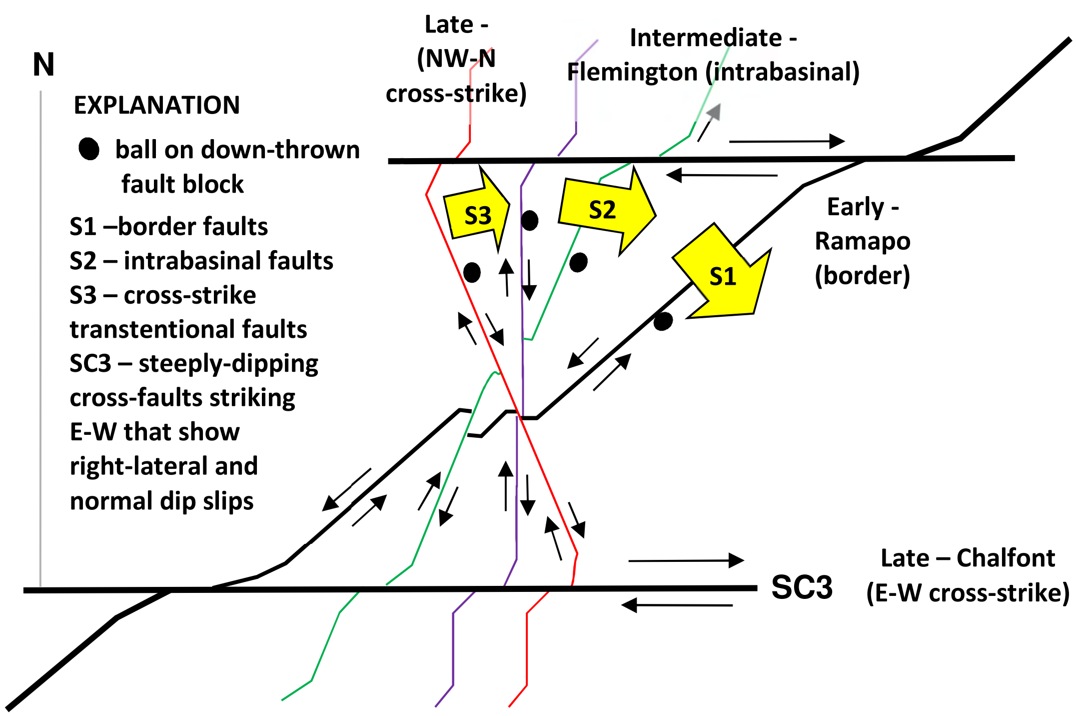

Figure 25. A schematic diagram illustrating how brittle rift-related structures mapped in the Newark Basin and surrounding region are oriented, overlap and interact. S1 (oldest) through S3 (youngest) sets of extension fractures (joints) and brittle faults fall within three sectors, have variable spatial distributions and densities in the basin, but consistently show the same orientations and structural interactions. S3C faults are complimentary to S3 fractures and may be coeval. The fracture and faults systems worked together to stretch and drop crustal blocks downward towards the southeast to northeast during rifting of the continental margin through time. The horizontal component of oblique slip is shown as arrows indicating observed slip directions on cross-strike, moderately- to steeply dipping fault planes.

with respect to kinematic indicators and secondary minerals infilling fracture interstices, we need to reappraise the nature of other brittle fractures (joints) mapped in the Appalachian foreland owing to the probability that the intense stretching phase resulting in S2 brittle structures probably reached well into the Pennsylvania Salient (fig. 27). Fractures systems of this strike are mapped in the Allegheny Plateau of New York and Pennsylvania that are currently thought to stem from Alleghanian orogenesis (Engelder and Geiser, 1985 among many others). But these fractures show congruency with both the Jurassic dikes, and subparallel reaches of the Susquehanna River and it's likely that many of these fracture systems, as well as other relatively late foreland strains reported in Pennsylvania will be reinterpreted to stem from Mesozoic and perhaps even Cenozoic strains. For example, a detailed structural analysis of late-stage Alleghanian structures at Bear Valley, Pennsylvania (Nickelsen, 1987) includes late-stage graben development consistent with S2-phase Mesozoic stretching. Moreover, the latest deformation phase reported there is oblique, foreland-directed slip found with slickensided shear planes showing sinistral wrenching of graben-bounding faults (fig. 28). Therefore, it's possible that prior, classic structural interpretations of the structural stages seen at the surface in Paleozoic strata of the Appalachian foreland needs reinterpretation, because two of the latest structural stages appear to post-date Paleozoic orogenesis in the Central Appalachian foreland. This point will be discussed further below with respect to the older tectonic structural groups.

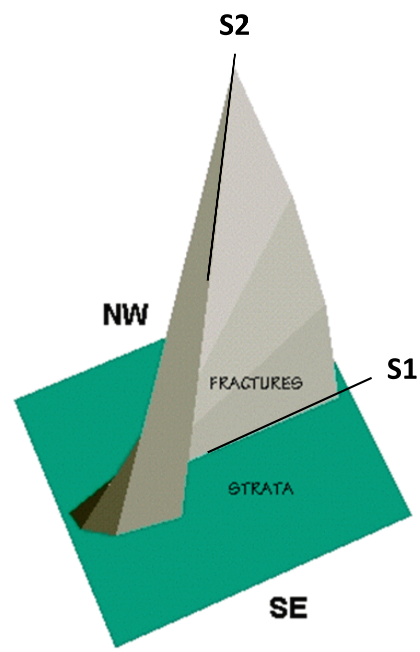

Figure 26. 3D diagram illustrating that extension fractures (joints) in the Newark basin are systematically arranged in the straigrpahic section with an upward, helical twist that reflects incremental rotation of the reigonal stetching direction from SE to E through the Meosozic. Strata mostly dip gently NW. The oldest srata commonly aligned paralell to the Appalachain grain (S1) whereas younger ones (S2 and S3) cut across it.

The Newark Basin Ramapo and border faults

Perhaps the most renowned fault that was active during the Mesozoic and has been appraised with respect to neotectonic activity is the Ramapo fault (Crone and Wheeler, 2000). This fault is one a series of linked faults that form the province boundary between the Ramapo-Hudson Highlands to the NW and the Piedmont to the SE (fig. 16). Originally thought to be a potentially active fault, or fault system, the Ramapo fault has probably been active to some degree throughout the entire Phanerozoic.

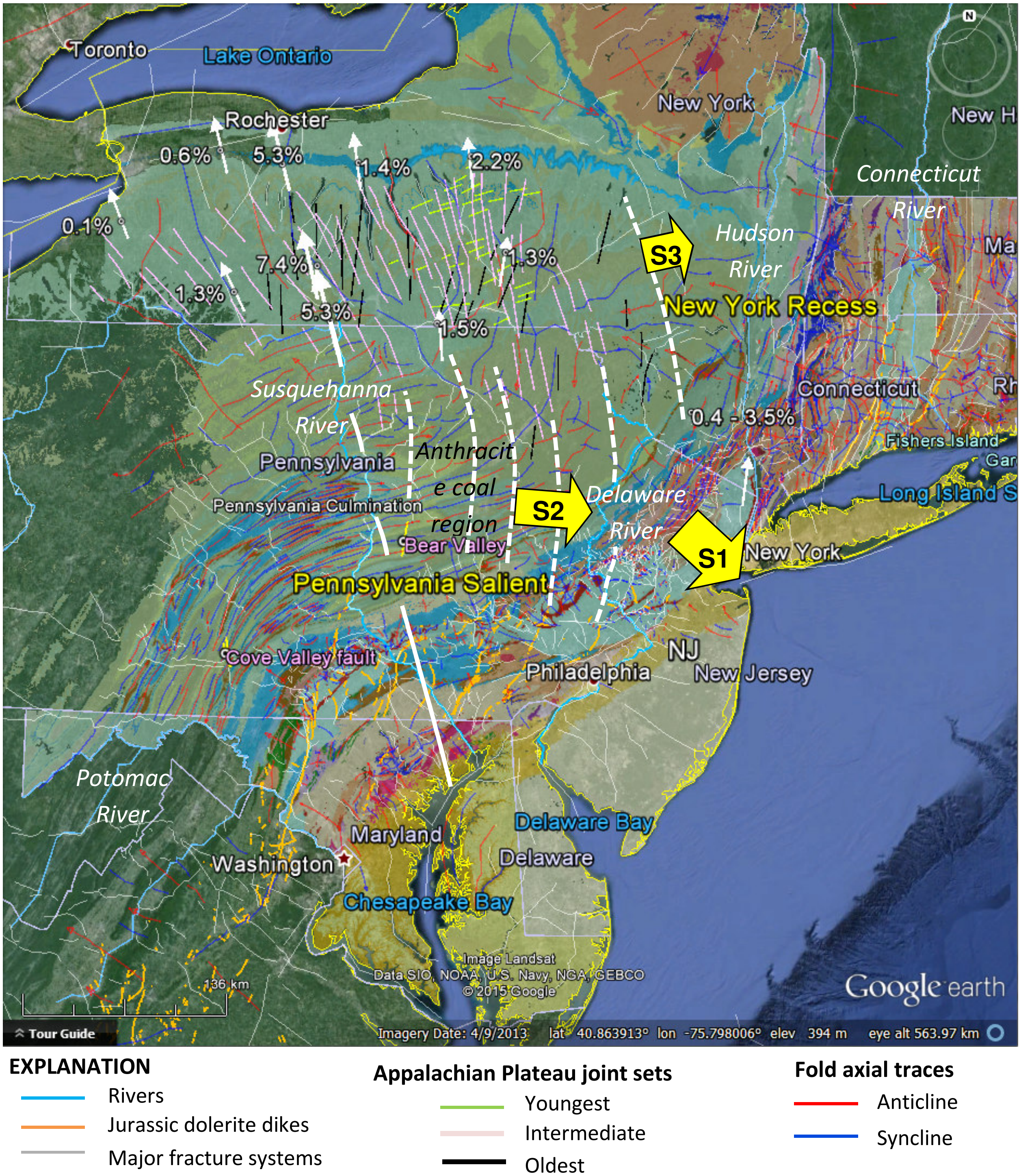

Figure 27. GE map showing regional joint sets of intermediate age on the Appalachian Plateau align with Jurassic dolerite dikes, river systems, and directions of regional stretching during the Mesozoic (thick yellow arrows labeled S1-S3). Joints sets adapted from Engelder and Geiser (1980) and Hancock and Engelder (1989). Note locations of the Cove Valley fault and Bear Valley. White arrows show directions and magnitudes of horizontal compaction measured in calcite grains in Paleozoic AND Mesozoic rocks (Engelder, 1979; Lomando and Engelder, 1984). The white line extending from Chesapeake Bay to the 7.4% value trends ~azimuth 347°.

The fault was a focus of research in the 1970's because it's a prominent, major fault occurring at a province boundary with historical crustal seismicity recorded near its map trace during a time requiring regional assessments of seismic risk for siting nuclear-power generating stations (Aggarwal and Sykes, 1978). Crone and Wheeler (2000), provide a thorough review of the historical reports of low-grade crustal seismicity in the area of the Ramapo fault both from map and profile perspectives. They cite several lines of reasoning disfavoring any significant, current activity on this fault. Detailed structural analyses of rock fabric at several locations showed mostly late- stage normal and oblique slips (Burton and Ratcliffe, 1985; Ratcliffe, 1980, 1982a; Ratcliffe and others, 1990) that are inconsistent with the existing, east–northeast-trending,

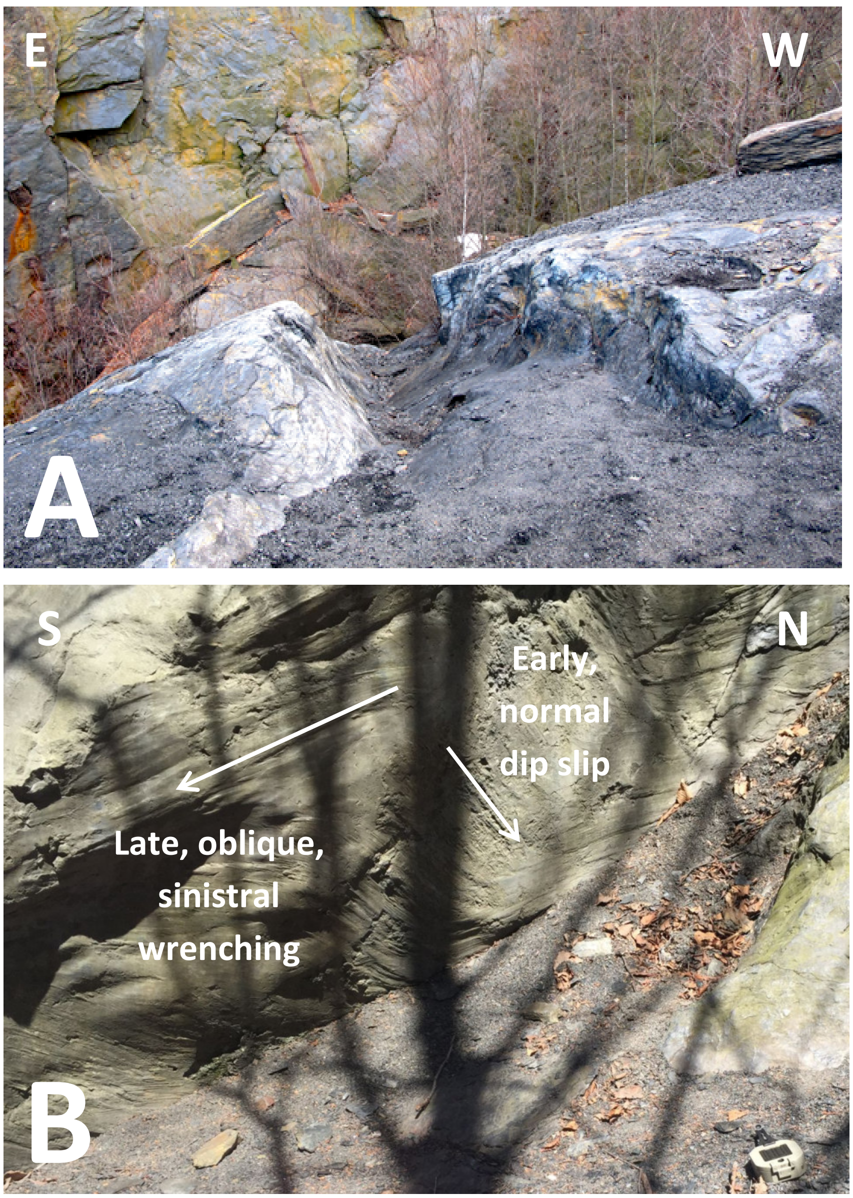

Figure 28. Photographs of probable Mesozoic and possible Cenozoic structures in upper Paleozoic strata at a coal mine in Bear Valley, Pa. (location noted in fig. 27). Late-stage structural grabens (A) of Newark S2 fault strike (fig. 25) dip steeply west and have two sets of slickenlines (B) on graben-bounding faults. The earlier slickenlines indicate normal, dip-slip shearing during graben development, and later ones indicate transcurrent wrenching (Nickelsen, 1963) that is also reported northward to the edge of the Appalachian plateau on regional joints sets of sub-prallel strike(Engleder and others, 2001). Photo a courtesy of www.princeton.edu.

contractional stress field (fig. 3). Also, Stone and Ratcliffe (1984) trenched the up dip projection of the Ramapo fault at two localities with both investigations finding no evidence of quaternary tectonic faulting. As Crone and Wheeler (2000) summarize, “No available arguments or evidence can preclude the possibility of occasional small earthquakes on the Ramapo fault or other strands of the fault system, or of rarer large earthquakes whose geologic record has not been recognized. Nonetheless, there is no clear evidence of quaternary tectonic faulting on the fault system aside from the small earthquakes scattered within and outside the Ramapo fault system”.

Other geological features that may indicate neotectonic structural reactivation or overprinting of Newark structures

There are only a few reports detailing relatively young, brittle strains that overprint Newark structures. A couple stem from outcrop evidence whereas many others have been emerging from the deployment of borehole-televiewer (BTV) cameras that capture oriented photographic images of the borehole walls and that are used to interpret subsurface water-bearing features within different strata (fig. 29; Herman and Curran, 2010). Lucas and others (1998) were the first to map and report compressional overprinting of Newark strata in the Jacksonwald syncline where foreland-type folding occurs with penetrative structures and shearing indicating “shortening at a high angle to the border fault”, that strikes about E-W there (fig. 30). Since then, there have been only a few, relatively recent reports of compressive overprinting or potential neotectonic reactivation of Newark structures, including the structural overprint of the discordant, compressional folds found along E-W striking segments of the Hopewell fault system as reported in Chapter 5, STOP 2. A more recent report of possible neotectonic reactivation of Newark structures stems from optical BTV records of Triassic mudstone from Elizabeth, New Jersey (Herman and others, 2015). The BTV data show apparent evidence of oblique slip on steeply dipping S1 (border-fault parallel) extension fractures, based on the offset of sub-horizontal veins that are probably relatively young, sub horizontal gypsum veins found in this part of the basin, and that have been cited as being the youngest, mineralized veins set in basin strata (El Tabakh and others, 1998). The Elizabeth report shows how older, S1 extension fractures of Newark age are favorably aligned to slip in our contemporary, compressional stress field.

One isolated patch of Late Pleistocene, very-fine grained alluvium bearing charcoal was recently uncovered along the trace of the Flemington fault that may signal relatively recent tectonic movement (Herman and others, 2012). This unusual deposit sits atop soft red shale and butts up against the fault, thereby inviting speculation of structural control of Quaternary age, but it could also be the result of selective preservation in a depositional trough. There is no fracturing in this silty clay bed, and therefore this one point of observation doesn't provide enough information to verify neotectonic activity. However, subsurface evidence of late-stage reactivation and shearing of Mesozoic and older bedrock is rather common in optical BTV images like those shown in figure 28. These records stem from fractured-bedrock aquifer subsurface investigations throughout northern New Jersey in Mesozoic through Proterozoic

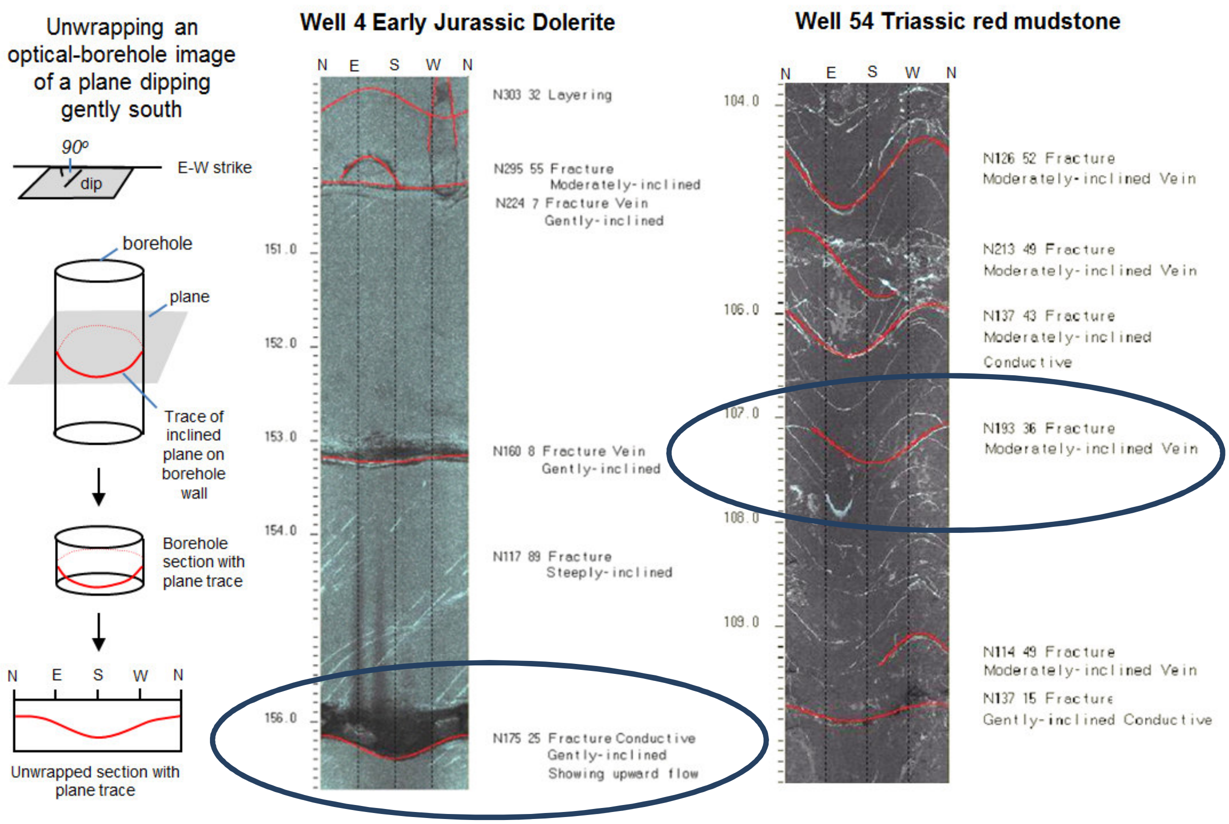

Figure 29. Optical BTV imagery collected in fractured-bedrock aquifers in New Jersey commonly show late-stage, ~E-W-striking, reverse shear fractures that dip gently SE (circled), less so to the NW, that are among the most open and permeable fracture conduits in the region. The schematic diagrams on the left illustrates how a gently dipping plane that is cut but a borehole appears in an unwrapped, optical-borehole image that is 'flattened' for interpretation. Note how early, inerlzied (S1) fractures are sheared and offset in the image to the right along one of these shear planes. The locations of these two wells are noted in figure 29. Depth units for the BTV imagery are feet below land surface.

bedrock and show sporadically distributed, late-stage, brittle, reverse shear planes that commonly strike ~E-W (fig. 28). These features are among the among the most open, permeable fracture systems in the area.

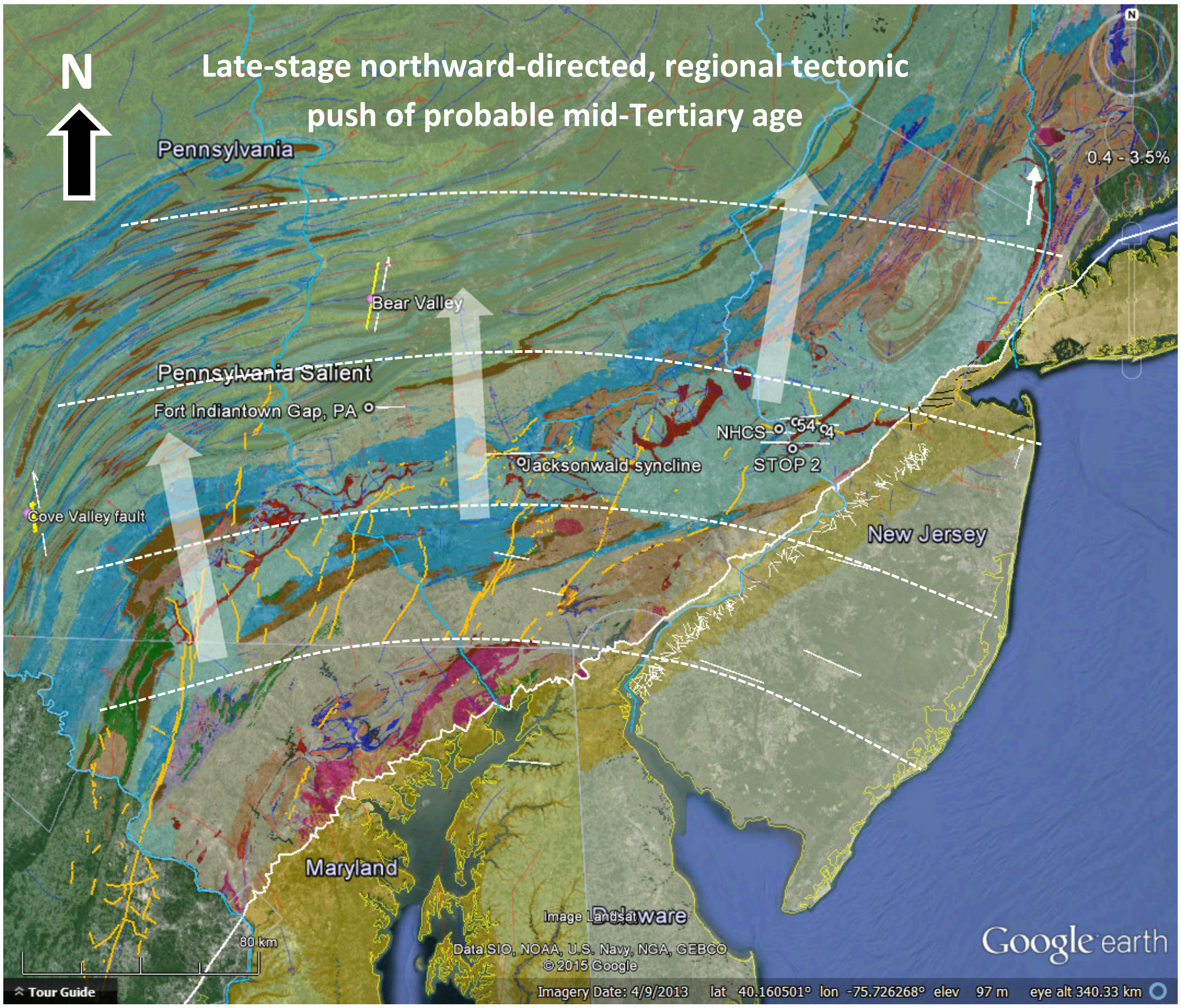

Figure 30. GE map showing the radial distribution of late-stage, probable Tertiary compressional push resulting in a north-directed, compressional, structrual overprinting of this region. The systematic orienntation of these late-stage features fans in an arcuate, convex manner above upper reaches of the Chesapeake Bay. This push laterally compacted both Palezoic and Mesozoic bedrock by a few percent, imparted mineralized shear fractures that cross-cut and offset earlier structres, and now are among the most, open, permeable features seen in the subsurface (fig. 28). NHCS-New Hope Crushed Stone quarry, locations labeled 4 and 54 refer to well records of Herman and Curran (2013). Key to geological units on figure 2.

Tectonic Groups G2 (Paleozoic >260 Ma) and G1 (Proterozoic >~765)

These two groups are covered together because we are just beginning to understand how to view the commonly mapped structures in basement rocks of the Highlands and cover rocks of the Valley and Ridge provinces with respect to both Mesozoic and Cenozoic strains. The sequence of pre-Mesozoic tectonics events in our region is diverse and complex. The summary in figure 3 provides no tectonic and structural details surrounding the series of orogenic pulses that helped form our Appalachian highlands, lowlands, and plateaus. To this point, a few key studies of classic Appalachian structural chronology and studies of foreland penetrative strains are reported in this region, and figure into this neotectonic survey, and are discussed and reevaluated with respect to some newly emerging map patterns and tectonic concepts.

As reported in Chapter 2, Merguerian (2015) provides a retrospective of his work in identifying the different sets of brittle discontinuities cutting Proterozoic basement and Paleozoic cover rocks in the New York City (NYC) area. He denotes these as Groups A to E, with the latter two, D and E showing good evidence of post-Paleozoic movements. His Group D fractures strike NNE parallel to Herman's (2007) S2 tensional fractures and they both dip steeply with predominately normal dip-slip kinematic indicators. They also share the same zeolite-to-calcite epithermal mineral assemblages infilling fracture interstices and coating fault surfaces (Chapter 2, fig. 11 and Chapter 5, fig. 30). Similarly, the latest NW-NNW striking (Group E) structures in NYC parallel the S3 Newark structures (noted above, that overprint and reactivate older ones (fig. 25). The 'E-S3' fractures show the largest post-metamorphic movements of both dextral and sinistral oblique slips (Baskerville, 1982; Merguerian and Sanders, 1996; Merguerian and Sanders, 1997). Dextral separations are measurably larger in the range of 100-200 m whereas the sinistral movements are reported on the order of centimeters (Merguerian, 2015). The Mosholu fault is one of the largest northwest-striking faults in the New York City area with a map throw of about 35 m of dextral slip (Baskerville, 1992). The interpretation of its recent tectonic uplift is suggestive but not yet conclusive. However, as Merguerian (2015) points out, sinistral slip along these systems is more probable in the present-day stress field (figs. 8 and 9). Seeber and Dawers (1989) also favor interpretation having dextral-slip movements on cross-strike structures of 'E-~S3' orientation resulting from Mesozoic rifting.

Richard Nickelsen (1963, 1987) chronicled the relative sequence of brittle strain events in the Appalachian Valley and Ridge province Pennsylvania, and his work figures prominently into this neotenic evaluation. It was demonstrated above that his latest two phases of structural deformation in the foreland corresponds with the intermediate 'D orS2', extensive Mesozoic stretch seen in this region as CAMP bodies rose from beneath the emerging proto-continental margins to feed massive sills and volcanic flows (Herman and others, 2013). The latest, sinistral wrench slips on the graben-bounding faults in the anthracite coal measures also agrees kinematically with more recent work that he conducted on the western flank of the Pennsylvania culmination, marked as the Cove Valley fault in figures 17 and 27 (Nickelsen, 1996). This is another area where sinistral wrenching occurs on latest-stage structures in the Appalachian foreland. He described these late-stage faults as having brecciated Silurian quartzite, but elusive in outcrop "because the surfaces are never slickensided or slickenlined. Proof of their existence rests in finding truncation of previous structures and the unique, brittle, fracture surfaces" … "that are coated with thin layers of extremely angular breccia that does not show evidence of progressing toward a finer cataclasite". In other words, this episode of rock fracturing doesn't appear to have been part of a progressive continuum, but more of a solitary episodic overprint. Additionally, this fault and other nearby similarly aligned cross faults offset rock ridges and locally coincide with limonite mines, some of which have reported hydrothermal pyrite. These are critical observations in light of other detailed microstructural studies of the foreland section by Engelder (1979) and Lomando and Engelder (1984) using techniques pioneered by Groshong (1972) of microscopically measuring twinned calcite grains to resolve principal axes of compressive tectonic shortening, and gauge the magnitude of penetrative, bulk, lateral compaction. This work shows foreland, penetrative shortening of Paleozoic AND Mesozoic rocks approaching 8% along a medial line roughly coinciding with the right side of the Pennsylvania culmination and intermediate north-south stretches of the Susquehanna River running along ~347^{o} azimuth (fig. 27). The strain field dies out laterally with diminishing strains fanning outward towards Lake Erie to the west and Long Island, NY to the east.

Geiser and Engelder (1983) postulated that two compressive pushes seen in the Pennsylvania salient, referred to as "Lackawanna" and "Main" phases were discreet tectonic episodes, perhaps separated by millions of years. A very interesting aspect of their work is they also note a very rapid strain rate for the latest push that reportedly happened is less than 1 million years. Gray and Mitra (1993) recognized five stages of foreland brittle tectonism in the Pennsylvania salient (Stages A-E) including three compressive phases that are probably Alleghanian followed by two post-Alleghanian trends. As seen before, stage 4 (D) conjugate extension faults are grouped with late-thrust faults and associated slickensides and gash veins, POST-folding crenulation cleavages, and finally veining and fracturing of stage 5 (E). They report that the three, earliest stages were continuous, but not necessarily the latter two. The more recent detailed structural analyses of penetrative strain and shortening directions in the Pennsylvania culmination by Saks and others (2014) also points to two phases of non-coaxial strain, with mean orientations of the early-stage of azimuth ~336 +16.3 and the later one along ~343^{o}. This latter one deviates less than 5^{o} azimuth from the ~347^{o} (NNE) axis of maximum shortening occurring along the east side of culmination (fig. 27).

Gwinn (1970) reintroduced the Pennsylvania culmination as the 'Juniata Culmination' and noted that both Nickelsen (1963) and Wise (in Nickelsen 1963) and Rodgers (1964) speculated that it may be partly a product of post Appalachian basement uplift transverse to trends of Paleozoic folding, although evidence of basement involvement is lacking. Blackmer and others (1994) used fluid inclusion geothermometry in the region and found initial rapid burial and unroofing during the Late-Permian through Early Jurassic that they attributed to flexure and rebound of the foreland to erosional loading and unloading of the Alleghanian thrust sheets. An episode of little to no unroofing (Middle-Jurassic-late Oligocene) possibly began with inception of drift at the Atlantic continental margin. Then, an episode of rapid unroofing over the full width of the basin occurred from the Miocene to the present. The driving mechanism for this renewed unroofing was not identified. Despite the earlier speculations of Davis (1902) and the more recent ones noted above, a popular consensus is that most tectonic structures in the Pennsylvania salient reflect Late Paleozoic orogenesis. As demonstrated herein, the latter viewpoint seems improbable as both Mesozoic and Cenozoic uplifts probably occurred here. With respect to just how many happened, and when they happened, and if they happened during our current, compressional state of crustal stress is the focus of the following discussion.

Discussion

Some key points are summarized below from this work that leads to a reinterpretation of the late-stage neotectonic events affecting our region:

1) Actual plate drift determined using ground-fixed GPS systems show increasing horizontal velocities progressing northeastward up the Appalachian grain from Chesapeake Bay at ~ 13 mm/yr into southern New England at ~17 mm/yr. Actual vertical motions of the crust oscillate on the order of 10-20 mm/yr, but in the region south of Adirondack Mountains through the Hudson Valley and New Jersey, the continental crust is slowly sinking at rates approaching 4 mm/yr except in an area lying west of the Pennsylvania culmination and other small, isolated spots that are rising very slowly with rates of less than 1 mm/yr (figs. 4, 8, 9, 17 and 23). A pronounced, NNW-trending, linear break in vertical crustal motion is seen bounding the west side of the Pennsylvania culmination that is mirrored to the east where the Delaware River watershed is separated from the Atlantic watershed by a topographic divide that zig zags from south to north up through New Jersey into New York, mimicking the river's course (fig. 4). These two velocity breaks bracket the Pennsylvania culmination, where the largest areas are sinking the fastest, and they both verge southward towards Chesapeake Bay (fig. 4).

2) The east-central continental margin of the NAP is seismically active with patterns of historical seismicity showing remarkable congruency with not only GPS-derived estimates of actual crustal motions, but also with major physiographic features including surface water drainage patterns and regional watershed boundaries (figs 4,8,9, and 11). A careful look at the historical seismicity in this region also shows that seismogenic zones preferentially occur where deep-seated igneous plutons are present, including ultramafic plutons of the Adirondacks (fig. 11) and of the Cortland intrusive complex in the Ramapo seismic zone (fig. 9). These areas appear as crustal sticking points that resist drift and leading to accumulated elastic strain and consequential, periodic seismic releases. The GPS plate motions at this scale show southward crustal deflection around the Adirondack Mountains (figs 11 and 17). The systematic, arcuate patterns of crustal seismicity bowing around and opening westward behind the Adirondacks have a symmetric, but reflected counterpart lying generally conforming in alignment to the New England coastline (fig. 11). This latter lineament opens eastward and runs southward from Maine through Long Island Sound, trending about normal to the direction of current horizontal plate drift. The closest P-axes solutions plotted in this region are near Stamford, CT with some easterly trends that also oppose the current direction of plate drift (figs. 8 and 9).

3) The intermediate stage of crustal rifting during the Mesozoic (D-S2 above) is regionally pervasive, and part of a strain continuum that likely stretched the entire Appalachian margin and well into the continental interior. This is supported by kimberlites of Mesozoic age occurring on west-side of the Pennsylvania culmination and in southwest Pennsylvania (Bikerman and others, 1997; Parrish and Lavin, 1982).

4) Right-lateral displacements are noted along the ~E-W striking Kelvin-Cornwall transform fault marked by the New England seamount chain, that links to ~E-W, late-stage transtensional fault components displaying the same kinematics and that cut the continental margin through New Jersey where they involve complementary sets of N-S to NNE, cross-strike normal faults having right-lateral-oblique slip components.

5) Late-stage penetrative tectonic compaction and wrenching strains are found in the Appalachian foreland not only in Paleozoic rocks but also Mesozoic rocks of the NY-NJ Piedmont, and therefore, the tectonic event responsible for these strains must be, at least in part, Cenozoic, and probably mid-Tertiary in age; strata older than the mid-Tertiary unconformity (~40-36 Mya; figure 20) contain visible, mapped structures whereas younger strata generally do not. The only exceptions are where structurally disrupted Miocene sediments in the Delaware coastal plain occur in a small area coinciding with the fastest rates of GPS-based subsidence (~3-4 mm/yr; Pollack Farm fig.

17 and 23). Late-stage kinematic indicators at Bear Valley and Cove Valley shows consistent sinistral-oblique slip kinematics, and when considering the late N-S directed push found in the central part of the Appalachian foreland, the Newark basin and the NJ Coastal Plain (fig. 30) it appears that an episodic, rapid tectonic push occurred during the mid-Tertiary period, resulting in crustal uplift and the pronounced, mid-Tertiary unconformity in this region (fig. 20). This push seems to have originated near the head of Chesapeake Bay as measured from compressive strains that systematically dissipate laterally away from maximum strain axis running along a medial line up the right side of the Pennsylvania culmination and coinciding with intermediate stretches of the Susquehanna River (fig. 2). The relatively rapid rate of current subsidence in the Pennsylvania culmination is probably a continuing, neotectonic response to a Tertiary uplift event lying foreland of the Chesapeake Bay as revealed by the aforementioned, observed breaks in the GPS vertical-velocity field, the radiometric age work detailed in Chapter 3 (Mathur and others, 2015), and pressure- and temperature-dependent fluid inclusion work in the region by Blackmer and others (1994).

6) The distributions and orientations of the various p-axes measurements plotted in figure 31 show varying stress regimes with respect to the Appalachian Mountain chain. For example, foreland and west of the Appalachian Mountain belt, stress axes in more interior regions of the NAP consistently plunge gently northeastward along a bearing that fans slightly from 53^{o} to 73^{o}. When these trends are projected SW up-plunge, they verge to the southwest somewhere in the lower Mississippi River Valley. Another regime is seen plunging southward off the rising Canadian Shield (fig. 31). An interesting break in orientation of these P-axes solutions also occur across the Saint Lawrence Seaway that developed along a historically active seismogenic zone (fig. 10) and an ancient fault system of at least Mesozoic age (Tremblay and Lemieux, 2001; Mazzotti and others, 2004). Another region occurs along the continental margin where two principal directions of current crustal compression are resolved, one of similar trends seen in the Appalachian foreland (gently plunging NE) and another that nearly opposes current plate drift (fig. 31). This implies that the more interior, aseismic parts of the NAP have remnant compressive stresses nearly aligned parallel to the Appalachian Mountains, and that were deflected backward by rising areas to the north, whereas coastal areas near the continent-ocean boundary have a variable stress regime that is evolving to reflect current plate drift. This raises the question as to the nature of the old, remnant stress field of the continental interior that points southwestward and north of the Gulf of Mexico. Could the Chicxulub impact have triggered subsequent plate reorganization and reversed not only the polarity of the stress regime, but also the rotation of our plate (Herman, 2009)?

7) The sets of cross-strike fold axe depicting late-stage folding, warping, and in essence, crenulation of older Appalachian structures along trends paralleling current plate drift are intriguing but perplexing. As for the proposed Rochester-Watchung synclinorium (figs. 11 and 17), the nature and timing of these structures need more study. In a simple sense, one would anticipate seeing a structural trough situated between two structural culminations; the Adirondacks to the north and the Pennsylvania to the south. Definition of the Watchung synclinorium and other, similarly trending, en-echelon fold structures crossing the New York Recess (fig. 17) is based on an visual analysis of the systematic irregularities expressed as patterns seen in regional and local geological and physiographic features, and they are probably slowly growing neotectonic accommodation features reflecting progressively increasing strain rates in a direction trending NE up the Appalachian Mountain chain because of increasing drift rates. It is interesting to note that the cross-strike pattern, paralleling Merguerian (2015) latest-stage brittle structures in NYC, is apparently limited in distribution, occurring only north of the Rochester-Watchung synclinorium, with this pattern only continuing southward along continental-oceanic marginal areas of the piedmont and coastal areas.

In a general sense, tectonics encompasses all geological processes which control the structure and properties of the Earth's crust, and its evolution through time, in particular, with respect to mountain building. Therefore, in addition to considering our current, actual plate movements and historical seismicity records collected over such a brief time, many other geological processes bear on our current states of crustal stress and the resulting patterns of our crustal seismicity. In a similar sense that we see the variable, oscillatory motion of Earth’s vertical ground motion, oscillatory, lower-frequency regional variations must also occur in response to long-period isostatic adjustments stemming from growth and retreat of continental ice sheets and encroachment and withdrawal of marginal seas. These longer-wavelength and longer-period lithospheric flexures and crustal adjustments probably take place over the course of tens of thousands to millions of years’ time and exceed the capabilities of day-to-day GPS monitoring. These processes however cannot possibly be gauged solely through inspection of historical plate motions and seismicity records, but also rely on other geomorphological, sedimentological-stratigraphic, and geochemical processes that merit further consideration in more thorough neotectonic treatment that one day will exceed the scope of this work.

Because the GPS-derived rates of vertical plate motion align with apparent trends in the historical seismogenic patterns, especially with respect to the distribution of large, ultramafic plutons, then subsequent snapshots of the vertical-velocity field should show localized variations with time, but the longer trends should persist given the lack of any catastrophic, regional energy flux that would perturb our on-going, relatively uniform, plate drift. A few spot

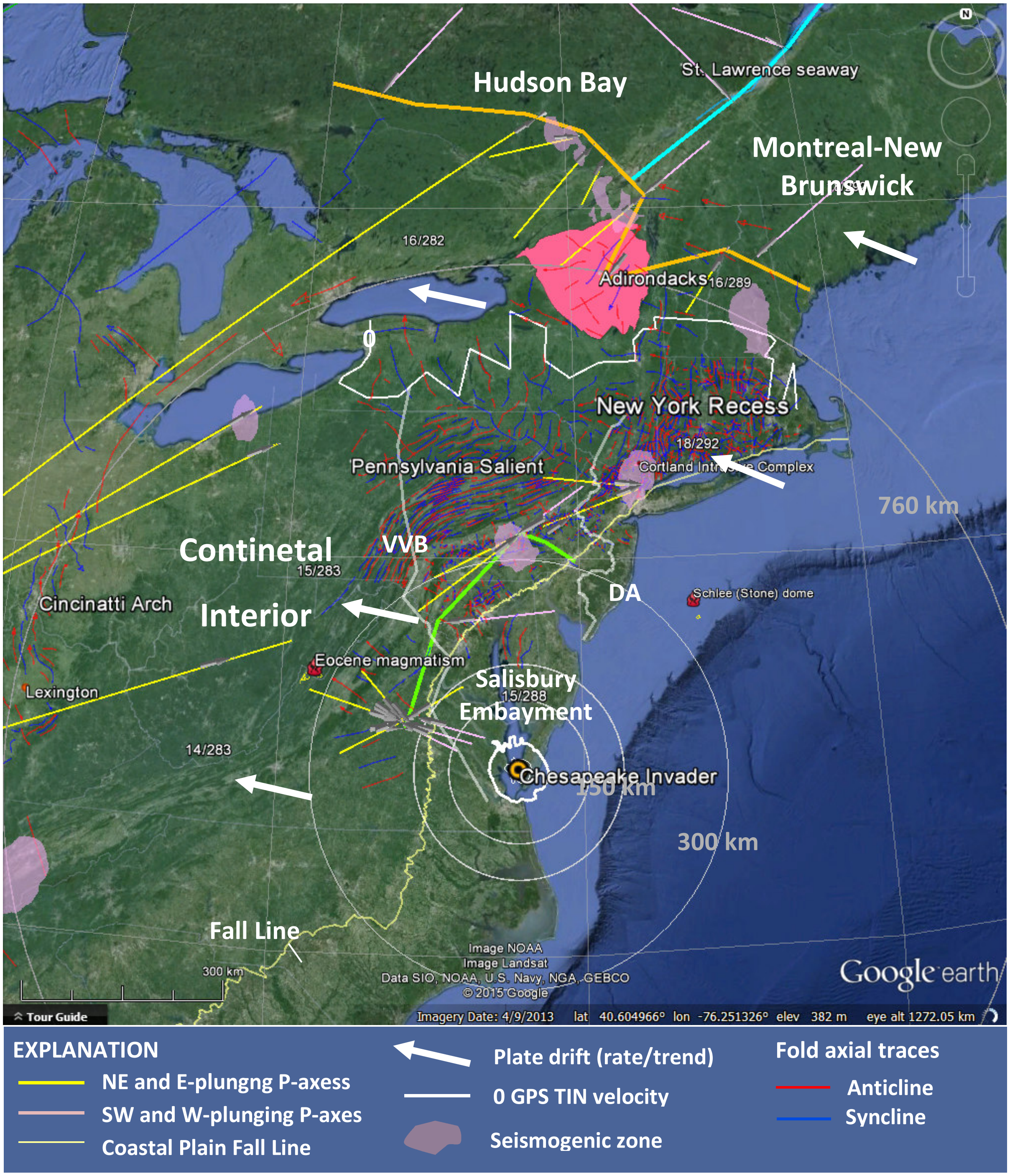

Figure 31. GE map showing stress-regimes (defined where P-axes display different trends and plunges), pronounced breaks in the TIN surface of vertical-crustal motion, the Delaware-Atlantic drainage divide (DA), the Coastal Plain boundary, compiled fold axes, and the Chesapeake impacts crater with concentric rings at varying radii. Colored straight lines emphasize plunge directions of compiled P-axes whereas colored (green, orange, and light-blue) polylines define stress regimes including the Hudson Bay, Montreal-New Brunswick, Salisbury Embayment, and Continetal Interior. The Pennsylvnia Salient NY Recess resemble the Continetal Interior but are evolving near the Fall Line. Rate of plate dirft in mm/yr.

checks of the vertical GPS rates in 2014 closely match the long-term values used to generate the TIN velocity surface, and the 2009 TIN surface is the best snapshot of vertical-plate motions that we currently have. As previously mentioned, plans are underway at the NJGWS to develop methods of automating computer retrievals of newer CORS data at successive, regular time intervals to facilitate further study of crustal dynamics, and one-day perhaps, be able to animate dynamic fluctuation of the surface over time. But for now, these results are encouraging, because the GPS rates of crustal subsidence in this regional generally agree with estimated rates of crustal erosion and denudation arrived independently. Specifically, Pazzaglia and others (2006) provide a synthesis of late Cenozoic deformation of the middle Atlantic passive margin. They report a deeply eroded early Tertiary Appalachian landscape of lower relief than today. Climate change, epeirogenic uplift, or rapid increase in the size of the Atlantic slope drainage basin, or some combination of all three factors, initiated the stripping of mature regolith in the middle Miocene and delivery to the Fall Zone. Increased sediment flux into the Baltimore Canyon trough (BCT), coupled with erosional unloading caused flexure of the margin with the Fall Zone located at the flexural hinge. Continued Middle Tertiary flexural warping of the margin arched early Miocene terraces and contributes to the continued incision by the Susquehanna River channel. The incised Appalachian landscape now delivers an immature, heterolithic load to the Coastal Plain and shelf region that reflect both periodic, positive and negative, isostatic adjustment to the loading and removal of Quaternary continental glaciers. Erosion rates vary across the Appalachian landscape depending on local relief, rock type, and proximity to the fall zone along the NW edge of the coastal plain, but current erosion rates of about ~ 5 to 10 mm/yr are estimated using present-day solute loads. Rates may have peaked at ~80-100 mm/yr during Quaternary periglacial erosion (Pazzaglia and others, 2009). Stanford and others (2002) derived much lower, long-term denudation rates of denudation rates of ~ 0.01 mm/yr from Late Tertiary to recent times for a 2800 km2 section of the U.S. Atlantic Coastal Plain and Piedmont. This work used reconstructed topography at five different times from the late Miocene to the present based on mapping of fluvial strata, colluvium, and marginal-marine deposits that are constrained with radiocarbon dates, palynostratigraphy, and correlation to adjacent glacial and marine units. These rates are reported as agreeing with other denudation rates found in similar regions, but as pointed out, local erosional rates can clearly vary widely, over at least two orders of magnitude depending upon the setting. Additional work relating observed GPS trends with local geomorphological variations is needed and may prove very useful in the future. With respect to Pazzaglia and others (2009) work, one additional, critical piece of information supports the hypothesis that this region contains far-field crustal strains imparted by the Chesapeake Invader (Poag, 1999). They report that erosion rates in Susquehanna River basin doubled from prior amounts immediately after the Chesapeake impact at ~ 35.5 Mya. This work is based on cosmogenic dating of the oldest river terraces and associated upland gravel at 36.1 + 7.3 Ma (Pazzaglia and others, 2009). Younger terraces yield averages dates of 19.8 +2.7 Ma and 14.4 +2.7 ka respectively. This last point brings us to a few concluding remarks and thoughts.

In more than one way, GANJ 32 provides closure on many, puzzling aspects of my work in the central Appalachians over the past 30 years. In 1981-82 during the time when I was helping unravel the geological complexities of the Pennsylvania culmination with Dr. Peter Geiser at the University of Connecticut (Herman, 1984; 1985), I found some unusual tectonic structures in the culmination that didn't quite fit the model paradigm of foreland fold-and-thrust belt that develops with an ideal 'break-forward' advance of stacked thrust sheets, one-at-a-time, transported northwestward from Alleghanian plate convergence. Rather, the manner with which the Pennsylvania crust was crumpled and compounded from thrust faulting was uncharacteristically 'out of sequence' in the most tightly compacted areas that appear to have been selectively raised by a quick, uncharacteristic tectonic push. Moreover, from attempting to palinspatically reconstruct the Pennsylvania Valley and Ridge province using a set of serial, balanced cross section line traces across the salient to estimate crustal shortening and pre-orogenic spatial positions, the serial reconstructions merged toward a point at the head of Chesapeake Bay. At the time, we simply thought "how strange"', and "orogenic thrust belts shouldn't do that", so we temporarily stopped that aspect of the work then, which was subsequently included in later work by Geiser (1988).

Another curious aspect of my MS work in the Pennsylvania culmination is that conjugate, deformation lamellae were petrographically seen in each oriented sample of ridge-forming Silurian quartzite collected across the width of the culmination. I noted this curiosity at the time (Herman, 1985), and was assured then, and over the following decades by many structural experts working in the region, that these were not uncommon, and that they probably are ordinary, brittle orogenic strain mechanisms. The problem is that I haven't seen them reported elsewhere in this arrangement in other orogenic settings, but they do occur as such near crustal impact craters , albeit with much higher concentrations and grain densities near the crater. Quartz deformation lamellae by definition are sharply defined crystal defects, or glassy, extremely narrow (~1 Um) bands that only form at high orogenic stresses of 110-200 Mpa in quartz (Blenkinskop and Rutter, 2014). Similar microstructures referred to as basal quartz, planar deformation features/lamellae (PDFs) also occurs in many silicates that have been shocked by terrestrial bolide impacts, and are best represented in quartz and feldspar. Apparently, their orientation is sensitive to pressure, and is a shock barometer at pressures between 15 and 35 GPa (Lee and Leroux, 2015), or values approximately an order of magnitude higher than those cited above for orogenic lamellae. Clearly, more work is needed in order to understand if these conjugate deformation lamellae in the culmination result from standard orogenic process or shock geodynamics. But cross-section representation of the out-of-sequence, tightened fault slices (Herman, 1984; Sak and others, 2012) are identical to those portrayed near the Cove Valley fault by Nickelsen (1989), where late stage, wrench faults like this belie a late, N-S push centered along the spine of Chesapeake Bay. Also at this time, everyone working on Appalachian structural chronology in the region, including the Appalachian Tectonics Study Group[6] were interpreting root causes for observed effects without any knowledge of the nearby Chesapeake impact crater (Poag, 1999), or for that matter, actual plate motions. This was at the advent of computerized mapping and satellite-based Earth imaging and monitoring of Earth's surface and geosystems. I began conducting neotectonic studies in this region just after the crater's discovery while working at the NJGWS and finishing a PhD at Rutgers, New Brunswick on the crustal structure of pre-Cretaceous bedrock in New Jersey (Herman, 1997). When first accessing and plotting the NASA GPS plate-motion data I was struck (no pun intended) by the manner in which the North and central American plates rotated in concert around the Gulf of Mexico, and the approximate location of the recently discovered Chicxulub impact crater lying off the tip of Mexico's Yucatan peninsula. This crustal impact structure is an order of magnitude larger than the Chesapeake crater (www.passc.net/EarthImpactDatabase/index.html) and is temporally associated with the Mesozoic-Cenozoic geological revolution across the K/T boundary (fig. 3). It soon became clear to me that these sites of such massive energy fluxes somehow factored into current plate structures and geodynamics (Herman, 2006). But the hypothesis needed refinement and testing, and it thereafter became my hobby (www.impacttectonics.org) rather than my job, the latter of which focused on fractured-bedrock hydrogeology. Now, one-decade later, this GANJ meeting provides the opportunity to fill in some details that have puzzled me for nearly three decades and allow me to help report corroborating evidence in the form of absolute, radiometric age dates indicating a widespread, regional, far-field brittle strain field fanning outward in front the Chesapeake Bay impact crater for distances greater than 500 km away through foreland areas of Pennsylvania and New Jersey (Chapter 3, Mathur and others, 2015). When combined with the abstract notion of the aforementioned Chicxulub effects, I sincerely hope that this work helps advance some anemic aspects of plate tectonic theory that currently lacks any consideration of large, hypervelocity impacts on Earth. From my, and some others perspectives (Ribiero, 2002) these effects are real and measurable and will prove one day as a factor into a more complete, robust plate-tectonic paradigm, one that includes intraplate crustal deformation and epeirogenesis stemming directly from periodic and catastrophic bombardment by large bolides. For now though, it is important to understand the need for more work in examining magnitudes of ground-energy generated by such events, both short- and long-term strain mechanisms serving to dissipate the energy fluxes, and the geometry of associated crustal and mantle strain fields. Also, according to the definition prefaced in this book, neotectonic strains are those that form in our current stress regime. If proven correct, does a catastrophic event qualify as a neotectonic feature, or is that reserved to the more accepted, standard, uniformitarian viewpoints only?

[6] http://www.impacttectonics.org/ATSG/

Regretfully, this work leaves many aspects of this neotectonic treatment and some conclusions unaddressed. For example, the scalloped, curved nature of our continental interior has been historically chronicled and debated for decades (Thomas, 1977; Wise and Werner, 2004; Marshak, 2004). The along-strike transition from the Pennsylvania salient in to the New York recess is perhaps the most studied and reported instance of a scalloped, passive margin that has historically been treated mostly as a byproduct of differential plate convergence with irregular docking of land masses at different places, times and directions as the orogenic suture closed. The evidence presented here supports the rather unheralded notion that much of our regional architecture, and especially the geometry of our scalloped margin, is a product of continental rifting, for it's much easier to tear earth material apart with tension that assemble it through compression, The Mohr circle shows how siliceous crustal material do not sustain tension for long and fail quickly in comparison to compression strain responses. Consequently, tensional strains should be distributed over wide regions in comparison to compressional fold-and-thrust belts.

There have also been many studies conducted of plate dynamics in this region of the NAP that lends credence to the impact-tectonic aspects of these hypotheses. For example, at the dawn of the Cenozoic, shortly after the Chicxulub impact in the Gulf of Mexico, major plate reorganizations began that involved the North American, Eurasian, and African Plates that and resulted in major changes in the deep water circulation, permitting cold polar waters to move southward in the Atlantic Ocean basin (Klitgord and Schouten, 1986). Similarly, shortly after the Chesapeake impact oceanic sea-floor spreading halted west of Greenland and suddenly accelerated to the east by Iceland where it's currently focused in the North Atlantic region (Dore´ and others, 2015). There are many such corroborative lines of evidence supporting this concept that almost forces serious consideration of how these two, known, large-bolide impacts on the NAP, at the beginning of and during the Cenozoic Era, have not only helped shaped the crust, but continue to exert a dynamic neotectonic signature on our landscape that is so remote to the causative agents. But as this work puts forth new hypotheses, new tools and sophisticated means are being developed that will help us gain new perspectives on these problems. Overall, I am very encouraged by the rate at which technical advances along these lines are developing, and although our region is comparatively passive in a tectonic sense with respect convergent or transcurrent plate margins, this part of the NAP in the region of the New York Recess is demonstrably active and passive only in regard to lacking a nearby, major plate boundary. For it continuously drifts and cracks, and rises and sinks as part of a larger set of spinning and shifting lithospheric plates on a planet that we call home.

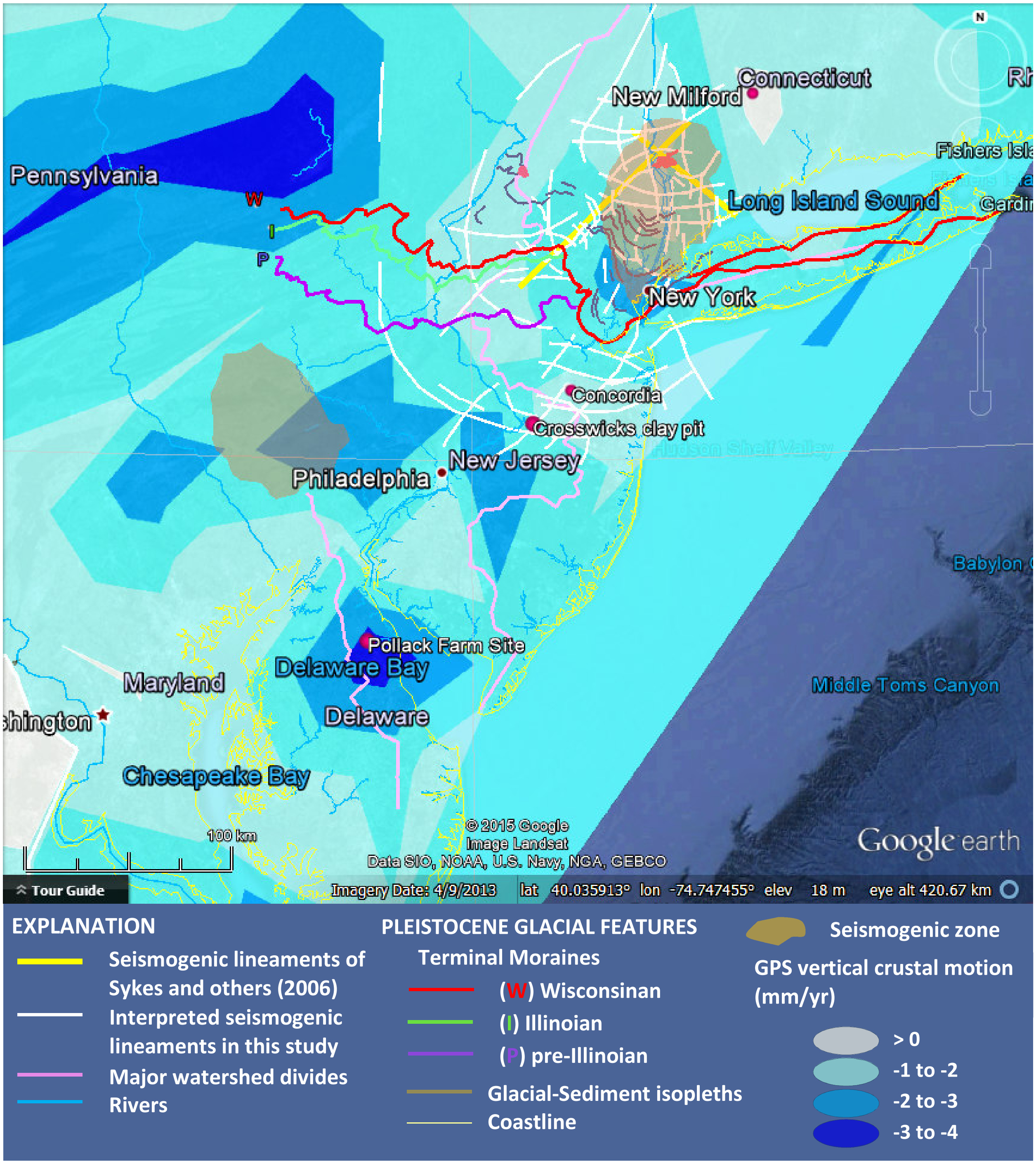

Figure 32. GE map showing interpreted sesimogenic lineaments of Sykes and and others (2006) in relation to others proposed here (white, thick, lines). Also shown are glacial sedimentary lines (see Chapter 1, exrercise 2), the TIN surface of vertical-crustal motion, sesimogenic zones, major watershed divides separating Delaware River and Atlantic drainages (DA), and bisecting the Del-Mar peninsula (DMP) divide (DA). Note the conformance of the TIN velocity break lines wi the interpreted sesimogenic linemanets and zones and their sptial arrangment reltaive to the Cortland Intruive Complex (CIC). Small areas showing positve crustal movemnts in Connecticut (New Milford) and New Jersey (Concordia) are highlighted.

Acknowledgments

This work is the culmination of over ten years of collaboration with many people at the NJGWS and elsewhere that I have had the privilege of mapping bedrock, conducting fractured-aquifer hydrogeological investigations, or sharing time in introductory geology class at TCNJ with. With respect to the latter, Jack Jamieson recently brought a renewed vigor into the mix from temporarily working at the survey, and has been brilliant in implementing web-based computing solutions to aid in GE data visualization. It has been my privilege to work other geologists at the NJGWS over the past few decades including Don Monteverde, Ron Witte, Peter Sugarman, Scott Stanford, James Boyle, Karl Muessig, Gregg Steidl, Hugh Houghton, Rich Volkert and Jim Mitchell. Dr. Sugarman brought me to the Vincentown Formation outcrop (fig. 21) and helped refine the chronostratigraphic groups in this report, as did Dr. Kenneth Miller of Rutgers University. Dr. Steve Spayd, Mark French, John Curran, Mike Gagliano, and Michelle Kuhn helped collect and interpret subsurface geophysical data. A special note of thanks is given to Dr. Monteverde who first pointed out the GPS data to me, and thereby generated a branch along the path of this neotectonic research. Don and I have shared many fine moments mapping together and his devotion to bridling my enthusiasm for fringe scientific elements has paid off (for the most part). I thank Dr. Peter Geiser, Richard Dalton, Bob Canace, and Haig Kasabach for giving me my first post-graduate employment and full-time job as a professional geologist. Having an opportunity to apply structural geological methods acquired with Peter and the Appalachian Tectonics Study Group (ATSG) for a cooperative, statewide mapping campaign with the USGS was a rewarding experience that I cherish. During the 2014 Pennsylvania Conference of Field Geologists (PCFG), Bob Ganis and Gail Blakmer told me about Ryan Mathur's work in the Pennsylvania foreland that we are fortunate to include in Chapter 3. This work is ground-breaking, insofar as it establishes absolute ages for mid-Tertiary tectonism herein hypothesized to stem from catastrophic tectonism, and as such, may be one of the first demonstrations of far-field, impact-tectonic strains on Earth that is given both map expression and radiometric-age control. I am grateful to the PCFG and for the advice and direction given by Bob and Gail. Drs. Richard (Nick) Nickelsen and Rodger Faill are two, recently deceased (2014) patriarchs of Appalachian geology that I owe much to. Rodger worked many years in deciphering geological structures in Pennsylvania and provided critical foundations into complicated tectonic processes. Nick not only was a member of my dissertation committee, but presided over the conference session where I presented my masters work. His thoughtful, gentle guidance and tenacious structural skills are greatly appreciated. Throughout the course of this work, Emmanuel 'Manny' Charles has been a friend and advocate. Manny dropped a hardbound copy of Wiley Poag's book about the Chesapeake Invader on my doorstep shortly after its release in 1999, and he has been influential in helping directing the course of this research. His reviews of various aspects of this work have been thoughtful and helpful, and I benefited from his insights into and enthusiasm for these ideas. Representatives of Trap Rock Industries (TRI) and Eastern Concrete Material have greatly facilitated this study and GANJ activities over the past decade. I thank George Conway, John Lyons, Kim Booth, Frank Bray, and Bill Warger of TRI and Michael Guida of ECM for their help and support of our mapping and research, and providing access their facilities. We gained a lot of geological insights from the unique glimpses that their facilities provide into the shallow subsurface. I thank Dr. Charles Merguerian for reviewing and improving this manuscript. I especially thank the GANJ board members, and in particular Dr. Michael Hozik, Dr. Emma Rainforth, Dr. Alan Benimoff, Dr. William Montgomery, Pierre Lacombe, and Stephen Urbanik, and Alan Uminski in working closely together with me over the past years to faithfully execute association duties. Without Suzanne Macaoay Ferguson's help, this year's guidebook would be of much less quality and possibly unfinished. Suzanne helped me through an unexpected event and I am very grateful for her help and advice. GANJ has given me a forum no expressed my viewpoints, some of which are controversial, and to repeat the words of Butch Grossman, editor of the GANJ 6 volume, "It is hoped that the resulting fire and fury generate light as well as heat". And most of all, thank you Heidi Sue for putting up with me.

References

Aggarwal, Y. P., and Sykes, L. R., 1978, earthquakes, faults, and nuclear power plants in Southern New York and Northern New Jersey: Science, vol. 200, no. 28, p. 425-49.

Aki, K., 1972, Scaling law of earthquake source-time function: Geophysical Journal of the Royal Astronomical Society, vol. 31, no. 3-25,

Assistant Secretary of Defense for Command, Control, Communications, and Intelligence, 2001, Global Positioning System standard positioning service and performance standard, United States of America Department of Defense, Washington, D.C., 66 p.

Bartholomew, M.J., and Whitaker, A.E., 2010, The Alleghanian deformational sequence at the foreland junction of the Central and Southern Appalachians *in* Tollo, R.P., Bartholomew, M.J., Hibbard, J.P., and Karabinos, P.M., eds., From Rodinia to Pangea: The Lithotectonic Record of the Appalachian Region, GSA Memoir 206, p. 431-454.

Baskerville, C.A., 1982, The foundation geology of New York City, in Legget, R.F., ed., Geology under cities: Geological Society of America Reviews in Engineering Geology, v. 5, p. 95-117.

Bikerman, M., Prellwitz, H. S., Dembosky, J., Simonetti, A., and Bell, K., 1997, New phlogopite K-Ar dates and the age of southwestern Pennsylvania kimberlite dikes: Northeastern Geology and Environmental Sciences, v. 19, p. 302–308.

Blackmer, G. C., Omar, G., I., And Gold, D. P., 1994, Alleghanian unroofing history of the Appalachian Basin, Pennsylvania, from apatite fission track analysis and thermal models: Tectonics, v.13, p. 1259-1276

Blenkinskop, T. G. and Rutter, E. H., 2014, Quartz microstructures in a fault process zone, *in* Snoke, A. W., Tullis, J., and Todd, V. R., Fault-related rocks: A photographic atlas: Princeton University Press, Princeton, NJ, p. 44-49.

Boucher, C., Altamimi, Z., and Sillard, P., 1999, The 1997 International Terrestrial Reference Frame (ITRF97), IERS Technical Note 27, Observatoire de Paris, Paris.

Brenner, G. J., 1963, The spores and pollen of the Potomac Group of Maryland: Maryland Department of Geology, Mines, and Water Resources Bulletin 27, 215 p.

Browning, J.V., Miller, K.G., Sugarman, P.J., Kominz, M.A., McLaughlin, P.P., Kulpecz, A.A. and Feigenson, M.D.2008, 100 Myr record of sequences, sedimentary facies and sea level change from Ocean Drilling Program onshore coreholes, U.S. Mid-Atlantic coastal plain: Basin Research, v. 20, p. 227-248.

Burton, W.C., and Ratcliffe, N.M., 1985, Attitude, movement history, and structure of cataclastic rocks of the Flemington fault—Results of core drilling near Oldwick, New Jersey: U.S. Geological Survey Miscellaneous Field Studies Map MF-1781, 1 sheet.

Crone, A. J., and Wheeler, R. L., 2000, Data for Quaternary faults, liquefaction fractures, and possible tectonic features on the central and eastern United States, east of the Rocky Mountain front, U.S. Geological Survey Open-file report OFM-00-260.

Davis, W. M., 1902, The rivers and valleys of Pennsylvania: National Geographic Magazine: Harvard College, Cambridge, Mass., 71 p.

Dombroski, D. R., 1987, Review of the Permeability characteristics of the Woodbury-Merchantville confining layer in New Jersey: Northeastern geology, vol. 9, no. 4, p. 191-200.

Drake, C. L. and Woodward, H. P. , 1963, Section of geological sciences: Appalachian curvature, wrench faulting, and offshore structures: Transactions of the New York Academy of Sciences, Series 11, no. 26: 48–63.

Duncan, R. A., 1984, Age progressive volcanism in the New England Seamounts and the opening of the central Atlantic Ocean: Journal of Geophysical Research, v. 89, no. B12, p. 9980-9990.

Dore´, A. G., Lundin, E. R., Kusznir, N. J., and Pascal, C., 2015, Potential mechanisms for the genesis of Cenozoic domal structures on the NE Atlantic margin: pros, cons and some new ideas, in, Johnson, H., Dore´, A. G., Gatliff, R. W., Holdsworth, R., Lundin, E. R., and Ritchie, E, J. D. , eds., The Nature and Origin of Compression in Passive Margins: Geological Society, London, Special Publications, v. 306, p. 1–26

Du, Ween-xuan, Kim, Won-Young, and Sykes, L. R., 2003, Earthquake source parameters and state of stress for the Northeastern United States and Southeastern Canada from analysis of regional seismograms: Bulletin of the Seismological Society of America, vol. 93, no. 4, p. 1633-1648.

El Tabakh, M. E., Schreiber, B. C., Warren, J. K., 1998. Origin of fibrous gypsum in the Newark rift basin, eastern North America. Journal of Sedimentary Research 68, p. 88–99.

Engelder, T., and Geiser, P., 1980, On the use of regional joint sets as trajectories of paleostress fields during the development of the Appalachian Plateau, New York: Journal of Geophysical Research, vol. 85, no. B11, p. 6319-6341.

Engelder, T., 1979, The nature of deformation within the outer limits of the central Appalachian foreland fold and thrust belt in New York State, Tectonophysics, 55, 289-310.

Engelder, T., Haith, B.F., and Younes, A., 2001, Horizontal slip along Alleghanian joints of the Appalachian plateau: evidence showing that mild penetrative strain does little to change the pristine appearance of early joints: Tectonophysics, v. 336, p. 31-41.

Engelder, T., and A. Whitaker, 2006, Early jointing in coal and black shale: Evidence for an Appalachian-wide stress field as a prelude to the Alleghanian orogeny: Geology, v. 34, p. 581–584

Ettensohn, F. R., 2008, The Appalachian foreland basin in Eastern united States, *in*, Miall, A. D., ed., The Sedimentary Basins of the United States and Canada, Chapter 4,vol. 5: Sedimentary Basins of the World, Elsevier, The Netherlands: 2008, pp. 105 – 179.

Gravity Anomaly Map Committee, 1987. Gravity Anomaly Map of North America (1:5,000,000). Boulder, Colorado: Geological Society of America, Continent-Scale Map-002 (5 sheets). Geophysics of North America CD-ROM, National Geophysical Data Center, 1989

Gray, M.B., and Mitra, G., 1993, Migration of deformation fronts during progressive deformation: Evidence from detailed structural studies in the Pennsylvania anthracite region, U.S.A.: Journal of Structural Geology, v. 15, p. 435–449, doi: 10.1016/0191-8141(93)90139-2.

Groshong, R. H., 1972, Strain calculated from twinning in calcite: Geological Society of America Bulletin, V. 83, p. 2025-2038.,

Gwinn, V. E., 1970. Kinematic patterns and estimates of lateral shortening, Valley and Ridge and Great Valley Provinces, Central Appalachians, South-Central Pennsylvania: in Fisher, G. W., Pettijohn, F. J., Reed, J. C., and Weaver, K. N., eds., Studies of Appalachian Geology: Central & Southern. Wiley Interscience, New York, NY, p. 127-146.

Hancock, P.L. and Engelder, T., 1989, Neotectonic Joints: Geological Society of America Bulletin, v. 101, p. 1197-1208.

Hatcher, R. D., Jr., 2008, Tracking Lower-to-Mid-to-Upper Crustal Deformation Processes through Time and Space through Three Paleozoic Orogenies in the Southern Appalachians Using Dated Metamorphic Assemblages and Faults: Geological Society of America Abstracts with Programs, Vol. 40, No. 6, p. 513.

Herman, G.C., 1984, A structural analysis of a portion of the Valley and Ridge Province of Pennsylvania [M.S. thesis]: Storrs, University of Connecticut, 107 p.

Herman, G. C., 1997, Digital mapping of fractures in the Mesozoic Newark basin, New Jersey: Developing a geological framework for interpreting movement of groundwater contaminants: Environmental Geosciences, v. 4, no. 2, p. 68-84.

Herman, G. C., 2005, Joints and veins in the Newark basin, New Jersey, in regional tectonic perspective: in Gates, A. E., editor, Newark Basin – View from the 21st Century, 22nd Annual Meeting of the Geological Association of New Jersey, College of New Jersey, Ewing, New Jersey, p. 75-116.

Herman, G. C., 2006, Neotectonic setting of the North American Plate in relation to the Chicxulub impact: Geological Society America Abstracts with Programs, Vol. 38, No. 7, p. 415 (1.3 MB PDF file)

Herman, G. C., 2009, Steeply-dipping extension fractures in the Newark basin, Journal of Structural Geology, V. 31, p. 996-1011.

Herman, G. C., 2010, Hydrogeology and borehole geophysics of fractured-bedrock aquifers (5 MB PDF), *in* Herman, G. C., and Serfes, M. E., eds., Contributions to the geology and hydrogeology of the Newark basin: N.J. Geological Survey Bulletin 77, Chapter F., p. F1-F45.

Herman, G. C., 2013, Utilizing Google Earth for geospatial, tectonic, and hydrogeological research at the New Jersey Geological and Water Survey: Geological Society America Abstracts with Programs, Vol. 45, No. 17, p. 110

Herman, G. C. and Curran, John, 2010, Borehole geophysics and hydrogeology studies in the Newark basin, New Jersey (38 MB PDF), *in* Herman, G. C., and Serfes, M. E., eds., Contributions to the geology and hydrogeology of the Newark basin: N.J. Geological Survey Bulletin 77, Appendexes 1-4, 245 p.

Klewsaat, D. R, and Gates, A. E., 1994: Northeastern Geology, vol. 16, no. 3&4, p. 237-250.

Klitgord, K. D., and Schouten, H., 1986, Plate kinematics of the central Atlantic; in Vogt, P. R., and Tucholke, B. E., eds., The Geology of North America, Volume M., The Western North Atlantic Region: Geological Society of America.

Komitz, M. A., and Pekar, S. F., 2001, Oligocene eustasy from two-dimensional sequence stratigraphic backstripping: Geological Society of America Bulletin, vol. 113, no. 3, p. 291-304

Lee, M. R., and Leroux, H., 2015, Planetary minerology: The mineralogical society of Great Britain and Ireland, 314 p.

Lomando, A. J. and Engelder, Terry, 1984, Strain indicated by calcite twinning: Implications for deformation of the Early Mesozoic Northern Newark Basin, New York: Northeastern Geology, vol. 6, no. 4, p. 192-195.

Lucas, M., Hall, J., and Manspeizer, W., 1988, A foreland-type fold and related structures in the Newark rift basin, *in* Manspeizer, W., ed., Triassic-Jurassic rifting, continental breakup and the origin of the Atlantic Ocean and passive margin: Elsevier, Amsterdam, p. 307-332.

Magnetic Anomaly Map Committee, 1987, Geophysics of North America CD-ROM, National Geophysical Data Center, 1989.

Marshak, S., 2004, Salients, recesses, arcs, oroclines, and syntaxes – A review of ideas concerning the formation of map-view curves in fold-thrust-belts, in McClay, K. R., ed., Thrust tectonics and hydrocarbon systems: American Association of Petroleum Geologists Memoir 82., p. 131-156.

Meeus, Jean, 1997, Mathematical Astronomy Morsels, Richmond, Virginia: Willmann-Bell. 379p.

Merguerian, C., 2002, Brittle faults of the Queens tunnel complex, NYC water tunnel #3, in Hanson, G. N., chairmen: Ninth annual conference on geology of Long Island and metropolitan New York, State University of New York at Stony Brook, NY, Long Island Geologist Program with Abstracts, 116 p.

Merguerian, C. and Sanders, J. E., 1994, Post-Newark folds and -faults: implications for the geologic history of the Newark basin, p. 57-64 *in* Hanson, G. N., chm., Geology of Long Island and metropolitan New York, 23 April 1994, State University of New York at Stony Brook, NY, Long Island Geologists Program with Abstracts, 165 p.

Merguerian, C. and Sanders, J. E., 1996, Diversion of the Bronx River in New York City; evidence for postglacial surface faulting?, in Geology of Long Island and metropolitan New York: Stony Brook, State University of New York at Stony Brook, Long Island Geologists, p. 131-145.

Merguerian, C. and Sanders, J. E., 1997, Bronx River diversion—Neotectonic implications: International Journal of Rock Mechanics and Mining Sciences, v. 34, no. 3-4, paper no. 198.

Metzger, J. M., Flemings, P. B., Christie-Blick, N., Mountain, G. S., Austin, J. A. Jr., Hesselbo, S. P., 2000, Late Miocene to Pleistocene Sequences at the New Jersey Outer Continental Shelf (ODP Leg 174A, Sites 1071 and 1072), Columbia University Academic Commons.

Miller, K. G., Mountain, G. S., and Tucholke, B. E., 1985, Oligocene glacio-eustasy and erosion on the margin of the North Atlantic: Geology, v. 13.p. 10-13.

Miller, K. G., Kent, D. V., Brower, A. N., Bybell, L. M., Feigenson, M. D., Olsson, R. K., and Poore, R. Z., 1990, Eocene-Oligocene sea-level changes on the New Jersey coastal plain linked to the deep-sea record, Columbia University Academic Commons, http://hdl.handle.net/10022/AC:P:12247.

Miller, K. G., Browning, J. V., Mountain, G. S., Sheridan, R. E., Sugarman, P. J., Glenn, S., and Christensen, B. A., 2014, History of continental shelf and slope sedimentation on the US Atlantic margin: Geological Society of London Memoirs, v. 41, p. 21-34.

Molinsky, Linda, and Bartlett, G. A., 1975, Environmental and stratigraphic zonation of the Oligocene and Miocene off Nova Scotia and Newfoundland: Continental Margins and Offshore Petroleum Exploration — Memoir 4, Abstracts, p. 897

Mazzotti, S., Henton, J., and Adams, J., 2004, Crustal strain rates and seismic hazard from seismicity and GPS measurements along the St Lawrence Valley, Quebec, American Geophysical Union, Spring Meeting 2004, abstract #S14A-02.

Nickelsen, R. P., 1963, Fold patterns and continuous deformation mechanisms of the central Pennsylvania folded Appalachians, *in* Cate., A., ed., Guidebook: Tectonics and Cambro-Ordovician stratigraphy, central Appalachians of Pennsylvania: Pittsburgh Geological Society with the Appalachian Geological Society, Pittsburgh, Pa., p. 13-29.

Nickelsen, R. P 1987, Sequence of structural stages of the Alleghany orogeny at the Bear Valley Strip Mine, Shamokin, Pennsylvania. (Dept. of Geology, Bucknell University) Geological Society of America Centennial Field Guide—Northeastern Section, 1987

Nickelsen, R. P., 1996, Alleghanian sequential deformation on the SW limb of the Pennsylvania salient in Fulton and Franklin Counties, South-Central Pennsylvania, *in* Nickelsen, ed., 61st Annual field conference of Pennsylvania geologists guidebook, Chambersburg, Pa., 108 p.

Nickelsen, R. P., 1997, Overprinted strike-slip deformation in the southern Valley and Ridge in Pennsylvania: Journal of Structural Geology, vol. 31, Issue 9, p. 865-873.

Olsson, R.K., Miller, K.G., and Ungrady, T.E., 1980, Late Oligocene transgression of middle Atlantic coastal plain: Geology, v. 8, p. 549-554.

Owens, J. P., Miller, K. G., and Sugarman, P. J., 1997, Lithostratigraphy and paleoenvironments of the Island Beach Borehole, New Jersey Coastal plain Drilling project, in Miller, K. G., and Snyder, S. W., eds., Proceedings of the Ocean Drilling Program, Scientific Reports, vol. 150X., p. 15-23.

Parrish, J. B. and Levin, P. M., 1982 Tectonic model for kimberlite emplacement in the Appalachian Plateau of Pennsylvania: Geology, v. 10, p. 344-347

Pazzaglia, F. J., and Gardner, 1994, Late Cenozoic flexural deformation of the middle U.S. Atlantic passive margin: Journal of Geophysical Research, vol. 99, no. B6, 12,143- 12,157.

Pazzaglia, F. J., and 8 others, 2006, Rivers, glaciers, landscape evolution, and active tectonics of the central Appalachians, Pennsylvania and Maryland, *in* Pazzaglia, F. J., ed., Excursions in Geology and history: Field trips in the Middle Atlantic States: Geological Society of America Field Guide 8, p. 169-197.

Parrish, J. B. and Lavin, P. M., 1982, Tectonic model for kimberlite emplacement in the Appalachian Plateau of Pennsylvania Geology: Geology, v. 10, p. 344-347,

Poag, W., 1999, Chesapeake Invader: Princeton University Press, Princeton, NJ, 168 p.

Ratcliffe, N.M., 1980, Brittle faults (Ramapo fault) and phyllonitic ductile shear zones in the basement rocks of the Ramapo seismic zones New York and New Jersey, and their relationship to current seismicity, *in* Manspeizer, W., ed. Field studies of New Jersey geology and guide to field trips: Newark, New Jersey, Rutgers University, Geology Department, New York State Geological Association, 52nd annual meeting, October 10, 1980, Guidebook, p. 278-312.

Ratcliffe, N.M., 1982, Results of core drilling of the Ramapo fault at Sky Meadow Road, Rockland County, New York, and assessment of evidence for reactivation to produce current seismicity: U.S. Geological Survey Miscellaneous Investigations Map I-1401, 1 sheet.

Ratcliffe, N. M., Burton, W. C., and Pavich, M. J., 1990, Orientation, movement history, and cataclastic rocks of Ramapo fault based on core drilling and trenching along the western margin of the Newark basin near Berndardsville, New Jersey: U.S. Geological Survey Miscellaneous Investigations Map I-1982, 1 sheet.

Ribiero, 2002, Soft plate and impact tectonics, with a contribution of Antonio Mateuus: Springer, Berlin, German, 324 p.

Ries, H., Kummel, H. B., and Knapp, G. N., 1904, The lay y and clay industry of New Jersey: Volume VI of the Final Report of the State Geologist, Trenton, NJ: MacCrellish & Quigley, Book and Job Printers, 548 p.

Seeber, L. and Dawers, N., 1989, Characterization of an intraplate seismogenic fault in the Manhattan Prong, Westchester Co., N.Y.: Seismological Research Letters, No. 60, p.71-78.

Shah, Wang, Jaw-Nan, and Samanti, N. C., 1998, Geological hazards in the consideration of design and construction activities of the New York City area: Environmental & Engineering Geoscience, vol. IV, No. 4, p. 525-533

Sheridan, R. E., Olsson, R. K., Miller, J. J., 1991. Seismic reflection and gravity study of proposed Taconic suture under the New Jersey Atlantic Coastal Plain: implications for continental growth: Geological Society of America Bulletin, vol. 103, p. 402–414.

Stanford, S.D., Jagel, D.L., and Hall, D.W., 1995, Possible Pliocene-Pleistocene movement on a reactivated Mesozoic fault in central New Jersey: Geological Society of America Abstracts with Programs, v. 27, no. 1, p. 83.

Stanford, S.D., Ashley, G.M., Russell, E.W.B., and Brenner, G.J. 2002, Rates and patterns of late Cenozoic denudation in the northernmost Atlantic Coastal Plain and Piedmont Geological Society of America Bulletin(2002),114(11):1422

Stone, B.M., and Ratcliffe, N.M., 1984, Faults in Pleistocene sediments at trace of Ramapo fault, *in* Geological Survey research, fiscal year 1981: U.S. Geological Survey Professional Paper 1375, p. 49.

Stewart, I. S., and Hancock, P. L., 1994, in Hancock, P. L., ed., Continental Deformation: Neotectonics, New York, Pergammon Press, p. 370-409.

Sykes, L. R., Armbruster, John, Kim, Won-Young, and Jacob, Klaus, 2006, Earthquakes in Greater New York-Philadelphia Area: Catalog 1677 to 2005 and Tectonic Setting; Appendices to paper Earthquakes in the Greater New York City-Philadelphia Area: 1677-2004. http://www.ldeo.columbia.edu/research/seismology-geology-tectonophysics/earthquakes-greater-new-york-philadelphia-area-catalog-an

Thomas, W.A., 1977, Evolution of salient and recesses from re-entrants and promontories in the continental margin: American Journal of Science, v. 277, p.

Tollo, R. P., Corriveau, L., McClelland, J., and Bartholomew, M. J., 2004, Proterozoic Tectonic Evolution of the Grenville Orogeny in North America, *in*, Tollo, R. P., ed., Proterozoic tectonic evolution of the Grenville orogen in North America, Geological Society of America, 820 p.1-18.

Tremblay, A., and Lemieux, Y., 2001, Supracrustal faults of the St;. Lawrence rift system between Cap-Tourmente and Baie-Saaint-Paul, Quebec: Geological Survey of Canada, Current research 2001-D15 (http://publications.gc.ca/collections/Collection/M44-2001-D15E.pdf).

Volkert, R. A., Monteverde, D. H., Friehauf, K. C., Gates, A. E., Dalton, R. F., and Smith, R. C., 2010, Geochemistry and origin of Neoproterozoic ironstone deposits in the New Jersey Highlands and implications for the eastern Laurentian rifted margin in the north-central Appalachians, USA, *in* Tollo, R. P., Bartholomew, M. J., Hibbard, J P., and Karabinos, P. M., eds., From Rodinia to Pangea: The Lithotectonic record of the Appalachian Region: Geological society of America Memoir 206, p., 283-306.

Weems, R. M., and Olsen, P. E., 1997, Synthesis and revision of groups within the Newark Supergroup, eastern North America: Geological Society of America Bulletin, vol. 109, no. 2, p. 195-209.

Wernicke, B., and Tilke, P. G., 1989, Extensional tectonic framework of the U.S. central Atlantic passive margin: in AAPG Memoir 46

Willard, B., McLaughlin, D. B., and Watson, E. H., 1950, Geologic map of Bucks County, Pennsylvania: Pennsylvania Topographic and Geologic Survey, Harrisburg, Pa., 1 map at the 1:62,500 scale.

Wise, D. U. and Werner, M. L., 2004, Pennsylvania salient of the Appalachians: A two-stage model for Alleghanian motion based on new compilations of Piedmont data: Geological Society of America Special Papers, v. 383, p. 109-120.

Woodward, H. P., 1968, A possible major fault zone crossing central New Jersey,: New Jersey Academy of Science, The Bulletin, vol. 13., No. 1, p. 40-46.

Woodworth, J. B., 1932, Contributions to the study of mountain building: American Journal of Science, series 5, vol. 23, no. 134, p. 155-171.

York, J.E. and Oliver, J.E., 1976, Cretaceous and Cenozoic Faulting in Eastern North America. Geological society of America Bulletin, vol. 87, p. 1105-1114.

Zoback, M.L., and Zoback, M.D., 1989, Tectonic stress field of the continental United States, in Pakiser, L.C., and Mooney, W.D., eds., Geophysical framework of the continental United States: Geological Society of America Memoir 172, p. 523-539.

Geomorphic paleogeodesy and intraplate deformation associated with the Mineral, VA earthquake and surrounding Central Virginia Seismic Zone (CVSZ).

Frank J. Pazzaglia and Helen, F. Malenda, Department of Earth and Environmental Sciences, Lehigh University, 1 West Packer Ave, Bethlehem, PA 18015

Abstract

The 2011 M 5.8 Mineral, VA earthquake was a sobering reminder that the central and eastern U.S. (CEUS) plate interior deforms, but unlike plate boundaries, plate interiors lack a systems-level model that describes their various components, deformation processes, process linkages, and feedbacks. Similarly, we know little about the sources of seismic stresses and why earthquakes appear to be concentrated in specific zones of low-level, but persistent activity such as the CVSZ. Earthquakes deform the crust and as this deformation propagates to the surface it should be geodetically recorded. Lying in the Piedmont of Virginia, the CVSZ is traversed by numerous entrenched bedrock streams flanked by Pleistocene fluvial terraces, geomorphic markers commonly used for geomorphic paleogeodesy in active tectonic regions. Detailed surficial mapping along the South Anna River in the Mineral epicentral region has defined a middle-late Pleistocene fluvial stratigraphy and channel morphologic changes that are distinct in the hanging wall and footwall of the fault that ruptured during the earthquake. River terraces are defined using textural, compositional, and soil stratigraphic criteria. OSL and IRSL geochronology provides ages for a key, ~70 ka terrace that we use as the anchor of a regional correlation that is further informed by dated terraces on the nearby James River and upland gravels preserved on the inner Coastal Plain. The long term incision rate in the footwall of the fault that ruptured during the Mineral earthquake is ~40-50 m/Ma, indistinguishable from the background, regional Pleistocene rate of Piedmont fluvial incision. However, in the hanging wall, the incision rate may be as much as double at ~90-100 m/Ma and the terraces are arched up and over the surface projection of the fault plane that ruptured in 2011. The Mineral earthquake has been geodynamically modeled to have generated ~ 0.07 m of surface deformation distributed over a wavelength consistent with the terrace arch. Generating ~50 m of incision in the hanging wall in a million years would require ~700 Mineral-sized events, with a mean recurrence interval of ~1500 years. Although crude and carrying huge uncertainties, these estimates offer some insights into the rates and scale of stress concentration and release in the CEUS.

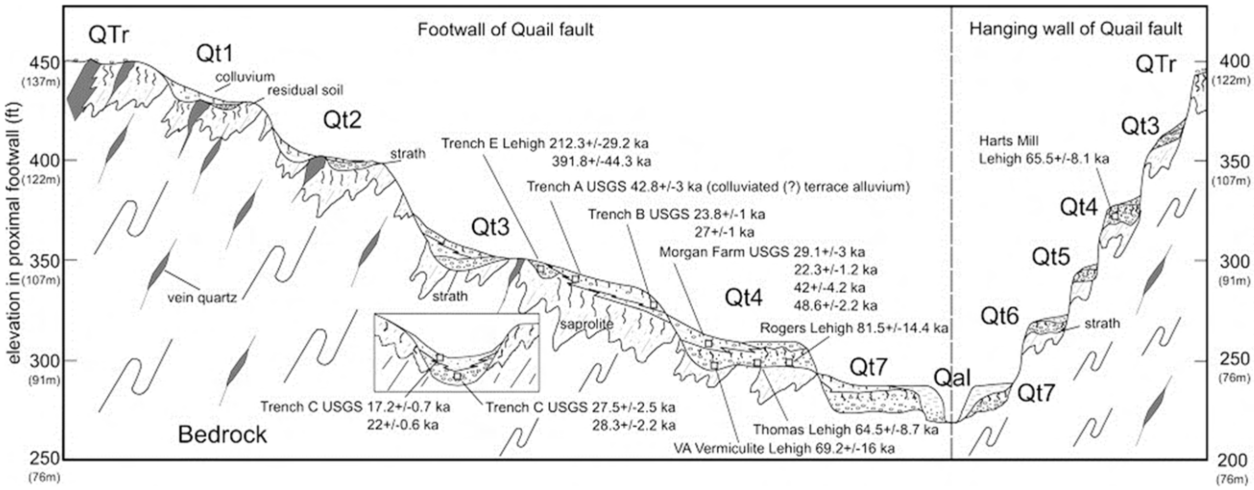

Figure 1 Stratigraphy of terraces (alluvium), colluvium, saprolite, and residual soils for the reach of the South Anna River crossing from the proximal footwall to the hanging wall of the Quail Fault

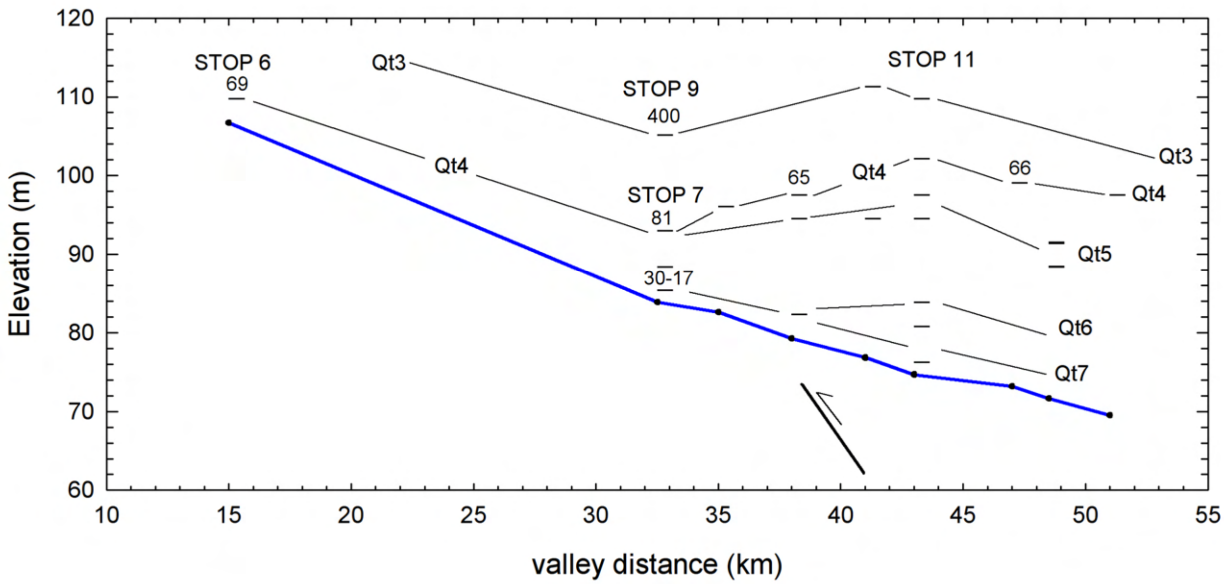

Figure 2. Proposed correlation of the Qt4 and Qt3 terraces from the footwall to the hanging wall of the Mineral earthquake fault with field trip stops indicated. Numbers are OSL/IRSL rounded ages rounded to the nearest ka. All data are projected to a vertical plane oriented NW to SE along the South Anna River valley. The lower solid line with dots is a simplified projection of the South Anna River. The horizontal tic-lines are projections of selected terraces. Thin lines between horizontal tics are the proposed terrace correlation. Approximate position of the updip projection of the Quail Fault is shown below the channel

Keynote abstract. The New Jersey Coastal Plain: A key to deciphering past, present, and future sea-level change.

Kenneth G. Miller, Distinguished Professor of Earth and Planetary Science, J.V. Rutgers University, New Brunswick , New Jersey

Abstract

The sands and muds of the U.S. Atlantic coastal plain (Fig. 1) record sea-level change of the past 100+ Myr. Starting in 1993, 16 holes drilled in the coastal plain in New Jersey, 1 in Delaware, and 1 in the Chesapeake Bay crater (Virginia)(Fig. 1) have provided an unprecedented core record that allows reconstruction of water depth changes through time. These transgressions and regressions reflect processes of global average sea-level change (eustasy), tectonism (thermal subsidence, glacial isostatic adjustment (GIA), and mantle dynamic changes), and sediment supply. We systematically backstrip sedimentary sequences to progressively remove the effects of compaction, loading, and thermal subsidence, the residual is a measure of eustasy and non-thermal subsidence (Fig. 2). By comparing records from numerous locations, we can decipher sea-level changes over the past 100 Myr. Prior to the Oligocene (ca. 33.5 Ma), the Earth had been a warm, high CO_2 Greenhouse world that was largely ice-free back to the Late Permian Period (ca. 260 Ma), though recent evidence from New Jersey suggests that 15-25 m sea-level changes may have been caused by growth and decay of small, ephemeral ice sheets. Our New Jersey records show 50-60 m variations on the 10^6 yr scale beginning ~33.5 million years ago (Ma), reflecting growth and decay of a continental-scale ice sheet in Antarctica. We compare our backstripped eustatic estimate with those obtained by scaling deep-sea benthic foraminiferal $\delta^{18}O$ records using Mg/Ca to constrain temperature effects. Both show the same amplitudes and timings and testify to a primary glacioeustatic control on the stratigraphic record on the Myr scale.

Regional differences document that mantle dynamic changes strongly imprint the stratigraphic and geomorphologic evolution of the passive U.S. Middle Atlantic continental margin. We note that the margin shows a patchwork preservation of blocks of sequences from Miocene, is attributed to mantle dynamics that overprinted the stratigraphic and geomorphologic evolution of this passive-aggressive margin

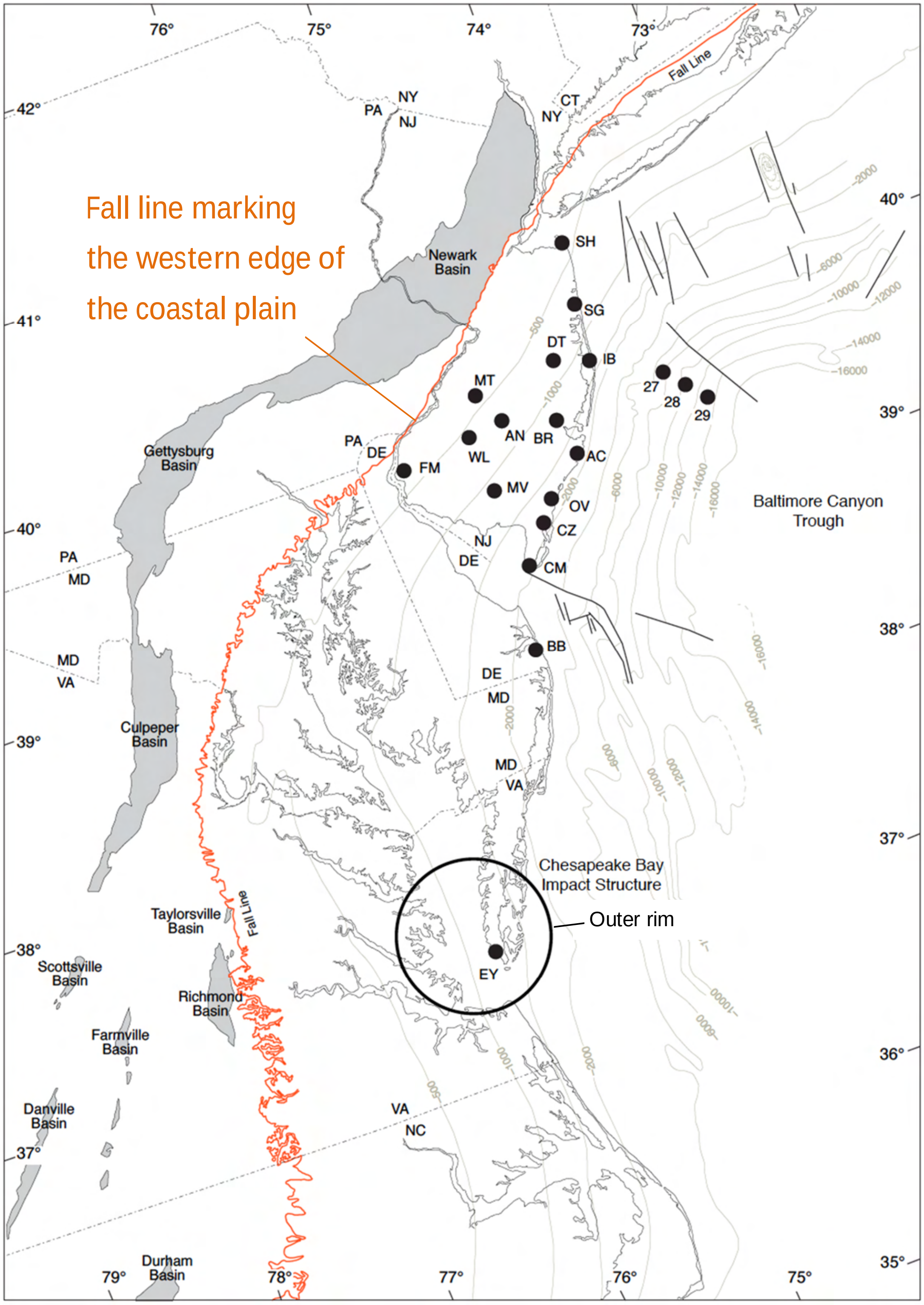

Figure 1. Map of the middle Atlantic coastal plain. Black dots indicate locations of drilled boreholes included in this summary. Adapted from Miller et al. (2013).

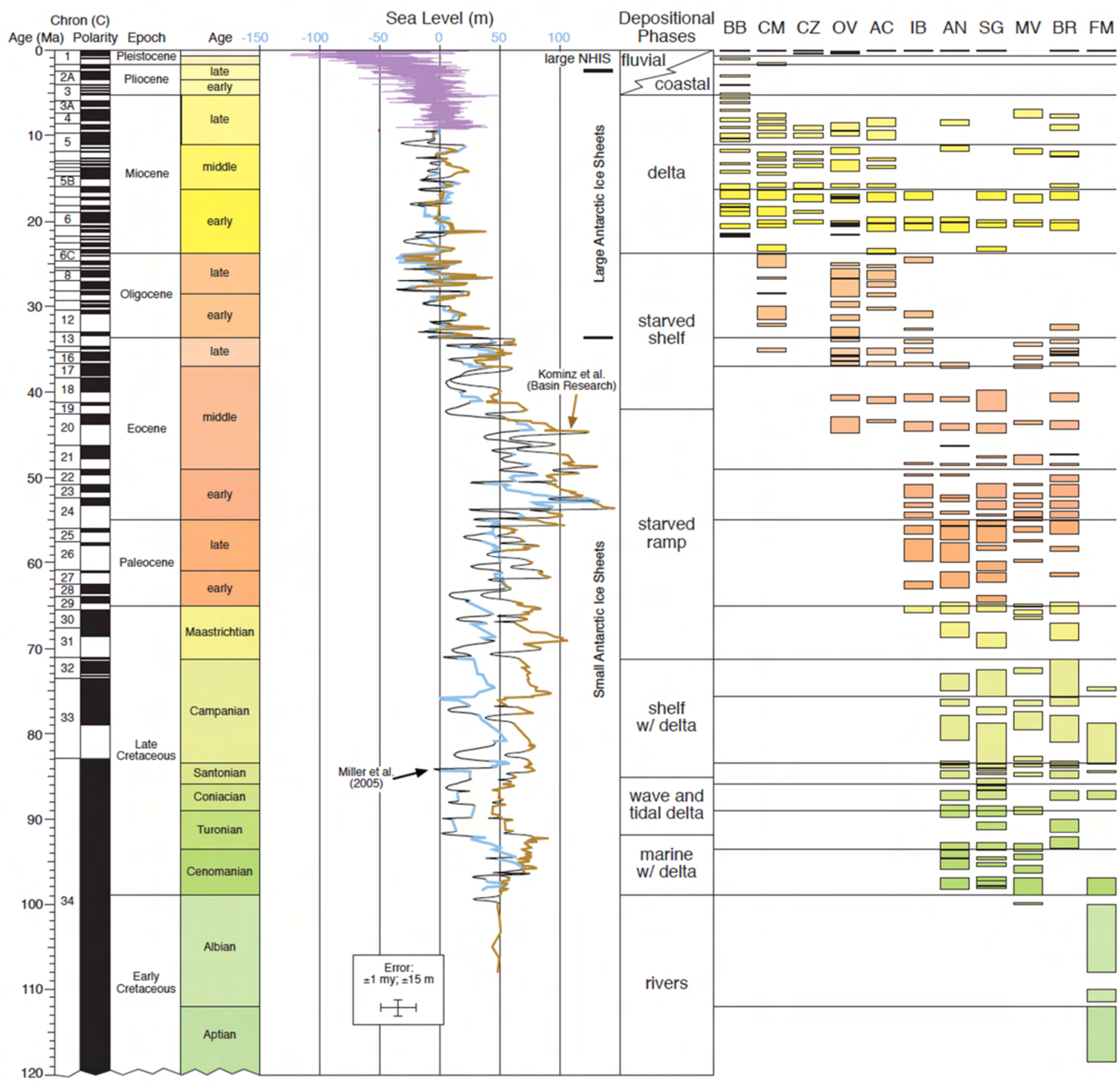

Figure 2. Distribution of sediments in sequences found in New Jersey coastal plain core holes plot as a function of time. BB-Bethany Beach core, CM-Cape May core, CZ-Cape May Zoo core, OV-Ocean View core, AC-Atlantic city core, IB-Island Beach core, AN-Ancora core, SG-Sea Girt core, MV-Millville core, BR-Bass River core, FM-Fort Mott core.

Sea-level is rising today due to increased anthropogenic warming and subsidence, threatening shoreline systems (Fig. 3). During the Common Era, sea level was globally stable, though it rose in NJ by ~1.6 mm/yr due to GIA and local subsidence. During the 20th century global sea level rose ~1.2±0.2 mm/yr and the rise is accelerating. Sea level is rising ~1.3±0.4

mm/yr faster than global at bedrock locations (e.g., New York City, Philadelphia, Baltimore, and Washington D.C.) due to GIA subsidence. At coastal plain locations, the rate of rise is an additional 0.3-1.3 mm/yr higher than at the bedrock locations due to groundwater withdrawal and compaction. Miller et al. (2013) constructed 21st century relative sea-level rise scenarios that include global, regional, and local processes. They projected a 22 cm rise at bedrock locations by 2030 (central scenario; low- and high-end scenarios with a range of 16-38 cm), 40 cm by 2050 (range 28-65 cm), and 96 cm by 2100 (range 66-168 cm), with coastal plain locations having higher rises (3, 5-6, and 10-12 cm higher, respectively). By 2050 CE in the central scenario, a storm with a 10-year recurrence interval will exceed all historic storms at coastal locations.

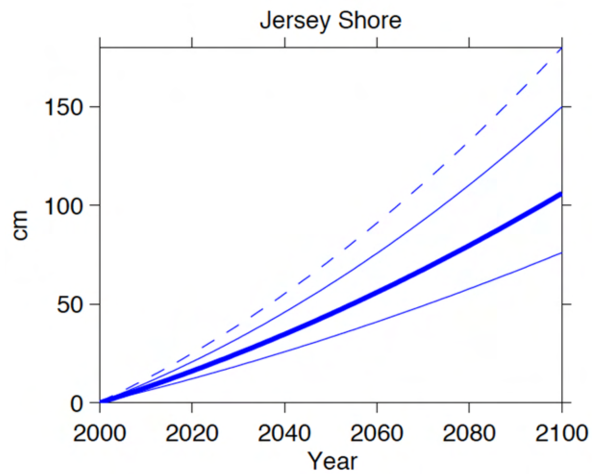

Figure 3. Projections of relative sea level rise on the Jersey shore. Various scenarios of projected sea-level rise plot along curves having higher (dashed), high (upper solid), low (heavy solid), and lower (solid) trends.

Acknowledgements

The ideas presented here were derived by interaction with numerous people; I especially thank J.V., Browning, M.A. Kominz, R.E. Kopp, P.P. McLaughlin, G.S. Mountain, P.S. Sugarman, and J.D. Wright. I thank NSF 1463759, the Midwestern Regional Carbon Sequestration Partnership (MCRSP), and New Jersey Sea Grant for support. The Coastal Plain drilling project is part of Ocean Drilling Program Legs 150X and 174AX and all cores examined here are available from the Rutgers Core Repository http://geology.rutgers.edu/research-facilities/rutgers-core-repository

Reference

Miller, K.G., Kopp, R.E., Horton, B.P., Browning, J.V., Kemp, A.C., 2013, A geological perspective on sea-level rise and impacts along the U.S. mid-Atlantic coast: Earth's Future, v. 1, p. 3-18.

Field Excursion Departure Location and Time

Liberty Village Commuter Parking Lot, 81 Route 12 W, Flemington NJ

Buses will leave at 8:15 am, please park in the eastern lot highlighted below

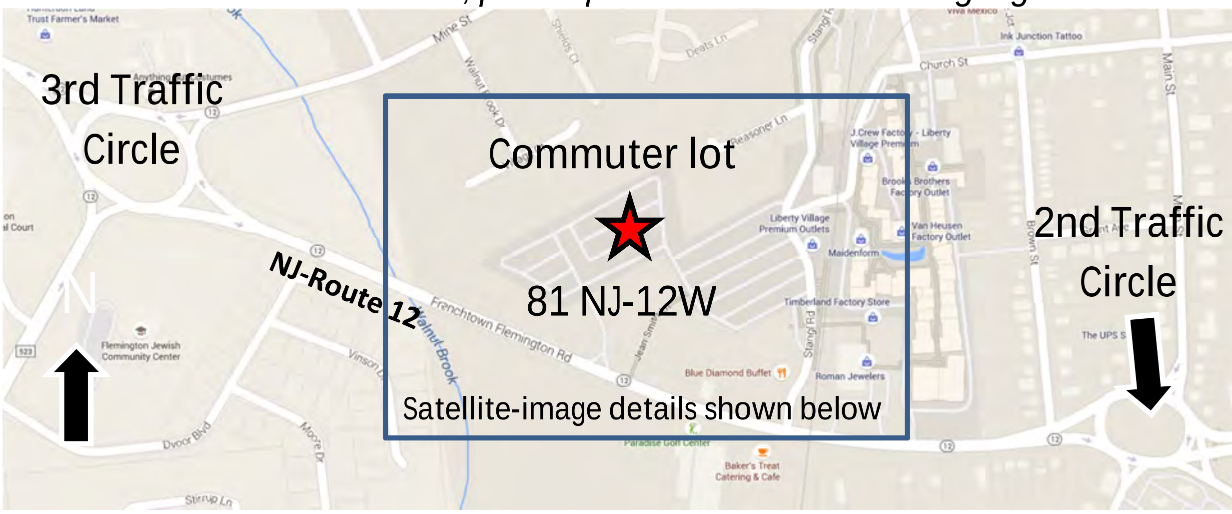

Maps show the commuter lot where we embark. upper-overview and lower details

Chapter 5. GANJ 32 Field Guide

Gregory C. Herman[1], Donald H. Monteverde[1], John H. Dooley[1], Larry F. Mueller[1], and Michael J. Hozik[2]

[1] New Jersey Geological & Water Survey, Trenton, NJ 08625
[2] Richard Stockton State College, Galloway, NJ 08205

Field Trip Itinerary

Saturday October 17, 2015

Assemble at NJ Liberty Village Commuter Lot at 81 RJ-12W (see previous page)

Time	Activity	Approximate Distance/ Driving Time
8:00 AM	Leave Flemington NJ Liberty Village Commuter Lot	16 miles/ 30 minutes
8:30 AM	Arrive at STOP 1: *Eastern Concrete Materials plant*	
10:30 AM	Leave for STOP 2	30 miles/ 46 minutes
11:15 AM	Arrive at STOP 2: *Mercer County Park at Valley Road*	
1:15 PM	Leave for STOP 3	2 miles/ 3 minutes
1:20 PM	Arrive at STOP 3: *Trap Rock Industries Moore's Station Plant*	
2:00 PM	Leave for STOP 4	13 miles/ 19 minutes
2:30 PM	Arrive at STOP 4: *Delaware & Raritan Canal State Park Trail*	
4:30 PM	Leave for return to Flemington	15 miles/ 20 minutes
4:50 PM	Return to Flemington NJ Liberty Village Commuter Lot	

Introduction

This field guide includes detailed geological maps covering the region and details for areas of interest, including the four (4) STOPS included in this year's field excursion (see fig. 1).

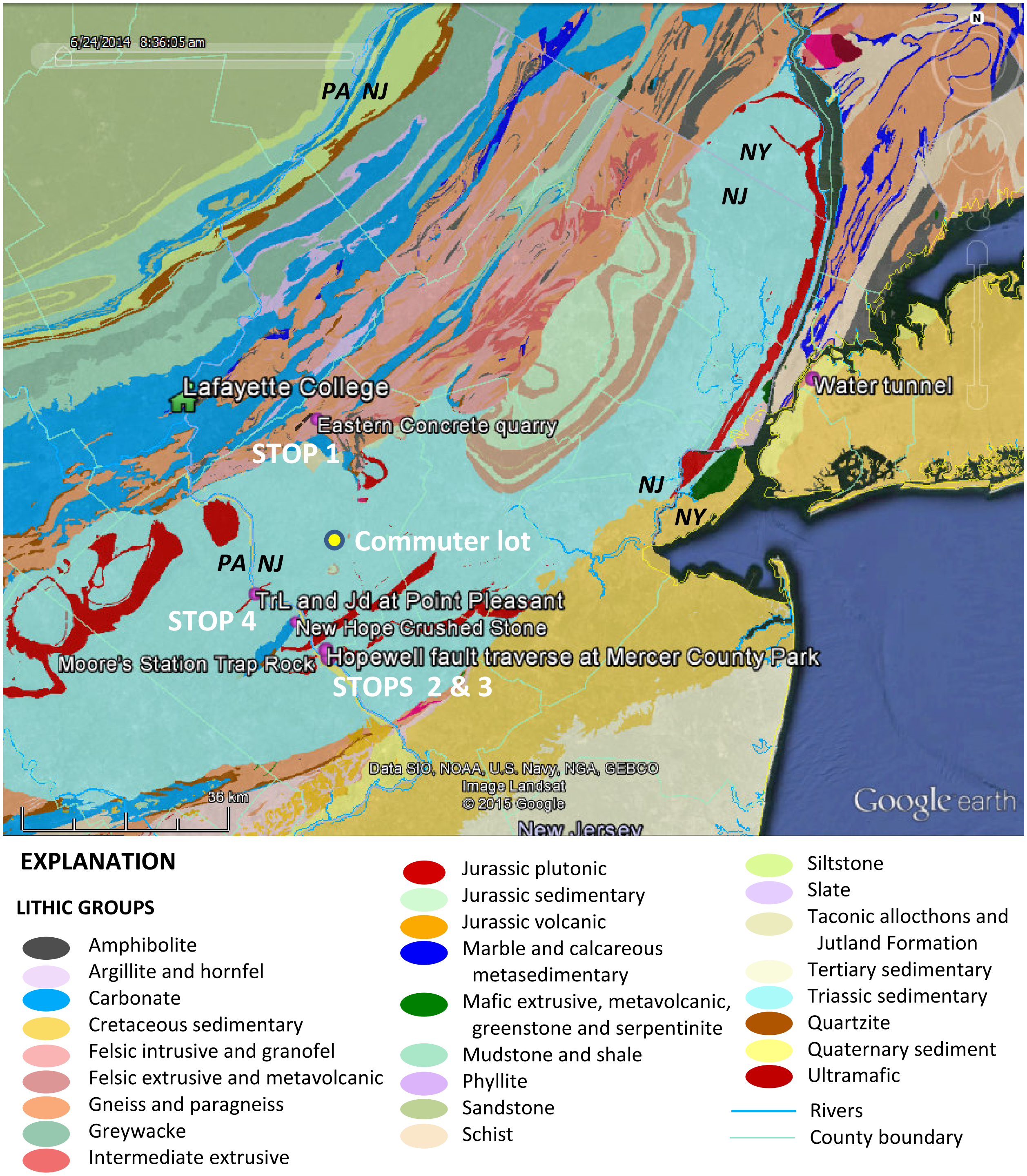

Figure 1. GE display of the GANJ 32 circuit showing Lafayette College, points of interest, and US Geological Survey statewide geology themes integrated by lithic groups.

Additionally, because of its proximity to the field STOPS and its geological relevance with respect to this year's theme, this guide also includes a geologic note detailing some recent work done in the New Hope Crushed Stone quarry in Buck's County, Pennsylvania. Much of this work stems from recent 1:24,000 scale mapping efforts performed with Don Monteverde and Ron Witte as part of their STATEMAP grant work within the geological mapping section of the New Jersey Geological and Water Survey (NJGWS). These efforts include work on the NJ parts of the Lambertville, Lumberville, and Stockton, NJ-PA 7-1/2' topographic quadrangles that straddle the state boundary between Pennsylvania (PA) and New Jersey (NJ) along the Delaware River (fig. 2) that has required some mapping in adjacent parts of Pennsylvania to address mismatches of geological contacts, faults, and bedrock units across the river based on prior mapping. Accordingly, this work revises some recent bedrock mapping along the Hopewell fault system in the NJ part of the Lambertville quadrangle (Owens and others, 1998) and prior work in Buck's County, PA (Willard and others, 1958).

Geological details are mapped using Google Earth (GE). In some instances, these include gray-colored, hill-shaded, digital-elevation models (DEMS) are included that add topographic-relief to the historical imagery available in GE, and together provide accurate constraints for geological revisions such as those mentioned above. These hill-shaded image overlays are derived from high-resolution DEMS that are produced from airborne surveys of ground altimetry using Light Detecting and Ranging (LiDAR) methods[1]. Pennsylvania provides statewide LiDAR DEM coverage through their on-line spatial-data clearinghouse (PASDA[2]). Metadata[3] for the PASDA LiDAR specifies horizontal accuracy of ~5 feet, with vertical accuracy tested between one-half to one foot. Hill-shade data for areas of interest were first displayed at a desired resolution using their digital-image navigator.[4] Each screen display was captured and saved as a JPEG image to tile with similar imagery by manually geo-registering them in GE as overlapping, image overlies, as shown in figure 3.

Although statewide, on-line LiDAR data are currently unavailable for NJ, LiDAR data for different areas of NJ have been obtained by various interests, as summarized by the State's Office of GIS.[5] As NJ State employees, direct access to these data is provided within our department's computerized geographic information system (GIS), and we use these data as detailed base maps to help refine our 1:24,000-scale geological interpretations. Some of the LiDAR data for NJ are included here as screen-captured image overlays in GE using the same methods outlined above for the PASDA imagery, except screen captures were done using GIS displays rather than an on-line image navigator. The horizontal and vertical accuracies for the

[1] www.ngs.noaa.gov/RESEARCH/RSD/main/lidar/lidar.shtml
[2] www.pasda.psu.edu
[3] www.dcnr.state.pa.us/topogeo/pamap/lidar/index.htm
[4] http://maps.psiee.psu.edu/ImageryNavigator/
[5] https://njgin.state.nj.us/NJ_NJGINExplorer/jviewer.jsp?pg=lidar

NJ data varies, however a statewide theme has been assembled with about half the resolution as that previously detailed for the PASDA data. The reader is referred to the fourth footnote

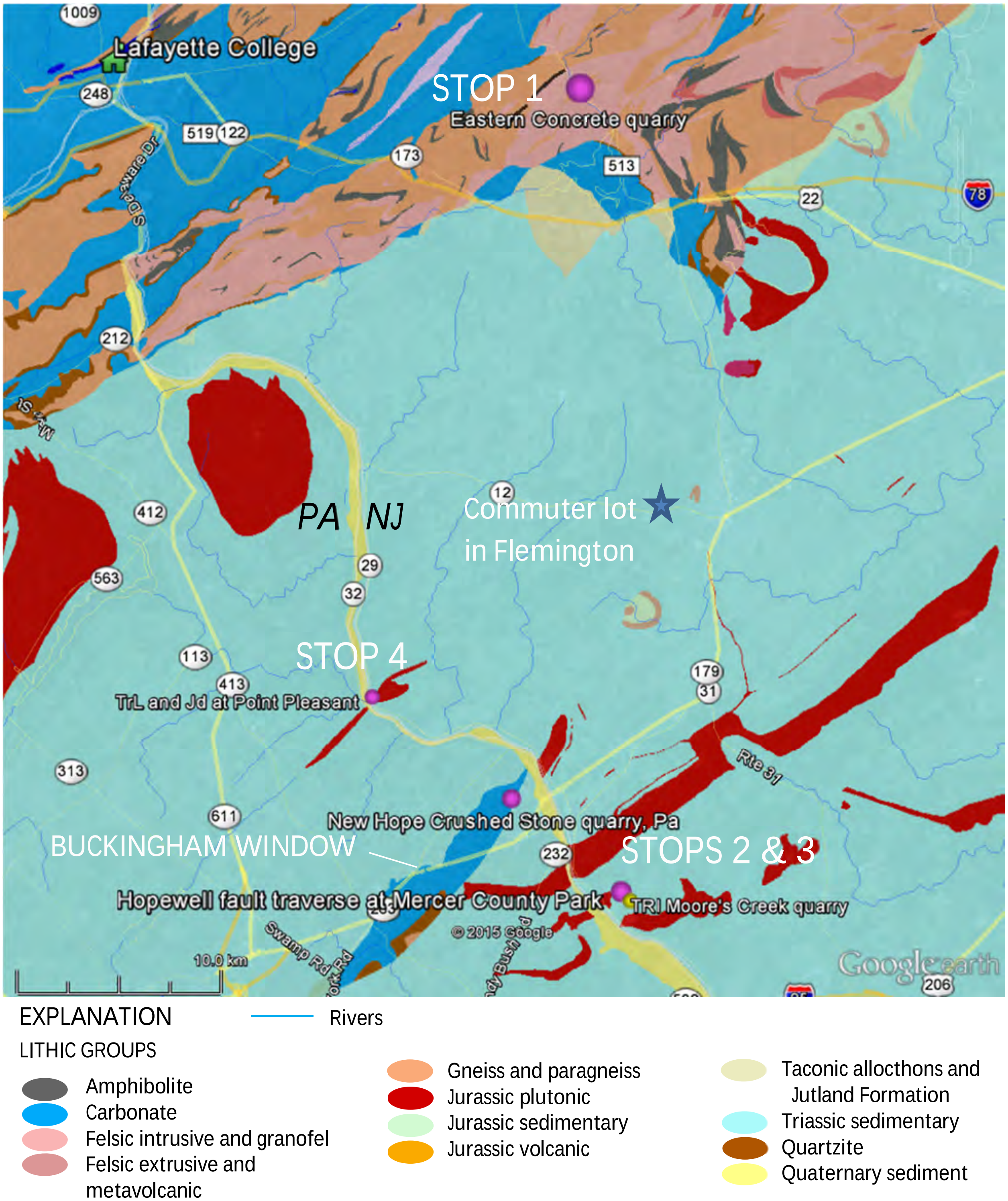

Figure 2. GE display of the GANJ 32 circuit showing Lafayette College, the Saturday morning place to assemble for the field trip (81 NJ-12), and other places of interest for this year's trip.

below for more information regarding the areas of coverage, resolutions, and requirements for obtaining NJ LiDAR data. Using five different LiDAR source themes covering northern NJ, a group of preliminary, GIS polyline themes of LiDAR-based bedrock features visible at land surface were generated for areas underlain by near-surface, pre-Cretaceous bedrock having less than 50-ft of sedimentary cover (Stanford and others, 2005). Apparent bedrock ridges, faults, and folds for those areas were manually digitized by tracing features using a computer mouse within the ESRI ArcGIS desktop environment, then checked against outcrop observations

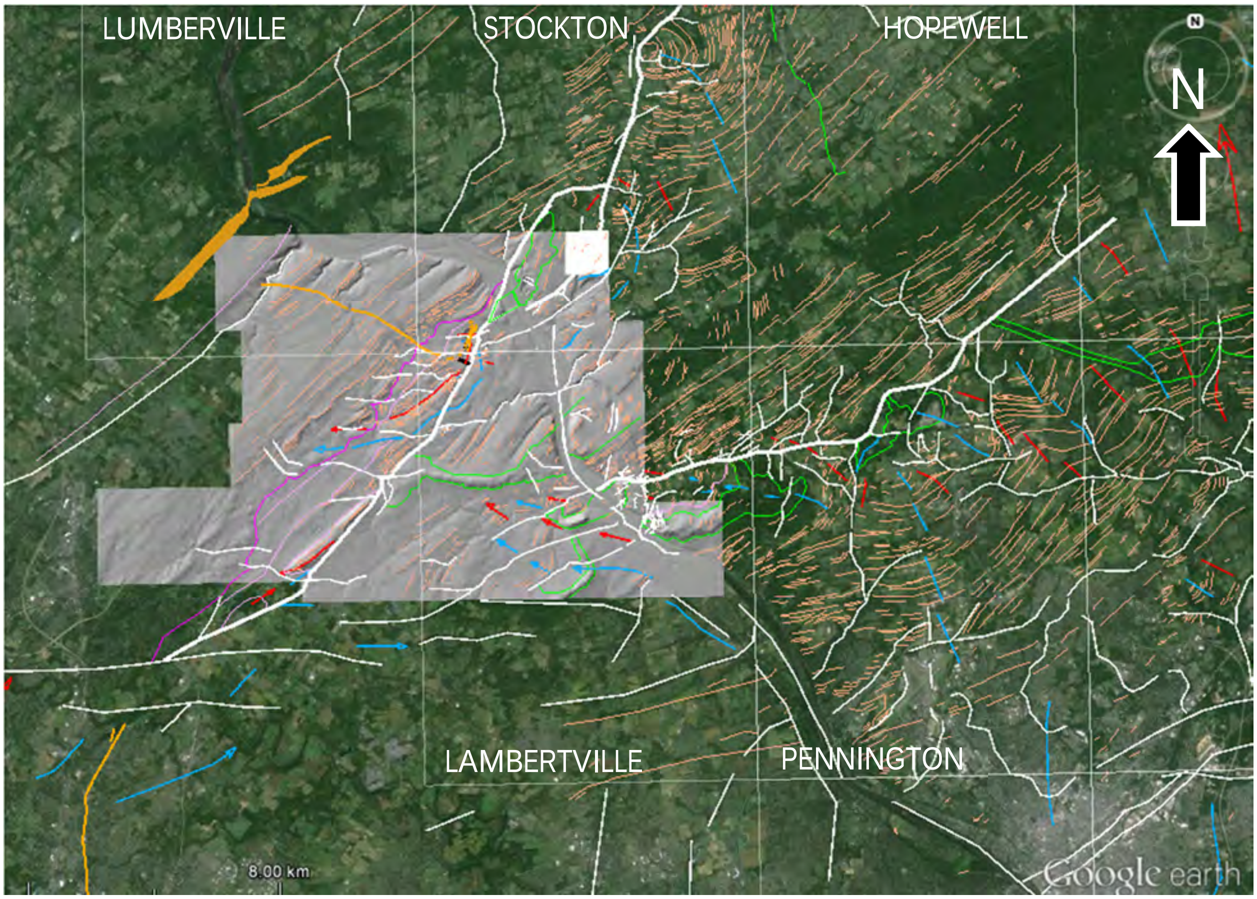

Figure 3. Screen-captured GE display of revised geological features based on LiDAR-derived imagery for the Delaware Valley in the area of west-central NJ and Buck's County, PA. Note the five named, 7-1/2' quadrangle tiles. Polyline themes covering NJ show bedrock ridges (tan lines), geological contacts (green lines), fold axes (red-anticlines and blue-synclines), and fault traces (bold-white lines are major faults, thin-white are minor faults). For PA, nine image overlays of PASDA hill-shaded DEMs are shown covering parts of the Lumberville, Stockton, and Lambertville quadrangles. The colored line elements are the same as for NJ, but dolerite dikes and sills are colored orange.

and prior geological mapping in order to ground-truth by spot checking the interpretations. To combine and refine the overlapping Pennsylvania and New Jersey data, the GIS- and LiDAR-based geology themes were converted into a GE file format (KMZ files), as shown in figure 4. These digital geological themes are preliminary in nature and are subject to further review and refinement as part of the NJGWS map-publication process. Accordingly, we intend to use this field conference as a forum to help vet some of this new work and advance some new thoughts regarding some old geological problems. Your input as part of this forum is welcomed. The complete set of KMZ files used for these analyses is available from the GANJ web site (www.ganj.org/2015/data.html).

This year's field excursion begins in Hunterdon County with STOP 1 in Proterozoic granite and gneiss exposed in the cut walls of an active bedrock quarry where crushed aggregate is produced for concrete mix. This quarry is located in the midst of Musconetcong Mountain along a cross-strike transtentional fault system (fig. 4) of probable Mesozoic age, as it cross-cuts and modified earlier, ancient compressional structures that are probably Grenville to Alleghanian in age. The purpose of this stop is threefold. We first want to demonstrate that Mesozoic extensional strains extend far into the Appalachian foreland, far beyond the limits of the Newark Basin. Then, we emphasize that in order to recognize very late, neotectonic strains in multiply deformed basement rocks, it is critical to first be able to recognize prior strain, older strains, and we get a glimpse of most of them in this quarry. And finally, that the Mesozoic-age, brittle strain features have the characteristics of those in Early Mesozoic rocks of the Newark Basin that we will see at STOP 2. We thank Eastern Concrete Materials for their kind assistance in making this stop possible.

The remaining STOPS are located in Mercer and Hunterdon Counties in the Delaware River valley, within a 3/4 hour's drive of STOP 1 (fig. 2). STOP 2 focuses on late-stage, brittle strains that we see in Mesozoic rocks along the Hopewell Fault, the second largest, intrabasinal fault system in the Newark Basin, where it occurs in Mercer County. These strains occur sporadically, are incongruent with respect to extensional structures stemming from continental rifting, and as such qualify as potential, neotectonic structures. At this stop we will see a stream cut through gray and red argillite of the Lockatong formation in the fault footwall, and softer red argillite and shale of the Passaic Formation in the hanging wall.

Nearby, STOP 3 is an opportunity to visit an active trap-rock quarry where crushed aggregate is produced for a variety of reasons. The reader is referred to Herman and others (2013) for a review of the trap rock industry in the area and additional details surrounding its production and use as a mineral resource. Moore's Station is renowned for its mineral assemblages and this stop will be an opportunity for mineral-collecting, as well as one where we will see many late-stage faults cutting some of the youngest (Early Jurassic) rocks in the area and demonstrably stemming from Mesozoic rifting. This opportunity to collect museum-quality zeolite and sulfide minerals in Passaic Formation hornfels is kindly provided by Trap Rock Industries through coordination with Mr. George Conway. Both the stratigraphic and structural aspects revealed in this quarry are amazing. Please note that this will be a brief stop. Mineral collecting will be restricted to the berms of loose material that have been positioned to buffer access to the high wall cuts. THERE WILL BE NO DIRECT CONTACT WITH THE HIGH WALLS AT THIS STOP.

This year's field trip concludes with STOP 4, a scramble of moderate difficulty up a small gorge cut through Lockatong argillite and Jurassic dolerite at Point Pleasant, NJ-PA (fig. 2). This STOP is unique to the area and includes some very bizarre, shatter-cone structures within faulted argillite that are difficult to explain.

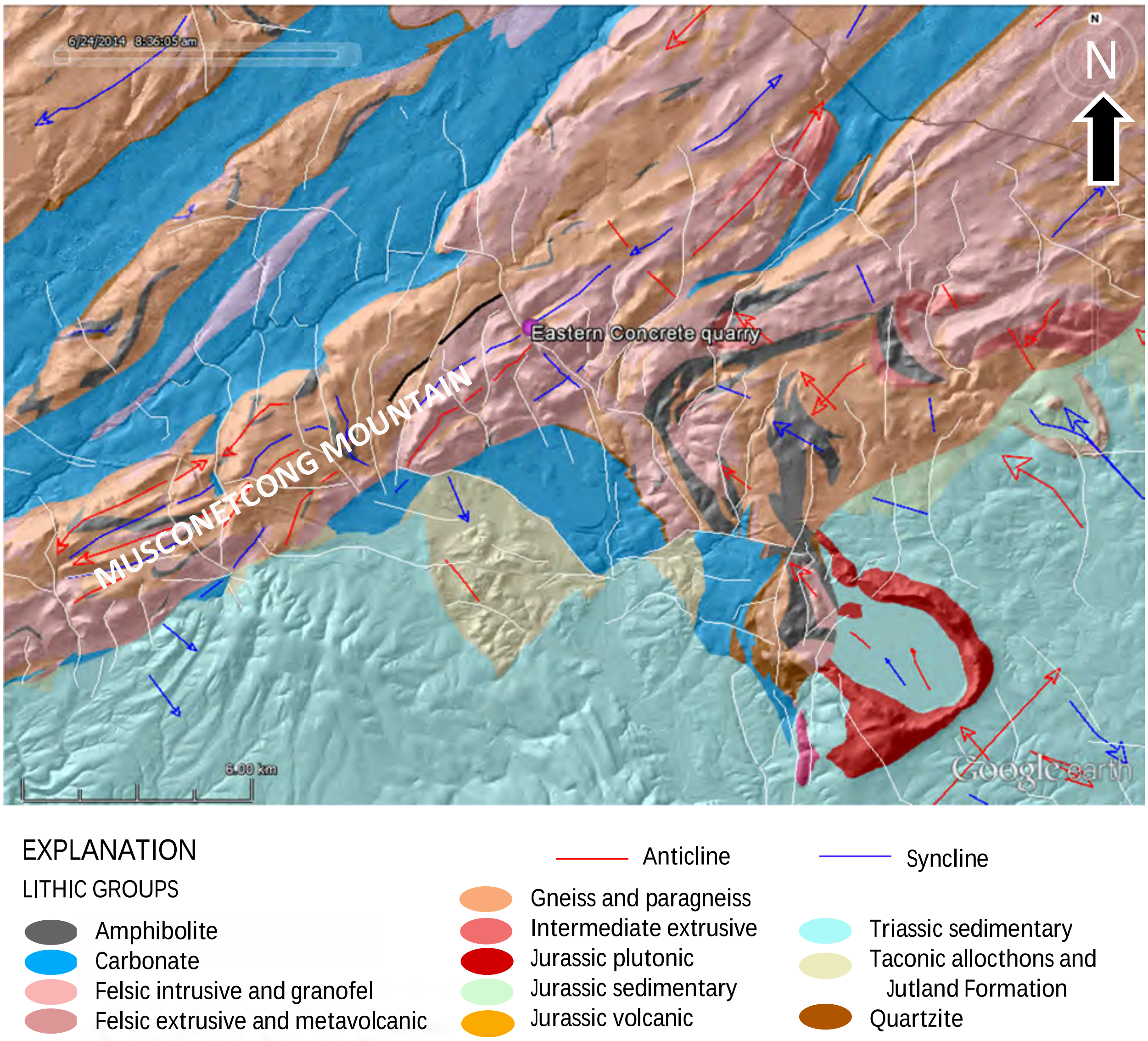

Figure **4.** Hill-shaded DEM overlay set at 50% transparent atop bedrock geology theme displayed using lithic groups. Note: 1) the abrupt width change in Musconetcong Mountain along the NW-SE trend along which the Eastern Concrete Materials plant resides, 2) the segmented nature of the mountain continuing along strike to the southwest, and 3) the interpreted continuity of cross-strike faults across the Proterozoic ridge and flanking carbonate and Triassic valleys.

STOP 1. Eastern Concrete Crushed Stone Quarry, 1 Railroad Ave, Glen Gardner, NJ

<u>HARD HATS REQUIRED HERE!</u>

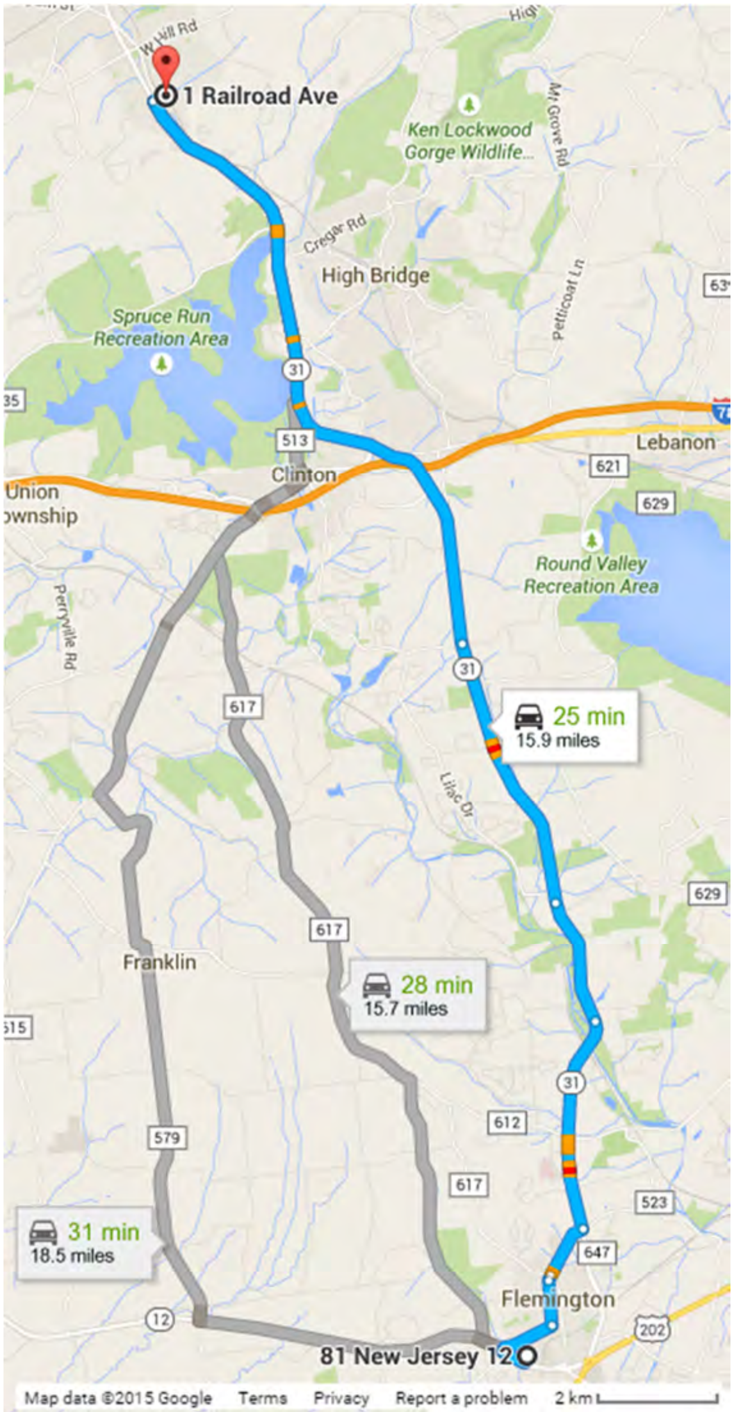

Figure 5. Google maps route (thick blue line) from the Commuter Lot at 81 NJ-12, Flemington to the Eastern Concrete quarry at 1 Railroad Ave, Glen Gardner, NJ.

Figure 5 summarizes highway routes and estimated times in driving from the meeting place to STOP 1, a crushed-stone quarry and processing plant developed on Musconetcong Mountain within crystalline basement rocks of the NJ Highlands. This quarry was targeted for study because it sits directly on a cross-strike, transtentional fault system of probable Mesozoic age that segments and offsets the mountain along its length from here to the southwest, as seen in LiDAR-based imagery (fig. 4). We see outcrop evidence of this fault system in the quarry where joints (extension fractures) and systematic, brittle, slickensided and mineralized shear planes overprint and strain earlier, ductile and brittle compressional structures stemming from earlier orogenic events. We'll examine the metamorphic compositional layering and the various ductile to brittle structures exposed in the quarry walls. The purpose of this stop is to characterize relatively late-stage, brittle strain features in the Highlands province that are also seen in the Newark Basin and demonstrate that many of the brittle, low-grade metamorphic strain mechanisms that are also seen the New Jersey Highlands and Valley

& Ridge provinces probably stem from continental rifting occurring during the Early Mesozoic period. As such, the strain effects stemming from continental breakup preceding passive-margin development are widespread, reaching past New Jersey into the Appalachian foreland of Pennsylvania (see Chapter 4). We will see evidence of copper mineralization on N-S to N20°E extension fractures, the same sets of fractures that occur in the Newark Basin and parallel deep-seated Jurassic dikes that cross-cut the Appalachian interior into the Juniata Culmination of Pennsylvania (see Chapter 4).

This quarry was mapped by the NJGWS as part of the Muessig and others (1992) field excursion focused on characterizing links between lithology and Radon occurrences in New Jersey. The geological map accompanying this report is reproduced below (fig. 6). To summarize this work with respect to our goals for this stop: the quarry is developed in Proterozoic gneisses and granites and the Longwood valley fault mapped as the contact between granitic bedrock to the southeast and gneissic bedrock to the northwest. The quartzofeldspathic gneisses contain conformable layers of amphibolite that generally strike N40°E and dip moderately to steeply southeast as well as locally disconformable alaskite lenses. Most of the rock in the quarry is sheared and shows both brittle and greenschist-grade retrograde deformation. Gross shearing appears to be sub parallel to the foliation (metamorphic layering), but small, locally localized northwest-striking brittle deformation zones are common. Most of these shear planes are coated with chlorite or epidote. Films and fibrous growths of blue crocidolite occur as an

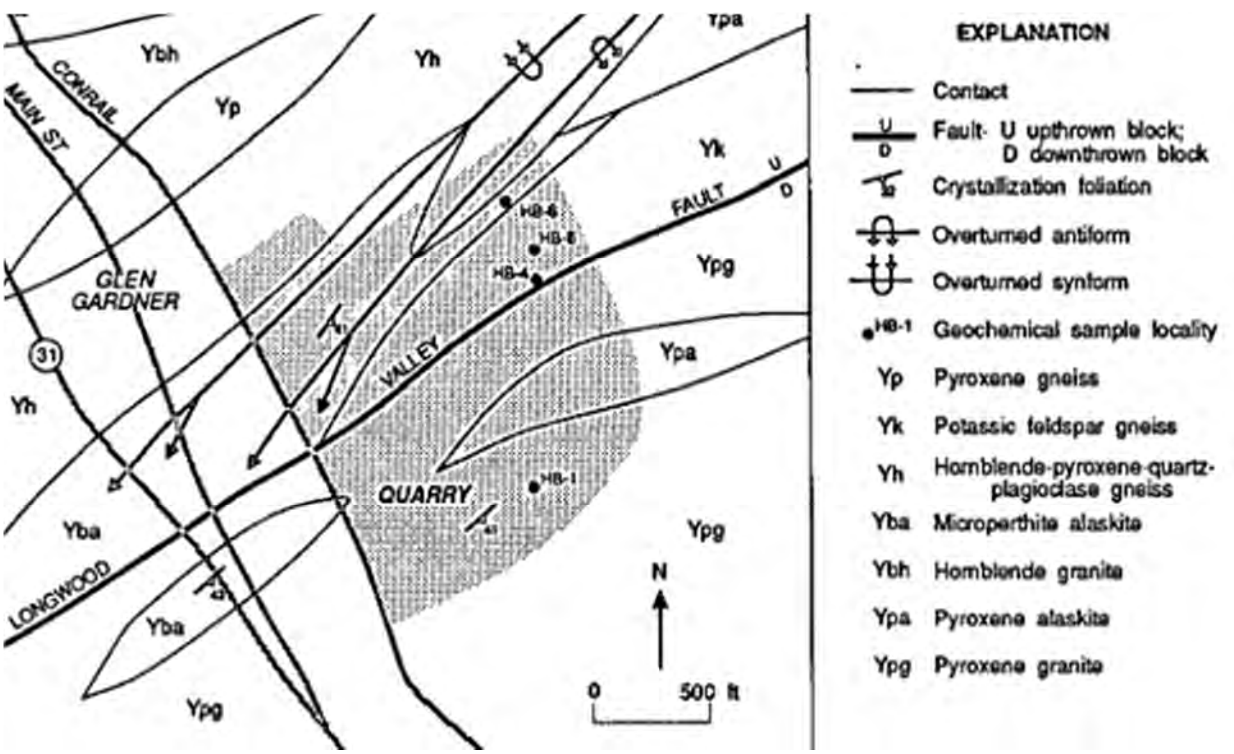

Figure 6. Geological map of the quarry in Muessig and others,

alteration product on some shear planes in the gneisses. This work also included detailed geochemical analyses of five different rock types in the quarry, documenting the link between relatively high scintillometer readings in the granites relative to the gneisses owing to increased concentrations of Uranium and Thorium. A particularly interesting part of this work is the mention and geochemical analysis of an unusual 'magnetite-rich cataclasite gneiss' that we will examine in outcrop.

I visited this quarry on a number of occasions beginning in June 2014 with various geologists from the NJGWS, Rider and Rutgers Universities in an attempt to characterize the nature of the late-stage, cross-strike faults that can be seen in LiDAR imagery (fig. 5), and that was characterized by Muessig and others (1992) as being composed of 'small' but 'common', lower-greenschist-grade, brittle shear planes. This quarry also contains two deep monitoring wells that we were given permission to log using an array of geophysical tools, including an optical borehole televiewer (BTV). Figures 7 to 15 and table 1 and 2 provide details of this recent work and a guide to the different ductile and brittle features that we will see in outcrop during this stop, including photographic details of various primary (crystalline layering) and secondary (fractures, faults, and slip lineation) structures (figs. 7, 9–12), GE maps showing some NJGWS field stations and logged wells (figs. 7 and 8), a summary of the subsurface BTV work (figs. 13 and 14), and a detailed cross-section of the hydrogeological framework based on the BTV analyses (fig. 15). Table 1 details the physical parameters for the two deep bedrock wells, and table 2 details some locations and measurement of some representative geological structures.

Outcrop data

As we enter the quarry (fig. 7), we see systematic, brittle joints, and shear planes cutting the northeast wall to our left within a well-layered quartzofeldspathic with hornblende and pyroxene. Figure 7C places these fractures into a geospatial context using an oblique southeast viewpoint and red-colored elliptical planes to show the locations and orientations of some measured metamorphic layers and superimposed shear structure detailed in table 2. The buses will park at a temporary lot located along the northern end of the eastern bench cuts near the upper quarry benches (fig. 8). We will park and assemble for a brief safety briefing and geological introduction to the quarry before walking southeast along the upper bench where the NJGWS field stations are noted in figure 8 and illustrated photographically in figure 9.

Upon starting our traverse, please be mindful that we will be examining outcrops excavated from quarrying operations. As such, before approaching any wall for close inspection, please look up above the outcrop to assess potential overhangs that look loose/perilous and avoid these locals. Please keep direct contact with the all rocks at a minimum and use rock hammers with caution as to minimize the potential for loosening any overhanging materials.

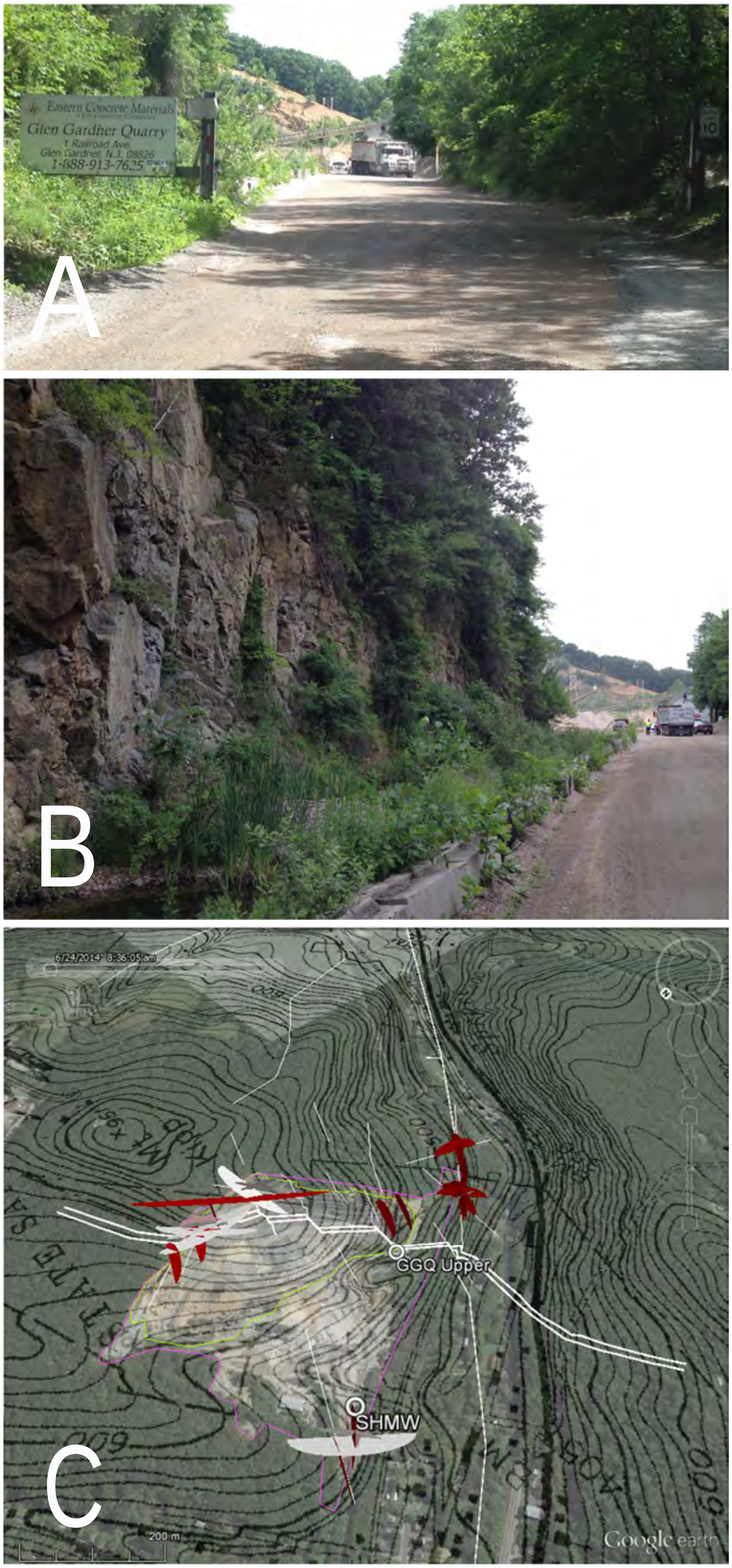

Figure 7. Photos and a map of the Glen Gardner Quarry of Eastern Concrete Materials, 1 Railroad Ave, Glen Gardner, NJ. All views are looking southeast.

A. Photo of the quarry entrance

B. Photo of the North wall just past the entrance shown above, showing a pervasive joint set in Hornblende-quartz-plagioclase gneiss that is part of the cross-strike fault system that cuts and offsets basement rocks of Musconetcong Mountain. These brittle, en-echelon, steeply dipping extension fractures show evidence of normal- and oblique-shear strain that are placed into structural and topographic context below using 3D objects (colored ellipses) in GE.

C. GE display with a monochromatic (black and white) image of the High Bridge 7-1/2' topographic quadrangle overlain atop GE imagery and set at 50% transparent. Note the two well locations (SHMW and GGQ Upper) relative to the colored ellipses represent shear fractures (red) and metamorphic compositional layering (gray). The trace of an iron (Magnetite Fe2O3)-infused, mylonite of Granville age is projected outside of the quarry along regional strike (NW-SW).

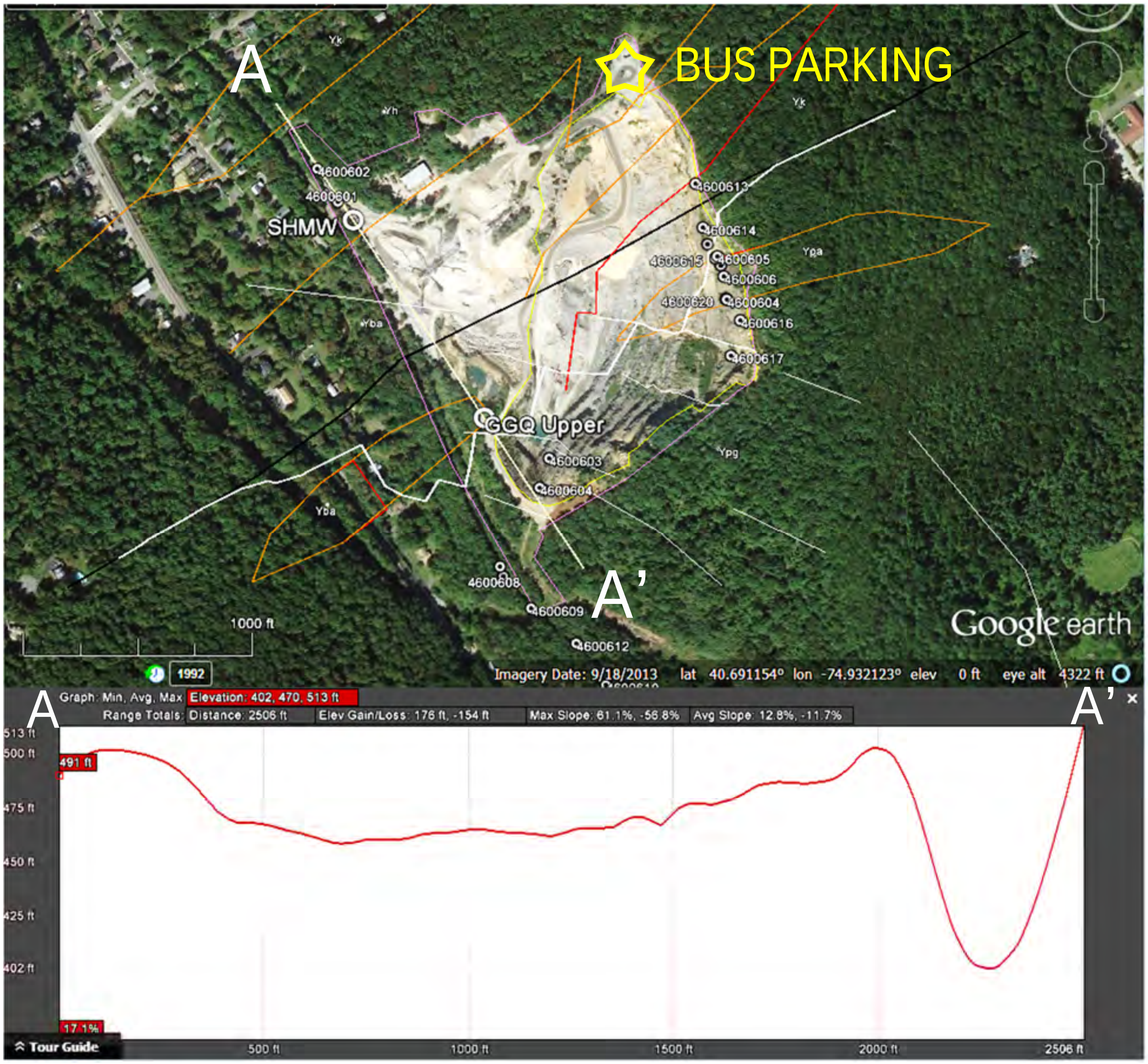

Figure 8. GE display of the quarry showing NJGWS field stations, current geological contacts (orange lines; Drake and others, 1997), a cross-section trace through two wells, and the trace of cross-strike faults that offset an older reverse fault (heavy white line). The topographic profile at the bottom was used to generate the trace of land surface for cross section A-A' (fig. 15).

Table 1. Well parameters. Geographic coordinates (WGS84 - decimal degrees), depth in feet (meters).

ID	Longitude	Latitude	Land surface (NGVD88)	Stickup	Casing depth	Total depth
SHMW	-74.933511°	40.689855°	462 (141)	2.8 (0.85)	50.0 (15.2)	
GGQ-upper	-74.933511°	40.689855°	501 (153)		25.5 (7.6)	

Table 2. NJGWS outcrop data for the Glen Garner quarry for the locations shown in figure 5-12.

Station	NJGWS-ID	Longitude	Latitude	Altitude	Dip Azimuth or Trend	Dip or Plunge	Note
GGQ1	4600601	-74.935810	40.692460	437.2	41	74	fault
GGQ1	4600601	-74.935810	40.692460	437.2	60	49	joint
GGQ1	4600601	-74.935810	40.692460	437.2	144	87	joint
GGQ1	4600601	-74.935810	40.692460	437.2	130	34	layering
GGQ1	4600601	-74.935810	40.692460	437.2	136	35	slip-lineation
GGQ2	4600602	-74.936140	40.692860	439.6	25	85	fault
GGQ2	4600602	-74.936140	40.692860	439.6	26	84	slip-lineation
GGQ3	4600603	-74.932480	40.689380	390.7	23	66	fault
GGQ4	4600604	-74.932630	40.689030	482.2	25	85	shear plane
GGQ5	4600605	-74.929830	40.691810	669.8	130	40	shear plane
GGQ5	4600605	-74.929830	40.691810	669.8	135	35	joint
GGQ5	4600605	-74.929830	40.691810	669.8	315	58	joint
GGQ5	4600605	-74.929830	40.691810	669.8	95	22	layering
GGQ6	4600606	-74.929720	40.691560	677.7	20	83	shear plane
GGQ6	4600606	-74.929720	40.691560	677.7	102	32	layering
GGQ7	4600607	-74.929670	40.691280	685.6	105	75	blue-shear-plane
GGQ8	4600608	-74.933253	40.688080	476.0	5	74	shear plane
GGQ8	4600608	-74.933253	40.688080	476.0	35	85	shear plane
GGQ8	4600608	-74.933253	40.688080	476.0	10	75	shear plane
GGQ8	4600608	-74.933253	40.688080	476.0	102	74	shear plane
GGQ8	4600608	-74.933253	40.688080	476.0	40	50	shear plane
GGQ8	4600608	-74.933253	40.688080	476.0	30	80	shear plane
GGQ8	4600608	-74.933253	40.688080	476.0	215	20	slip-lineation
GGQ9	4600609	-74.932760	40.687580	453.0	55	80	shear plane
GGQ9	4600609	-74.932760	40.687580	453.0	42	70	shear plane
GGQ11	4600611	-74.933200	40.687962	481.0	318	80	shear plane
GGQ12	4600612	-74.932050	40.687160	446.7	290	66	shear plane
GGQ12	4600612	-74.932050	40.687160	446.7	38	58	shear plane
GGQ13	4600613	-74.930170	40.692680	683.2	22	34	shear plane
GGQ14	4600614	-74.930050	40.692150	670.6	20	30	shear plane
GGQ14	4600614	-74.930050	40.692150	670.6	125	19	slip-lineation
GGQ15	4600615	-74.929860	40.691780	670.6	130	77	fault
GGQ15	4600615	-74.929860	40.691780	670.6	135	33	layering
GGQ15	4600615	-74.929860	40.691780	670.6	165	70	slip-lineation
GGQ16	4600616	-74.929460	40.691030	666.7	128	40	thrust fault
GGQ17	4600617	-74.929610	40.690610	674.6	145	70	shear plane
GGQ17	4600617	-74.929610	40.690610	674.6	105	70	shear plane
GGQ17	4600617	-74.929610	40.690610	674.6	175	29	layering

South-southwest view. The white line highlights the bench that we walk out on.

Southwest view along Musconetcong Mountain from midway along the upper bench noted above

Northeast view of the southeast bench cuts with the southeastern contact of the iron-impregnated shear zone traced with a white line. The numbered points indicate where photos were taken.

Figure 9. Photographs of the quarry. ECM mining engineer Michael Guida looks on.

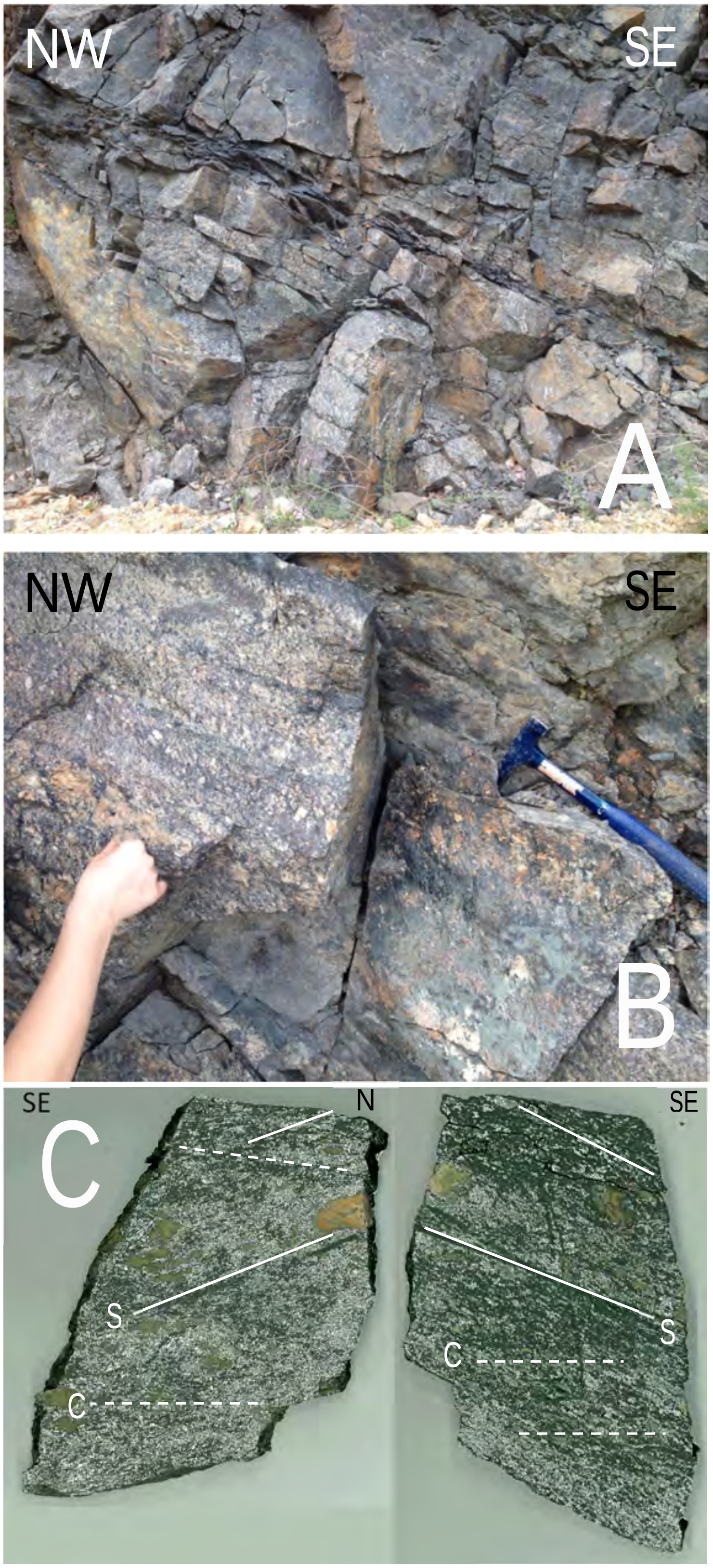

Figure 10. Outcrops near point 2 on fig. 8 showing a gently dipping brittle reverse fault (probable Alleghanian-aged) with reactivated normal slip dipping southeast and sub-parallel to a thick, Grenville-age, iron-rich (magnetite) ductile-brittle shear zone (tectonite).
A. A brittle reverse fault of probable Alleghanian age places dark grayish green pyroxene granite in the hanging wall over a very thick iron-rich tectonite occupying the footwall.
B. A close up of the old tectonite showing compositional layering with large phenocrysts and porphyroclasts including K-spar (pinkish-orange). This footwall sequence is about 20 meters thick and composed of about 20-30% magnetite in places, some of which forms in pressure shadows around siliceous porphyroclasts. This material probably formed deep within the crust (~>12 km) by synchronous magmatic intrusion and shearing between a large, granitic intrusion and older gneiss. Note the cross-cutting, brittle, slickensided shear plane to the left of the letter B with slickenlines pitching steeply to the southeast.
C. Photographs of a slabbed section of the iron-rich tectonite with white graphics emphasizing the SC-mylonite fabric. The area with magnetite is accentuated by adjusting image palette colors for pixels corresponding to magnetite from dark gray to light gray to contrast with the dark green and pink (K-spar) siliceous material.

Relatively fresh bedrock begins in the wall cuts near the red line drawn on figure 8, about one-third of our way to the southeast from where the buses are parked to the southeastern corner of the quarry. Before this, on your left, you can see bench cuts in sedimentary colluvium atop bedrock residuum and regolith as you proceed towards point 1 in figure 9. Here we see well-layered gneiss dipping moderately southeast before crossing the Longwood fault into the more granitic material at stations 2 to 4 (fig. 9). As illustrated above in figure 9C, the contact between the gneiss and granite is the old, magnetite-infused shear zone of Muessig and others (1992). The mining engineer excludes this from aggregate-resource use owing to its anomalously high iron content and specific gravity (density). Muessig and others (1992) geochemical analysis of this material shows Fe_2O_3 levels at about 23%, without providing photographs or further description of the material, other than designating it as a "Magnetite-rich cataclasite." As shown in figure 11, this cataclasite is a thick tectonite having a SC-planar fabric arising from heterogeneous layering and alignment of feldspar-dominated porphyroclasts (S-plane) and a second set of less-pronounced, but penetrative, mineralized (C) planes aligned acutely to layering.

At least two, brittle-deformation phases cross cut this old, ductile-brittle fabric (figs. 10A and B). SC cataclasite can form at mid-crustal depths of 5-10 km as a result of synchronous shearing, brecciating, and recrystallization (Lin, 1999), but these rocks are feldspar dominated and could have formed at deeper crustal levels (Fossen, 2010). Muessig and others (1992) report geochemical dissimilarities in some trace-element concentrations for the respective pyroxene granites, alaskite, and cataclasite, but only a few geochemical analyses were reported for representative samples of each metamorphic body, and it's probably more than coincidental that this iron deposit lies at the contact between the large igneous body of pyroxene alaskite and granite continuing southeast of the shear zone in contrast with the large body of country gneiss in the footwall to the northwest; that is, it's likely that the iron-impregnated shear zone formed during synchronous emplacement of the granite and deep crustal shearing occurring deep within the roots of the Grenville Orogen. The immiscibility of iron and silica within crustal melts is well known (Phillpotts, 1979), and this deposit either represents deep crustal fractionation of immiscible liquids during granitic emplacement into gneissic crust with synchronous shearing, crystallization and brecciation, or as Rich Volkert suggests,[1] it may be a mid- to upper crustal brittle fault of Grenville age that developed within a precursor, iron-laden metamorphic layer. The nature of this unusual iron deposit could benefit from a more thorough petrologic investigation, and serve as a key for understanding the petrogenesis of other magnetite deposits in the Reading Prong.

[1] Personal communication July 6th, 2015

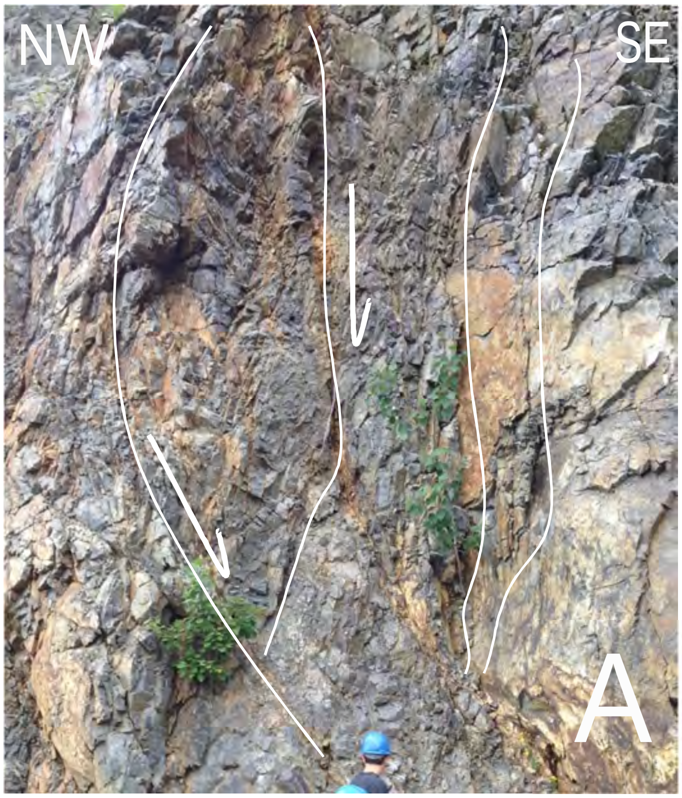

Figure 11. Photos taken near points 3 and 4 on figure 9.

A. Steeply dipping normal faults of probable Mesozoic age have branching and anastomosing fault geometry with fault blocks bounded by slickensided shear planes.

B. Electric-blue chrysocolla, a hydrated copper cyclosilicate mineral ($(Cu,Al)_2H_2Si_2O_5(OH)_4 \cdot nH_2O$) occurs on steeply dipping extension fractures striking north to northeast, the same joint sets commonly mapped in the Newark Basin (Herman, 2009).

C. Photomicrograph at about 20X of botryoidal microcrystalline silica atop greenish chrysocolla with an unidentified rusty mineral.

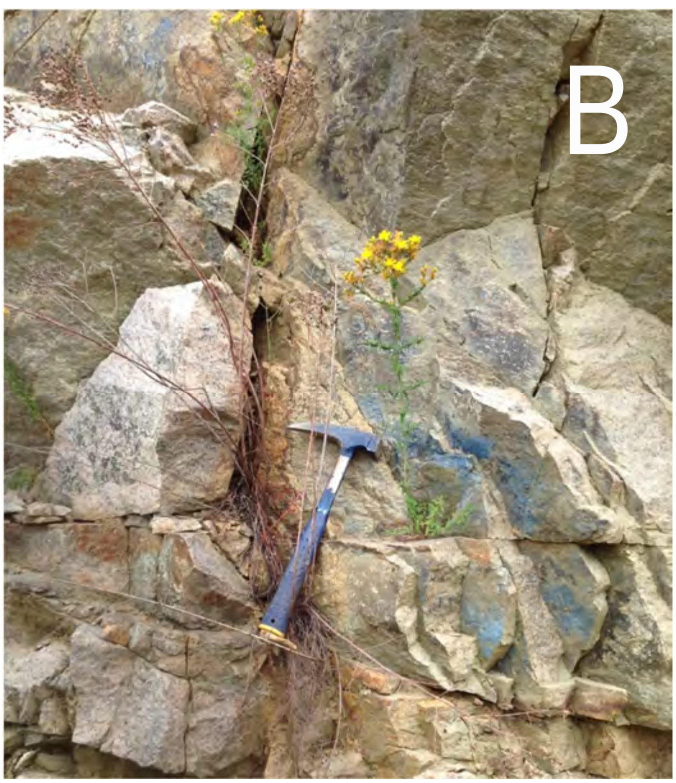

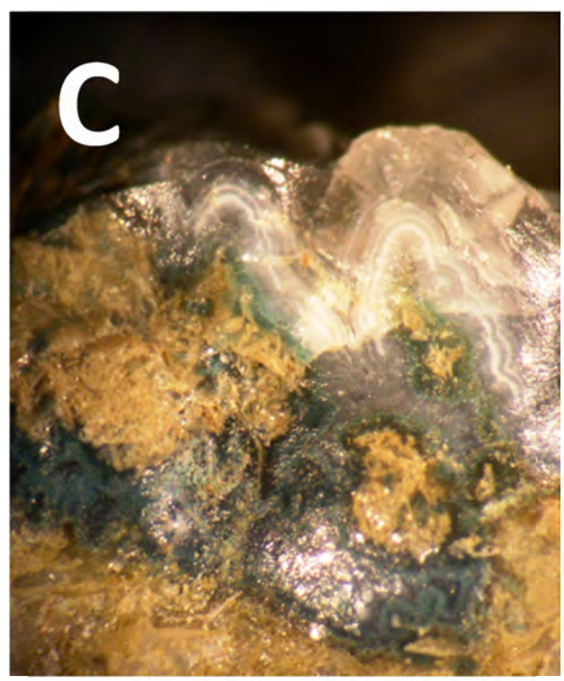

Other, gently dipping, ductile-brittle, shear zones having SC fabric occur further along in these cuts (fig. 12A) that strike sub parallel to the SC cataclasite. These older shear zones are

Figure 12. Outcrops along the upper bench near point 3 (fig. 9) on the Northeast cut face.

A. Probable Grenville-age (Precambrian) ductile-brittle shear zones cutting pyroxene alaskite. These shear zones also have anastomosing (SC- tectonite) fabric and, iron-rich (chloritic) shear planes showing top-to-the-left (northwestern-directed) synthetic shearing.

B. Brittle shear zone of probable Alleghanian (late Paleozoic) age reverse (thrust) fault with reactivated, probable Mesozoic, dip-slip to the southeast. Mike Castilli of the NJGWS provides a scale.

then cut by younger, southeast-dipping, brittle reverse faults (fig. 10A and 12B) of probable Paleozoic age. Lastly, the brittle reverse faults that we see here are both reactivated with normal slip and interact with steeply-dipping normal and oblique-slip shear planes that together (figs. 10B and 12) comprise a cross-strike transtentional fault system as portrayed in figures 5 and 7C, and further described in a regional perspective in Chapter 4. As we will see in the BTV-based cross section below, this type of penetrative, brittle fracturing and shearing occurs on penetrative sets fault blocks that take on a rhombohedral-form through the interaction of faults and extension fractures of both synthetic (SE) and antithetic (NW) dips. A schematic portrayal of the angular shear and shear sense that metamorphic layering sustains from these distributed strains, at the scale of the outcrop, are characterized below using the structural results of the two BTV surveys in the quarry wells used to monitor the water table (fig. 8 and Table 1) allows the crust to stretch and sag during continental rifting.

Borehole Televiewer (BTV) study

ECM mining engineer Michael Guida arranged for the NJGWS to log ECM's monitoring wells using our suite of slim-line geophysical equipment in order to assess the framework of this fractured-bedrock aquifer. Michael Gagliano and Michelle Kuhn of the NJGWS collected borehole and fluid electrical, caliper (borehole diameter), natural gamma radiation, and optical borehole imaging logs on June 24, 2014. The well location and construction parameters are listed in table 1. Each record was interpreted by measuring primary metamorphic layering and secondary brittle structures in each borehole image to determine the types and relative densities of the most commonly fracture and fault planes (figs. 13-15). The BTV imagery and structural results were then used to characterize some stratigraphic and structural details of the hydrogeological framework.

Many details surrounding the logging, interpretation, and structural methods used to characterize this fracture-bedrock aquifer surpass the scope of this field report, and additional structural analyses remain to be done on these records. For example, the structural classification and analyses included here stem from an initial interpretation of these records that combines the structural analyses of both wells for the purpose of constructing a representative, a schematic cross-section interpretation (figs. 13-15). Further discrimination between primary and secondary structures in each well and for the different rock type (gneiss and granite) waits, but some interesting geological relationships can be gained from the details shown here. For example, what appears to be good stratigraphic control across the distance of the quarry using a key bed (fig. 13) cannot be simply interpolated between wells based on using a n average mean orientation of metamorphic layering; that is, if one assumes that the marker horizon is the same stratigraphic layer, then there appears to be a significant amount of stratigraphic offset between the wells.

Also, the primary, reverse shear zones are oriented parallel to layering whereas the most frequently occurring shear plane is a normal, synthetic (southeast-dipping) shear plane (fig. 14) Normal reactivated slip seen on the primary, synthetic reverse work appear to have worked together to form a rhombohedral fault pattern like that commonly seen within fault zones in the Newark Basin. The apparent stratigraphic mismatch between the two wells may simply stem from an incorrect identification of two different beds as the same one. However, if the marker bed is indeed the same one, then this implies that the southeastern section here has been structurally elevated with respect to the footwall section which could arise from having intervening, unidentified reverse fault running through this quarry in the footwall of the Longwood fault. As previously mapped (fig. 6), we should have encountered the Longwood Valley and high-iron section in the wells, but we didn't. Our alternative interpretation of the

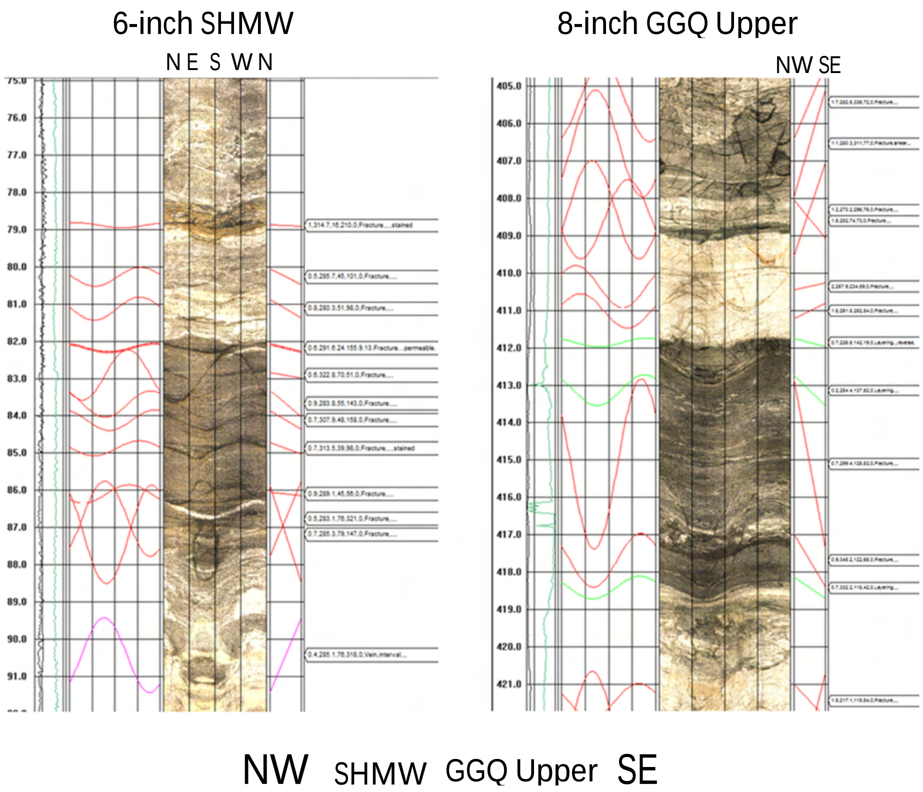

Figure 13. BTV sections from two bedrock wells in the quarry that provide stratigraphic correlation of a metamorphic contact between gneiss (NW) and granite (alaskite SE) for a distance of about 1,040 feet across strike. Well locations are mapped on figure 8.

A. Detailed sections showing unwrapped (flattened) BTV optical records next to their structural interpretations, appearing as sinusoidal line traces of fractures (red), layers (green), and shear-planes (purple).

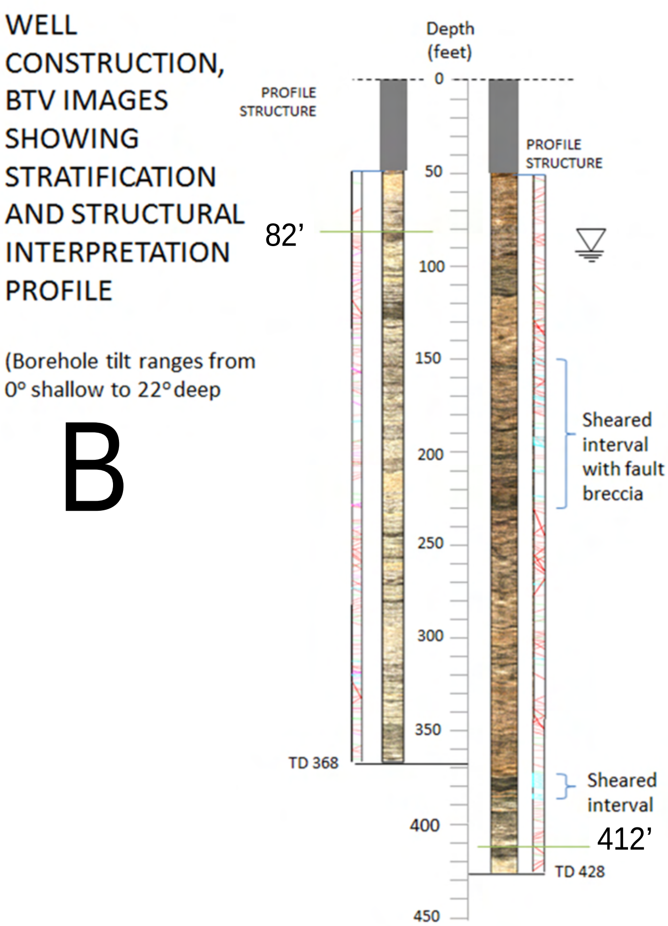

The directions noted above the SHWM BTV record are the same as for the structural interpretation to its left, and for each record. A profile depiction oriented NW-SE is shown to the right of each BTV image. The contact highlighted with the thick black arrow is a marker horizon where a thick amphibolite (darker) layer is sandwiched between quartzofeldspathic gneiss (lighter). Note the many layer-parallel brittle fractures

B. Complete optical BTV records and profile structures reproduced and placed into depth perspective relative to land surface to emphasize the color contrast between footwall gneiss on the left and hanging wall granite to the right (SE). Subsurface fault zones are also noted for the GGQ Upper well.

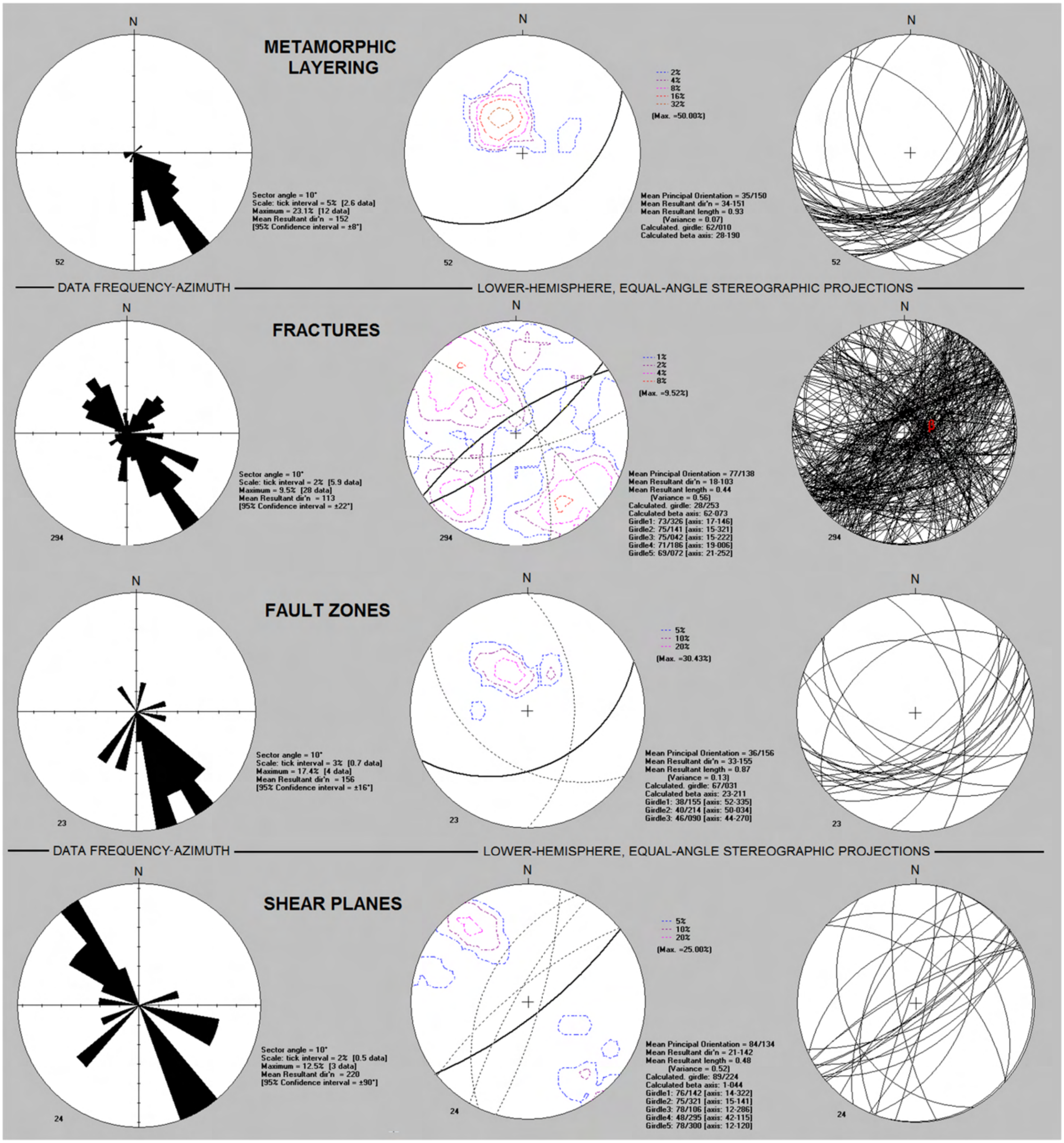

Figure 14. Stereonet analyses of primary (crystalline compositional layering in metamorphic rocks) and secondary fractures, shear planes, and fault zones.

Layering	Shear fractures	Fault zones
35/150 (20%)	76/142 (20%)	38/155
	75/321 (10%)	40/214

Representative structural maximums with the highest percentage of occurrence are used for depicting a schematic cross-section framework of the fractured-bedrock aquifer in figure 15.

Longwood Fault, as shown in figure 8, explains why this happened. The older (1:00000-scale) version of this area didn't take into account the topographic effects on a moderately southeast-dipping fault with respect to the manner in which it deviates from a straight line on the map in coming into and leaving the quarry excavations. The actual fault trace ends up bowing considerably southeast of that previously portrayed and likely crops out in deep levels in the quarry immediately southeast of the GGQ Upper well (fig. 8).

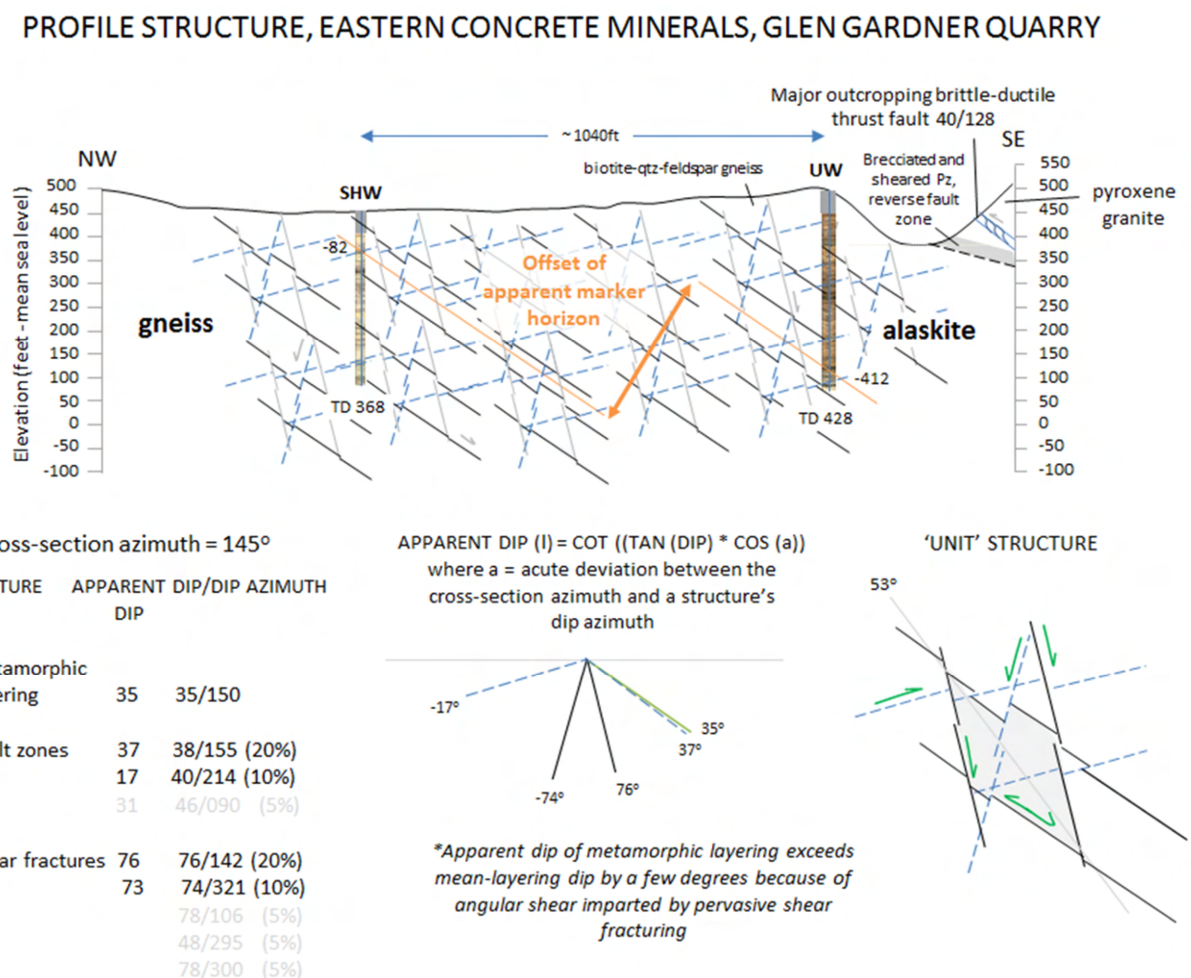

Figure 15. Schematic cross section of the Eastern Concrete quarry showing apparent dips of metamorphic layering with respect to the four principal fault planes measured in the OBI records of the quarry wells. Note the major reverse faults mapped along the SE edge of the site, and the apparent structural offset of a key bed identified in figure 13.

STOP 2. Youngest structural features in the Hopewell fault zone at Mercer County Park, 41 Valley Road, Hopewell Twp., Mercer County, NJ

WATERPROOF BOOTS AND/OR A CHANGE OF SOCKS ARE RECOMMENDED FOR THIS STOP!!

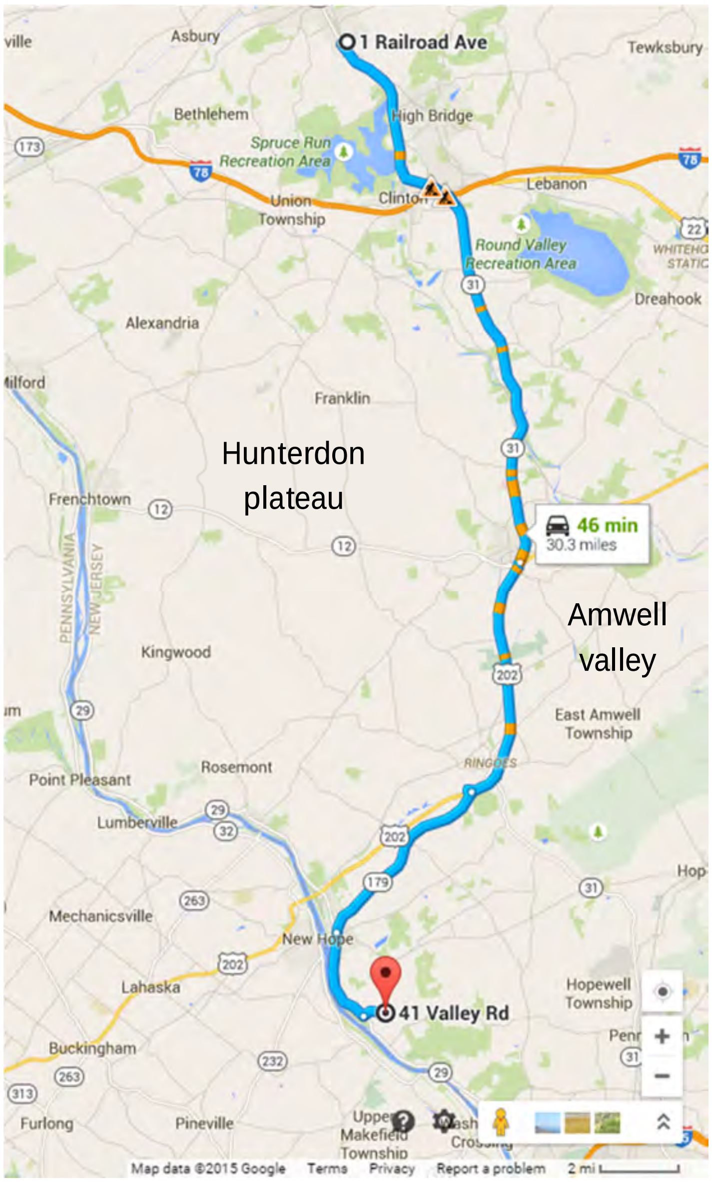

Figure 16. Google maps display of the route from STOP 1 to STOP 2. From Railroad Ave in Glen Gardner take Route 31 South to Route 202 South at Flemington towards, then Route 179 South to Valley Road.

In leaving the Glen Garner quarry, we proceed south along NJ Route 31 South to US Route 202 South towards Lambertville, NJ and STOP 2 at 41 Valley Road (fig. 16). We are using Mercer County Park at Valley Road (fig. 17) for STOP 2 and lunch afterwards. STOP 2 is a traverse in and along the stream running alongside the western side of the park. After this hike, we get out of the stream bed near the pavilion for lunch. Afterwards, we'll drive a very short distance to STOP 3 to collect some minerals in Trap Rock Industries (TRI) Moore's Station quarry.

The route from STOP 1 to STOP 2 crosses the boundary between the Highlands and Piedmont physiographic provinces that correspond with the system of border faults separating crystalline uplands of the Reading Prong from shale lowlands of the Newark Basin. After crossing the border fault near Clinton, NJ, we drive south along the Flemington fault system. To your right is the Hunterdon Plateau, an upland propped up by the relatively resistant, indurated black, gray and red argillite of the Lockatong Formation, a thick, deep-lacustrine mud rock deposited in deep lakes within the subsiding Newark rift basin. This unit was once deeply buried and has been uplifted or structurally inverted to its present position sometime after it was deposited and buried during the Triassic period. Beneath you and to your left, red shale of the Passaic Formation underlies most of the Amwell Valley in the hanging-wall block of the Flemington fault.

We take the NJ Route 29 (Lambertville-Stockton) exit off of US Route 202, and proceed about 3.5 miles South on Daniel Bray Highway (NJ Route 29) to Valley Road. We turn left onto Valley Road and drive east for ~0.8 miles to 48 Valley Road. The park entrance will be on your right (fig. 17A). Figure 17B shows the pavilion where we end STOP 2 and assemble for lunch.

Figure 17. Photographs of Mercer County Park

A. Entrance looking south from Valley Road.

B. South view of the picnic area just beyond the park entrance. The stream runs North to South in the tree line to the right (west).

Figure 18 details the bedrock geology in the area and places STOPS 2 and 3 in perspective with the Hopewell fault system. As seen in figures 18 -20, the main traces of the Flemington, Hopewell, and Furlong faults are highlighted to show how they branch, splay, and interconnect as part of an intrabasinal *fault system*.

STOP 2 is a walk within and along the creek bed of a tributary to Moore's Creek that cuts across the main Hopewell fault trace and reveals the many complexities surrounding the Hopewell fault system (figs. 21 and 22). Prior versions of the 1:100,000 –scale bedrock geology (figure 18; Owens and others, 1998) have lately been modified based on more recent detailed mapping at the 1:24,000 scale (figs. 20-22). This year's conference highlights this recent work and ties together strata and structures across the river into Buck's County Pennsylvania (fig. 19) with a new interpretation that includes LiDAR hill-shaded imagery (fig. 19 and /www.ganj.org/2015/Data.html). With these updates, mismatch stratigraphic units across the river have tentatively been resolved, and more accurate depictions of the fault system are available for review and interim use in GE (www.ganj.org/2015/Data.html).

STOP 2 begins by crossing Valley Road and entering the tributary on the North side of the bridge abutment. Lockatong argillite is exposed intermittently in the stream here that strikes at high angles to the fault trace and dips steeply west (figs. 21-22). It can be difficult to see bedding in these rocks for they are highly fractured and strained. Our primary goal is to proceed as quickly and quietly as we can up the stream for about 500 meters, while keeping mindful of the slippery rock conditions. There will be a few places where you will need to cross the shallow and intermittently flowing stream to proceed among the bank flora.

Our destination is a series of ~1-meter high benches and bedrock ridges running parallel to the stream that show late-stage, cross-cutting compressional structures discordantly cutting and offsetting all earlier fault, bed, and fold structures (fig. 23). This sequence of Lockatong beds is probably a middle section of the roughly, 2000-ft thick argillite sequence of the Lockatong Formation (fig. 20). The member exposed here has not been determined. One can best see sedimentary bedding on the joint faces striking normal to the stream when looking North (upstream). Many primary sedimentary features are apparent including mud cracks and other desiccation features within dark- and light-gray, red, and tan argillite that is severely fractured.

The benches and ridges that we focus on dip about 45^{o}W and spatially bracketed by the more steeply dipping beds to the SE (~65^{o}W) and more gently dipping beds to the NW (~22^{o}NW). Regional, gentle dips less than 20^{o}NW occur at a distance of over 600 meters from the trace of the Hopewell fault into the footwall block to the NW, and attests to the distributed, penetrative nature of the strain along this complex fault system (figs. 21-22). In addition to the late-stage (neotectonic?), folded joints, we also see brittle deformation zones occurring from isolated fault splays striking parallel to the main trace of the Hopewell fault here (~N40E) and other later-stage faults generally showing southeastern to eastern normal and oblique slip (figs. 20-24).

The late-stage structures are small and upright, but moderately plunging crenulations and mineral veins in bedrock (figs. 23-24) that qualify, from my perspective, as the relatively youngest tectonic structures seen in Triassic rocks. They have not been absolutely dated;

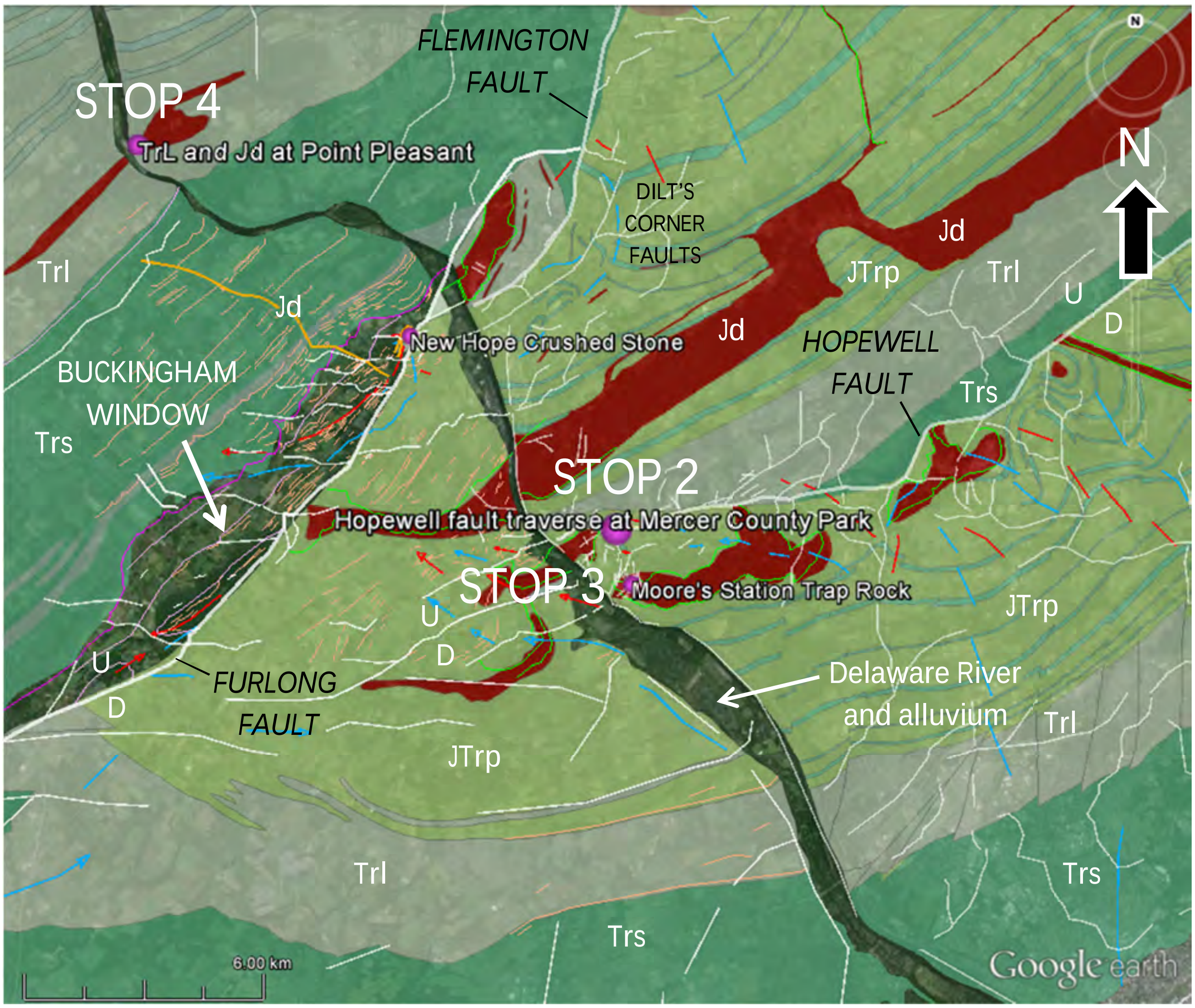

Figure 18. GE map showing the integrated USGS bedrock geology of the Delaware River valley near STOPS 2 and 3 and the confluence of the Flemington, Furlong, and Hopewell faults. Lower Paleozoic carbonate and quartzite crop out in the Buckingham window, whereas the course of Delaware River is covered by water and alluvium. The colored and white line traces are structural interpretations that used LiDAR hill-shaded imagery, as shown in figures 19 and 22. Line colors: Green – contacts, Tan - bedrock ridges, Red – anticline, Blue – syncline, White - faults. Note the varying fault interpretations in the lower right hand corner between prior and revised interpretations. Jd – Jurassic dolerite, JTrp – Passaic Formation, Trl – Triassic Lockatong Formation, Trs – Triassic Stockton Formation. The darker-green striping in the Lockatong and Passaic Formation are gray-bed sequences.

however, as shown here, they cross-cut all other structures and fold pre-existing extension fractures (joints). The simple fact that they are discordant structures that plunge the opposite direction from encompassing, large bed flexures and folds in Triassic bedrock, suggests that these features stem from a completely different stressor, one seemingly reflective of a crustal contraction event directed about N-S.

After spending about ½ hour at the northern end of this traverse (fig.22 location A) we return back down the stream, and either walk under the bridge, or if the stream flow is too high, go up and over the bridge to continue southward in the creek to see fault-proximal Lockatong gray breccia and sheared red shale of the Passaic Formation (fig. 22 traverse B). Immediately after passing under the bridge, brecciated and tectonized gray argillite of the Lockatong Formation is seen in about a 20-meter span, before crossing over the concealed Hopewell fault and further on to fractured red beds of the Passaic Formation (fig. 24). This section of sheared red mudstone is a middle section of the Passaic Formation about 11,000-foot thick in the region (fig. 20). As for the footwall at location A, the formation member here is undetermined.

The most noticeable features in the first outcrops of red beds that we see are the network of brittle, steeply-dipping, slickensided shear planes that form irregular faces paralleling the stream banks dip steeply (fig. 24A). The planes are mineralized with streaks of green epidote and chlorite, and white calcite that are streaked with slickenlines plunging gently to moderately east to northeast. Bedding is difficult to see here, as the fracturing is dominant and causes the red beds to break and spall into the creek. Be careful when hammering these rocks, especially with other people around you as they can easily spill into the creek and onto feet in a crowd. Figure 24B shows the next outcrop located about 50 m south along the creek bed, but these outcrops are commonly overgrown or laden with debris from storms, so we will probably not venture beyond the first set of red beds before climbing up the eastern bank of the creek and heading over to the pavilion for lunch.

An MS-Excel worksheet including field stations, their spatial coordinates, and measured structures for this area is available at www.ganj.org/2015/Data.html. This worksheet covers the area of STOPS 2 and 3 and contains 256 structural readings, geospatial coordinates in WGS84 decimal degrees, and lists of structural attributes. Three-dimensional (3D) planar objects were plotted in GE, where they were measured in outcrop using the same methods as outlined for STOP 1. Figures 21 and 22 show the results of generating 2D bed symbols and 3D planes representing igneous compositional layering (pink) and faults (red) and using them in GE to help map geological structures.

For lunch, we will take about 45 minutes to eat and cleanup before heading back to the bus for departure to STOP 3.

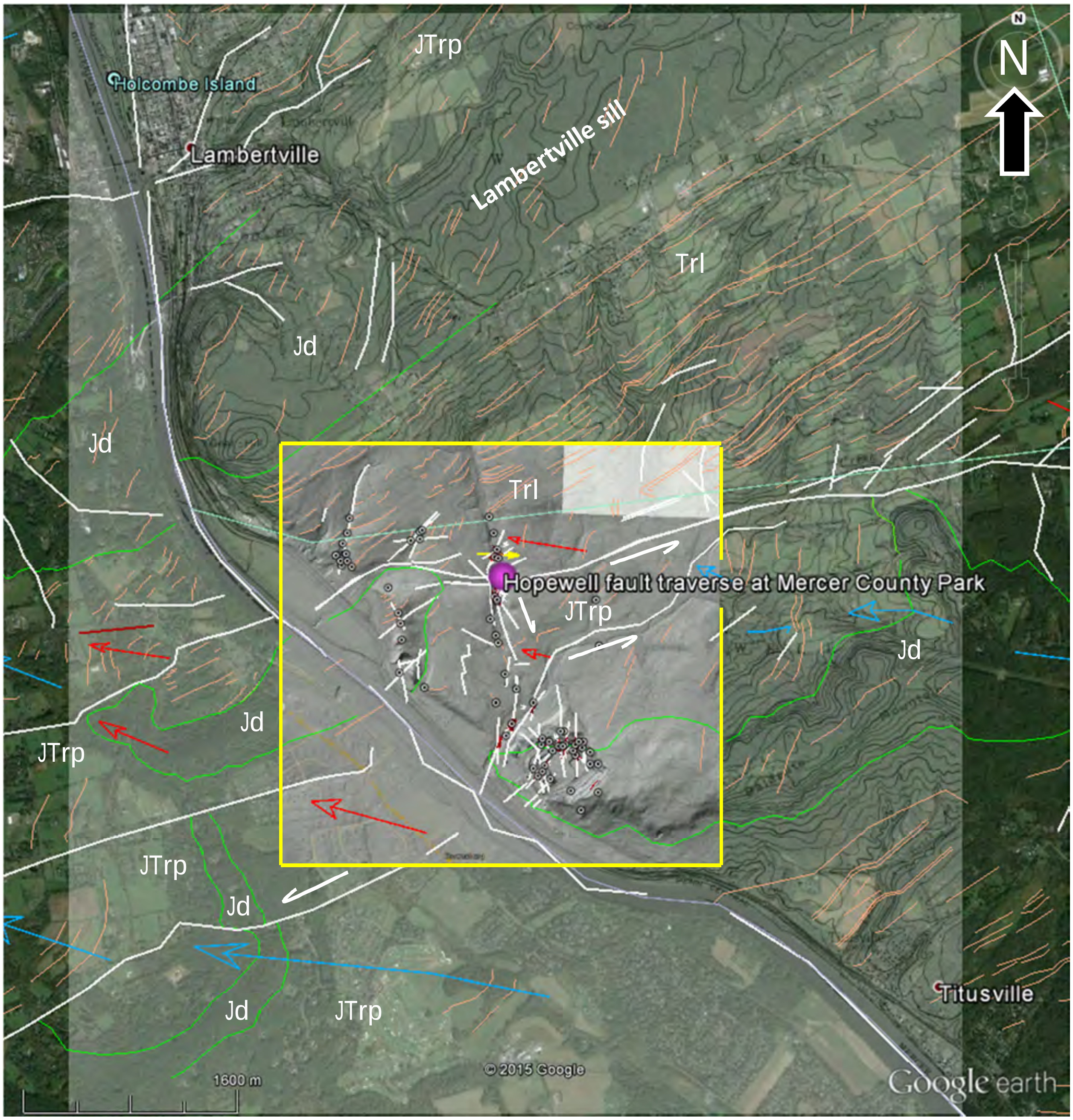

Figure 19. GE map of the area of focus for STOP 2 and 3 showing PASDA LiDAR hill shade imagery and geological interpretations, including structural details of component faults within the Hopewell fault system. Note the apparent stratigraphic offset of the sedimentary contact with trap rock (green lines) across the Delaware River and the likelihood of having river-parallel shear fractures accounting for the offset. Unit abbreviations and line colors are the same as those noted in figure 18.

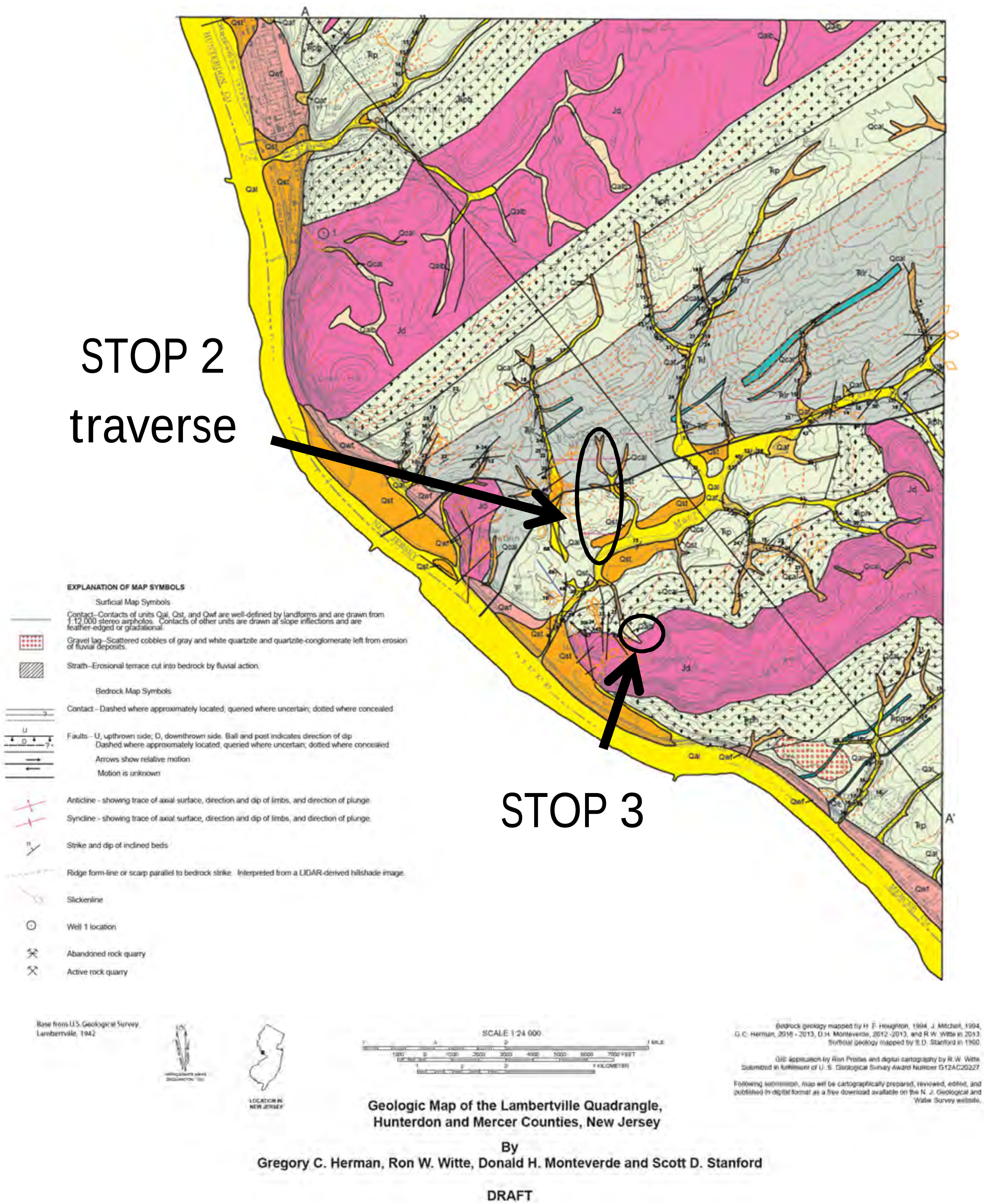

Figure 20. Excerpt from part of the draft, open-file NJGWS 1:24,000-scale Geological Map of Lambertville Quadrangle, showing the locations of STOPS 2 & 3. Unit legend is on opposite page.

DESCRIPTIONS OF MAP UNITS

Qal

Alluvium -- Silt, pebble-to-cobble gravel, minor fine sand and clay. Moderately to well-sorted and stratified. Contains minor amounts of organic matter. Color of fine sediment is reddish-brown to brown, locally yellowish-brown. Gravel is dominantly flagstones and chips of red and gray shale and mudstone with minor pebbles and cobbles of basalt, diabase, sandstone, and hornfels. Silt, fine sand, and clay occur as overbank deposits on floodplains along low-gradient stream reaches. Overbank silts are sparse or absent along steeper stream reaches. Gravel is deposited in stream channels and is the dominant floodplain material along steeper stream reaches. Flagstone gravel typically shows strong imbrication. As much as 10 feet thick.

Qalb

Alluvium and boulder lag -- Silt, sand, minor clay and organic matter, dark brown, brown, yellowish-brown, reddish-yellow, moderately sorted, weakly stratified, overlying and alternating with surface concentrations (lags) of rounded to subrounded diabase (and, in places, hornfels) boulders and cobbles. As much as 10 feet thick (estimated). Formed by washing of weathered diabase and hornfels by surface water and groundwater seepage.

Qcal

Colluvium and alluvium, undivided -- Interbedded alluvium as in unit Qal and colluvium as in unit Qcs in narrow headwater valleys. As much as 10 feet thick (estimated).

Qaf

Alluvial fan deposits -- Flagstone gravel as in unit Qal and minor reddish-brown silt and fine sand. Moderately sorted and stratified. As much as 15 feet thick. Form fans at mouths of steep tributary streams.

Qst

Stream-terrace deposits -- Silt, fine sand, and pebble-to-cobble gravel, moderately sorted, weakly stratified. Deposits in the Neshanic River basin are chiefly reddish-yellow to reddish-brown silt with minor fine sand and trace of red and gray shale, mudstone, and sandstone pebble gravel, and are generally less than 10 feet thick. They form terraces 5 to 10 feet above the modern floodplain and are likely of late Wisconsinan age. Deposits along the Delaware River are chiefly yellowish-brown silt and fine sand as much as 25 feet thick that form a terrace 15 to 20 feet above the modern floodplain. They rest on a strath cut into the glaciofluvial gravel (unit Qwf) and so are of postglacial age. Deposits along Wickecheoke Creek are dominantly flagstone gravel and minor reddish-brown silt and fine sand. They are as much as 15 feet thick and form terraces 5 to 10 feet above the modern floodplain. They are likely of both late Wisconsinan and postglacial age.

Qe

Eolian deposits -- Silt and very fine-to-fine sand, reddish yellow. Well-sorted, nonstratified. As much as 5 feet thick. These are windblown deposits blown from the glaciofluvial plain in the Delaware River valley.

Qwf

Glaciofluvial deposit -- Pebble-to-cobble gravel and pebbly sand, moderately to well-sorted and stratified. Sand is yellowish-brown, brown, light gray. Gravel includes chiefly red and gray mudstone and sandstone, gray and white quartzite and conglomerate, and some gray and white gneiss, dark gray chert, and dark gray diabase. As much as 40 feet thick. Forms an eroded plain in the Delaware River valley with a top surface about 35-40 feet above the modern floodplain. Deposited by glacial meltwater descending the Delaware River valley during the late Wisconsinan glaciation.

Jd

Diabase (Lower Jurassic) -- Fine-grained to aphanitic dikes (?) and sills and medium-grained, discordant, sheet-like intrusion of dark-gray to dark greenish-gray, sub-ophitic diabase; massive-textured, hard, and sparsely fractured. Composed dominantly of plagioclase, clinopyroxene, and opaque minerals. Contacts are typically fine-grained, display chilled, sharp margins and may be vesicular adja-cent to enclosing sedimentary rock. Exposed in map area in sills, southeast of Stockton and east of Lambertville, and in the Sourland Mountain diabase sheet on the southern edge of the mapped area. This sheet may be the southern extension of the Palisades sill. The thickness of the Rocky Hill diabase in the quadrangle, known mainly from drill-hole data, is approximately 1,325 feet.

JRp

JRpg

JRph

Passaic Formation - (Lower Jurassic and Upper Triassic) (Olsen, 1980) - Interbedded sequence of reddish-brown to maroon and purple, fine-grained sandstone, siltstone, shaly siltstone, silty mudstone and mudstone, separated by interbedded olive-gray, dark-gray, or black siltstone, silty mudstone, shale and lesser silty argillite. Reddish-brown siltstone is medium- to fine-grained, thin- to medium-bedded, planar to cross-bedded, micaceous, locally containing mud cracks, ripple cross-lamination, root casts and load casts. Shaly siltstone, silty mudstone, and mudstone form rhythmically fining upward sequences up to 15 feet thick. They are fine-grained, very-thin- to thin-bedded, planar to ripple cross-laminated, fissile, locally bioturbated, and locally contain evaporate minerals. Gray bed sequences (JRpg) are medium- to fine-grained, thin- to medium-bedded, planar to cross-bedded siltstone and silty mudstone. Gray to black mudstone, shale and argillite are laminated to thin-bedded, and commonly grade upwards into desiccated purple to reddish-brown siltstone to mudstone. Thickness of gray bed sequences ranges from less than 1 foot to several feet thick. Several inches of unit have been thermally metamorphosed along contact with Orange Mountain Basalt (Jo). Thicker thermally metamorphosed sections(JRph) exist on the southern flank of Sourland Mountain, on the southern part of the mapped area. Unit is approximately 11,000 feet thick in the map area.

Rl

Rlr

Lockatong Formation (Upper Triassic) (Kummel, 1897) - Cyclically deposited sequences of mainly gray to greenish-gray, and in upper part of unit, locally reddish-brown siltstone to silty argillite (Rlr) and dark-gray to black shale and mudstone. Siltstone is medium- to fine-grained, thin-bedded, planar to cross-bedded with mud cracks, ripple cross-laminations and locally abundant pyrite. Shale and mudstone are very thin-bedded to thin laminated, platy, locally containing desiccation features. Lower contact gradational into Stockton Formation and placed at base of lowest continuous black siltstone bed (Olsen, 1980). Maximum thickness of unit regionally is about 2,200 feet (Parker and Houghton, 1990).

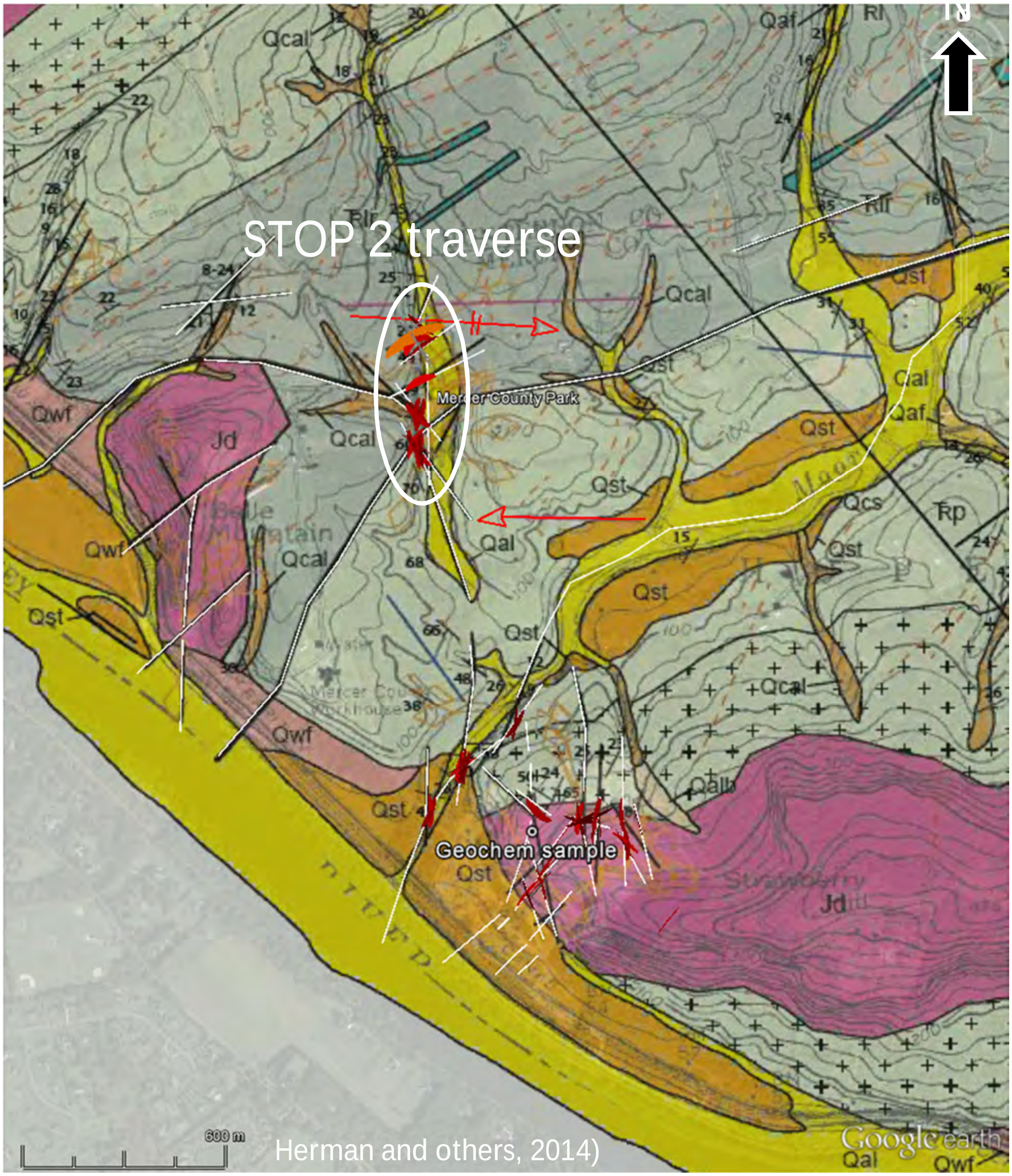

Figure 21. Part of the NJGWS Lambertville Geological Map (fig. 20). A JPEG version of the Open-File, digital map was register in GE and is shown here with traces of faults (white lines) digitized in GE, and 3D fault that are portrayed using 100 x 50 m red ellipses (collada 3D circle object model s scaled with a 2:1 strike:dip aspect ratio). *Note* the faint, pink line on the map below the words 'STOP 2 traverse' is the draft version of the late-stage fold trend. The map legend key is included on figure 20.

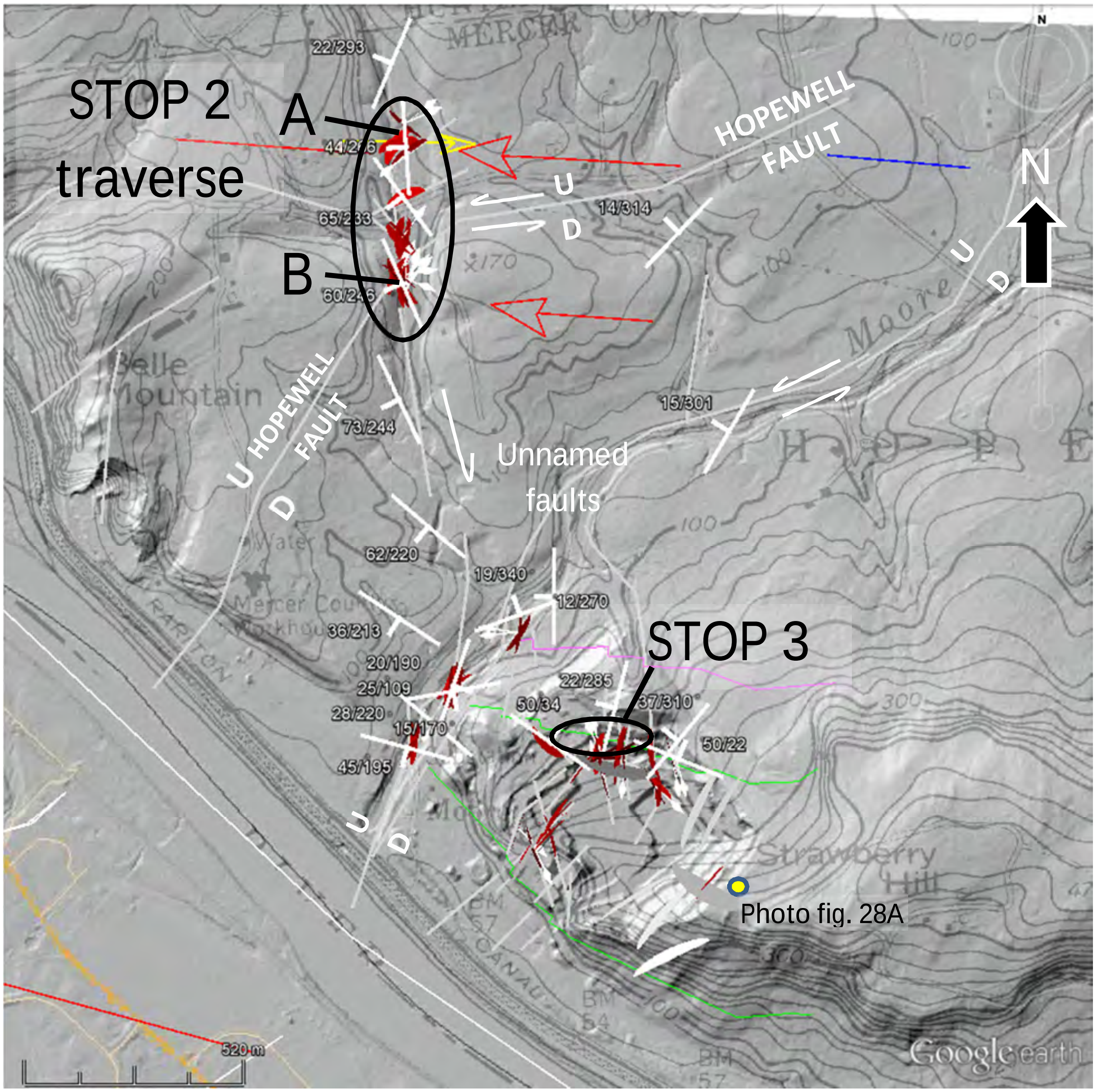

Figure 22. GE display of the area covering STOP 2 and 3. A PASDA LiDAR, gray, hill-shaded image is overlain by a monochromatic, 1:24,000-scale, Lambertville, NJ-PA 7-1/2’ USGS topographic quadrangle set at 50% transparency. The topography reflects old quarry activity on the west end of Strawberry Hill, with more recent bench cuts visible south of STOP 3. The upper contact of the Jd sill with superjacent Passaic Formation hornfels dips gently to moderately northwest in contrast with the steep-southeast-dipping compositional layering in the trap rock. White bed symbols use dip/dip azimuth notation. 3D colored disks are measured faults (red) and compositional layering (gray).

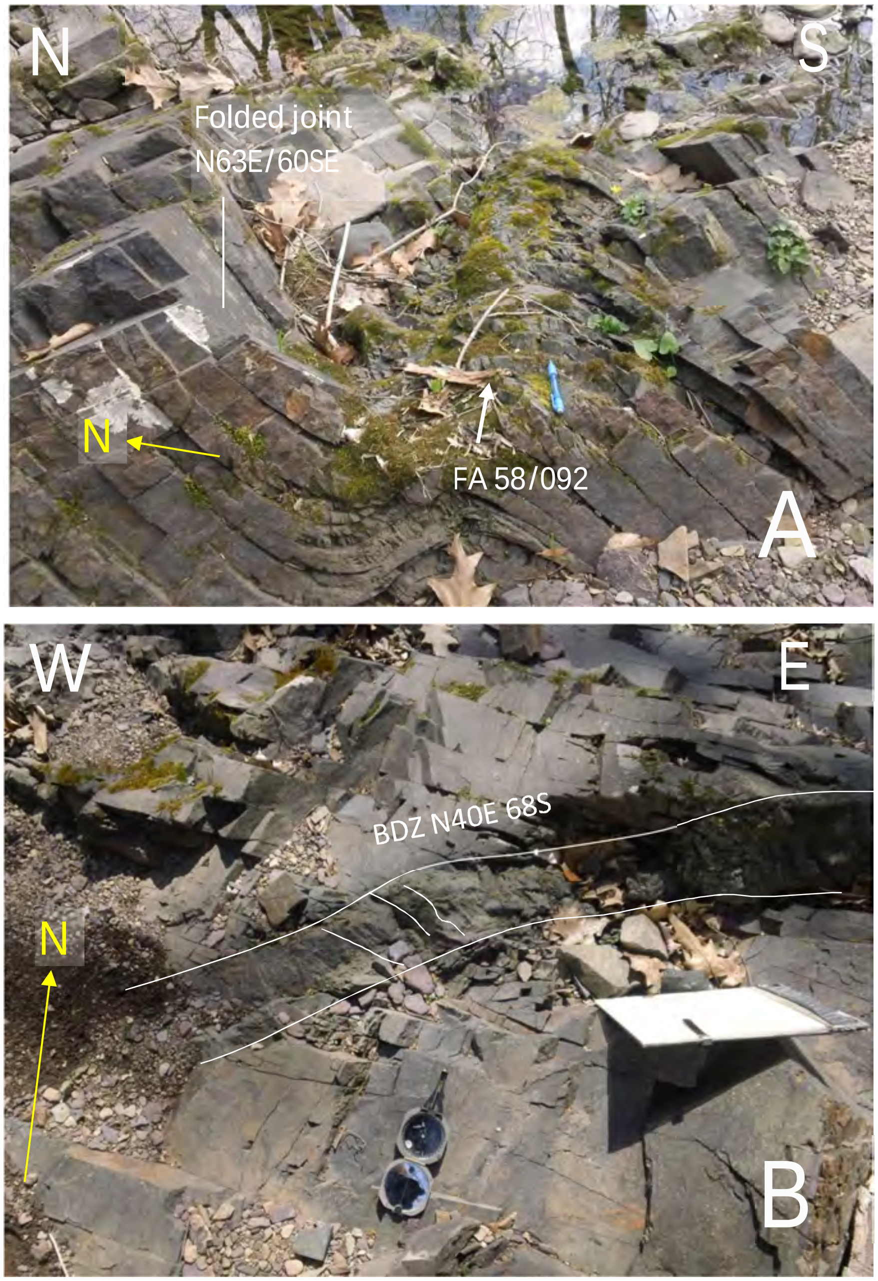

Figure 23. Outcrops near point A in figure22 in the footwall of the Hopewell fault.

A. Folded joints generally striking N63E/60-65 SE with small anticline-syncline pair plunging moderately eastward and opposed to westward-plunging bed folds (fig. 22). Note small shear faults showing bed duplication and contraction in the core of the anticline and associated, localized fracture cleavage. Bedding in the view is dipping 47° W toward the viewer and is not apparent.

B. Bed-discordant brittle deformation zones of S1 fault orientation (Herman, 2009) have shear morphology involving localized, band-normal fracturing showing a component of left-lateral (sinistral) slip.

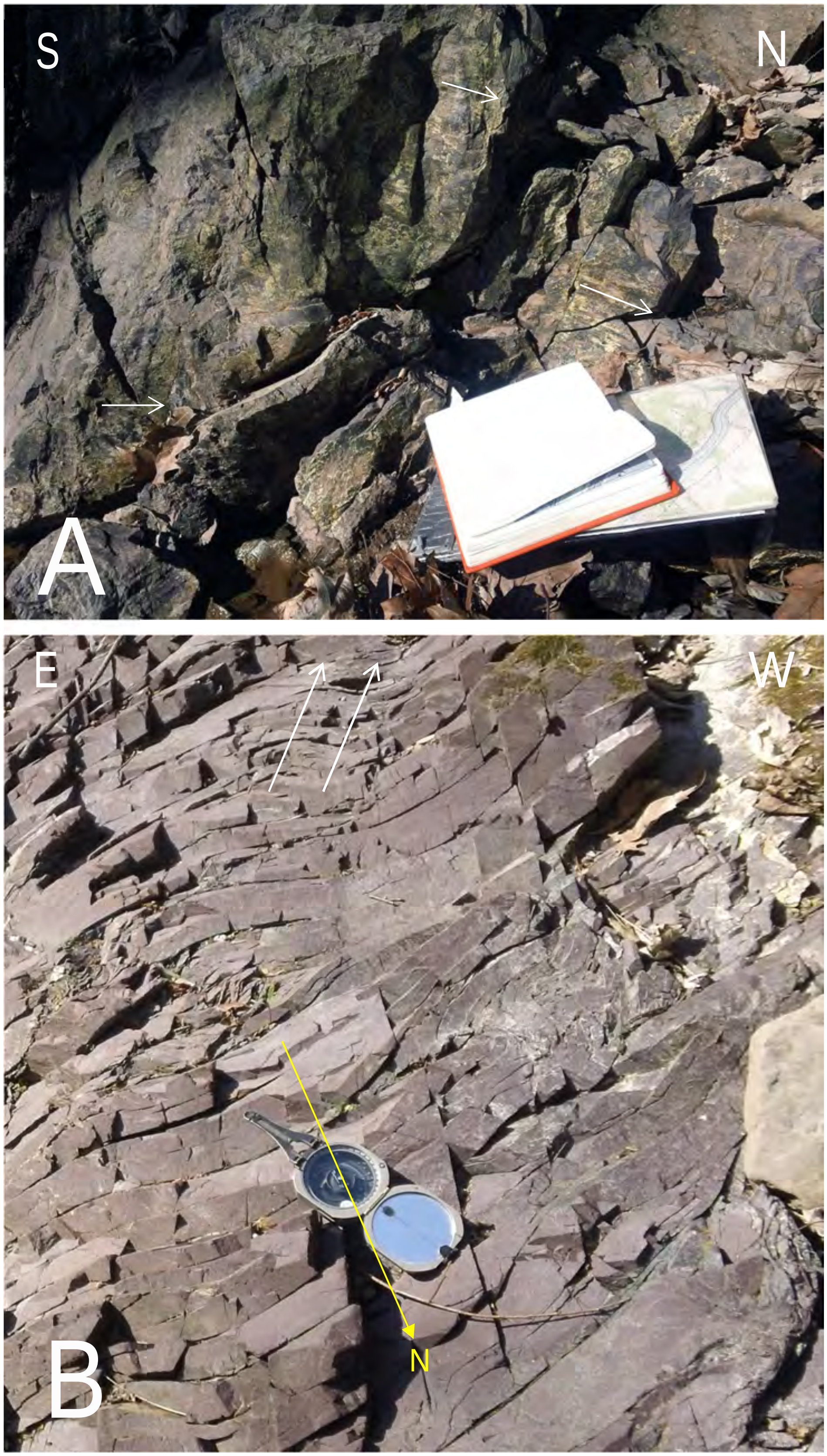

Figure 24. Outcrops of fractured and sheared red mudstone of the Passaic Formation. These outcrops are the first seen in the hanging-wall fault block and show complex incremental strains including slickensided shear planes with calcite (white) and epidote (green) mineralization.

A. Folded and compressed joint sets.

B. Slickenlines show left-lateral and normal oblique slips plunging shallow NE to SE (see fig. 22 STOP 2B).

STOP 3. Trap Rock Industries, Moore's Station Quarry

The quarry is located only about 5 minutes away from the park (fig. 25). We return to NJ Route 29 and head southeast for about a mile. The entrance of TRI's Moore's Station Quarry will be on our left. As a reminder:

HARD HATS ARE REQUIRED THERE, AND THERE WILL BE NO DIRECT CONTACT WITH HIGH WALLS IN THIS ACTIVE QUARRY.

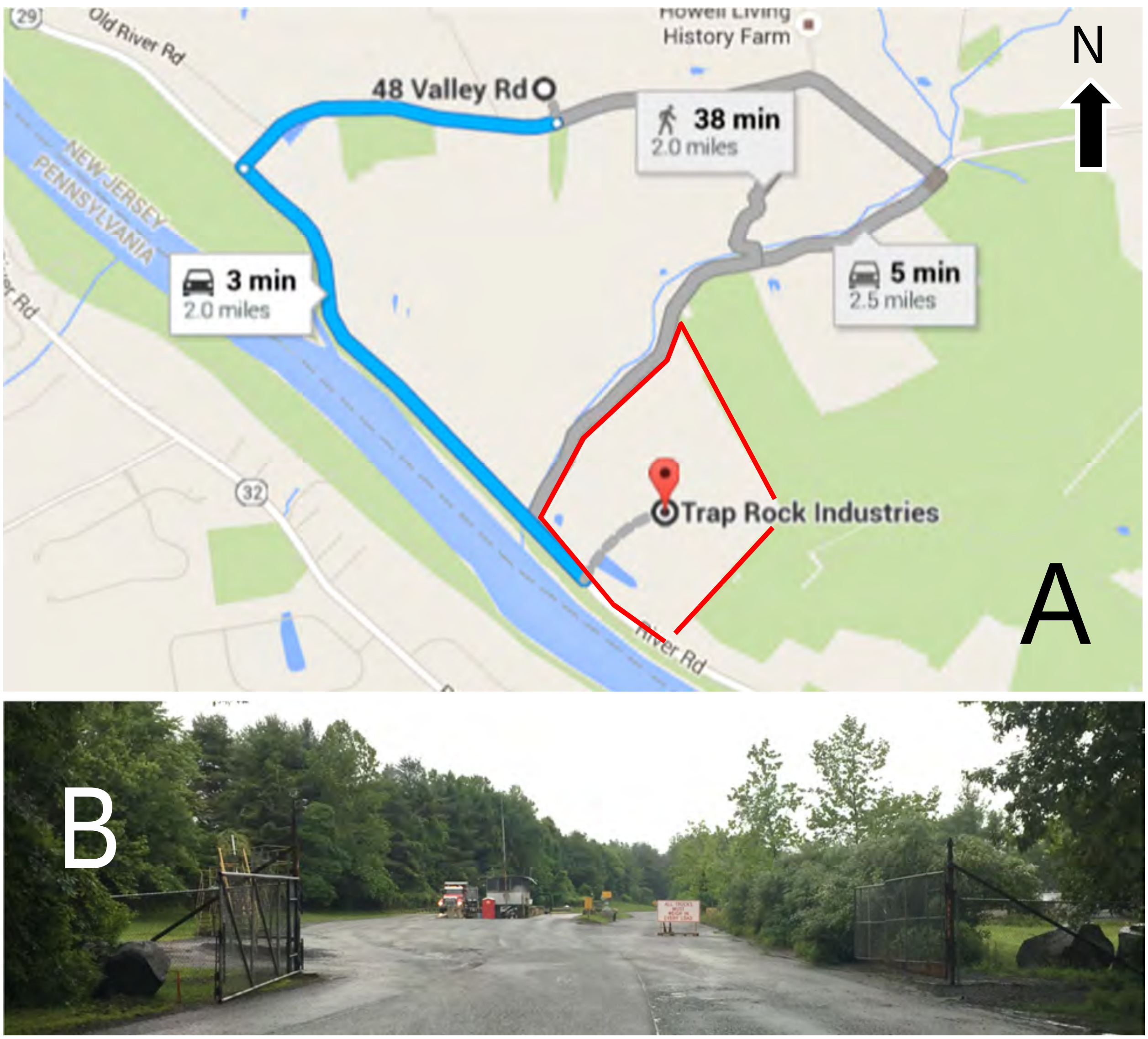

Figure 25. A. The route from Mercer County Park at 48 Valley Road to Trap Rock Industries' Moore's Station quarry. The Moore's Station quarry parcel is outline in red. B. Photo of the quarry's entry gate.

This STOP will be a relatively quick drive through – more a sight-seeing tour with one mineral-collecting opportunity near point B (fig. 27). It is expected that this STOP should take about 30 minutes. This quarry has thick, excavated exposures of red-bed hornfels (fig. 28) that rival anything that seen in the New Jersey part of the Newark Basin. This quarry is developed in the west end of the Baldpate Mountain dolerite body (figs. 18-22) in a manner reported by Herman and others (2013) as part of their work in detailing the plumbing geometry of the complex system of intrusive bodies in the center of the basin that are part of the Central Atlantic Magmatic Province (CAMP; Marzoli and others, 1999).

The Moore's Station quarry has a long and storied history. According to Mindat.org, an on-line Mining and minerals database:

> *"This is a large quarry located at the northwest end of Baldpate Mountain, adjacent to Rt. 29 and Pleasant Valley Road. It is very near the Delaware River. The quarry was abandoned in 1932, the same year the nearby Delaware and Raritan Canal went out of business, and lay dormant for 50 years. It was reactivated by Trap Rock Industries in 1982 and called the "Moore's Station Quarry. …This quarry is cut by splays from the Hopewell Fault. Some of the common members of the prehnite - zeolite mineral assemblage, typical of the New jersey trap rocks are present although significant collecting has not been possible in the large scale, industrial atmosphere that prevails at this site."*

According to correspondence from Mercer County addressed to the NJ Water Supply Authority (on file at the offices of the NJGWS), the County purchased the 166-acre property from TRI, Inc. subject to the stipulation that TRI retains the right to continue quarrying activities for a period of 25 years, terminating in 2022. The property is currently part of the 1,200-acre regional nature area and passive recreation park known as the Ted Stiles Preserve at Baldpate Mountain. The County is in the early stage of planning for future recreation use of this site, and evaluations are underway to see if this site might fit into New Jersey's future reservoir needs. A seen in figure 28A, the quarry is very deep, with over 6 benched levels and a range in elevation of about 120 m (~400 feet) from the nearby uplands on Baldpate Mountain down to the floor (~0m elevation). Current estimates are that the quarry is capable of holding about 2 billion gallons of water (written communication from Mercer County Division of Planning to the New Jersey Water Supply Authority dated 04-29-2015 on file at the NJGWS.).

As we drive into the main quarry area, we see the northeast wall in the distance, and the structural arrangement of the igneous layering relative to the overlying hornfels, as pictured in figure 28. A 3D display in GE of the igneous layers, sedimentary beds, and steeply dipping normal- and oblique-slip faults measured in outcrop within and around the quarry is shown in figure 27B. The Early Jurassic dolerite is steeply dipping to the right in the NE wall and the hornfels dip gently northwest and to the left. The dominant fracture pattern seen in the

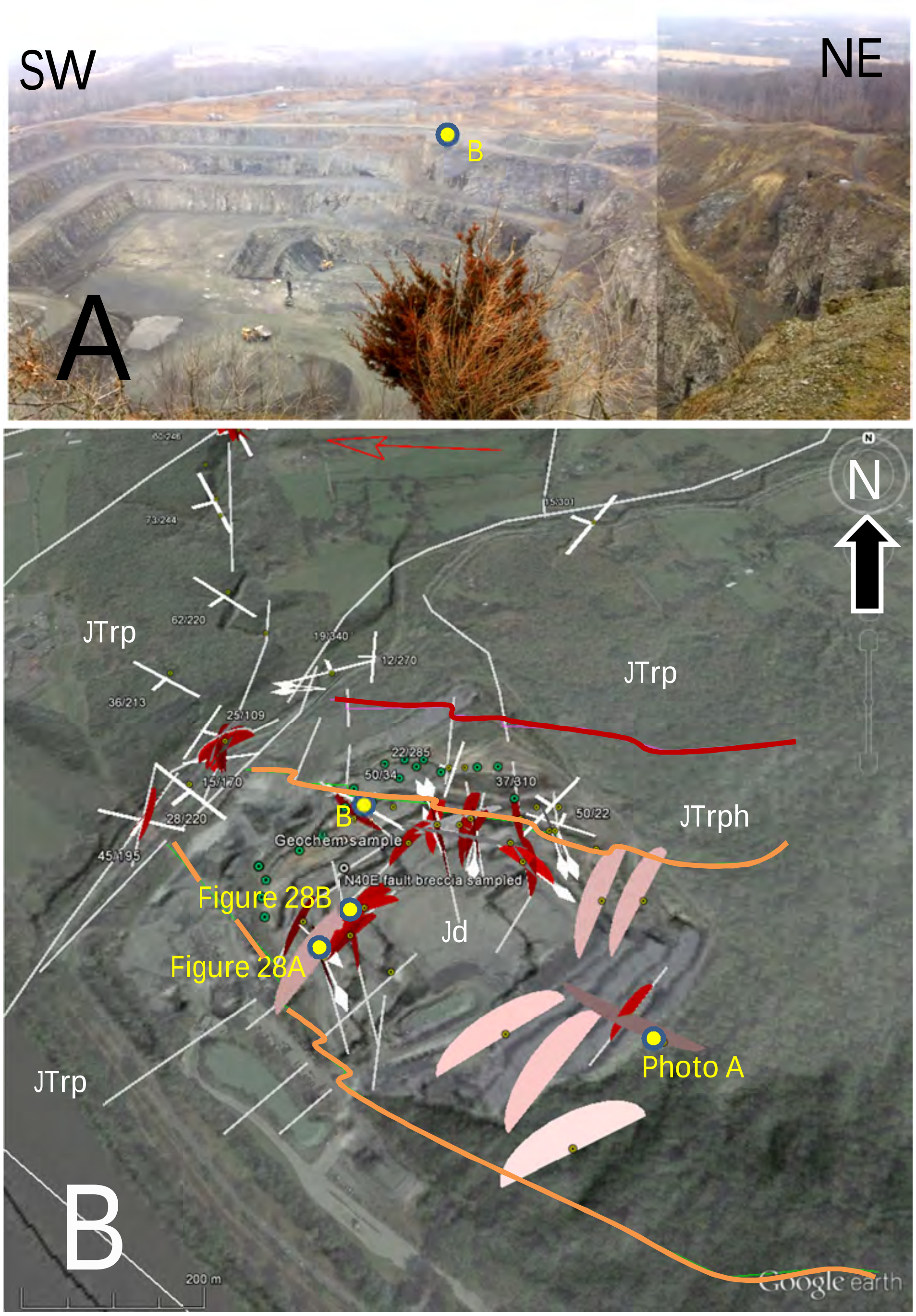

Figure 26. A. February 2012 overview of the Moore's Station quarry, looking SW from the ridge crest on Strawberry Hill (fig. 22). B. Obliquely tilted overhead view of the Moore's Station quarry showing some 2D and 3D structures. The PASDA grayscale hill-shade image overlay is set at 80% transparent. White bed symbols have dip/dip azimuth notation. Green points are the locations of TRI test borings. White points are NJGWS field stations. The white lines are fault traces, orange lines are trap (Jd) contacts, and the dark red line is the upper hornfels contact. The pink 3D ellipses represent compositional layering in dolerite-trap that generally dips SE to NE. The red 3D ellipses represent fault planes. White 2D arrows show slickenline trends and plunge directions. Fault movement is mostly down to the E-SE for most fault blocks although N-W fault slips occur. The northern Jd-JTrph contact is indicated where the trap nonconformably plunges beneath Passaic Formation hornfels, as seen in figure 27A. Point B is near where the Buses will park for mineral collecting from the gravel berms.

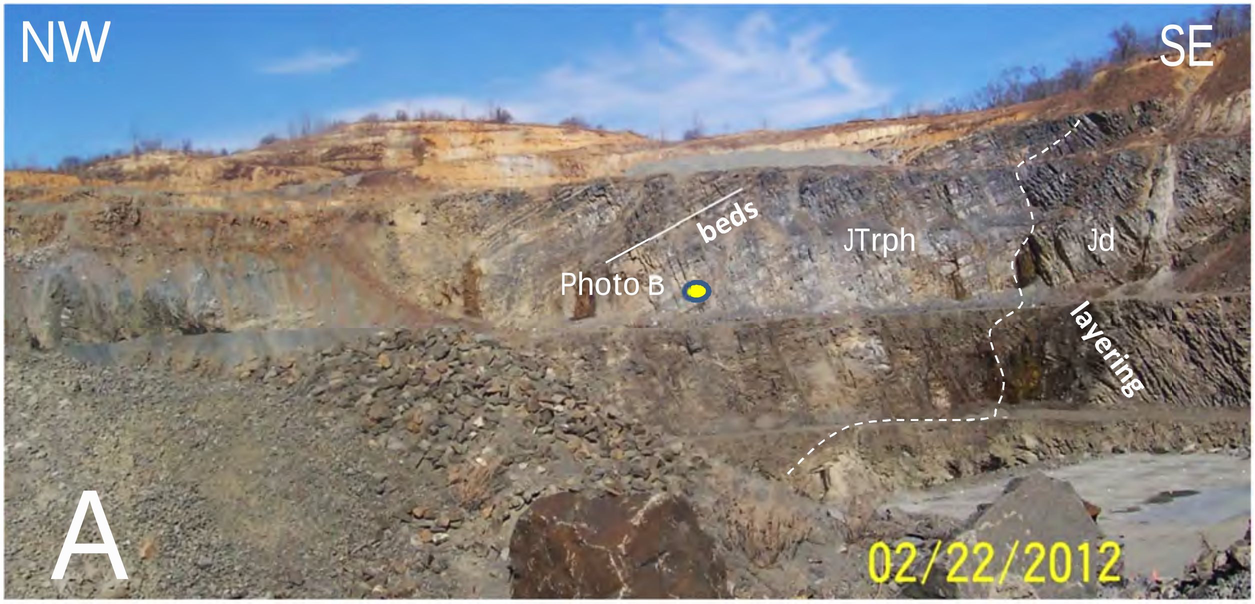

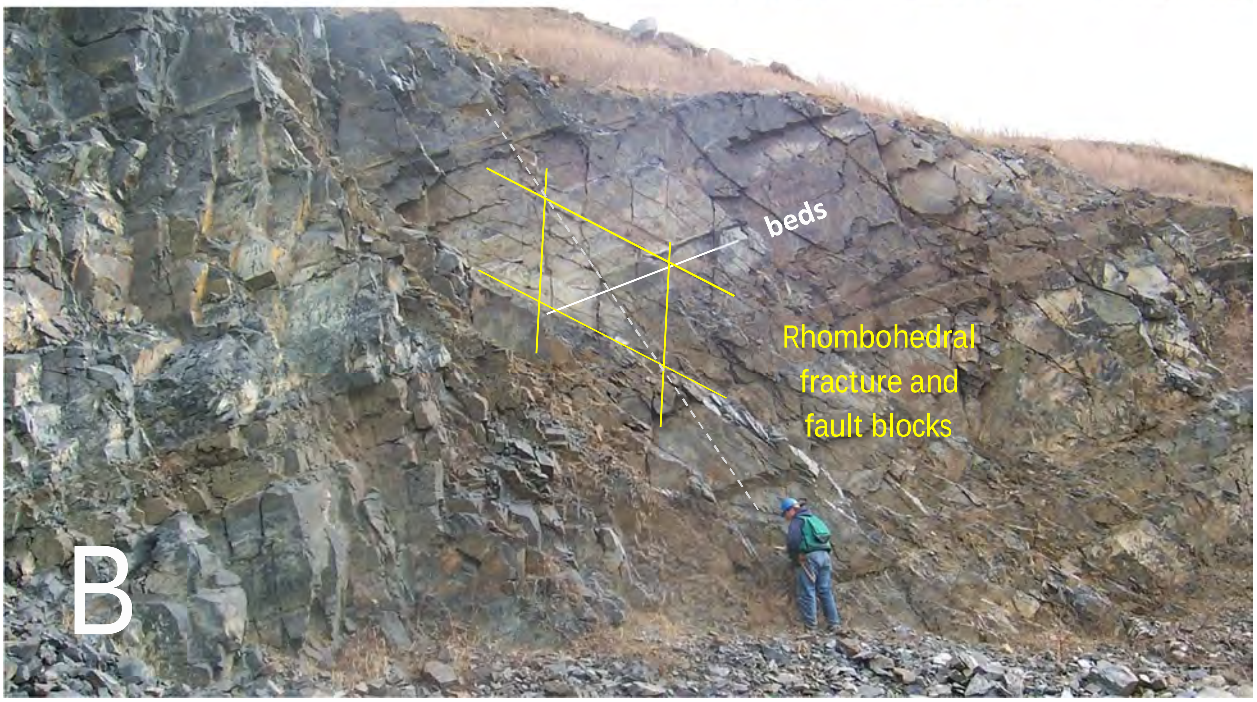

Figure 27. A. Northern view of the gray, brown, and purple hornfels of the Passaic Formation, dipping moderately west with the steep SE-dipping diabase cropping out beneath it to the right. B. Passaic Formation hornfels dipping gently NW showing a rhombohedra fracture geometry stemming from overlapping sets of tension fractures developed during the Mesozoic rifting (see cross-section in fig. 15 and Herman, 2009).

dolerite dips steeply southeast and reflects pervasive cooling fractures that formed parallel to compositional layering and that locally interacted with conjugate shear planes and other cooling fractures to impart sigmoidal shear structures to the igneous layering (fig. 30). These same relationships are observed in TRI's Pennington quarry (Herman and others, 2013). The structural form of igneous layering and sedimentary bedding are very well exposed here and provides evidence of the mechanics of magmatic stoping (Day, 1914), the process by which magma was intruded into the sedimentary section.

For example, figure 21 traces LiDAR lineaments in the Lambertville Sill striking at 30^{o}-60^{o} angles relative to the encompassing sedimentary-bedrock ridges. These traces also likely correspond to compositional layers representing individual magma pulses that were injected into the sedimentary section along developing, crustal fractures that were aligned normal to regional tension at that time (S2 structural phase of Herman, 2009). This means that for the Lambertville Sill, as for Baldpate and Pennington Mountains, igneous layering commonly strikes and dips at high angles relative to the upper nonconformity. This normal alignment of compositional layering with bounding nonconformities is also seen in the Mt. Rose dike leading to the Rocky Hill dolerite body (Herman and Curran, 2012) and the Stockton dolerite body hosting TRI's Lambertville quarry (Herman and others, 2013). The mechanics of magmatic stoping therefore includes compositional layers that were inserted into steeply dipping, extension fractures that developed within focused horizons during tensional rifting.

It's convenient to think of the injection process as magma rising through subsidening crust that is forming extension fractures to accommodate crustal stretching, rather than magma forcefully stoping into bedrock along a specific stratigraphic layer at low angles and uplifting suprajacent beds in the process. Magma is first injected from a subvertical feeder dike laterally into a thick, semi-consolidated sedimentary pile at a depth where lithostatic pressure equals magmatic injection-pressure. But as the injection process continues, the magma stopes upward at moderate to steep angles along rhombohedral-shaped, overlapping faults that we repeatedly see developed in transtentional crustal environments involving at least two phases of non-coaxial extension (figs. 16 and 29; Herman and others, 2009; 2013; Henza and others, 2009). A point to emphasize here is that dolerite intrusions in the Delaware Valley are igneous bodies with composite geometric form having igneous layers paralleling encompassing sedimentary beds in some places, but with angular nonconformance elsewhere. In the case of Baldpate Mountain, injection of this western limb appears to reflect an eastern source, because layering dips eastward to where the medial dike segment springs in a normal direction from the trace of the Hopewell fault, near a major fault branch (figs. 18-20). Similar intrusion geometry is seen for the Pennington trap body (fig. 18) and both intrusions have been shown to reflect fault-mediated ascent of CAMP dolerite from lower stratigraphic sections to the northwest into higher sections to the southeast (Husch and others, 2009; Herman, 2013).

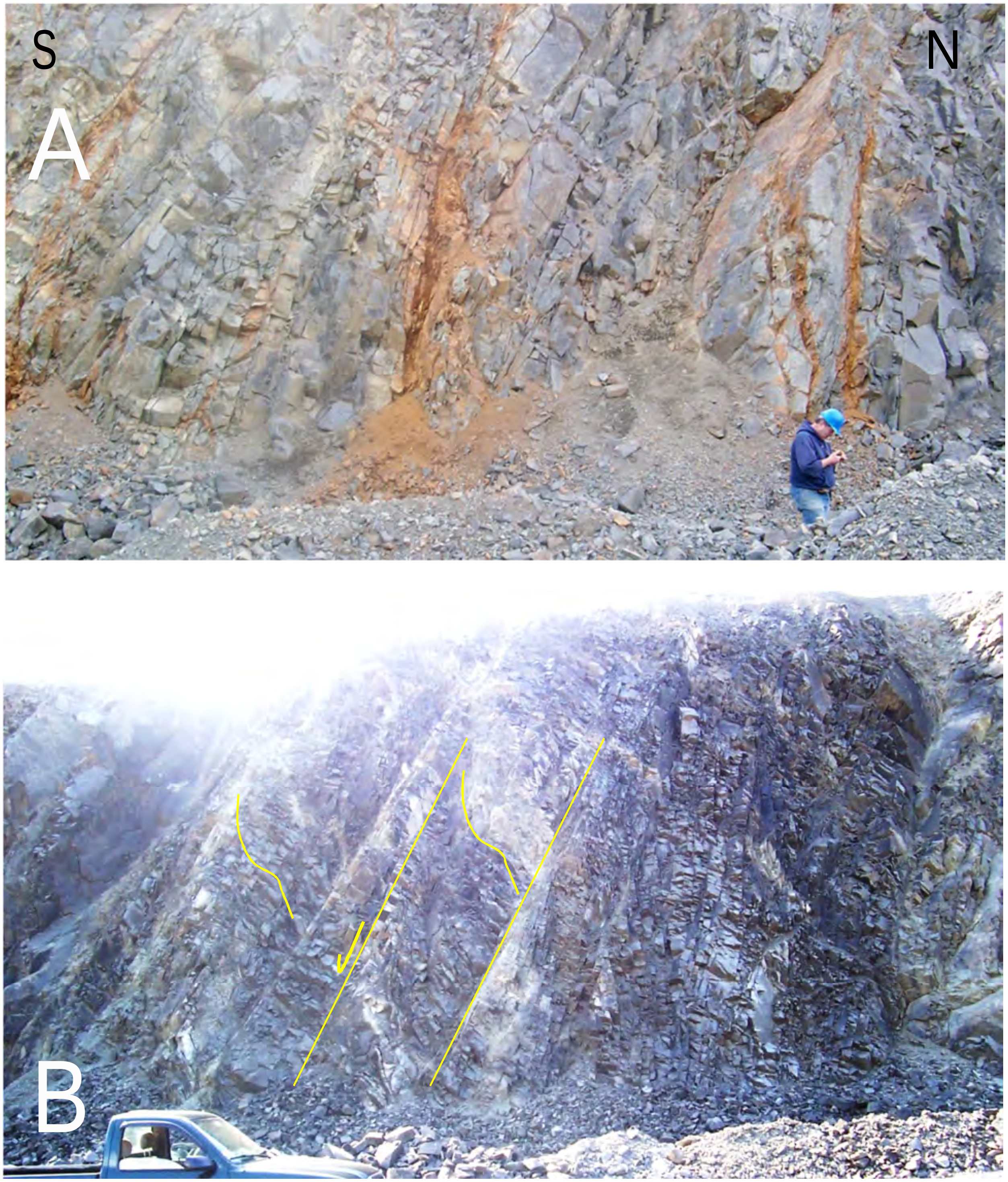

Figure 28. Outcrops along upper- and lower-level benches looking west towards the east face cuts noted in figure 26, where igneous layering dips moderately SE (upper right to lower left). In photo A, some rusty, layer-sub-parallel faults occur in upper-level faces near land surface where meteoric groundwater infiltrated fault surfaces and zones coated and impregnated with iron-rich minerals including chlorite, epidote, and sulfides In photo B, the sigmoidal interaction of cooling joints with shear fractures belies synchronous magmatic injection and normal shearing.

For STOP 3, we will drive through the quarry and out on the 1st or 2nd - level benches where mineralized hornfels are excavated (near point B on figure 28) and where the berms contain excavated, mineralized hornfels. Figure 29-31 and table 3 provide some details of the mineralized horizons and mineral specimens that have been documented at, and that we have collected from, this quarry. A list of minerals in table 3 below is tallied from www.mindat.org and expanded with chemical formulae and abstract descriptions adapted from Deer and others (2013) and Wikipedia. All of these minerals have petrogenesis in volcanogenic igneous settings associated with the mineral infilling of voids, amygdales, and veins in ore-bearing environments from transport during low-temperature hydrothermal circulation including sulfur and copper.

Table 3. List of minerals reported from TRI Moore's Station quarry on www.mindat.org

Mineral	Chemical Formula	Comment
Calcite	$CaCO_3$	
Chabazite	$(Ca,K_2,Na_2)_2[Al_2Si_4O_{12}]_2\cdot12H_2O$	Zeolite tectosilicate
Heulandite	$(Ca,Na)_{2-3}Al_3(Al,Si)_2Si_{13}O_{36}\cdot12H_2O$	Zeolite tectosilicate
Stilbite	$[NaCa_4$ or $Na_9](Si_{27}Al_9)O_{72}\cdot28(H_2O)$	Zeolite tectosilicate
Natrolite	$Na_2Al_2Si_3O_{10}\cdot2H_2O$	Zeolite tectosilicate
Apophyllite	$(K,Na)Ca_4Si_8O_{20}(F,OH)\cdot8H_2O$	Hydrated sheet silicate
Prehnite	$Ca_2Al(AlSi_3O_{10})(OH)_2$	Chain silicate – metamorphic-facies mineral
Schorl (Tourmaline)	$(Ca,K,Na,[\ ])(Al,Fe,Li,Mg,Mn)_3(Al,Cr,Fe,V)_6(BO_3)_3(Si,Al,B)_6O_{18}(OH,F)_4$	Trigonal Boron silicate
Pyrite	FeS_2	Isometric cubic
Marcasite	FeS_2 (white pyrite)	Orthorhombic
Chalcopyrite	$CuFeS_2$	Isometric hextetrahedral w/ perfect cleavage
Sphalerite	$(Zn,Fe)S_2$	

Note: [ ] An empty, double bracket denotes that the following combination of chemicals form repeating units in the chemical formulae.

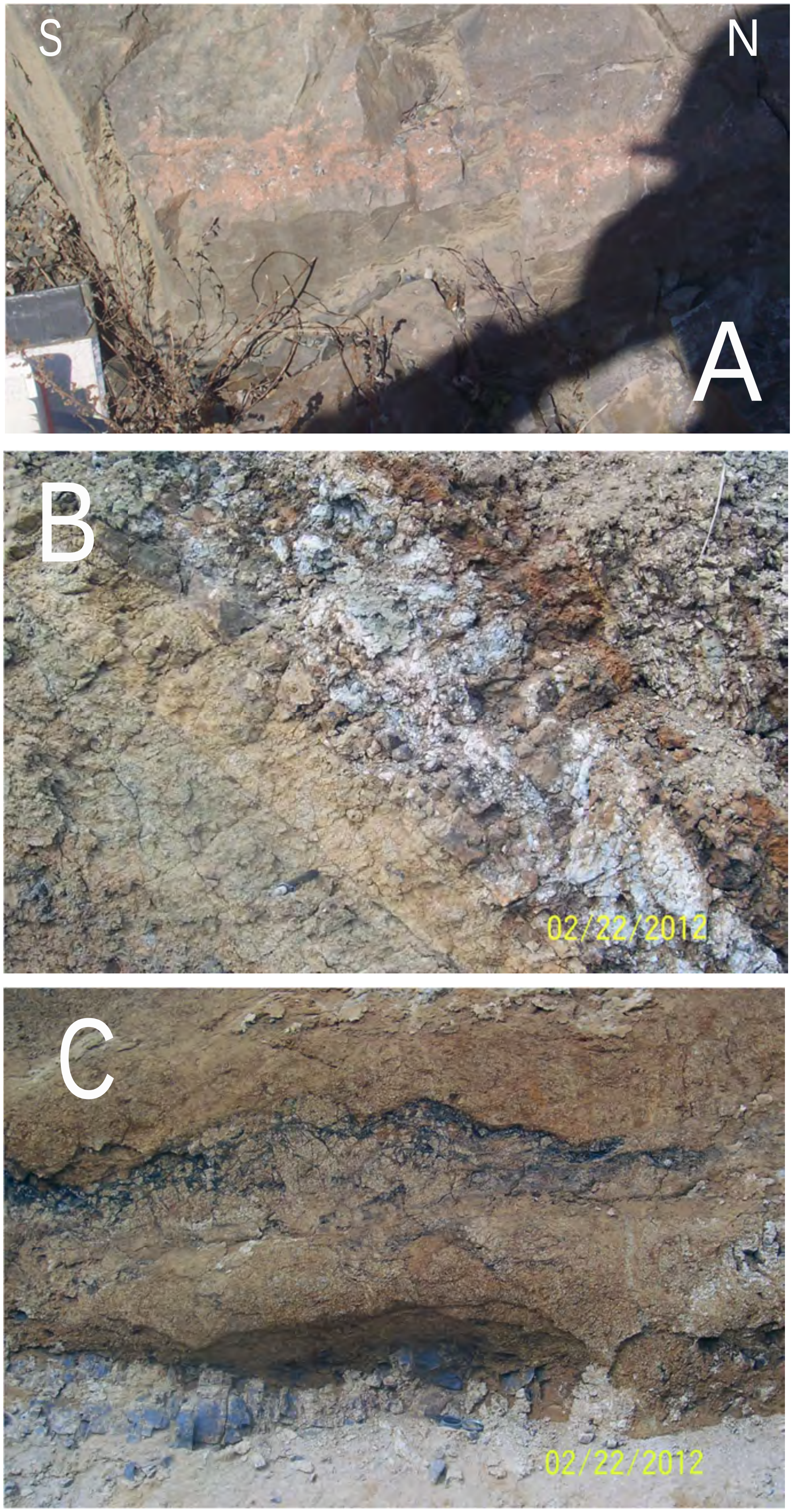

Figure 29. Outcrops along the upper benches on the northern and western face cuts showing epithermal mineralization associated with emplacement of trap into the Passaic Formation. Looking West in all photos.

A. In some places, melt lenses a few inches thick that are enriched in alkali-feldspar invaded Passaic red beds immediately above the nonconformity.

B. A light-greenish-blue supergene enrichment zone lying beneath a gossan cap was temporarily exposed on the uppermost bench of the east side of the quarry during removal of the hornfels cover to expose workable trap rock.

C. Manganese dendrites weather out along fractured horizons in saprolitic hornfels that were permeated with hydrothermal fluids from the nearby igneous intrusion. Upper bench on western limits of the quarry near the westernmost borings shown in figure 26B.

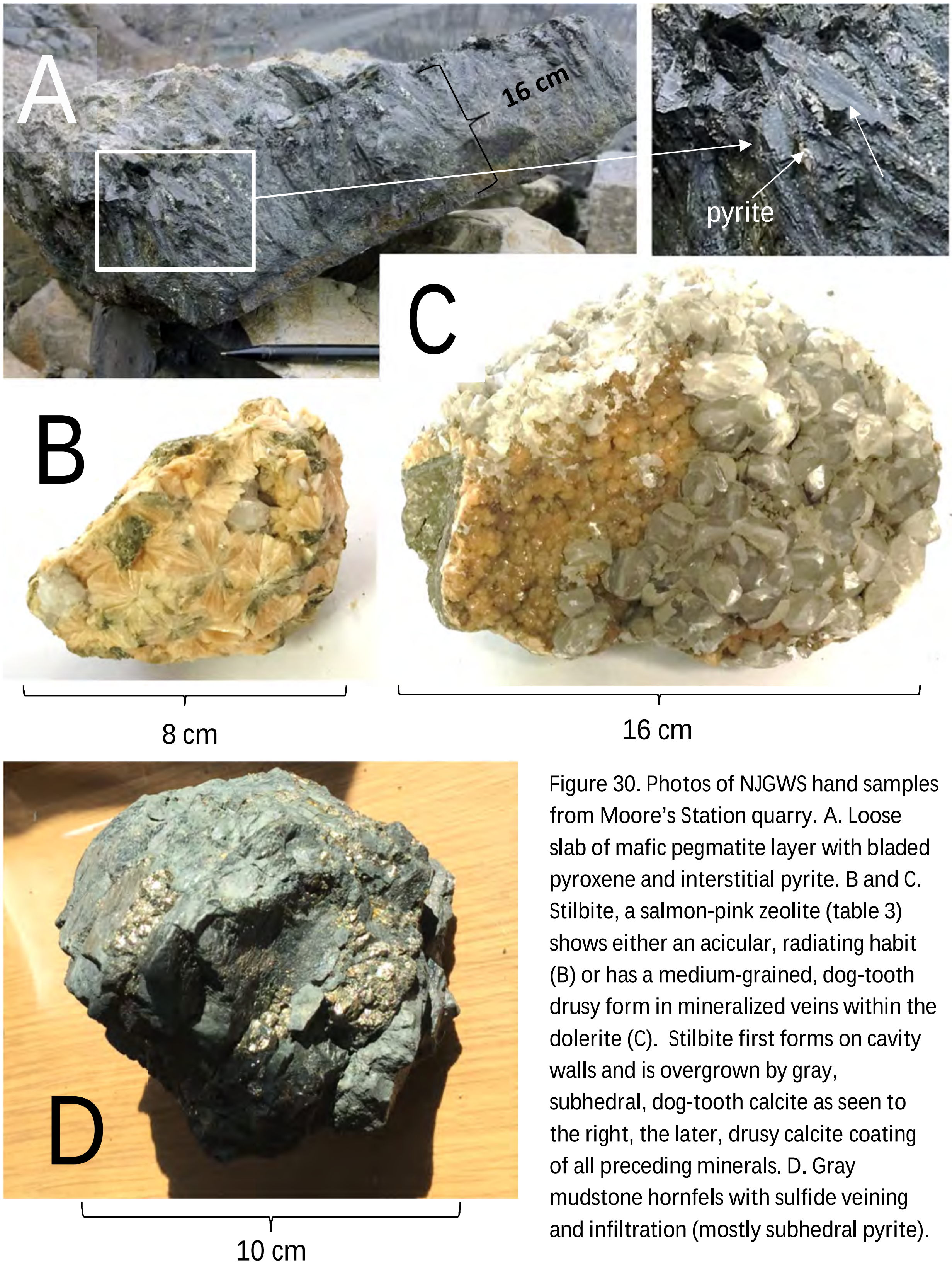

Figure 30. Photos of NJGWS hand samples from Moore's Station quarry. A. Loose slab of mafic pegmatite layer with bladed pyroxene and interstitial pyrite. B and C. Stilbite, a salmon-pink zeolite (table 3) shows either an acicular, radiating habit (B) or has a medium-grained, dog-tooth drusy form in mineralized veins within the dolerite (C). Stilbite first forms on cavity walls and is overgrown by gray, subhedral, dog-tooth calcite as seen to the right, the later, drusy calcite coating of all preceding minerals. D. Gray mudstone hornfels with sulfide veining and infiltration (mostly subhedral pyrite).

With respect to our work, we commonly find calcite, prehnite, stilbite, pyrite, and chalcopyrite (figs. 30 and 31).

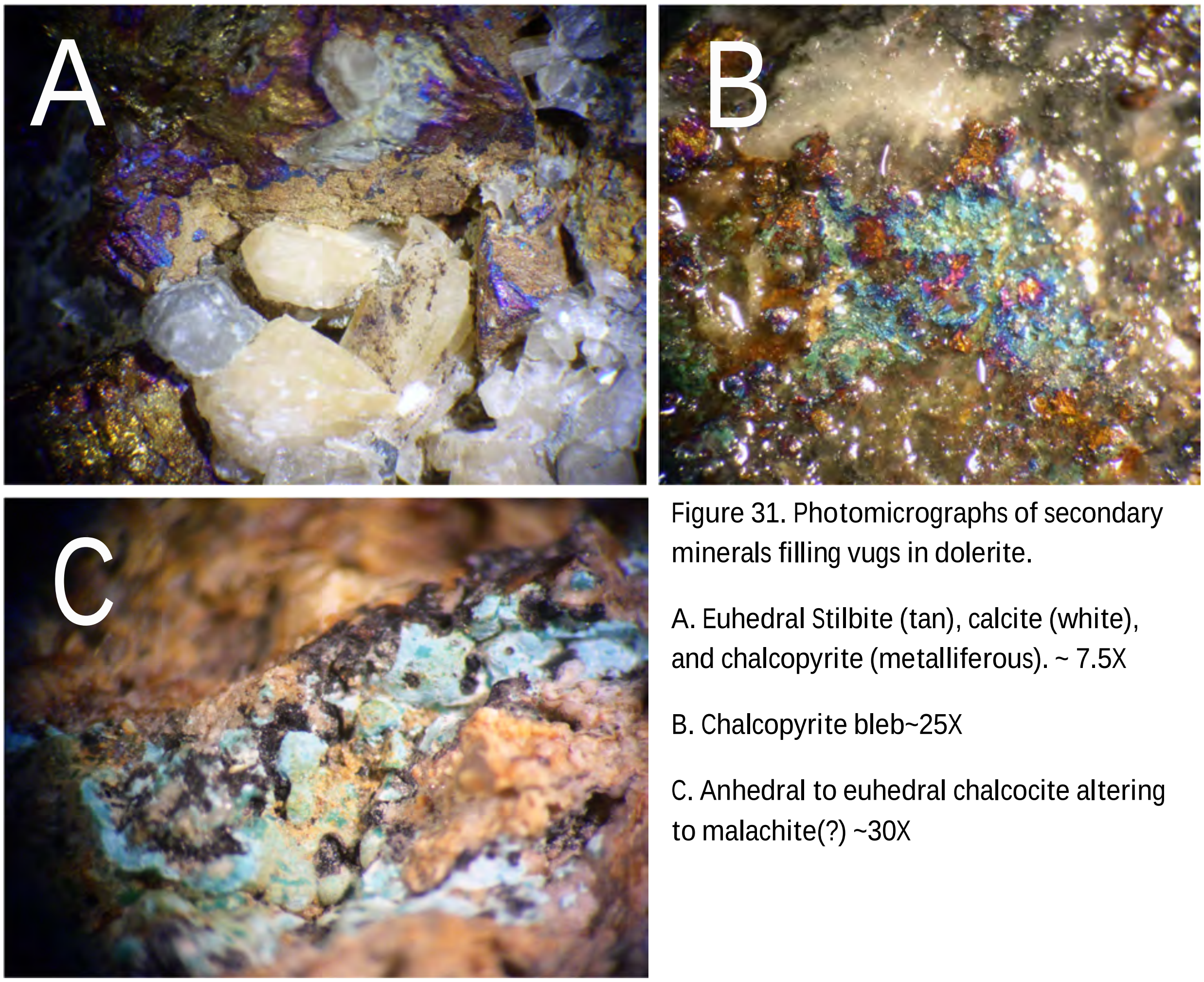

Figure 31. Photomicrographs of secondary minerals filling vugs in dolerite.

A. Euhedral Stilbite (tan), calcite (white), and chalcopyrite (metalliferous). ~ 7.5X

B. Chalcopyrite bleb~25X

C. Anhedral to euhedral chalcocite altering to malachite(?) ~30X

After picking through the berms for about 20 minutes, we will return to the buses and head to STOP 4.

STOP 4. Faulted and shattered Triassic Lockatong argillite and Jurassic dolerite at Byram-Point Pleasant, NJ-PA along the Delaware and Raritan Canal State Park Trail, Route 29, Hunterdon County, NJ

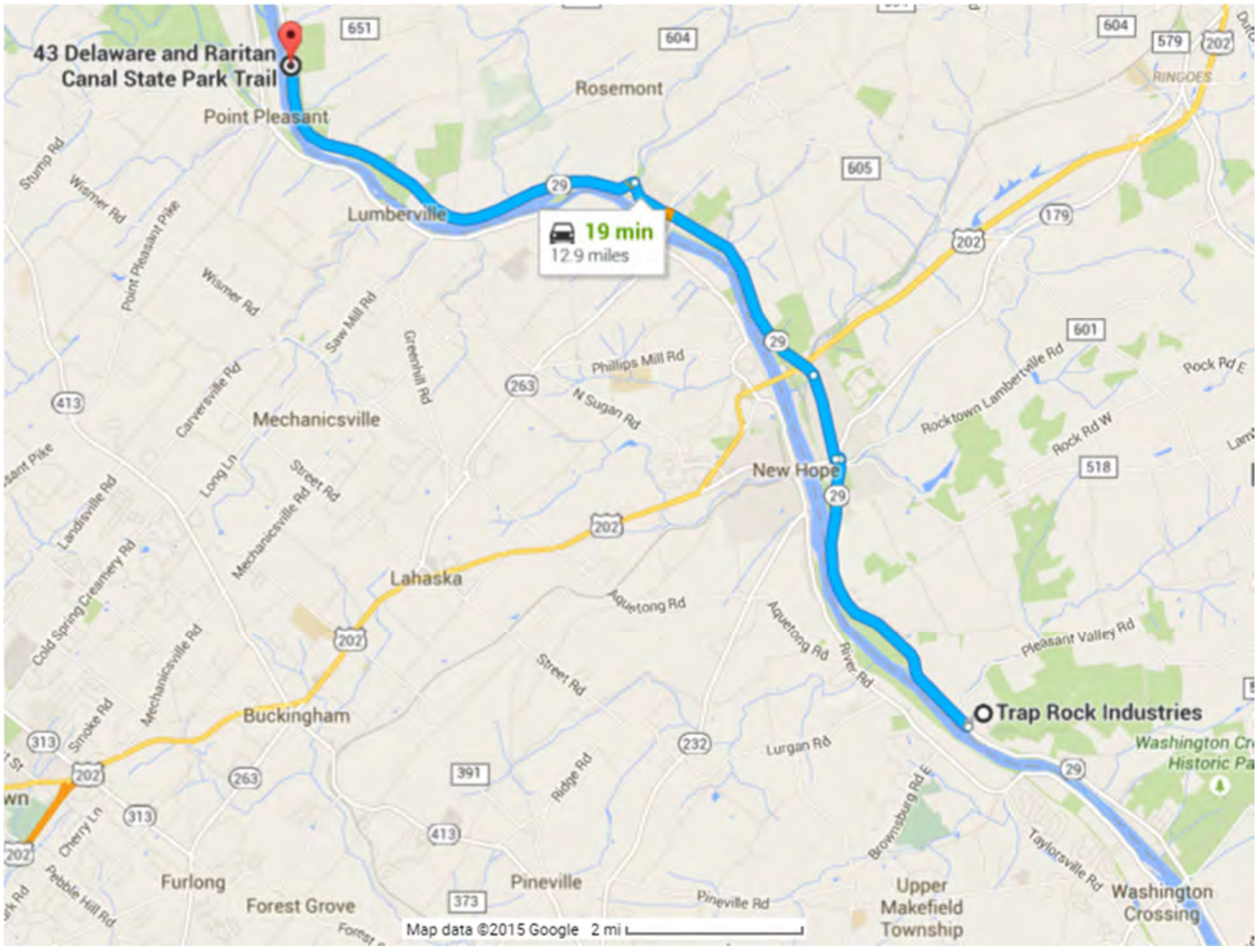

Figure 32. Google maps route from 48 Valley Road, Hopewell Township, NJ to 43 Delaware and Raritan Canal State Park Trail.

Our final STOP is in faulted and shattered dark-gray argillite of Lockatong Formation and overlying dolerite of the Byram sill (Van Houten, 1987). It includes outcropping, late-stage normal faults that cut, offset, and repeat the sill. This area is part of the Lumberville, PA-NJ US Geological Survey 7-1/2' topographic quadrangle. The geological mapping is being updated by the NJGWS as part of their STATEMAP 1:24,000 scale mapping project. Don Monteverde asked me to join in mapping this area because of the structural complexity seen along the stream gorge in which that the D&R Canal trail is developed. The 'trail' is poorly marked; it's actually three different trails that require scrambles up either the banks of the ravine or the creek bed. An old quarry road flanks the ravine on the north and ascends to an abandoned argillite quarry.

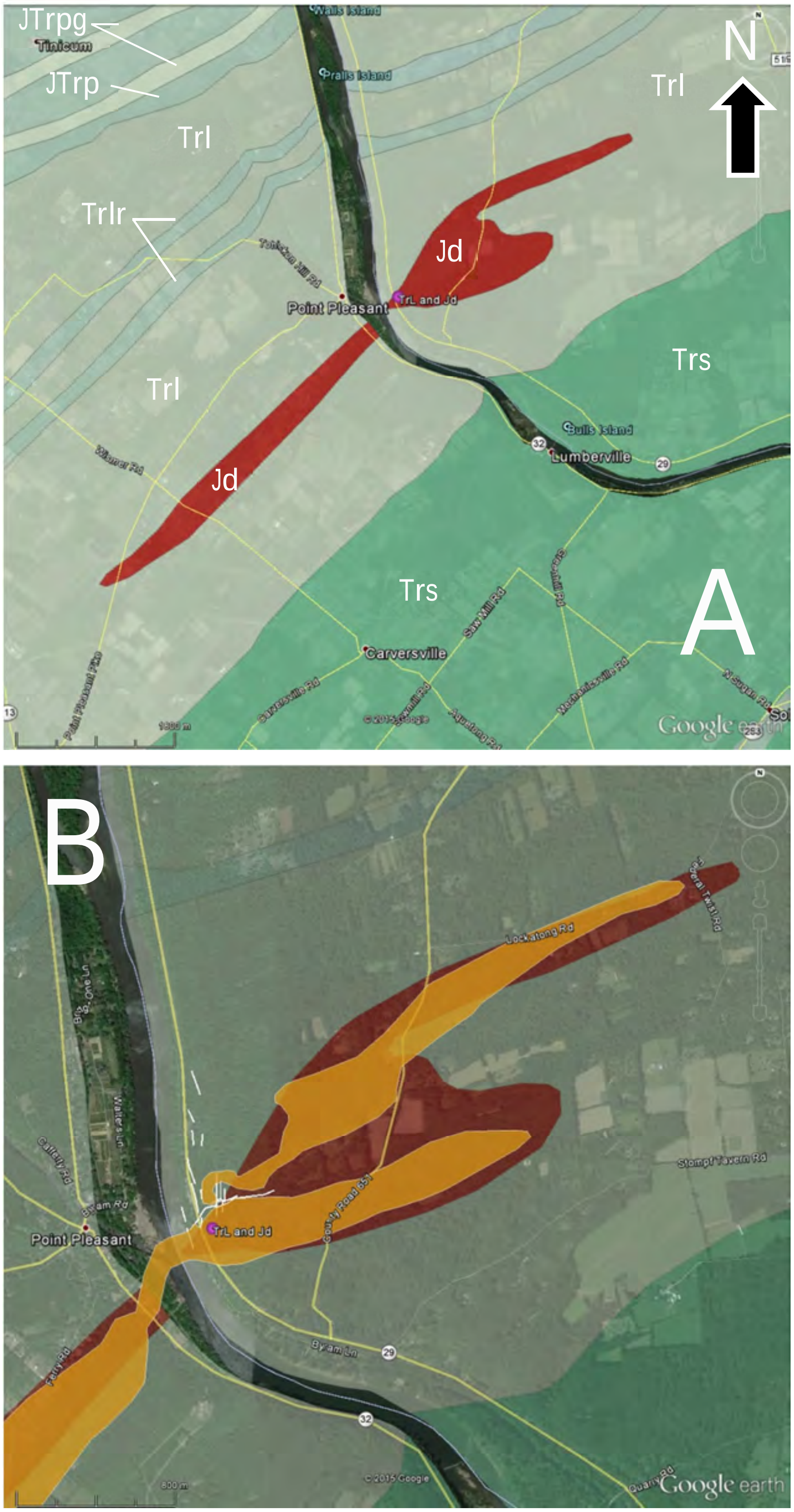

Figure 33. A comparison of old (A) and new (B) geological mapping near Point Pleasant, PA and Byram, NJ.

A. Bedrock geology as currently mapped in Pennsylvania (Berg and others, 1980) and New Jersey (Owens and others, 1998). Jd – Jurassic dolerite. JTrp –Triassic-Jurassic Passaic Formation, JTrpg – Passaic Formation gray bed, Trl – Triassic Lockatong Formation (argillite), Trlr – Triassic Lockatong Formation red bed, Trs – Stockton Formation (sandstone).

B. The contacts between the Lockatong Formation and the Byram sill in the old (red) and new (orange) forms. The new work by NJGWS stems from a combination of mapping outcrops in the Lumberville quadrangle at the 1:24,000 scale and using LiDAR hill-shaded imagery (fig. 35).

South of the ravine, a moderately steep bank follows the fault and hanging-wall contact upstream between the overlying trap (Jurassic dolerite – Jd) and the footwall argillite (Lockatong Formation – TrL).

The creek bed is strewn with sub-rounded to sub-angular boulders of trap rock that have cascaded down from cliffs that flank both sides of the stream. All three trails are difficult to navigate to varying degrees, but the features that occur here are unique and worth a patient, steady walk up a 30 meter elevation (~100 ft) over about a 0.2 km (0.12 miles) distance. If the day is dry and the path is clear, the walk up the stream bed is the preferred path. Once past the boulder talus and alluvial apron at the creek's mouth, fractured and shattered Lockatong Formation outcrops can be seen continuing up the stream for over 1 kilometer. This sequence of argillite has some unique brittle structures that obscure a late-extension stage or river-parallel faulting (fig. 35A), and a brittle overprint of some shatter cones with unusual tension gashes that may stem from an ancient bolide (asteroid or meteor) impact (see Chapter 4; Herman, 2015).

Prior Work

This area of the Delaware River valley has been previously studied and noted by many workers, including Lewis (1909) in a report regarding building stones of New Jersey. He described the Lockatong Formation within the quarry immediately north of this STOP as the 'Byram argillite':

> *"... dark slate-colored to brownish-black argillite, which is more massive that that at Princeton and Lawrenceville, and does not readily split into flat slabs or blocks suitable for building. Hence it is crushed for concrete, railroad ballast, etc. Beds occur 10 to 40 feet thick, which are entirely massive, and the stone breaks with a conchoidal fracture like dense flint... The beds dip 8 degrees toward the north (strike N. 80^o E). Calcite veins and pyrite nodules are abundant in parts of the quarry. Many of the joints are lined with beautiful radial clusters of the mineral laumontite*, which quickly loses its water of crystallization on exposure to the air and crumbles away....Under the microscope this rock crystallized into a dense aggregate of fine flakes of brown mica and granular scapolite, feldspar, and calcite --- a typical hornfel."*

* $CaAl_2Si_4O_{12} \cdot 4H_2O$ – Zeolite tectosilicate

The geological popularity of this area is spurred on by the extensive bedrock cliffs and ledges flanking the Delaware River and deep ravines cuts into the flanking Hunterdon Plateau by creeks, including the Lockatong and Wickecheoke. These conditions have facilitated close inspection of the Triassic strata in this central part of the basin as a continuous section. Dean

McLaughlin with the University of Michigan in the 1930's and 40's and Franklin Van Houten of Princeton University in the 1960's through 80's developed representative stratigraphic sections for this area as part of their work on formalizing the Triassic section in the basin. McLaughlin (1946) mentioned the creeks cutting deep gorges in the escarpment since their rejuvenation by uplift and "their upper courses have cut but little below the old erosion surface". They both noted the nearby stratigraphic transition from a lacustrine setting for the dark gray, muddy argillites of the Lockatong Formation into the subaerial mudflat environment for the red shale of the Passaic Formation.

McLaughlin (1944) also noted here that the two river-bank sections correlate closely with no appreciable offset of the beds from cross-strike faulting (in the river), but then he also asserts that "the evidence is equally convincing as regards absence of significant strike faults." As noted below, this is not the case, as we will see evidence of multiple, cross-strike faults paralleling the river here, as well as strike-parallel faulting noted by Van Houten (1987). The latter documented these cuts for a centennial field guide for the Northeast Section of the Geological Society of America. He noted that this section contains the 'Byram sill' in predominantly dark-gray and brown argillite that is only a few hundred feet above the lower

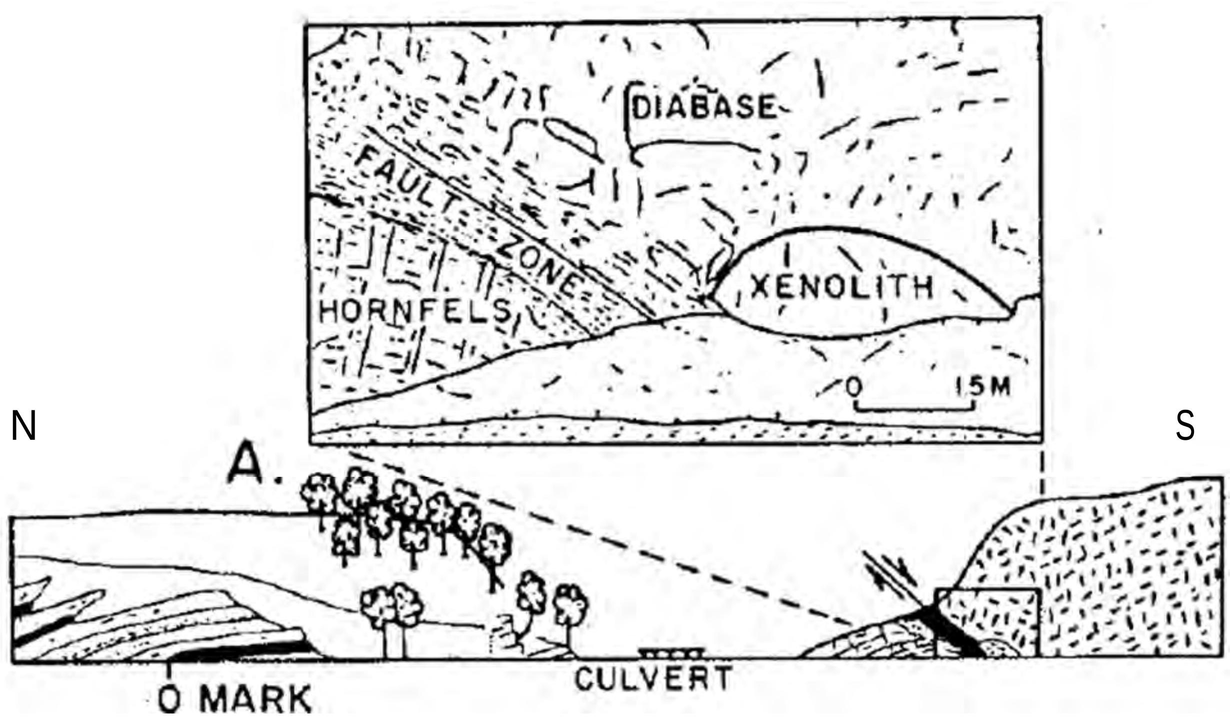

Figure 34. N-S cross section by Van Houten (1987) along Route 29. Note the synthetic, normal fault to the SE dropping dolerite down in contact with the Lockatong Formation. The detailed inset shows a Lockatong xenolith in the basal trap along the fault. We will visit this fault first before heading east up the trail.

contact with the Stockton Sandstone. He depicted this sill as being ~35 m thickness as part of a representative stratigraphic section. His cross section for this site parallels the river (NNW-SSE) and depicts a normal, synthetic fault cutting, offsetting, and repeating the sill (fig. 34). He also notes the occurrence of what he called "upward-concave surfaces and thin zones of shearing in tent-like structures 6 to 12 in (15 to 30 cm) high recurring laterally in wave lengths of 1.5 to 3.0 ft (0.5 to 1 m)", but offered no sketches or pictures of these features.

Michael Hozik has been using this site as a field laboratory for his Stockton University Field Geology class for many years. In addition to the obvious easterly-striking normal fault along the stream, they have documented several north striking oblique slip faults. Evidence for these will be presented as we hike up the stream.

NJGWS 1:24,000 Map Data

As noted previously, detailed geological mapping in the New Jersey part of the Lumberville 7-1/2' quadrangle is currently underway by the NJGWS for publication. The structural data presented here represent a small subset of the data collected in September 2014. These data are available for download at www.ganj.org/2015/Data.html. Figure 33B shows that the mapped shape of the trap body has been redefined and figures 37-39 detail some of the structural relationships mapped and photographed here.

STOP 4 Traverse

PLEASE BE CAREFUL, PROCEED SLOWLY, and DON'T HESITATE TO ASK FOR ASSISSTANCE IN NAVIGATING THE LEDGES AND BENCHES.

This stop includes a moderately difficult hike up the stream bed that will include hopping on boulders to cross the stream if you want to keep your feet dry. If not, plan on becoming wet and bring a change of dry socks and shoes. Hiking boots are a must as this hike involves climbing a 3 to 5-ft crevace cut through bedrock ledges and benches in the creek bed. Once we arrive at the upper level, across the fault trace, the argillite beds dip gently NW, and the creek flows along the bed tops.

THESE BEDS ARE SLIPPERY SO AGAIN, PLEASE PROCEED WITH CAUTION.

If you are not up for the hike up the creek bed, there is an alternative trail just to the North of the creek, along Route 29. This trail follows up a short, steep bank uphill to the old

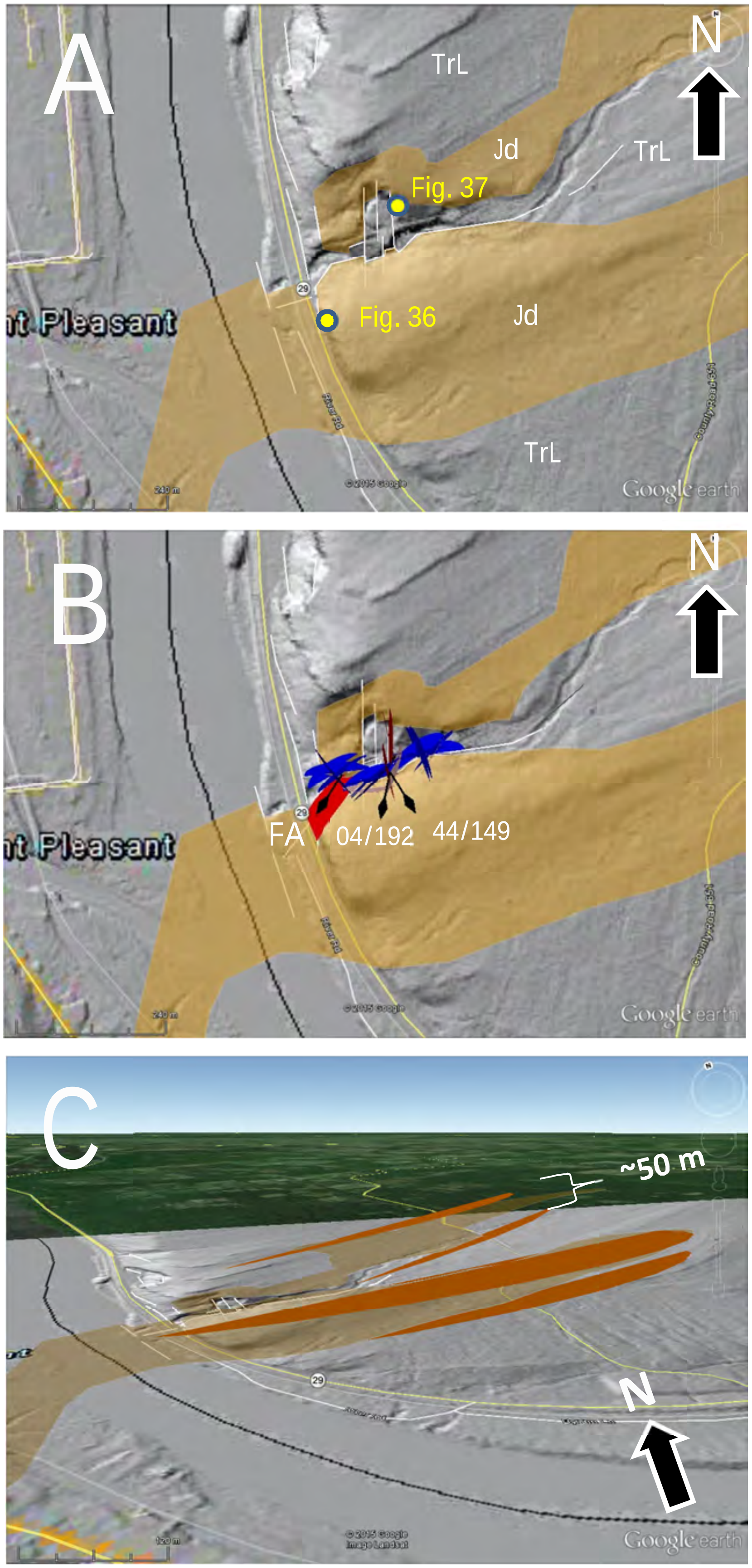

Figure 35. GE displays of STOP 4. A. PASDA LiDAR grayscale hill-shade image overlay with dolerite bodies mapped at the 1:24,000 scale as light-orange polygons. Note the locations of photographs shown in the next two figures. The stream largely follows a long, thin splinter of Lockatong Formation argillite (Trl) along a fault that offsets a thin dolerite sill. This body had been previously mapped as a continuous sill, as shown in fig. 33A. White, straight lines highlight two faults sets, one striking E-W along the stream, and many other's running N-S parallel to the river.

B. Same view as A but showing the 3D colored ellipses representing joints (blue) and faults (red). 2D black arrows represent a fold axis (FA) and slip lineation, or slickenlines noting plunge and trend. Each structural is about 100-m long. Elliptical planes are scaled 50% in the dip direction to accentuate strike

C. Obliquely tilted view looking NNE of the faulted and tilted sill. Orange circular disks were manually fit to the nonconformities to show that the body is about 50 meters thick here.

quarry trail. You can can follow this trail about a kilometer but will still need to descend down to the creek from above. This alternative trail can be very challenging as well.

Or, if you are hesitant to embark on a hike of moderate difficulty, we recommend sitting some or all of this hike out. You won't be bored if you do; the road cuts in the dolerite here are very interesting and include blueberry-sized black tourmaline nodules in the compositional layering seen at road level (fig. 36).

Before we start up the stream channel, it is worth walking a short distance to the south to view the major normal fault in outcrop. Our first stop, located near the entrance to the D&R Trail, is marked by a wooden sign and bulletin board. Outcrop along the road immediately to he south show gently dipping dolerite overlying and in fault contact with the argillite to the NW as portrayed in cross section by Van Houten (fig. 34). The southerly dip of the fault is obvious,

Figure 36. Outcrop along Route 29 North showing compositional layering highlighted with solid white lines dipping gently NE and small splay faults with normal slip dipping steeply SE that highlighted with white dashed lines.

Figure 37. Outcrops location noted in re along the upper bench on the Northeast cut face. The shatter-cone features occur at different places throughout the Lockatong for the full length of the stream and fault to the point where outcrop is lost under alluvium. The dark gray argillite is so dense that no discernible internal structure can be seen other than a peculiar, rolling, linear fracture pattern. The argillite splinters when the rock is cracked open.

A. Certain sections are shattered on steeply dipping planes and sub-horizontal, bed-sub parallel gashes.

B. The conical features radiate inward from gash edges and meet along suture lines where cones merge with flat tops (center by folded eyeglasses).

C. When they remain open and do not meet, they terminate as cones.

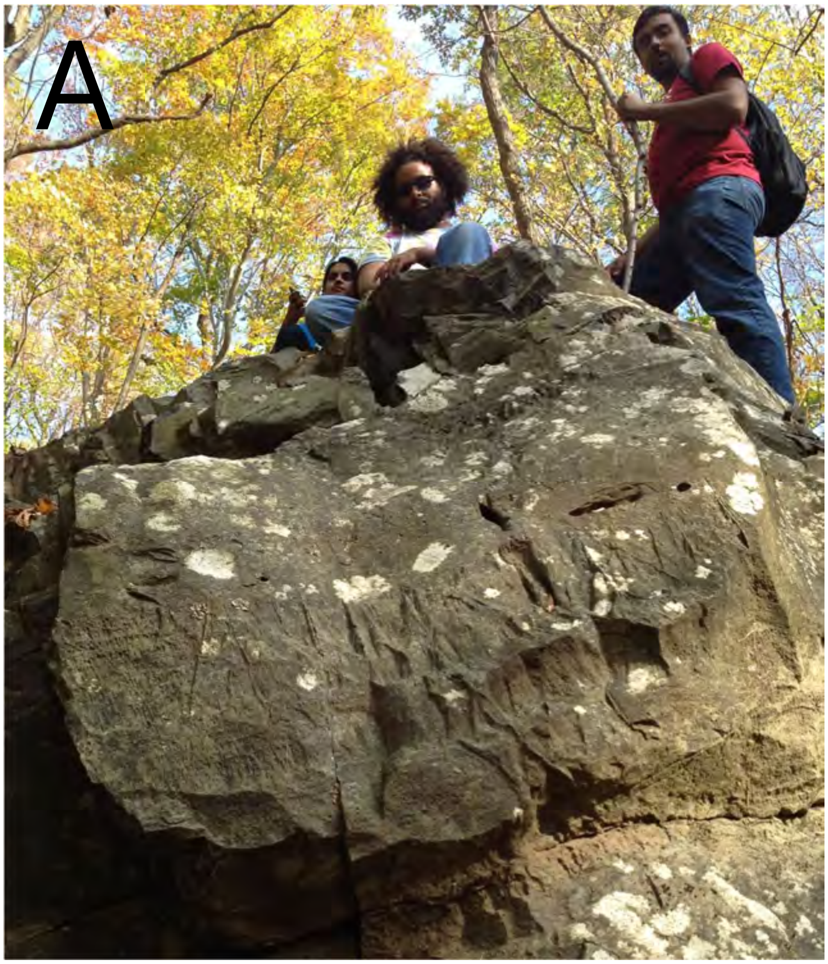

Figure 38. Photographs of the shattercones.

A. View looking NE of a Lockatong bed dipping gently NW. Atop the bed are Rider University geology students Suvarna, Paul, and Muhammad. Note the cone-shaped fractured patter in the lower meter of the bed and the sutured lower contact.

B. A large piece of shattered argillite float found in the stream bed showing some of the best morphology of these cone structures that we could photograph.

as is parallel fracturing in the diabase. More importantly, the bedding in the argillite is dragged toward parallelism with the fault, indicating normal motion on the fault.

Soon after the wooden sign, the trail breaks uphill and the scrambling begins. Prcoceeding up the ravine, Lockatong argillite is first seen as a gently NW-diping pavement in the stream bed. Some of the first of a set of unusaul, cone-shaped structures are visible at the very base of the northern stream in joint faces immediately below the lower nonconfomrity mapped about 1/3 of the way up the stream on the north side. These small, subtle features are only teasers for the more pristine versions exposed farther up the traverse as shown in figure 37 and 38. From here the traverse remains completely in argillite, except for the dolerite

A short way up the stream, the channel widens into a pool. The east side of the pool is dolerite, and if we are able to proceed eastward along the stream there is dolerite on both the north and south sides of the channel. Hozik interprets this as evidence for a north-striking oblique-slip fault intersecting the main east-striking normal fault. In this section of channel, it is worth noting the extensive jointing.

Continuing eastward along the stream, the channel gets steeper, and we will reach a prominent step that has to be climbed. On top of this bench are more of the features mentioned near the start of the traverse. Additionally, the north wall of the channel is argillite, while the east wall is dolerite float. Hozik interprets this as indicative of a second north-striking oblique-slip fault. Slickenlines measured on a fault in the quarry on the bench above this locality plunge gently to the south.

Continuing farther up the stream, nearly to the level of the base of the dolerite, one can observe that the bedding in the argillite has a much less steep dip than in the north wall of the channel. Hozik interprets this as drag indicating normal motion on the east-striking fault in the vicinity of the stream. If we have sufficient time to continue farther upstream, we will see a small area where argillite again crops out in a small area. Hozik suggests that this is another indication of a third north-striking oblique-slip fault.

We finally return to the buses and proceed back to the parking lot in Flemington.

References

Berg, T. M., Edmunds, W. E., Geyer, A. R., and others, compilers, 1980, Geologic map of Pennsylvania: Pennsylvania Geological Survey, 4th ser., Map 1, scale 1:250,000.

Boucher, C., Altamimi, Z., and Sillard, P., 1999, The 1997 International Terrestrial Reference Frame (ITRF97), IERS Technical Note 27, Observatoire de Paris, Paris.

Daly, R. A., 1914, Igneous rocks and their origin: Harvard Press, Cambridge Massachusetts, 563. P.

Deer, W.A., Howie, R.A. and Zussman. J., 2013, An Introduction to the Rock-Forming Minerals. London: Mineralogical Society. 3rd ed., 498 p.

Muessig, K., Houghton, H., Monteverde, D., and Volkert, R., 1992, Field guide to the geology of Radon hazard areas in New Jersey: NJ Geological Survey Open-File OFR 92-2, 22 p.

Fossan, Haakon, 2012: Structural Geology, Cambridge University Press, 480 p.

Grieve, A. F., 2005, Economic mineral resource deposits at terrestrial impact structures, in McDonald, L., ed., Mineral deposits and Earth Evolution: Geological Society of London, p. 1-29.

Henza, A.A., Withjack, M. O., and Schlische, R. W., 2009, Normal-fault development during two phases of non-coaxial extension: An experimental study: Journal of Structural Geology, Vol. 32, Issue 11, p. 1656-1667.

Herman, G. C., 2009, Steeply-dipping extension fractures in the Newark basin: Journal of Structural Geology, V. 31, p. 996-1011.

Herman, G. C. and Curran, John, 2010, Borehole geophysics and hydrogeology studies in the Newark basin, New Jersey (38 MB PDF), in Herman, G. C., and Serfes, M. E., eds., Contributions to the geology and hydrogeology of the Newark basin: N.J. Geological Survey Bulletin 77, Appendixes 1-4, 245 p.

Herman, G. C., Dooley, J. H., and Mueller, L. F., 2010, Geology of the Pennington Trap Rock (Diabase) Quarry, Mercer County (6 MB PDF), in LaCombe, Pierre, ed., Geology of Trenton and its impact on the Capitol City: 27th Annual Meeting of the Geological Association of New Jersey, Trenton, NJ, p. 92-119.

Herman, G. C., Dooley, J. H., and Monteverde, D. H., 2013, Structure of the CAMP bodies and positive Bouger gravity anomalies of the New York Recess, in Benimoff, A. I., ed., Igneous processes during the assembly and breakup of Pangaea: Northern New Jersey and New York City: Proceedings of the 30th Annual Meeting of the Geological Association of New Jersey, College of Staten Island, N.Y., p. 103-142.

Husch, J. M., Bambrick,T. C., Eliason, W. M., Roth, E. A., Schwimmer, R. A., Sturgis, D. S., and Trione, C. W., 1988, A review of the petrology and geochemistry of Mesozoic diabase from the central Newark basin: New petrogenetic insights, in Husch, J. M. and Hozik, M. J., eds., Geology of the Central Newark Basin: Field Guide and Proceedings of the Fifth Annual Meeting of the Geological Association of New Jersey, Lawrenceville, NJ, p. 149-194.

Lewis, J.V., 1909, Building Stones of New Jersey: Geological Survey of New Jersey, Annual Report of the State Geologist for the year 1908, p. 95-96

Lin, Aiming, 1999, S C cataclasite in granitic rock: Tectonophysics, Volume 304, Issue 3, p. 257-273.

Lugli, S., Reimold, W. U., and Koerberl, K., 200?, Silicified Cone-in-_cone structures from Erfoud (Morocco): A comparison with Impact-generated shatter cones, in Koerberl, C., and Henkel, H., eds., Impact Tectonics: Springer-Verlag Berlin Heidelberg, p. 82-110.

McLaughlin, D. B., 1944, Triassic stratigraphy in the Pont Pleasant district: Pennsylvania Academy of Sciences Proceedings, v. 18, p. 89-98.

Marzoli, A., Renne, P., Piccirillo, E., Ernesto, M., Bellieni, G., and De Min, A, 1999. Extensive 200-million-yearold continental flood basalts of the Central Atlantic Magmatic Province: Science v. 284, p. 616–618

Owens, J. P., Sugarman, P. J., Sohl, N. F., Parker, R. A., Houghton, H. F., Volkert, R. A., Drake, A. A., Jr., and Orndorff, R.C., 1998, Bedrock Geologic Map of Central and Southern New Jersey, U. S. Geological Survey Miscellaneous Investigation Series Map I-2540-B, scale 1:100,000, 4 sheets.

Philpotts, A. R., 1982. Composition of immiscible liquids in volcanic rocks: Contributions to Mineralogy and Petrology, v. 80, p. 201-218.